

**Nutrient availability as a driver of soil green-
house gas fluxes and nitrogen leaching in a native
tropical forest and large-scale sugarcane
plantations in north-western Uganda**

Kumulative Dissertation zur Erlangung des naturwissenschaftlichen
Doktorgrades (Dr. rer. nat.) der Universität Augsburg (Fakultät für
Angewandte Informatik)

vorgelegt von

Joseph Tamale

geboren in Wobulenzi, Uganda

Augsburg, 2023

First Reviewer: Prof. Dr. Peter Fiener

Second Reviewer: Prof. Dr. Wolfgang Buermann

Third Reviewer: Prof. Dr. Sebastian Doetterl

Date of oral examination: October 2nd, 2023

Summary

Soil macronutrient availability (particularly nitrogen (N) and phosphorus (P)) is a crucial abiotic control for the cycling of carbon (C) and N in terrestrial ecosystems. However, empirical evidence on macronutrient regulation of soil greenhouse gas (GHG; carbon dioxide (CO₂), methane (CH₄), nitrous oxide (N₂O)) and N leaching fluxes from tropical forests and agricultural systems in sub-Saharan Africa (SSA) is still lacking. Yet, currently, SSA accounts for nearly one-third of all tropical forests. It is also expected to become a hotspot for increased N deposition, large-scale deforestation, and agricultural intensification in the near future. Hence, high-resolution measurements (spatially and temporally) on C and N fluxes from SSA terrestrial ecosystems are needed to constrain global C and N budgets properly. Thus, this PhD study evaluated the regulation effect of soil macronutrients on soil GHG and N leaching fluxes in a nutrient-limited tropical forest and a fertilized sugarcane plantation in north-western Uganda. The PhD study is based upon three interconnected work packages (WP).

In WP1, it is investigated how soil GHG fluxes (CO₂, CH₄, and N₂O) were affected by macronutrient limitations in a Ugandan tropical forest. Hence, a large-scale nutrient manipulation experiment (NME) was setup in Budongo Forest Reserve consisting of four times replicated plots with N, P, N + P, and control treatments. In every replicate plot, soil CO₂, CH₄, and N₂O fluxes were measured monthly (between May 2019 and June 2020) using static vented chamber bases. The study findings show that N addition (N and N + P) resulted in significantly higher N₂O fluxes in the transitory phase (0-28 days (d) after fertilization). N fertilization likely increased soil N beyond the microbial immobilization and plant nutritional demands, leaving the excess to nitrification or denitrification. Prolonged N fertilization, however, did not elicit a significant response in background N₂O fluxes (measured more than 28 d after fertilization). P fertilization marginally and significantly increased transitory and background CH₄ consumption, probably because it enhanced methanotrophic activity. Adding N and P together (N + P) resulted in larger CO₂ effluxes in the transitory phase, suggesting a possible co-limitation of both N and P on soil respiration. Heterotrophic (microbial) CO₂ effluxes were significantly higher than the autotrophic (root) CO₂ effluxes across all treatment plots, with microbes contributing about two-thirds of the total soil CO₂ effluxes. However, neither heterotrophic nor autotrophic respiration significantly differed between treatments.

In WP2, it is assessed how forest conversion to intensively fertilized sugarcane plantations affected soil GHG fluxes (CO₂, CH₄, and N₂O). Here, soil GHG fluxes from the control plots in WP1 were compared to those measured in every treatment plot of a completely randomized design (CRD) experiment in a sugarcane plantation. The CRD experiment was established in a

5.6-hectare ratoon sugarcane field 6 km south of the forest NME. It consisted of fertilizer treatments (low, standard, and high) that represented a gradient of N fertilization rates used by sugarcane farmers in north-western Uganda. Similarly (like in the NME), all the CRD treatments were replicated four times. Soil GHG fluxes were determined with static vented chambers intensively in the six months that followed fertilization before switching to monthly measurements for the remaining period of the sampling campaign. Additionally, for every land use, fine root biomass was determined based on 20 x 20 x 10 cm soil monoliths while soil organic carbon (SOC) stocks were determined based on oven-dry bulk densities and SOC concentrations in the first 1-meter soil depth. Soil CO₂ effluxes were higher under sugarcane compared to the forest because of the higher autotrophic respiration from the sugarcane's fine root biomass and the microbial decomposition of the sugarcane's larger SOC stocks. Conversely, soil CH₄ uptake under sugarcane was three times lower than under forest, owing to the likely alteration of methanotroph abundance upon conversion. Likewise, soil N₂O emissions were much smaller under sugarcane than in the forest because excess N from fertilizer addition in the sugarcane was either lost through leaching or taken up by the sugarcane crop. All the results combined demonstrate that even with the higher soil CO₂ effluxes under sugarcane compared to the forest, the fact that there was higher SOC sequestration in sugarcane plantations of different ages relative to the native forest, suggests that sugarcane systems in the study area acted as a C sink since the uptake of CO₂ far exceeds SOM mineralization. However, the SOC sequestration under sugarcane does not offset the initial significant loss in the above and belowground biomass C loss immediately after forest conversion. Moreover, the C sink under sugarcane can change if CO₂-equivalents related to N₂O and CH₄ fluxes are considered in the calculation of the sugarcane's C footprint.

In WP3, it is evaluated how increasing N fertilization rates affected N dynamics, productivity, and profitability of sugarcane plantations established on Ferralsols. Here, soil N₂O fluxes from WP2 were used in combination with the measured N leaching fluxes and field fresh weight (yield/biomass) from the respective treatment plots of the CRD experiment established in WP2. N leaching fluxes were determined based on drainage fluxes estimated with the Leaching Estimation and Chemistry Model and leachate N concentrations obtained from suction cup lysimeters installed at the soil depth of 90 cm. However, estimation of N leaching fluxes was limited by the lack of site-specific measurements of soil hydraulic properties and pedotransfer functions (PTFs) trained and calibrated for Ferralsols in tropical Africa. This challenge was overcome by testing a suite of American, Brazilian, and European PTFs for their suitability in determining soil hydraulic properties for the study test site. Sugarcane field fresh weight was estimated by

randomly harvesting four (1 m x 1 m) quadrants in every replicate plot. In WP3, it is demonstrated that three of the five tested PTFs reliably estimated drainage fluxes for the study test site in Uganda based on the match between the measured and predicted soil matric water potentials. Therefore, despite the tested PTFs being developed using American, Brazilian, and European soil datasets, some of them were robust enough to be used outside their training and validation geographical confines with a satisfactory degree of accuracy. N leaching fluxes marginally increased when N rates were increased from low to standard but significantly when the N rates exceeded the standard rate. The measured soil N₂O emissions were unaffected by N fertilization. Sugarcane yields did not respond to increasing N rates, despite a significant to marginal increase in crop N uptake between low and standard N rates and at N rates higher than the standard, respectively. All the findings from WP3 suggest that surpassing the standard N rate for sugarcane in north-western Uganda would be less economically viable since it would only marginally increase yields, while the substantial increase in N leaching will affect groundwater quality. Additionally, despite demonstrating that sugarcane cultivation can still be profitable at lower-than-standard N rates since part of the N requirement is met by mineralizing the high soil organic matter levels in sugarcane fields, it remains unreconciled from this short-term study whether reducing N rates below the standard N rate will not counterintuitively lower SOC stocks in the long term. The high SOC stocks under sugarcane reflect the long-term C input dynamics obtained with the standard N rates.

Zusammenfassung

Die Verfügbarkeit von Makronährstoffen im Boden (insbesondere von Stickstoff (N) und Phosphor (P)) ist ein wichtiger abiotischer Einflussfaktor für den Stickstoff- und Kohlenstoffkreislauf in terrestrischen Ökosystemen. Allerdings fehlen bisher empirische Studien aus den tropischen Regionen Afrikas südlich der Sahara (SSA), die die Einflüsse von Makronährstoffen auf die Stoffflüsse von N und Treibhausgasen (GHG), wie Kohlendioxid (CO₂), Methan (CH₄) und Lachgas (N₂O) in Wald und landwirtschaftlichen Systemen betrachten. Dabei befinden sich nahezu ein Drittel der globalen tropischen Wälder in der SSA Region. Es wird zudem erwartet, dass die SSA Region in naher Zukunft durch großflächige Entwaldung und Intensivierung der Landwirtschaft verändert wird. Als Konsequenz dieses Wandels, werden sich auch die Stickstoffeinträge erhöhen. Daher sind hochauflösende Messungen (räumlich und zeitlich) der C- und N-Flüsse aus den terrestrischen Ökosystemen der SSA Region erforderlich, um die gesamten C- und N-Haushalte angemessen abzuschätzen. Diese Doktorarbeit untersucht die Regulierung der Treibhausgas- und Stickstoffauswaschungsflüsse durch Makronährstoffe in einem nährstofflimitierten tropischen Wald und einer gedüngten Zuckerrohrplantage im Nordwesten Ugandas. Die Arbeit lässt sich in drei Arbeitspakete (WP) untergliedern.

In WP1 wurde untersucht, wie GHG-Flüsse (CO₂, CH₄ und N₂O) im Boden durch Makronährstoffbeschränkungen in einem tropischen Wald in Uganda beeinflusst werden können. Im Bundongo-Waldreservat wurden Untersuchungspartellen für ein großskaliges Nährstoffmanipulationsexperiment (NME) angelegt. Die Partellen wurden jeweils viermal mit N, P und N + P gedüngt und mit einer Kontrollgruppe, ohne Zugabe, verglichen. Auf jeder Partelle wurden die CO₂-, CH₄- und N₂O-Emissionen des Bodens monatlich (zwischen Mai 2019 und Juni 2020) mit stationären Haubenkammern gemessen. Die Ergebnisse zeigten, dass die N-Zugabe (N und N + P) kurzzeitig (0 - 28 Tage nach der Düngung) zu signifikant höheren N₂O-Emissionen führte. Die Düngung erhöhte den N-Gehalt des Bodens so stark, dass sich ein Überschuss ergab, der die mikrobielle Immobilisierung und den Nährstoffbedarf der Pflanzen überschritt und zur Nitrifikation oder Denitrifikation führte. Die Düngung führte jedoch zu keiner signifikanten Veränderung der langfristigen (mehr als 28 Tage nach der Düngung gemessen) N₂O-Emissionen. Die P-Düngung erhöhte den kurzfristigen und langfristigen CH₄-Emissionen geringfügig aber signifikant, da sich die Aktivität methanotropher Bakterien erhöhte. Die gemeinsame Zugabe von N und P (N + P) führte kurzfristig zu größeren CO₂-Emissionen (0-28 Tage), was auf eine mögliche gemeinsame Limitierung von N und P für die Bodenatmung hindeutet. Auf allen Untersuchungspartellen war die heterotrophe (mikrobielle) Atmung signifikant höher als der au-

totrophe Atmung, wobei die heterotrophe Atmung etwa zwei Drittel des gesamten CO₂-Emissionen ausmachte. Allerdings unterschied sich weder die heterotrophe noch die autotrophe Atmung signifikant zwischen den unterschiedlichen Düngevarianten.

In WP2 wurde untersucht, wie sich die Umwandlung von Wäldern in intensiv gedüngte Zuckerrohrplantagen auf die GHG-Flüsse (CO₂, CH₄ und N₂O) der Böden auswirkte. Auf Untersuchungsparzellen einer Zuckerrohrplantage mit vollständig randomisiertem Design (CRD), wurden ebenfalls die GHG-Flüsse im Boden gemessen und mit den Kontrollparzellen aus WP1 verglichen. Das CRD-Experiment wurde in einem 5,6 Hektar großem Zuckerrohrfeld 6 km südlich der NME-Waldflächen eingerichtet. Die im CRD-Experiment verwendeten N-Zugaben repräsentierten einen Gradienten von Düngungsraten (niedrig, Standard und hoch), die von Zuckerrohrbauern im Nordwesten Ugandas verwendet werden. Die GHG-Emissionen wurden mit stationären Haubenkammern in den ersten sechs Monaten nach der Düngung intensiv gemessen und anschließend wurden die Messungen monatlich bis zum Ende der Messkampagne weitergeführt. Außerdem wurde für jede Landnutzung die Biomasse der Feinwurzeln (basierend auf 20 x 20 x 10 cm großen Bodenmonolithen) und der organische Bodenkohlenstoffvorrat (SOC) im obersten Meter des Bodens (basierend auf der ofentrockenen Rohdichte und SOC-Konzentrationen) bestimmt. Die CO₂-Emissionen des Bodens waren unter Zuckerrohr höher als im Wald, was auf die höhere autotrophe Atmung der Feinwurzeln des Zuckerrohrs und den mikrobiellen Abbau der höheren organischen Kohlenstoffvorräte zurückzuführen ist. Umgekehrt war die CH₄-Aufnahme des Bodens unter Zuckerrohr dreimal niedriger als unter Wald, was wahrscheinlich auf die kurzfristige Veränderung der Aktivität methanotropher Mikroorganismen zurückzuführen ist. Die N₂O-Emissionen des Bodens waren ebenfalls unter Zuckerrohr geringer als im Wald und überschüssiger N wurde ausgewaschen oder von der Zuckerrohrpflanze aufgenommen. Alle Ergebnisse zusammengenommen zeigen, dass trotz der höheren CO₂-Emission des Bodens unter Zuckerrohr im Vergleich zum Wald, eine höhere SOC-Sequestrierung in Zuckerrohrplantagen mit verschiedenem Alter erreicht werden kann. Des Weiteren hat sich gezeigt, dass die Zuckerrohrsysteme im Untersuchungsgebiet als C-Senke fungierten, da die Assimilierung von atmosphärischen CO₂ die Mineralisierung der organischen Bodensubstanz (SOM) bei weitem übersteigt. Jedoch, gleicht die SOC-Sequestrierung durch Zuckerrohr die erheblichen Verluste von C aus der ober- und unterirdischer Biomasse des Waldes durch die Umwandlung von Wald zu Zuckerrohrplantage nicht aus. Darüber hinaus ändert sich das Potential der C-Senke unter Zuckerrohr, wenn die realen CO₂-Äquivalente von N₂O- und CH₄-Flüssen bei der Berechnung des C-Fußabdrucks berücksichtigt werden.

In WP3 wurde untersucht, wie steigende N-Düngungsraten die N-Dynamik, Produktivität und Rentabilität von Zuckerrohrplantagen auf Ferralsolen beeinflussen. Hierzu wurden die gemessenen N_2O - Flüsse aus WP2 die gemessenen N-Auswaschungen aus dem Wurzelraum, sowie N-Gehalte der Erntebiomasse aus den jeweiligen Parzellen verwendet. Die Biomasse und der Ertrag von Zuckerrohr wurde in vier Quadranten (1 m x 1 m) in jeder Wiederholungsfläche geschätzt. Die N-Auswaschungsraten wurden auf der Grundlage von Durchflussraten, die mit dem *Leaching Estimation and Chemistry Model* geschätzt und mittels Saugkerzen gemessenen N-Konzentrationen im Sickerwasser in 90 cm Bodentiefe bestimmt. Für die Abschätzung der N-Auswaschung fehlten jedoch Daten und Messungen der hydraulischen Eigenschaften des Bodens sowie Pedotransferfunktionen (PTF), die für das Untersuchungsgebiet im tropischen Afrika angepasst und kalibriert wurden. Diese Herausforderung wurde innovativ angegangen, indem eine Reihe PTFs aus amerikanischer, brasilianischer und europäischer Regionen auf ihre Eignung zur Bestimmung der hydraulischen Bodeneigenschaften für den tropischen Standort hier evaluiert wurden. In WP3 wurde gezeigt, dass drei der fünf getesteten PTFs die Durchflussraten für das Untersuchungsgebiet in Uganda basierend auf der Übereinstimmung zwischen den gemessenen und vorhergesagten Bodenwasserpotenzialen zuverlässig abschätzen konnten. Obwohl die getesteten PTFs unter Verwendung klimatisch unterschiedlicher Bodendaten erstellt wurden, sind einige von ihnen robust genug, um auch bei tropischen Böden erfolgreich Anwendung zu finden. Darauf basierend hat sich gezeigt, dass die N-Auswaschung geringfügig aber signifikant ansteigt, wenn die N-Düngung von niedrigen auf die üblichen Standardraten erhöht wurden und signifikant, wenn diese N-Düngungsrate überschritten wurde. Die N_2O -Emissionen des Bodens wurden jedoch durch die N-Düngung nicht beeinflusst. Die Zuckerrohrerträge zeigten keine Veränderung mit steigender N-Düngung. Jedoch hat sich die N-Aufnahme mit zunehmender N-Düngung signifikant erhöht. Alle Ergebnisse von WP3 deuten darauf hin, dass eine Überschreitung der Standard-N- Düngerate für Zuckerrohr im Nordwesten Ugandas wirtschaftlich weniger rentabel wäre, da sie die Erträge nur geringfügig erhöhen und sich gleichzeitig eine potenziell höhere Auswaschung ins Grundwasser ergibt. Die hohen SOC-Vorräte unter Zuckerrohr wurden durch langfristige Bewirtschaftung mit üblichen Standardraten von N-Dünger erzielt. Obwohl gezeigt wurde, dass der Zuckerrohranbau auch bei N-Düngung unterhalb der Standardraten rentabel sein kann, da ein Teil des Stickstoffbedarfs durch die Mineralisierung der organische Bodensubstanz gedeckt werden kann, konnte in dieser Studie nicht geklärt werden, ob sich langfristig eine Verringerung der SOC-Vorräte ergeben würde.

Acknowledgment

The last 4.5 years of my PhD studies have been nothing short of a whale of a time and tremendous growth as a scientist. However, I attribute the outcome of my PhD thesis not to my strength, character, and intrinsic abilities but mainly to the generosity of many people and organizations that have invested their valuable time and financial resources to see me accomplish this incredible milestone.

First and foremost, I would like to thank the German Academic Exchange Service (DAAD), the International Foundation of Science (IFS), Sweden, and the National Agricultural Research Organization, Uganda, for the financial support towards my fieldwork in Uganda and my PhD stipend in Germany.

Next, I would like to thank my PhD supervisors: (1) Peter Fiener for our excellent scientific interactions and deliberations over the entire tenure of my PhD studies. Your outstanding mentorship, timely feedback, and positive criticism of my research articles and the thesis will forever be priceless. (2) I am also greatly indebted to Sebastian Doetterl for his critical feedback on my scientific pieces, and if there is one thing, I have learned from you, Sebastian, over the years, that would be the necessity to keep things precise. (3) Special thanks go to Oliver van Straaten for believing in my potential as a budding scientist, holding me by the hand on several occasions, and showing me how things are done in the world of flux measurements. Your feedback on my DAAD and IFS PhD proposals, research articles, and scientific chapters of my PhD dissertation was beyond immeasurable.

I want to convey my sincere thanks to John Hutson, University of Flinders, Australia, for the support you rendered me during the nitrogen modeling part of my thesis, particularly on using the Leaching Estimation and Chemistry Model (LEACHM). No combination of words can truly express how deeply grateful I am for all the time you spent to see me carry through with the modeling tasks. N modeling will undoubtedly be a part of my future scientific career, and I hope to ripple the favor you gave me to someone else who might need support with LEACHM in their project. That way, the LEACHM user community will even grow bigger and stronger. In the same respect, I would like to acknowledge Paolo Nasta, University of Naples Federico II, Italy, for his support towards modeling water and solute transport in the vadose zone using Hydrus.

I would also like to thank the management of the Johan Six and Soil resources laboratories ETH Zürich, particularly Roman Hüppi, Marco Griepentrog, and Matti Barthel, for analyzing all my gas samples.

Special thanks to the management of Budongo Conservation Field Station and the Walji Sugarcane Estate, Uganda, for hosting the two field experiments and providing me space to store the field equipment, consumables, and collected gas samples.

I am grateful to Ayo Brown Gerald and Adriko Moses for their unwavering commitment to successfully implementing all field activities. Your hard work and willingness to learn are reflected in the quality of the data we collected.

My colleagues: Raphael, Mario, Benjamin, Kathi, Pedro, Anna Stegmann, Ana Calorina, Florian, Tabea, and Alessandro, you have been terrific. I enjoyed all the moments we had at Unikum, especially the shared Pizza, Currywurst, and the ice-cold Helles after a hectic day at the office.

On a personal note, I would like to thank my Fiancée, Evelyn, for being extremely encouraging and patient and being deeply involved in my PhD as a grammatical checker and critical reviewer of all the proposals and manuscripts before I sent them out to my co-authors. Throughout this journey, the rule of thumb has been that if a piece of writing is clear for Evelyn, then it will be for those closest to my domain. Evelyn, thank you immensely for being that phenomenal support system during my PhD studies.

Finally, yet importantly, words cannot express how deeply grateful I am to my late mum, Ms. Erioth Matovu. I owe the zeal with which I have executed this PhD to the life lessons you taught me over the years. It is these lessons that have kept me going thus far. My brothers (Raymond and Julius) and sisters (Victoria, Diana, and Lillian), you guys have been fantastic throughout this journey. I hope this accomplishment inspires all of you to do more in life because you can.

Lastly, I would like to thank my children, Clarissa Nakanjako and Russell Tamale, for being a huge inspiration in my life. It is because of these two that I do not relent in my pursuit of success.

Dedication

This piece of work is dedicated to my late mum, two children (Clarissa and Russell), and to all the liked-minded humans who believe that the only way we can shield our dear kids from the adverse effects of the looming climate change catastrophe is to take formidable action now to address the ever-rising global temperatures.

Contribution of the author to the different peer-reviewed articles

Article I published.

Tamale, J., Hüppi, R., Griepentrog, M., Turyagyenda, L. F., Barthel, M., Doetterl, S., Fiener, P., and van Straaten, O. 2021. Nutrient limitations regulate soil greenhouse gas fluxes from tropical forests: evidence from an ecosystem-scale nutrient manipulation experiment in Uganda. *SOIL*, 7, 433–451.

Author contribution: Joseph Tamale and Oliver van Straaten conceptualized the study. Oliver van Straaten established the nutrient manipulation experiment. Joseph Tamale conducted the fieldwork, analyzed the data, and prepared the paper. Oliver van Straaten, Peter Fiener, and Sebastian Doetterl provided significant input on the experimental setup and data analysis. Roman Hüppi and Barthel Matti did the laboratory measurements and gave critical feedback on the paper. Oliver van Straaten, Peter Fiener, Sebastian Doetterl, Marco Griepentrog, and Laban Frank Turyagyenda critically reviewed and provided feedback on the paper

Article II published.

Tamale, J., van Straaten, O., Hüppi, R., Turyagyenda, L.F., Fiener, P. and Doetterl, S. 2022. Soil greenhouse gas fluxes following conversion of tropical forests to fertilizer-based sugarcane systems in north-western Uganda. *Agriculture, Ecosystems & Environment*, 333, p.107953.

Author contribution: Joseph Tamale, Sebastian Doetterl, Oliver van Straaten, and Peter Fiener conceptualized the study. Joseph Tamale did the soil GHG flux measurements, analyzed the data, and drafted the manuscript. Roman Hüppi, Laban Frank Turyagyenda, Sebastian Doetterl, Oliver van Straaten, and Peter Fiener reviewed and gave technical feedback on the manuscript.

Article III under review.

Tamale, J., Nasta, P., Hutson, J., van Straaten, O., Turyagyenda, L.F., Doetterl, D. and Fiener, F. 2023. Impact of urea fertilization rates on nitrogen dynamics, productivity, and profitability of Ugandan sugarcane plantations. Under review at *Soil Use and Management Journal* (SUM-2023-107)

Author contribution: Joseph Tamale, Sebastian Doetterl, Oliver van Straaten, and Peter Fiener conceptualized the study; Joseph Tamale did the nitrogen leaching and soil GHG flux measurements, analyzed the data, and drafted the manuscript; John Hutson, Paolo Nasta, Laban Frank Turyagyenda, Sebastian Doetterl, Oliver van Straaten, and Peter Fiener reviewed and gave technical feedback on the manuscript.

Table of Contents

Summary-----	iii
Zusammenfassung-----	vi
Acknowledgment-----	ix
Dedication-----	xi
Contribution of the author to the different peer-reviewed articles-----	xii
Table of Contents-----	xiii
List of figures-----	xvii
List of tables-----	xviii
List of appendices-----	xix
CHAPTER 1. GENERAL INTRODUCTION-----	1
1.1. Tropical forests and their role in global climate system regulation-----	2
1.2. Nutrient controls on soil greenhouse gas fluxes under humid tropical forests-----	3
1.3. Tropical deforestation: History and extent-----	6
1.4. Bittersweet: Emergence of the sugarcane sector at the expense of tropical forests-----	6
1.5. Forest conversion to cropland and global greenhouse gas flux budgets-----	8
1.6. Nitrogen and carbon dynamics under sugarcane plantations-----	9
1.7. Aims and structure of the thesis-----	13
1.8. PhD conceptual flow diagram-----	15
CHAPTER 2. NUTRIENT LIMITATIONS REGULATE SOIL GREENHOUSE GAS FLUXES FROM TROPICAL FORESTS: EVIDENCE FROM AN ECOSYSTEM-SCALE NUTRIENT MANIPULATION EXPERIMENT IN UGANDA-----	16
2.1. Abstract-----	17
2.2. Introduction-----	18

2.3. Materials and methods -----	21
2.3.1. Study site description -----	21
2.3.2. Experimental design-----	21
2.3.3. Baseline soil physico-chemical characterization-----	22
2.3.4. Soil greenhouse gas fluxes and soil environmental control measurements -----	22
2.3.5. Statistical analysis -----	27
2.4. Results-----	28
2.4.1. Soil physico-chemical characteristics, water-filled pore space, soil temperature, and nitrates -----	28
2.4.2. Soil CO ₂ fluxes -----	29
2.4.3. Soil CH ₄ fluxes -----	31
2.4.4. Soil N ₂ O fluxes -----	31
2.5. Discussion -----	33
2.5.1. Effect of nitrogen and phosphorus addition and soil environmental controls on soil CO ₂ fluxes-----	33
2.5.2. Effect of nitrogen and phosphorus addition and soil environmental controls on soil CH ₄ fluxes-----	37
2.5.3. Effect of nitrogen and phosphorus addition and soil environmental controls on soil N ₂ O fluxes-----	38
2.6. Conclusion-----	40
 CHAPTER 3. SOIL GREENHOUSE GAS FLUXES FOLLOWING CONVERSION OF TROPICAL FORESTS TO FERTILIZER-BASED SUGARCANE SYSTEMS IN NORTH-WESTERN UGANDA -----	 41
3.1. Abstract -----	42
3.2. Introduction-----	43
3.3. Materials and methods -----	45
3.3.1. Study area-----	45
3.3.2. Experimental design-----	45
3.3.3. Soil sampling and analysis -----	46
3.3.4. Aboveground and belowground biomass determination-----	47
3.3.5. Soil greenhouse gas flux measurements, auxiliary measurements, flux calculation, and soil greenhouse gas flux budget estimation -----	48

3.3.6. Statistical analysis -----	49
3.4. Results-----	50
3.4. 1. Auxiliary controls and soil greenhouse gas fluxes -----	50
3.4.2. Carbon stocks in biomass and soil -----	55
3.5. Discussion -----	55
3.5.1. Soil greenhouse gas flux dynamics in the reference forest and sugarcane plantations -----	55
3.6. Conclusion-----	59
 CHAPTER 4. IMPACT OF UREA FERTILIZATION RATES ON NITROGEN DYNAMICS, PRODUCTIVITY, AND PROFITABILITY FROM UGANDAN SUGARCANE PLANTATIONS-----	61
4.1. Abstract -----	62
4.2. Introduction-----	63
4.3. Materials and methods -----	65
4.3.1. Study area description and available datasets -----	65
4.3.2. Experimental design-----	66
4.3.3. Soil sampling-----	68
4.3.4. Nitrogen leaching estimation -----	68
4.3.4.1. Soil pore water sampling and nitrate concentration measurements -----	68
4.3.4.3. Soil water drainage flux modeling and nitrogen leaching loss estimation -----	69
4.3.5. Soil nitrous oxide flux measurements -----	71
4.3.6. Field fresh weight, crop nitrogen uptake, and soil nitrogen balance -----	72
4.3.7. Partial factor productivity and return on investment -----	73
4.3.8. Statistical analysis -----	73
4.3.9. Description of the methodology -----	73
4.4. Results-----	75
4.4.1. Soil nitrogen dynamics at increasing nitrogen fertilization rates -----	75
4.4.1.1. Estimation of the soil water retention and hydraulic conductivity function ---	75
4.4.1.2. Nitrogen leaching flux, soil nitrous oxide emissions, plant nitrogen uptake, and nitrogen balance -----	78
4.4.1.3. Productivity and profitability of sugarcane cultivation at increasing nitrogen rates-----	79

4.5. Discussion	82
4.5.1. Performance of pedotransfer functions in the estimation of the soil hydraulic properties of Ferralsols	82
4.5.2. Effect of increasing urea fertilization rates on nitrogen dynamics, productivity, and profitability of sugarcane	83
4.6. Conclusion	85
CHAPTER 5. SYNTHESIS	87
5.1. Main findings	88
5.2. How different are tropical forests from high-latitude forests in their soil greenhouse gas flux response to changes in nutrient dynamics?	90
5.3. How will increasing nitrogen and phosphorus deposition rates over the tropics affect tropical forest soil greenhouse gas fluxes?	92
5.4. How does forest-sugarcane conversion drive global change?	92
5.5. Implications for nutrient management under sugarcane	94
5.6. General conclusion and outlook	95
REFERENCES	97
APPENDIX	141
DECLARATION OF ORIGINALITY AND CERTIFICATE OF OWNERSHIP	xxvi
ABOUT THE AUTHOR	xxvii
Curriculum Vitae: Joseph Tamale	xxvii

List of figures

Figure 1.1. PhD conceptual flow diagram.-----	15
Figure 2.1. Pooled vs non-pooled gas sampling approach. -----	24
Figure 2.2. Spatial dynamics of proximal controls for soil GHG fluxes in the forest. -----	30
Figure 2.3. Seasonality of proximal controls and climatic variables in the forest. -----	32
Figure 2.4. Seasonality of soil GHG fluxes in the forest. -----	34
Figure 2.5. Spatial dynamics of soil GHG fluxes in the forest. -----	35
Figure 2.6. Macronutrient limitations on soil respiration sources in the forest. -----	36
Figure 2.7. Spearman correlation between soil GHG fluxes and proximal controls. -----	39
Figure 3.1. Seasonality of proximal controls for GHG fluxes under forest and sugarcane. ---	52
Figure 3.2. Soil GHG fluxes under forest and sugarcane. -----	53
Figure 3.3. Carbon stocks under forest and sugarcane.-----	56
Figure 4.1. Geographical location of study sites in Uganda. -----	67
Figure 4.2. Schematics of the surface and bottom boundary conditions under sugarcane. ----	72
Figure 4.3. Flow chart of the methodology underpinning the sugarcane study.-----	74
Figure 4.4. Performance of pedotransfer functions. -----	77
Figure 4.5. Nitrogen dynamics under sugarcane. -----	79
Figure 4.6. Temporal dynamics of nitrogen leaching under sugarcane. -----	80
Figure 4.7. Productivity and profitability under sugarcane. -----	81
Figure 5.1. Impact of forest conversion to sugarcane on the carbon balance. -----	94

List of tables

Table 2.1. Soil physico-chemical properties under forest.-----	28
Table 2.2. Macronutrient limitation on forest soil GHG fluxes.-----	33
Table 3.1. Seasonality of proximal controls under sugarcane and forest.-----	51
Table 3.2. Spearman correlation between soil GHG fluxes and proximal controls.-----	54
Table 3.3. Annual soil GHG fluxes from the forest and sugarcane plantations.-----	55
Table 4.1. Basic soil physical and chemical properties under sugarcane.-----	68
Table 4.2. Soil hydraulic parameters estimated with pedotransfer functions.-----	75
Table 4.3. Soil water balance components derived with pedotransfer functions.-----	76

List of appendices

Appendix F.1. Soil N ₂ O fluxes from sugarcane. -----	141
Appendix F.2. Soil water retention curves for sugarcane soils.-----	142
Appendix F.3. Soil hydraulic conductivity curve for sugarcane soils.-----	143
Appendix F.4. Soil water balance components. -----	144
Appendix F.5. Temporal dynamics of predicted matric potential. -----	145
Appendix T.1. Site-specific topographic, geological, soil and climatic characteristics. -----	145
Appendix T.2. Soil physico-chemical characteristics under forest and sugarcane. -----	146
Appendix T.3. Estimation of parameters of the van Genuchten (1980) equation. -----	146
Appendix T.4. Tabulated regression coefficients for predicting soil water content. -----	147
Appendix T.5. Tabulated regression coefficients for estimating water retention function.--	148

CHAPTER 1. GENERAL INTRODUCTION

1.1. Tropical forests and their role in global climate system regulation

The global climate system primarily revolves around the redistribution of incoming solar radiation as well as the exchange of both matter and energy between the Earth's surface and atmosphere, for which tropical forests play a dominant role (Spracklen *et al.*, 2012; Lawrence & Vandecar, 2015; Devaraju *et al.*, 2015). Like all other forest biomes, tropical forests emit biogenic volatile organic compounds necessary for producing secondary organic aerosols that facilitate cloud formation (Artaxo *et al.*, 2013). More importantly, once in the atmosphere, the secondary organic aerosols scatter solar radiation and enhance cloud albedo leading to additional biophysical cooling and increased carbon (C) uptake by the vegetation (Artaxo *et al.*, 2013).

In addition, tropical forests not only store significant amounts of C in their vegetation (about 360 Pg C) and soils (about 800 Pg C; Pan *et al.*, 2013) but also annually sequester appreciable amounts of carbon dioxide (CO₂) emissions via photosynthesis (about 15.6 Pg C; Friedlingstein *et al.*, 2019). Furthermore, soils under tropical forest biomes predominantly have high C turnover rates (Raich & Schlesinger, 1992). Hence, the shift in the balance between net primary productivity and soil respiration in tropical forests largely dominates the reported inter-annual variability in the global atmospheric CO₂ concentrations (Wang *et al.*, 2014b).

Besides the tropical forests' role in the exchange of CO₂ in the soil-plant-atmospheric continuum, they also sequester and/or emit significant amounts of nitrous oxide (N₂O; Werner *et al.*, 2007) and methane (CH₄; Dutaur & Verchot, 2007). It is estimated that 1.1 to 1.3 Tg N₂O (Stehfest & Bouwman, 2006; Butterbach-Bahl *et al.*, 2013) and 20 to 45 Tg CH₄-C (Schlesinger & Bernhardt, 2013) are emitted and sequestered annually by tropical forest soils accounting for 25 and 27% of the global N₂O emissions (Butterbach-Bahl *et al.*, 2004a) and CH₄ uptake (Dutaur & Verchot, 2007), respectively. Emerging evidence further indicates that woody tree trunks in tropical forests act as conduits for N₂O and CH₄ from soil to the atmosphere (Saunio *et al.*, 2016; Welch *et al.*, 2019). Hence, tropical forests are widely recognized as strong sinks and sources of all three biogenic climate-relevant greenhouse gases (GHGs). The drawback, however, is that the estimated GHG sink and source potential of tropical forests is based on sparse and unevenly distributed GHG measurements across the tropics (Don *et al.*, 2011; Powers *et al.*, 2011), which introduces significant uncertainties in global GHG budgets (Welch *et al.*, 2019).

1.2. Nutrient controls on soil greenhouse gas fluxes under humid tropical forests

Over the past decades, Ecologists have been keenly interested in understanding the primary controls of GHGs in tropical forest biomes (Smith, 1990; Malhi & Grace, 2000; Verchot *et al.*, 2020). This has been in light of the increasing atmospheric concentrations of the respective GHGs (CO₂ (47.3%; 409.9 ± 0.4 ppm), CH₄ (156%; 1866.3 ± 3.3 ppb), and N₂O (23%, 332.1 ± 0.4 ppb)) above their respective preindustrial levels (IPCC, 2021), underscored by heightened ambitions to limit the increase in the global mean- temperature to 1.5 °C (UNFCCC, 2015).

Decades of this ecological research indicate that besides soil temperature (Conant *et al.*, 2011; Wanyama *et al.*, 2019; Tchiofo Lontsi *et al.*, 2020) and soil moisture (Oertel *et al.*, 2016), macronutrient availability (especially nitrogen (N) and phosphorus (P)) equally exerts a crucial control on soil GHG fluxes from tropical forests (Müller *et al.*, 2015; Bréchet *et al.*, 2019). However, this assertion is highly debatable, since nearly all the evidence available so far on macronutrient regulation of GHGs in tropical forests is based on nutrient manipulation experiment studies premised in Southeast Asian (Feng & Zhu, 2019; Lu *et al.*, 2021) and Latin American tropical forests (Kaspari *et al.*, 2007; Fanin *et al.*, 2015; Bréchet *et al.*, 2019). African tropical forests remain largely understudied. To date, only one NME study has been conducted in the African tropical forests (Newbery *et al.*, 2002), despite the recognition that these biomes represent a significant proportion of the global forest cover (33%; Saatchi *et al.*, 2011). Furthermore, recent studies by Barkley *et al.* (2019) and Bauters *et al.* (2019) highlight significant N and P deposition rates over the African humid tropics. Hence, it remains unclear how the externally supplied N and P may affect GHG fluxes from African tropical forests, let alone their contribution to the global C and N budgets.

Nonetheless, evidence from NMEs premised in Latin American and Southeast Asian tropical forests indicate that adding N to these ecosystems triggers mixed soil respiration responses. For instance, N addition to tropical montane forest floors increased soil respiration (Hobbie & Vitousek, 2000; Wu *et al.*, 2022 p. 202), attributed to lifting the N limitation on microbial litter decomposition (Tanner *et al.*, 1992; Koehler *et al.*, 2009a). However, in the case of N-rich lowland tropical forests, either a reduction in soil respiration (Mo *et al.*, 2008) or no effect on soil CO₂ effluxes was reported (Cleveland *et al.*, 2006; Koehler *et al.*, 2009a; Barantal *et al.*, 2012). The counteracting responses in soil respiration following N addition in N-rich lowland tropical forests either suggest a concomitant reduction in microbial and fine root biomass (Mo *et al.*, 2008) or resilience of soil respiration components in these biomes to any N-induced changes in the soil biochemical characteristics (Koehler *et al.*, 2009a).

With respect to soil CH₄ fluxes, evidence of the effect of N addition on methanotrophic (obligate aerobes) or methanogenic (obligate anaerobes) activity in tropical forest floor soils is similarly inconclusive. We particularly lack a consensus on whether the expected increases in soil N availability in tropical forests (due to N deposition) would increase or decrease their soil CH₄ uptake. This is exemplified by some studies (Zhang *et al.*, 2008b; Li *et al.*, 2021) aligning with findings of temperate forest NMEs where N addition inhibited methanotrophic CH₄ oxidation (Steudler *et al.*, 1989; Brumme & Borken, 1999). Usually, the inhibition is a result of ammonium (NH₄⁺) ions from the added fertilizer competing for the reactive sites on CH₄ monooxygenase (the enzyme that initiates the CH₄ oxidation pathway), reducing the uptake of CH₄ by the enzyme (Bédard & Knowles, 1989). In contrast, some studies have reported a significant increase in CH₄ consumption following the addition of N to tropical forests (Veldkamp *et al.*, 2013; Matson *et al.*, 2017; Martinson *et al.*, 2021). Authors attribute the increase in CH₄ consumption to the likely switch by methanotrophs from the energy-demanding molecular N fixation to mineral N assimilation, thereby elevating their activity (Bodelier & Laanbroek, 2004).

Unlike in the case of soil respiration and CH₄ uptake, there is seemingly a consensus that adding N to the N-rich tropical forests results in increased soil N₂O emissions. This is because tropical forests have a leaky N cycle, given their large N cycling rates (Koehler *et al.*, 2009b); hence, any additional input of N immediately exceeds the plant and microbial N demand leaving excess to be denitrified/nitrified (Hall & Matson, 1999; Corre *et al.*, 2014 p. 201; Zheng *et al.*, 2016b).

Besides N, P availability has also been shown to have varying effects on the exchange of the three biogenic GHGs at the soil-atmospheric interface of the tropical forest understory. Tropical forests are known to exhibit a conservative P cycle due to the complexation of P with pedogenic oxides (iron and aluminum) and low weatherable minerals (kaolinites) (Hedin *et al.*, 2003) compared to their temperate forest counterparts growing on young soils and with higher P availability (Vitousek, 1984). Hence, lifting P-limitation on microbes in tropical forests increases soil respiration (Hobbie & Vitousek, 2000; Cleveland & Townsend, 2006; Kaspari *et al.*, 2007) by concomitantly stimulating litter and organic matter decomposition (Cleveland & Townsend, 2006). Counterintuitively, there is also evidence that P addition to the wetter tropical forest soils does not affect the mass loss rate during decomposition (Fanin *et al.*, 2016). In wetter tropical environments, dissolved organic matter is increasingly leached from the litter and transported to underlying mineral soil (Cleveland *et al.*, 2006), reducing the C substrate for microbial de-

composition (Cleveland *et al.*, 2006). Nonetheless, such inconsistencies among studies highlight our incomplete understanding of the P limitation on soil respiration and the uncertainty in predicting the future tropical C cycle response to changes in nutrient availability.

Nonetheless, P addition is thought to have both a direct and an indirect control on CH₄ uptake in tropical forest soils. Directly, P availability increases CH₄ uptake by significantly increasing microbial biomass (Liu *et al.*, 2012). However, some soil ecologists think this effect is usually exaggerated since methane-oxidizing bacteria only form a small proportion of the total soil microbial biomass (Zhang *et al.*, 2011). Indirectly, P availability increases soil pH and stimulates plant-root water uptake resulting in increased oxygen diffusivity and availability at the CH₄ oxidation sites in the soil (Zhang *et al.*, 2011).

Arguably, the effect of P on soil N₂O fluxes from the tropics is by far the most highly contested. Up until now, evidence of P limitation on soil N₂O fluxes has been largely based on either tropical plantations (Mori *et al.*, 2010; Zhang *et al.*, 2014) or secondary forests (Wang *et al.*, 2014a), and only a handful of these studies were conducted in old-growth (sub) tropical forests. Hence, an inhibition effect of P on soil denitrification and nitrification processes has been reported (Mori *et al.*, 2010; Zhang *et al.*, 2014), which is presumably a result of the stimulated increase in plant N uptake and microbial N immobilization upon P addition (Mori *et al.*, 2010). However, for the old-growth tropical forests, lifting the P limitation on (de) nitrifiers did not affect soil N₂O fluxes (Zheng *et al.*, 2016b).

Notably, it is becoming apparent that some microbial processes that produce and consume GHGs in tropical soils could be co-limited by the availability of both N and P (N + P), though just a handful of previous studies have evaluated this possibility. Nonetheless, Zheng *et al.* (2016) measured significantly higher N₂O emissions from N addition plots in comparison to the N+P treatment plots, whose soil N₂O emissions were not any different from the control plots. Here, the expected increase in N₂O emissions after N addition was likely to be counter-balanced by the alleviation of the P limitation on both the plants and soil microbes, resulting in increased plant N uptake and microbial N immobilization. Consequently, soil available N for the (de) nitrifiers was reduced and so were the soil N₂O emissions (Sundareshwar *et al.*, 2003). For CH₄ uptake, Gao *et al.* (2017) found a lower CH₄ consumption in N+P plots compared to when N or P were applied alone, suggesting an additive inhibition effect of N+P on soil methanotrophs in the Chinese mixed subtropical forest. Furthermore, soil respiration in the French Guiana tropical forest NME was significantly higher for N + P addition plots than either N or

P addition plots (Bréchet *et al.*, 2019), alluding to a positive impact of the combined effect of N and P on faunal and litter decomposers (Fanin *et al.*, 2016).

1.3. Tropical deforestation: History and extent

Besides the increasing enrichment of the humid tropics with N and P via wet deposition (Bauters *et al.*, 2019; Barkley *et al.*, 2019), ecosystem functions derived from tropical forests are equally threatened by (non) selective logging (Tchiofo Lontsi *et al.*, 2020) and the widespread conversion of these forests to other land uses (Verchot *et al.*, 2020). Human modification of tropical forest landscapes dates back to the late Pleistocene and early Holocene when megafauna in different tropical regions became extinct due to hunting by the *Homo sapiens* (Koch & Barnosky, 2006). However, it is the early Anthropocene that ushered in a myriad of pervasive conversion of tropical forests to agriculture, human settlement, logging, fragmentation, defaunation, and wildfires (Malhi *et al.*, 2014), which increased through the 19th century, reaching an apparent global peak in the 20th century (Geist & Lambin, 2002).

According to the FAO (1993), tropical forests occupied nearly 1756 million hectares (M ha) in the 1990s, distributed among lowland evergreen humid tropical forests (718 M ha), moist deciduous forests (587 M ha), dry deciduous forests (238 M ha), and montane forests (204 M ha). This expanse of tropical forests was mainly concentrated in Latin America (52%; 9178 M ha), Africa (30%; 526 M ha), and South East Asia (18%; 311 M ha; FAO, 1993). Fast forward to 2020, nearly 378 M ha of tropical forests have been lost to deforestation over the last three decades (1990-2020), representing more than 90% of global forest loss (FAO, 2020). The net loss in tropical forest cover was mainly in Africa and Latin America, with an estimated annual forest loss rate of 3.9 and 2.6 M ha, respectively. In stark contrast to Africa and Latin America, Asia registered a net gain in forest cover over the same period, which was even much higher than the respective net forest gains in Oceania and Europe due to Asia's reforestation and natural forest regeneration policies (FAO, 2020). Unfortunately, recent projections indicate that tropical forest loss in Africa will only increase in the coming decades (Hansen *et al.*, 2013) since it is home to the fastest growing yet poorest population in the world, expected to reach 4.2 billion people by the end of the 21st century (Gerland *et al.*, 2014).

1.4. Bittersweet: Emergence of the sugarcane sector at the expense of tropical forests

Sugarcane (*Saccharum officinarum*) is a semi-perennial and highly productive C4 grass originating from Asia, probably New Guinea (Daniels & Daniels, 1993; de Matos *et al.*, 2020) and currently endemic to nearly all hot tropical and subtropical regions of the world (Leff *et al.*,

2004; de Matos *et al.*, 2020). For centuries, sugarcane was mainly used for the production of crystal sugar globally (de Matos *et al.*, 2020), until the 1970s, when the world experienced the first global oil crisis forcing leading sugarcane producers like Brazil to also use sugarcane as a feedstock for ethanol production to reduce the dependency on fossil fuels (Hira & de Oliveira, 2009). Consequently, sugarcane is now widely recognized as a high-value agricultural crop given its contribution to the creation of both direct and indirect jobs in sub (tropical) countries (Australia; Wei *et al.*, 2022, Brazil; Deuss, 2012, India; Solomon, 2014, Pakistan; Usman, 2016) as well as significantly driving their economies (Satolo & Bacchi, 2013; Solomon, 2016 p. 2).

Sugarcane is currently grown on 26.5 M ha of arable land worldwide (Leff *et al.*, 2004) of which 70% of this land area is distributed among the top four world producers of sugarcane (Brazil, India, China, and Thailand) and the remaining 30% distributed among other sugarcane producers like Australia and Africa (de Matos *et al.*, 2020). However, in most of these countries, the land currently under sugarcane cultivation was created through widespread deforestation, with the initial forest clearing happening as early as the 1600s in the case of Caribbean islands (Griggs, 2007) and Brazil (de Matos *et al.*, 2020) and as early as the 1800s in the case of Australia (Griggs, 2007). Interestingly, historical records on the initial widespread deforestation for sugarcane remain scarce, probably because most of this land use shift happened 200-400 years ago (Griggs, 2007; Obidzinski *et al.*, 2015; de Matos *et al.*, 2020). Consequently, over time, the scientific discourse has shifted from the greatest environmental catastrophe that the emergence of the sugarcane sector was to how this sector can be expanded further to meet the growing demand for low-C biofuels as a replacement for C-packed fossil fuels (Altpeter & Oraby, 2010; Antunes *et al.*, 2019; Silveira & Khatiwada, 2019).

Nonetheless, what remains unresolved, is whether this expansion would not reverse the carbon-saving benefits derived from biofuels through accelerated deforestation in sugarcane growing frontiers across the world (Fargione *et al.*, 2008). Available evidence so far on the sustainability of the biofuel industry in leading countries like Brazil indicates that sugarcane expansion for biofuel will either have a negligible to no effect on existing forest cover (Sparovek *et al.*, 2009; Bordonal *et al.*, 2018; Hernandez *et al.*, 2022) or at worst indirectly drive deforestation (Lapola *et al.*, 2010; Jusys, 2017).

However, in the case of Africa, several studies indicate the contrary. Here, the sugarcane sector has been expanding (Jolly, 2012; Kalinda & Chisanga, 2014; Hess *et al.*, 2016) and will continue to do so at the expense of tropical forests (Gibbs *et al.*, 2010). This is because there is a

high demand for sugar by the continent's rapidly growing population (de Matos *et al.*, 2020) and an increased embracement of sugarcane biofuel as an environmentally friendly and low-carbon renewable energy source (Gasparatos *et al.*, 2015). Additionally, many African governments view the scaling up of sugarcane production as a viable route to resolving the problem of youth unemployment through the creation of new jobs (Amigun *et al.*, 2008, 2011; Pradhana & Mbohwa, 2014), and the Ugandan government is no exception (Mwavu & Witkowski, 2008; Zommers *et al.*, 2012). Forestland giveaways in Uganda represent the main incentive through which the government attracts foreign investment into the country's sugarcane sector. For instance, in 2006, the Ugandan government attempted to give away a huge portion of Mabira Forest Reserve to the Sugar Corporation of Uganda Limited, but the move was meted with wide condemnation from the civil society as well as deadly strikes across the country (Zommers *et al.*, 2012). These deterrents, however, were only short lived since in 2016, the Ugandan government through the National Environmental Management Authority and Uganda Land Commission, approved the conversion of 55,788 ha of Bugoma Forest to sugarcane growing (<https://ecotrust.or.ug/the-campaign-to-save-bugoma-forest/>). Evidently, the Ugandan population as well as the world will undoubtedly continue to enjoy a sugary cup of tea blended with a bitter spice of environmental implications that underpin the sugar production process.

1.5. Forest conversion to cropland and global greenhouse gas flux budgets

The conversion of tropical forests to other land uses (mainly cropland and pastures), and their degradation through nonselective logging remains the second most important driver of global climate change after fossil fuel combustion (Malhi & Grace, 2000). It is estimated that about 1.4 Pg C is released annually into the atmosphere from tropical forest clearing and biomass burning (Houghton, 2013). Upon conversion, both top- and subsoil dynamic properties (particularly bulk density, base saturation, effective cation exchange capacity, soil C: N, and soil pH) under formerly forested areas profoundly change, predisposing the large vulnerable SOC stocks to microbial degradation both in the short and long-term (Malhi *et al.*, 1999; Don *et al.*, 2011; Veldkamp *et al.*, 2020). Several studies suggest that about 18- 50% of the forest SOC stocks is lost within the first 25 years of forest conversion (Don *et al.*, 2011; Powers *et al.*, 2011), and these losses continue until the SOC stocks under cropland reach a new equilibrium (25-100 years; Hombegowda *et al.*, 2016). Overall, 50 Pg C of SOC has been lost to tropical deforestation since the onset of agriculture, accounting for nearly 37% of the net global SOC losses (133 Pg C; Sanderman *et al.*, 2017).

While CO₂ remains the dominant GHG released by tropical forest conversion, fluxes of both CH₄ and N₂O are equally affected by this land use shift (Saunois *et al.*, 2016; Verchot *et al.*, 2020). Tropical forests exhibit higher N₂O flux rates (about 1.2 kg N ha⁻¹ yr⁻¹; Werner *et al.*, 2007) relative to the converted cropland. However, soil N₂O emissions from the newly established croplands often significantly surpass background forest N₂O emissions shortly after forest conversion due to the deposition of nutrient-rich ashes from biomass burning (van Lent *et al.*, 2015). Sometimes, the flush of N₂O emissions in the newly established croplands may last several years before falling below the background forest N₂O flux rates (Verchot *et al.*, 1999). Conversely, croplands generally have weaker sinks of CH₄ compared to tropical forests (Verchot *et al.*, 2020), but forest-cropland paired site measurements are still rare in the tropics. Comparable studies premised in Northern European forests and croplands reported a 60% reduction in CH₄ uptake for the cropland relative to forests (Dobbie *et al.*, 1996), reflecting the negative impacts of land use change on methanotrophic activity (Tate, 2015).

1.6. Nitrogen and carbon dynamics under sugarcane plantations

The alteration in the biogeochemical nutrient cycling upon forest conversion to cropland, together with the associated decline in soil fertility, especially related to the concomitant reduction in soil pH, soil C and N stocks, exchangeable bases, and cation exchange capacity (CEC) in the newly established crop fields (Veldkamp *et al.*, 2020), makes application of synthetic fertilizers inevitable to sustain high yields. In sugarcane, large doses of synthetic inorganic N fertilizers (between 60 and 755 kg N ha⁻¹) are applied to the fields every growing cycle to sustain production, which together with the hot humid tropical climate and deeply weathered tropical soils, predisposes sugarcane plantations to large N losses (Robinson *et al.*, 2011). N losses under sugarcane can account for as high as 60% of the applied N fertilizers (Chapman *et al.*, 1994), leaving only about 40% available for uptake by the sugarcane crop (Meyer *et al.*, 2007; Kingston *et al.*, 2008; Franco *et al.*, 2011).

Firstly, ammonia volatilization represents one of the pathways through which N is lost from fertilized sugarcane plantations (da Silva Paredes *et al.*, 2014; Otto *et al.*, 2017; Pinheiro *et al.*, 2018) and accounts for nearly 10-40% of the added N fertilizers (Cantarella *et al.*, 2008; Faria *et al.*, 2013). Therefore, it is highest in conventional systems where crop residues are left standing on the field after harvest, creating a thick mulch barrier that prevents incorporating the added N fertilizers into the soil, thereby predisposing the fertilizers to ammonia volatilization (Pinheiro *et al.*, 2018). Hence, in such systems, the use of urease inhibitors or slow-releasing N fertilizers (Otto *et al.*, 2017), straw removal (Pinheiro *et al.*, 2018), and subsurface application

of N fertilizers (Prasertsak *et al.*, 2002) are highly recommended to mitigate ammonia volatilization.

Secondly, N is lost via nitrate (NO_3^-) leaching (Hartemink, 2008; Armour *et al.*, 2013; Otto *et al.*, 2016). However, N leaching budgets under sugarcane remain incredibly challenging to constrain due to differences in N fertilizer application rates, soil types, and climatic settings among studies. Consequently, the current literature is filled with large variabilities with some studies reporting low N leaching rates ($0.38\text{-}2.9 \text{ kg N ha}^{-1}$; de los A. Portocarrero & Acreche, 2013; Stewart *et al.*, 2006) while others reporting high N leaching rates ($9.2\text{-}34 \text{ kg N ha}^{-1}$; Armour *et al.*, 2013; Ghiberto *et al.*, 2009, 2015). Additionally, N leaching budgets still suffer from a geographical bias since the majority of the studies were premised in sugarcane fields in Australia (Armour *et al.*, 2013), Brazil (Blum *et al.*, 2013), Japan (Okamoto *et al.*, 2021), and United States (Xu *et al.*, 2022) and only a few studies were conducted in sub-Saharan Africa (Shishaye, 2015). This is mainly because sub-Saharan Africa, like many sites across the tropics, lacks information on soil hydraulic properties, primarily the soil water retention function and hydraulic conductivity function (Gupta *et al.*, 2022). Yet, this information is mandatory for predicting the downward movement of NO_3^- in the vadose zone (Jarvis *et al.*, 1991; Gupta *et al.*, 2022).

Soil water retention function describes the relationship between soil water content (θ) and matric potential (h ; Brooks & Corey, 1964; van Genuchten, 1980) and is influenced by soil texture, SOM, and soil structure (Tuller & Or, 2005) while hydraulic conductivity function describes water flow behavior in soil (Hao *et al.*, 2019) and is influenced by pore size distribution and pore connectivity (Chapuis, 2012). Conventionally, soil water retention function is determined directly in the field or laboratory based on flow experiments (Wolfgang & Kai, 2006) in which a series of discrete data points (representing the $\theta(h)$ relationship) are generated and fit to the desired soil water retention function model (e.g., van Genuchten (1980)). Hydraulic conductivity function is then estimated from soil water retention function provided the saturated hydraulic conductivity, K_s , is known (Peters & Durner, 2008). However, flow experiments are time-consuming, laborious, and expensive as they require many soil samples to overcome the inherent spatial and temporal variability in hydraulic properties (Wösten *et al.*, 2001; Patil & Singh, 2016). Additionally, taking numerous direct measurements of soil hydraulic properties at a large scale is impractical due to the size and complexity of the terrestrial systems (Vereecken *et al.*, 2010). Hence, indirect but cheaper soil water retention function and hydraulic conductivity function estimation methods are widely preferred and have gained significant traction in the

past decades (Wösten *et al.*, 2001; Vereecken *et al.*, 2010; Patil & Singh, 2016). Indirect methods entail applying pedotransfer functions (PTFs) to estimate soil hydraulic properties from easy-to-measure and readily available soil physicochemical data (grain size distribution, SOC, and bulk density; Nasta *et al.*, 2021; Pachepsky *et al.*, 2006; Shein & Arkhangel'skaya, 2006). Hence, PTFs, through empirical functional relationships, help translate basic soil survey information to broader practical applications, which would instead be untenable with direct measurements (Wagenet *et al.*, 1991).

Nonetheless, using PTFs is not without drawbacks (Wösten *et al.*, 2001; Pachepsky & van Genuchten, 2011). First, PTF-derived soil water retention function and hydraulic conductivity function estimates suffer from innate but rarely communicated differences among soil laboratories regarding how soil samples for textural analysis were processed (pre-treatment and dispersions); let alone, the techniques used to quantify the grain size classes (sedimentation or laser techniques) (Pachepsky & van Genuchten, 2011). These differences are important for iron rich Ferralsols whose aggregates tend to be very stable and resistant to dispersion leading to discrepancies between labs and the performance of PTFs for what would otherwise be identical soil sample sets. Second, PTFs assume that particle size classes used in estimating the soil water retention function and hydraulic conductivity function are similar to those used to develop the PTFs. However, this is not always the case since the definition of particle or grain size classes can widely differ from country to country. For instance, the USDA/FAO textural classification system defines the silt fraction diameter to be 2-50 μm while the Australian textural system defines the silt fraction diameter as 2-20 μm , presenting an immediate challenge to the adoption of PTFs (Minasny & McBratney, 2001). Third, PTFs are site and/ or region-specific (Vereecken *et al.*, 2010; Patil & Singh, 2016). Hence, applying them outside their training and validation geographical confines often results in a poor estimate of the soil hydraulic properties (Wösten *et al.*, 2001; Vereecken *et al.*, 2010). Notwithstanding, a few studies have reported the contrary. For instance, Hungarian Plain soil water retention PTFs were successfully applied to Caucasian Piedmont Plain soils suggesting that some PTFs can be robust (Pachepsky & van Genuchten, 2011). Surprisingly, despite this evidence, no studies have to date been carried out to evaluate the possibility of applying the widely used European and North American PTFs (e.g., McBratney *et al.*, 2011; Schaap & Leij, 1998; Wösten *et al.*, 1999) to test sites in sub-Saharan Africa which currently has a deficit of region-specific PTFs.

Thirdly, heavy N fertilization above the plant and microbial N needs increases N_2O -N losses (de Oliveira *et al.*, 2013; Wang *et al.*, 2016). Indeed, different studies conducted in Australian

(Weier, 1998; Denmead *et al.*, 2010), American (Cai *et al.*, 2013; Dattamudi *et al.*, 2019), and Brazilian sugarcane plantations (Macedo *et al.*, 2008; Carmo *et al.*, 2013) reported variable soil N₂O emission losses in the range of 0.3 and 45 kg N₂O-N ha⁻¹ due to the usage of N fertilizers. Two factors explain why N₂O emissions under sugarcane are highly variable. (1) The type of N fertilizers used (Dattamudi *et al.*, 2019). Farmers mainly apply urea and ammonia-based fertilizers to their sugarcane fields, with the former supplying NH₄⁺ and NO₃⁻ ions and the latter providing only NH₄⁺ ions (Faustino *et al.*, 2015). The ion species released by the fertilizer accelerate or slow down N₂O production in soil (Dattamudi *et al.*, 2019; de Carvalho *et al.*, 2021), which according to several accounts, is dominated by denitrification (Butterbach-Bahl *et al.*, 2013). Hence, numerous studies have shown a considerable increase in N₂O emissions after applying urea fertilizers because urea elevates soil NO₃⁻ concentrations—an essential precursor to denitrification (Dattamudi *et al.*, 2019; de Carvalho *et al.*, 2021). Conversely, the denitrification process is slowed down after applying ammonium-based fertilizers because the released NH₄⁺ ions from the fertilizer must first be converted to NO₃⁻ ions before N₂O is produced (Rahman & Forrester, 2021). (2) Management practices that conserve soil moisture—the second important direct control of N₂O production, given its role in regulating oxygen concentrations for the microbes (Butterbach-Bahl *et al.*, 2013). Until recently, sugarcane plantations were burned before harvest (De Figueiredo & La Scala, 2011; Chalco Vera *et al.*, 2017), but this is increasingly being replaced with green cane harvesting (GCH), involving leaving crop residues on the field after harvest (Carmo *et al.*, 2013). Despite the GCH system improving soil ecosystem functioning (Satiro *et al.*, 2017; Cherubin *et al.*, 2018), it also amplifies N₂O emissions (Yang *et al.*, 2021) by increasing water-filled pore space (Pinheiro *et al.*, 2019) and mineralization of labile N from the retained crop residues (Pugesgaard *et al.*, 2017; Kravchenko *et al.*, 2017). Notwithstanding, year-round measurements of soil N₂O emissions in the variably managed sugarcane systems are, in general, limited, creating a gap in our understanding of the sugarcane N budgets.

Similarly, N fertilization, crop residue management, and agronomic practices affect the exchange of C in the soil-crop-atmospheric continuum of sugarcane systems (Flores-Jiménez *et al.*, 2019; Gonzaga *et al.*, 2019). Residue retention on the fields and reduced or no tillage practices enhance long-term soil C sequestration under sugarcane (Lal, 2004). A study by Galdos *et al.* (2009) in Brazil reported higher total SOC, microbial biomass C, and particulate OC under unburned sugarcane fields compared to the burned ones. Therefore, burning residues transforms sugarcane systems from a C sink to a C source (Dominy *et al.*, 2002; Osher *et al.*, 2003; Chalco

Vera *et al.*, 2019). Accordingly, burned fields usually exhibit higher soil respiration rates compared to unburned ones because SOC decomposes faster than when residues are left standing on the fields (Moitinho *et al.*, 2021).

For soil CH₄ dynamics, several studies indicated that sugarcane soils remained a CH₄ sink irrespective of the application of organic and inorganic N fertilizers (Paredes *et al.*, 2015). This contrasts a wealth of evidence that suggested an inhibition (Denmead *et al.*, 2010) or stimulation effect of N fertilizers on CH₄ sequestration in agricultural soils (Bolinder *et al.*, 1999). There is, however, conflicting evidence on the impact of straw accumulation in soil CH₄ fluxes under sugarcane. For example, Paredes *et al.* (2015) found no effect of straw accumulation on CH₄ fluxes. They argued that sugarcane straw was a poor source of labile C, given its high C-N ratio; yet, C is a crucial substrate for methanogenesis. On the contrary, Dattamudi *et al.* (2019) found an increase in CH₄ emissions in treatment plots with crop residues because they had 15-20% higher water-filled pore space than those without crop residues. Evidently, the discrepancies in our current understanding of the C dynamics under sugarcane warrant a thorough investigation into the validity of the proposition that sugarcane-derived biofuel is environmentally friendly and C-neutral.

1.7. Aims and structure of the thesis

Despite the increasing N and P deposition rates and the rapidly expanding fertilizer-based commercial agriculture at the expense of tropical forests in Africa's humid tropics, it remains unclear how externally supplied macronutrients alter the cycling of C and N in tropical forests and managed croplands. The aim of the PhD study was to evaluate the regulation effect of soil macronutrients on soil GHG and N leaching fluxes in a nutrient-limited tropical forest and a fertilized sugarcane plantation in north-western Uganda. The PhD thesis storyline builds on three interconnected studies conducted in the north-western part of Uganda, which is home to some of the remaining tropical forests and a concentration of large-scale sugarcane plantations. The PhD thesis workflow is conceptually represented by Fig 1.1.

The first study evaluated how nutrient limitations regulated soil GHG fluxes from tropical forests based on the evidence from an ecosystem-scale nutrient manipulation experiment in Uganda. The hypotheses underpinning the first study were: (1) Adding N or N + P to a tropical forest ecosystem would result in increased N₂O emissions coming from excess availability of bio-available N beyond microbial immobilization and plant N demands, decreased CH₄ uptake due to negative effects of N addition on soil methanotrophs, and reduced CO₂ effluxes attributed mainly to reduction in both root and microbial respiration upon addition of N. (2) Adding P to

a tropical forest ecosystem would stimulate the release of N from soil organic matter and consequently lead to increased N₂O emissions, higher CO₂ effluxes linked to increased root activity and decomposition of soil organic matter, and increased CH₄ uptake due to stimulation of methanotrophic activity.

The second study, through a completely randomized design (CRD) experiment in the sugarcane and control plots in the forest, investigated how switching from tropical forests to intensively fertilizer-based sugarcane systems affects soil greenhouse gas fluxes. The underlying hypotheses were: (1) Increased CO₂ emissions from the respective sugarcane CRD treatment plots compared to the reference forest (low input > standard input > high input > reference forest plots) coming from the continuous loss of forest SOC until the soils under sugarcane reach a new equilibrium and the higher autotrophic respiration by the sugarcane's fibrous roots. (2) Reduced CH₄ uptake in the respective sugarcane CRD treatment plots compared to the reference forest plots (high input < standard input < low input < reference forest plots) resulting from reduced methanotrophic activity under the heavily fertilized and compacted (from machinery traffic) sugarcane fields. (3) Increased N₂O emissions from the respective sugarcane CRD treatment plots compared to the reference forest plots (high input > standard input > low input > reference forest plots) attributed to N fertilization and increased mineralization of the retained crop residues.

The third study evaluated the impact of urea fertilization rates on nitrogen dynamics, productivity, and profitability under sugarcane plantations in Uganda. The overarching hypotheses were: (1) It is feasible to use well-established PTFs developed in Europe, North America, and Brazil to predict the soil water retention function and hydraulic conductivity function for Ugandan Ferralsols since some PTFs are robust enough to be applied beyond their training and validation areas. (2) N dynamics under sugarcane, specifically N leaching losses, crop N recovery, and soil N₂O fluxes, will be altered along the fertilizer intensification gradient because N rates affect the magnitude of plant and soil microbial processes. (3) Applying N rates above the standard N rate for sugarcane would result in significant incremental profitability and productivity benefits for the farmer, given the expected increase in yield at increasing N rates.

1.8. PhD conceptual flow diagram

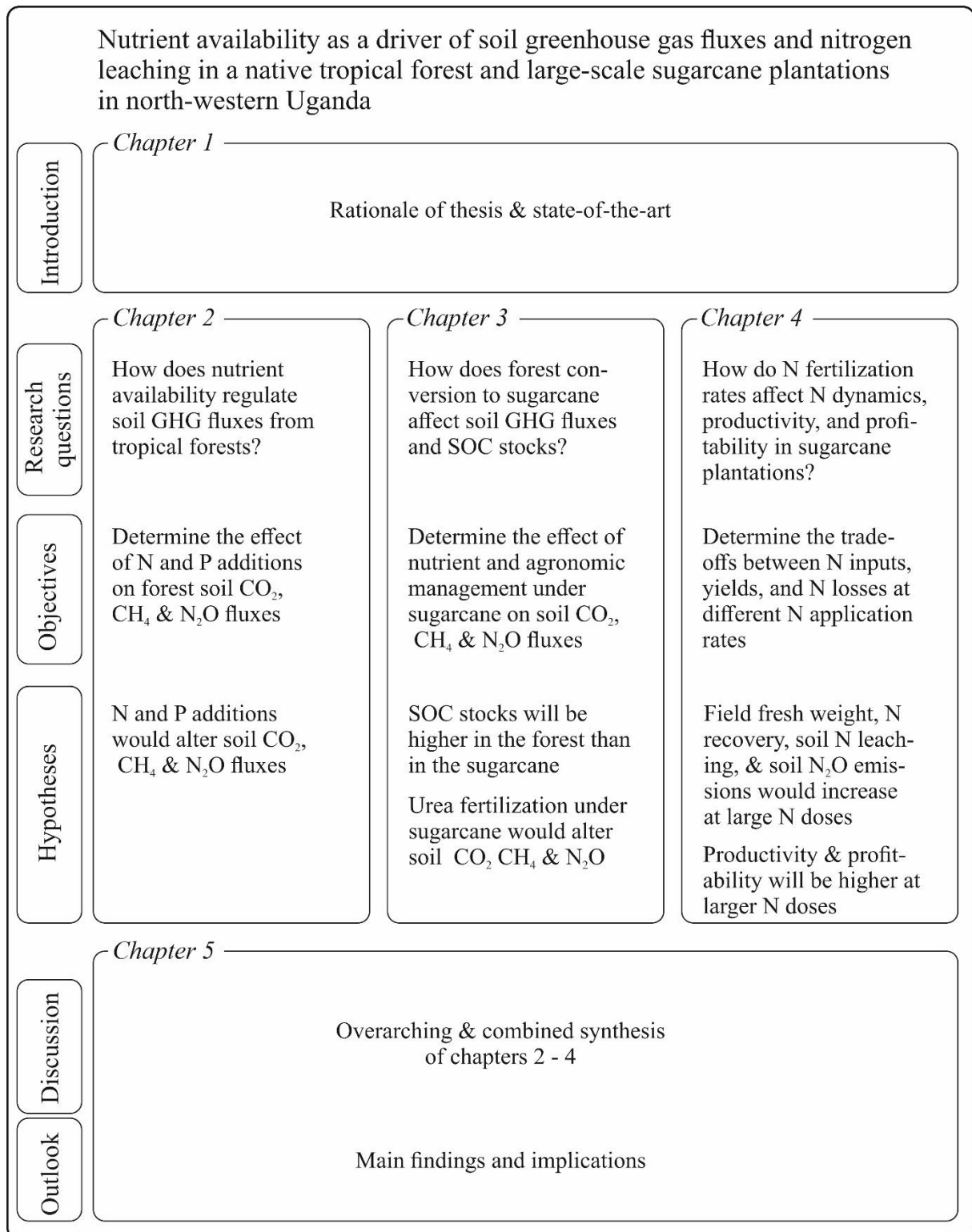


Figure 1.1. PhD conceptual flow diagram

CHAPTER 2. NUTRIENT LIMITATIONS REGULATE SOIL GREENHOUSE GAS FLUXES FROM TROPICAL FOR- ESTS: EVIDENCE FROM AN ECOSYSTEM-SCALE NUTRI- ENT MANIPULATION EXPERIMENT IN UGANDA

with minor editing differences, published as: Tamale, J., Hüppi, R., Griepentrog, M., Turyagyenda, L.F., Barthel, M., Doetterl, S., Fiener, P. and van Straaten, O. 2021. Nutrient limitations regulate soil greenhouse gas fluxes from tropical forests: evidence from an ecosystem-scale nutrient manipulation experiment in Uganda. *SOIL* 7 (2), 433-451.

2.1. Abstract

Soil macronutrient availability is one of the abiotic controls that alter the exchange of greenhouse gases (GHGs) between the soil and the atmosphere in tropical forests. However, evidence on the macronutrient regulation of soil GHG fluxes from central African tropical forests is still lacking, limiting our understanding of how these biomes could respond to potential future increases in nitrogen (N) and phosphorus (P) deposition. This study aimed to disentangle the regulation effect of soil nutrients on soil GHG fluxes from a Ugandan tropical forest reserve in the context of increasing N and P deposition. Therefore, a large-scale nutrient manipulation experiment (NME), based on 40 m × 40 m plots with different nutrient addition treatments (N, P, N + P, and control) was established in the Budongo Central Forest Reserve. Soil carbon dioxide (CO₂), methane (CH₄), and nitrous oxide (N₂O) fluxes were measured monthly, using permanently installed static chambers, for 14 months. Total soil CO₂ fluxes were partitioned into autotrophic and heterotrophic components through a root trenching treatment. In addition, soil temperature, soil water content, and nitrates were measured in parallel to GHG fluxes. N addition (N and N + P) resulted in significantly higher N₂O fluxes in the transitory phase (0–28 days after fertilization; $p < 0.01$) because N fertilization likely increased soil N beyond the microbial immobilization and plant nutritional demands, leaving the excess to be nitrified or denitrified. Prolonged N fertilization, however, did not elicit a significant response in the background (measured more than 28 days after fertilization) N₂O fluxes. P fertilization marginally and significantly increased transitory ($p = 0.05$) and background ($p = 0.01$) CH₄ consumption, probably because it enhanced methanotrophic activity. The addition of N and P together (N + P) resulted in larger CO₂ fluxes in the transitory phase ($p = 0.01$), suggesting a possible co-limitation of both N and P on soil respiration. Heterotrophic (microbial) CO₂ effluxes were significantly higher than the autotrophic (root) CO₂ effluxes ($p < 0.01$) across all treatment plots, with microbes contributing about two-thirds of the total soil CO₂ effluxes. However, neither heterotrophic nor autotrophic respiration significantly differed between treatments. The results from this study suggest that the feedback of tropical forests to the global soil GHG budget could be disproportionately altered by increases in N and P availability over these biomes.

2.2. Introduction

Tropical forest soils play an important role in the Earth's radiative balance by sequestering and releasing significant amounts of carbon dioxide (CO₂), methane (CH₄), and nitrous oxide (N₂O; Mosier *et al.*, 2004). It is estimated that tropical forest soils emit about 1.3 ± 0.3 Tg N₂O yr⁻¹ (Butterbach-Bahl *et al.*, 2004b), capture 6.4 Tg CH₄ yr⁻¹ (Dutaur & Verchot, 2007), sequester about 10% of the total atmospheric CO₂ via photosynthesis, and account for about 30% of the world's soil C stocks (Jobbágy & Jackson, 2000; Malhi & Phillips, 2004).

The rate and magnitude of the specific plant and soil microbial processes that produce (CO₂ – autotrophic and heterotrophic respiration; N₂O – denitrification and nitrification; CH₄ – enteric fermentation and methanogenesis) and consume (CO₂ – photosynthesis; CH₄ – oxidation) greenhouse gases (GHGs) in and at the soil–atmospheric interface are constrained by a multiplicity of biotic and abiotic controls (Mosier *et al.*, 2004). These controls include vegetation communities (Veber *et al.*, 2018), soil moisture (Sjögersten *et al.*, 2018), soil temperature (Holland *et al.*, 2000), geochemistry, given its control on microbial abundance (Gray *et al.*, 2014) and soil organic carbon stabilization (Doetterl *et al.*, 2015), and macronutrient availability (especially N and P; Oertel *et al.*, 2016).

Macronutrient replenishment in undisturbed tropical forests is inherently via litter input (for both N and P; Tanner *et al.*, 1998) and rock weathering (for P; Hedin *et al.*, 2003) processes. However, the past 3 decades have seen an increase in the levels of N and P deposition over most tropical regions (including central Africa) due to widespread deforestation and biomass burning (Galloway *et al.*, 2004; Bauters *et al.*, 2019). Currently, the central African region receives about 18.5 kg N ha⁻¹ (Bauters *et al.*, 2019) and 1.8–2.5 kg P ha⁻¹ (Tamatamah *et al.*, 2005) each year due to high fire-derived N deposition (Bauters *et al.*, 2019) and P-rich biomass aerosols (Barkley *et al.*, 2019), respectively. Increased anthropogenic N and P deposition over tropical forest biomes disrupts ecosystem stoichiometric equilibrium, thereby affecting the biogeochemical cycling of N and P (Bauters *et al.*, 2019) and the exchange of GHGs between the soil and atmosphere (Corre *et al.*, 2014). One way of understanding how increases in N and P availability (for instance, through deposition) affect soil GHG fluxes from tropical forests is through large-scale nutrient manipulation experiments (NMEs). NMEs purposely use large doses of N and P (e.g., Cleveland & Townsend, 2006– 150 kg N ha⁻¹ yr⁻¹ and 150 kg P ha⁻¹ yr⁻¹; Hall & Matson, 2003 – 100 kg N ha⁻¹ yr⁻¹ and 40 kg P ha⁻¹ yr⁻¹) to simulate how future nutrient enrichment of tropical forests (through deposition) could affect soil GHG fluxes

(among other ecosystem processes; Corre *et al.*, 2010).

To date, several NMEs have been carried out across the tropics (e.g., Wei *et al.*, 2008; Corre *et al.*, 2010), and the outcome has been a consensus that the addition of N to an already N-rich tropical forest ecosystem results in increased N₂O emissions (Zhang *et al.*, 2008a; Martinson *et al.*, 2013; Corre *et al.*, 2014). For N-rich forest ecosystems, an increase in available soil N beyond the microbial immobilization and plant nutritional demands results in the excess being nitrified or (and) denitrified by soil microbes (Corre *et al.*, 2014). However, several studies suggest that increased availability of N not only reduces fine root biomass but also curtails microbial activity, leading to reduced autotrophic (Cusack *et al.*, 2011) and heterotrophic respiration (DeForest *et al.*, 2006; Koehler *et al.*, 2009a; Chen *et al.*, 2010), respectively. Notably, there are varying results on how N addition affects CH₄ uptake from tropical forest soils. For instance, Veldkamp *et al.* (2013) found no effect of N on CH₄ uptake, while Du *et al.* (2019) measured reduced CH₄ consumption following the addition of N to a tropical forest, with the latter study suggesting an inhibitory effect of N on CH₄ uptake (Seghers *et al.*, 2003; Zhang *et al.*, 2011; Bodelier & Steenbergh, 2014). Aronson & Helliker (2010) argue that the observed differences in the measured CH₄ fluxes in the two separate studies were likely due to the different amounts of N added in the respective experimental setups. They argued that low amounts of N stimulate CH₄ uptake, while high amounts inhibit it.

With respect to P, it has been shown that P availability opens up the N cycle by stimulating soil organic matter mineralization, releasing excess N for soil nitrification and/ or denitrification processes (Mori *et al.*, 2010). It is also urged that P availability has a positive effect on both autotrophic and heterotrophic components of soil respiration (Mori *et al.*, 2013). P not only stimulates fine root growth (Chen *et al.*, 2010) but also regulates organic matter decomposition (Mori *et al.*, 2018). However, studies elucidating the P limitation of organic matter decomposition in the P-deficient tropics remain rare, and even the few available studies on the regulation effect of P on leaf litter mass loss rates are inconclusive (Cleveland & Townsend, 2006). This might explain why contrasting results were reported from two similar experiments carried out on P-depleted soils in Hawaii (Hobbie & Vitousek, 2000) and the Brazilian Amazon (McGroddy *et al.*, 2008). Hobbie & Vitousek (2000) reported an increase in the litter mass loss rate, while McGroddy *et al.* (2008) did not detect any change, suggesting that the relationship between P availability and organic matter decomposition is complex (Cleveland & Townsend, 2006). Similarly, the literature on the interaction between N and P in regulating CH₄ fluxes from tropical forests remains limited.

Despite the recognition that N and P affect soil GHG fluxes, and the fact that tropical forest

ecosystems could subtly respond to potential future increases in N and P deposition (Li *et al.*, 2006; Bobbink *et al.*, 2010), the magnitude and direction of this response remains unclear for African tropical forests. To date, only a handful of NMEs focusing on tropical forests' response to shifts in ecosystem N and P dynamics have been carried out. Of these studies, just a few included both N and P treatments in their experimental setups (e.g., Corre *et al.*, 2014). Yet, P deficiency typical of tropical soils can have direct impacts on ecosystem biomass production if the limitation is lifted (John *et al.*, 2007). Furthermore, nearly all the studies conducted in (sub-) tropical forest ecosystems were, so far, concentrated in China (Yan *et al.*, 2008; Jiang *et al.*, 2016; Zheng *et al.*, 2016a), Central America (Koehler *et al.*, 2009a; Corre *et al.*, 2014; Matson *et al.*, 2014), and South America (Wolf *et al.*, 2011; Martinson *et al.*, 2013; Müller *et al.*, 2015). Unfortunately, no single controlled experiment has simulated the effects of elevated soil nutrient inputs on soil greenhouse gas fluxes from African tropical forests, despite the projected increase in N and P deposition over these biomes (Galloway *et al.*, 2004) and the fact that they represent a significant proportion of global tropical forests (27%; Saatchi *et al.*, 2011). It was for this reason that a replicated, completely randomized NME was established in a Ugandan tropical forest reserve to investigate the role N and P have in regulating soil GHG fluxes in the context of changing N and P deposition rates over the tropics. In the following, it was hypothesized that:

1. the addition of N or N + P to a tropical forest ecosystem would result in increased N₂O emissions coming from the excess availability of bio-available N beyond microbial immobilization and plant N demands, decreased CH₄ uptake due to negative effects of N addition on soil methanotrophs, and reduced CO₂ effluxes largely attributed to the reduction in both root and microbial respiration upon the addition of N.
2. the addition of P to a tropical forest ecosystem would stimulate the release of N from soil organic matter and, consequently, lead to increased N₂O emissions, higher CO₂ effluxes linked to increased root activity and decomposition of soil organic matter, and increased CH₄ uptake due to stimulation of methanotrophic activity.

2.3. Materials and methods

2.3.1. Study site description

The study was conducted in the Budongo Central Forest Reserve, a semi-deciduous tropical forest, located in the north-western part of Uganda ($1^{\circ}44'28.4''$ N, $31^{\circ}32'11.0''$ E). The forest reserve spans over 825 km² and is extensively diverse with respect to forest communities, with *Cynometra alexandri*, *Chrysophyllum albidum*, *Maesopsis eminii*, and *Diospyros abyssinica* as the dominant tree species (Eggeling, 1947). The long-term mean annual temperature and precipitation over the study area is 25 °C and 1700 mm, respectively (Lukwago *et al.*, 2020). Rainfall is distributed into two rainy seasons (i.e., March to May and August to November) punctuated by a strong dry season (December to February) and a weak dry season (June to July; Lukwago *et al.* (2020)). It is worth noting that the amount of rainfall received during the field campaign (2385 mm) was higher than the long-term mean annual precipitation for this region. The weather data for the experiment period were obtained from a climatic station installed at the Budongo Conservation Field station (2 km northwest of the study site) and was beneficial for understanding how precipitation affected soil greenhouse gas fluxes given its direct control on water-filled pore space. The soils at the experimental site are highly weathered, are classified as Lixisols (IUSS Working Group WRB, 2015), and are developed on a Precambrian gneissic–granulitic basement complex (van Straaten, 1976).

2.3.2. Experimental design

The study was conducted within the framework of a running nutrient manipulation experiment (NME). The NME study used a completely randomized design to investigate how the three macronutrients (applied individually as nitrogen, phosphorus, and potassium (K) and in all possible combinations, i.e., N + P, N + K, P + K, and N + P + K, as treatments) constrained key ecosystem processes (particularly nutrient cycling and net primary productivity) in comparison to the unamended control. Each of the eight treatments was replicated four times (hence, $n = 32$ plots; eight treatments \times four replications). While the NME included a K treatment, the soil GHG flux study (the basis for this paper) was conducted on the N, P, and N + P (combination of N and P) plots and compared to the untreated control plots ($n = 16$). Only N and P (among nutrient addition plots) were exclusively considered for soil GHG flux measurements because their availability has been shown to limit soil greenhouse gas fluxes from tropical forest biomes. Each treatment plot measured 40 m \times 40 m in size, but measurements were conducted in the inner measurement core (30 m \times 30 m) to avoid boundary effects. A spacing of at least 40 m between experimental plots was ensured to prevent the spillover of applied nutrients from the neighboring plots. To elicit an ecosystem response, N was applied at a rate of 125 kg N ha⁻¹

yr⁻¹, in the form of urea ((NH₂)₂CO), and P at 50 kg P ha⁻¹ yr⁻¹, as triple superphosphate (Ca (H₂PO₄)₂). The types of fertilizers and application rates used in this study were identical to those used in the Wright *et al.* (2011) NME. The fertilizer was applied by hand and in four split doses every year. Specifically, 31.3 kg N ha⁻¹ and 12.5 kg P ha⁻¹ were applied to the plots of the NME every 3 months between May 2018 and June 2020.

2.3.3. Baseline soil physico-chemical characterization

Before the first fertilizer application, soil samples were taken from all the treatment plots of the NME (for the topsoil) and the close proximity of the NME (for deeper soil layers) for baseline soil physico-chemical analyses. The analyses included texture, bulk density, soil pH, total soil organic carbon (TOC) stocks, total nitrogen stocks, C-N ratio, exchangeable bases, effective cation exchange capacity (ECEC), and Bray-extractable P. For the topsoil (0–10 cm depth), soil monoliths (20 cm (*L*) × 20 cm (*W*) × 10 cm (*D*)) were carefully taken from 10 different locations within each plot of the NME (*n* = 32 plots) using a spade. For deeper soil layers (0–30 and 30–50 cm), samples were obtained outside the established NME plots to minimize modifications to the microenvironment inside the NME plots. Deeper soil sampling was done during a reconnaissance survey conducted at approximately 500 m from the current location of the NME site. During the reconnaissance survey, 16 plots (*n* = 16) were established and samples were taken from five different locations in each plot for every depth interval (i.e., 0–30 and 30–50 cm) using an auger (diameter = 30 mm). The samples from the same depth within each plot were mixed thoroughly in a basin, and about 500 g of the homogenized samples were sent to the soil laboratory of the University of Göttingen, Germany, for analysis. Soil texture was determined using a Bouyoucos hydrometer. Soil pH was determined in a 1: 2.5 (soil water) suspension. Soil bulk density for every depth in each plot was calculated from the mass of oven-dried soil (at 105 °C for 48 h) and the volume of the Kopecky ring (volume = 251 cm³) used in collecting the soil sample. Note that soil bulk density was corrected for stone content. The soils were tested for the presence of inorganic carbon (IC) using dilute hydrochloric acid and were found to be devoid of any IC. Hence, TOC and N were determined using a CN elemental analyzer (vario EL cube; Elementar Analysis Systems GmbH, Hanau, Germany) and stocks were later calculated from bulk density measurements. Exchangeable base cations (Ca, Mg, K, Na, and Al) and ECEC were determined on the 1–2 mm Earth fraction of the collected soil samples.

2.3.4. Soil greenhouse gas fluxes and soil environmental control measurements

Soil CO₂, CH₄, and N₂O fluxes were measured monthly for 14 months (May 2019 to June 2020). In every replicate plot's inner measurement core, four chamber bases (fabricated from a 250 mm PN10 PVC pipe and each with an area equal to 0.044 m² and volume equal to about 12 L)

were randomly installed at the soil surface to a depth of about 0.03 m. Installation of chamber bases was done at the beginning of April 2019, a month before the GHG flux measurements, and chamber bases remained permanently in place for the entire measurement period. The litter was not removed from the chambers. However, all the chamber bases were always maintained to be vegetation-free throughout the gas-sampling period to avoid measuring plant night respiration during chamber closure. On the sampling day, chamber bases were covered with vented polyvinyl hoods fitted with sampling ports. A pooled gas sample was then obtained every 3, 13, 23, and 33 min using an airtight Luer lock syringe, following the pooling approach described in detail by Arias-Navarro *et al.* (2013). The 33 min maximum chamber closure period used in this study was well under the threshold recommended by Pavelka *et al.* (2018) but comparable to other tropical GHG flux studies (e.g., Koehler *et al.*, 2009; Corre *et al.*, 2010; Matson *et al.*, 2017). To check if the pooling worked correctly, both the pooled and unpooled (an average of four individual chamber measurements) samples were taken for February 2020 for analysis. Both methods produced very comparable results (Fig. 2.1). Soil GHG fluxes were always measured between 09:00 and 16:00 EAT throughout the entire study period, while, for each measurement day, the sequence of plots to be measured was randomly chosen. Together with the very low diurnal variability in the air (0.6 ± 0.04 °C; mean \pm SE) and soil (0.2 ± 0.03 °C; mean \pm SE) temperatures at this tropical forest site, the time of the measurement of individual gas chambers should, if at all, only have a minimal effect on the measured gas fluxes. All collected gas samples were stored in Labco exetainers (Labco Limited, Lampeter, UK) with screw-on plastic caps fitted with Labco gray chlorobutyl septum because these exetainers have been demonstrated to remain airtight for periods spanning up to 6 months (Hassler *et al.*, 2015). Additionally, all the plastic caps were screwed on to the exetainers by hand and quarter-turned before sampling to ensure that they were airtight (Pavelka *et al.*, 2018). All the gas-filled exetainers were shipped to the Department of Environmental Systems Science, ETH Zürich, Switzerland, for analysis using a gas chromatograph (GC; SCION 456-GC; Bruker, Germany) within 4 months from sampling.

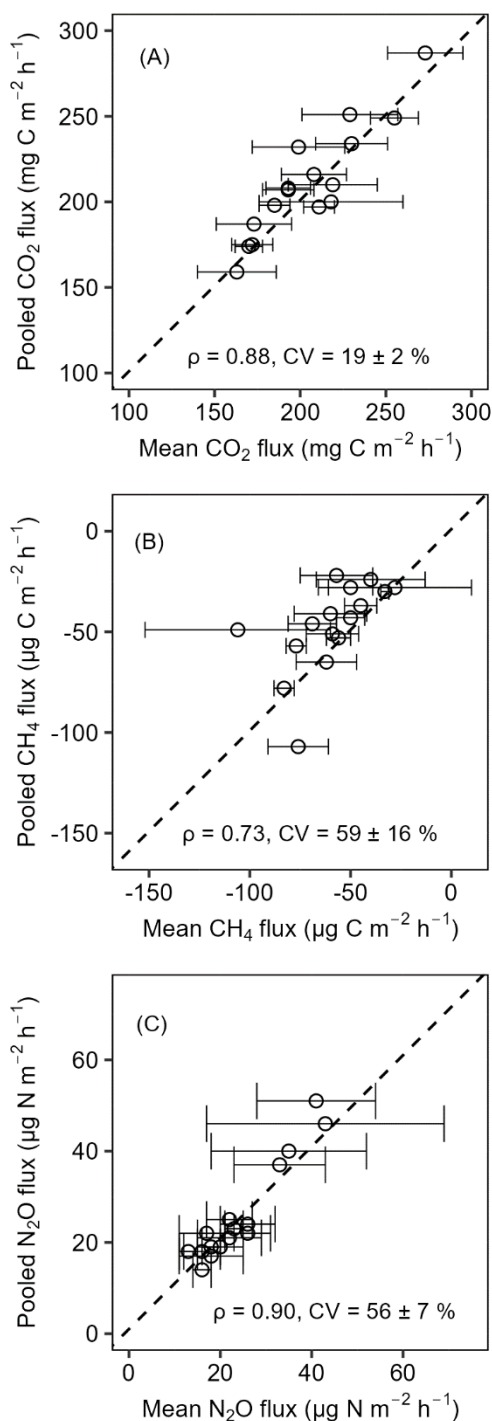


Figure 2.1. Comparison of the soil CO₂ fluxes (A), soil CH₄ fluxes (B), and soil N₂O fluxes (C) from pooled sampling and the mean of four chamber measurements for the month of February 2020 in the Budongo Central Forest Reserve. ρ is the Spearman correlation coefficient, and CV is the coefficient of variation. Error bars are derived from standard error of the mean.

The GC was equipped with an electron capture detector (N₂O), flame ionization detector (CH₄), thermal conductivity detector (CO₂), and auto-sampler. GC concentrations of the individual gas species of interest (CO₂, CH₄, and N₂O) were then calculated by comparing the peak areas of the measured samples to the respective peak areas of a suite of standard gas samples. Next, flux rates of individual gases at the soil–atmosphere interface were calculated based on either linear

increase or decrease in gas concentrations during chamber closure, following Eq. (2.1) in Butterbach-Bahl et al. (2011).

$$GHG_{flux} = \frac{V_{ch} * GHG_m * S * 10^6 * 60}{A_{ch} * GHG_v * 10^9} \quad (2.1)$$

where GHG_{flux} is given as a positive flux to the atmosphere or a negative flux into the soil (micrograms per square meters per hour; hereafter $\mu\text{g m}^{-2} \text{h}^{-1}$), V_{ch} is the chamber volume (cubic meters), GHG_m is the molar mass of the different gases (grams per mole; hereafter g mol^{-1}), S is the slope of a linear regression calculated based on the increase or decrease in gas concentrations during chamber closure (parts per million per minute), A_{ch} is the chamber ground area (square meters), and GHG_v is the molar volume of the different gases (cubic meters per mole; hereafter $\text{m}^3 \text{mol}^{-1}$). Note that the constants 10^6 , 10^9 , and 60 were used to convert grams into micrograms, parts per million into cubic meters, and minutes into hours. GHG_v was adjusted to air temperature and pressure in the field using the ideal gas law, following Eq. (2.2):

$$GHG_v = 0.02241 * \frac{273.15 + T_f}{273.15} * \frac{P_f}{P_s} \quad (2.2)$$

where T_f is the air temperature (degrees Celsius) and P_f is the pressure (Pascal) at the field site, and P_s is the pressure at sea level (Pascal). As a quality check, the linearity of the CO_2 increase during chamber closure was inspected by comparing the CO_2 concentrations (of each chamber measurement) with time since chamber closure and, thereafter, determining the goodness of fit for the linear regression model (R^2). The R^2 for all the measurements was 0.992 ± 0.001 (mean \pm SE). Additionally, the measured gas concentrations from the GC were checked against the standards and the GC's minimum detection limit to ensure that the changes in gas concentrations during chamber closure were well above its minimum detection limit.

In parallel to gas flux measurements, soil environmental controls, particularly soil temperature, volumetric water content, and soil mineral nitrogen (ammonium – NH_4^+ ; nitrate – NO_3^-), were measured. Soil temperature and volumetric water content were determined at 0.05 m soil depth adjacent to each of the four installed chamber bases per replicate plot. A digital thermometer (Greisinger GMH 3230; GHM Messtechnik GmbH Standort Greisinger, Germany) fitted with an insertion probe and a calibrated ML3 Theta Probe soil moisture sensor (Delta-T Devices Ltd, United Kingdom) was used to determine soil temperature and soil volumetric water content, respectively. Soil mineral nitrogen was determined by obtaining a soil sample in a Kopecky ring at 0.05 m depth (from the soil surface) and 1 m distance from each of the installed chambers per replicate plot. The obtained soil samples (from each replicate plot) were pooled together

and thoroughly mixed. Next, 100 and 150 g of the pooled soil samples were extracted with 100 and 600 mL CaCl₂ solution to determine NO₃⁻ and NH₄⁺ concentrations, respectively, using the RQflex®10 reflectometer. The RQflex®10 reflectometer is part of the Reflectoquant ® system comprising a reflectometer, a batch-specific barcode, and test strips. The test strips used in this study had a 3 – 90 and 0.2 – 7 mg L⁻¹ detection range for nitrates (NO₃ - N) and ammonium (NH₄ - N), respectively.

To understand the contribution of autotrophic (root) and heterotrophic (microbial) sources to total soil respiration, a trenching treatment was done in all the plots, following the protocol of Wang & Yang (2007). Before trenching, root biomass distribution with depth was determined to establish where most roots were located. Root biomass estimation involved digging three profile pits measuring 1 m (*L*) × 1 m (*W*) × 1.1 m (*D*) at the forest site. In every pit, 10 soil monoliths (each measuring 20 cm (*L*) × 20 cm (*W*)) were carefully cut out (using a spade and hoe), following a 10 cm depth interval from the surface down to 1 m. The soil monoliths were thoroughly washed to isolate the roots from the bulk soil. The root samples were oven-dried at 60 °C for 48 h and weighed to determine the root biomass per depth increment. The root biomass for each depth interval was calculated as the mean of the root biomass from the three pits for that interval. It was established that over 90% of the roots were within the top 0.60 m of the soil profile. Therefore, a circular trench (about 0.60 m in diameter) was dug to a depth of about 0.60 m at the center of all the plots, thereby creating a soil mass free of roots. All the trenches were lined with a heavy-duty plastic sheet to prevent roots from growing back into the trenched soil mass. The trenched soil mass and the proximally neighboring untrenched (reference) zone (about 1 m apart) were, respectively, installed with a chamber base. Both the trenched and reference chamber bases had a design (an area equal to 0.044 m² and a volume equal to about 12 L) identical to the one used in the NME soil GHG flux study. The installed chamber bases were left standing for 6 months before the first measurements began in November 2019. This ensured that a large proportion of the cut roots in the trenched soil mass decomposed before the start of the CO₂ measurements. CO₂ measurements were conducted monthly for 4 months (starting in November 2019 and ending in February 2020). The selected measurement time window represented the transition between the wet season and the long dry season, allowing us to capture how soil moisture constrained the different soil CO₂ efflux sources. After the completion of the flux measurements, root coring was done to a depth of 0.30 m at two locations directly adjacent to both the trenched and untrenched chambers to determine if the trenching approach was effective in reducing the amount of living root biomass in the trenched zone. It was established that there was a 73% and 63% reduction in fine root biomass and coarse root biomass, respec-

tively, in the trenched zone in comparison to the reference zone. Heterotrophic (microbial) respiration was equal to the CO₂ effluxes from the trenched chamber, while autotrophic (root) respiration was the difference between CO₂ effluxes from the reference and trenched chambers.

2.3.5. Statistical analysis

Before statistical analysis, transitory N₂O fluxes from N addition plots (N and N + P) were detrended to compensate for the absence of frequent measurements immediately after fertilization coming from sampling GHGs monthly. Detrending involved using a lognormal fit between the measured N₂O fluxes and time since fertilization (until day 42), and this explained 43% of the observed variability in the N₂O data during the transitory phase ($p < 0.05$). Additionally, GHG flux and soil environmental control data were aggregated based on seasons (wet and dry) and phases (transitory – 0 – 28 days from the date of fertilization; background – more than 28 days after fertilization). Furthermore, despite monitoring soil NO₃⁻ and NH₄⁺ contents monthly throughout the measurement period, only the soil NO₃⁻ data set was used in the analysis because soil NH₄⁺ was mostly low and often below the detection limit of the reflectometer at the majority of the sampling time points. Data were checked for normality and homogeneity of variance (homoscedasticity) across treatment groups, seasons, and phases before implementing parametric tests (i.e., linear mixed-effects models – LMEMs; one-way analysis of variance – ANOVA). The normality of the respective data was inspected by using diagnostic plots (histograms and quantile – quantile plots) and the Shapiro – Wilk normality test, while heteroscedasticity was determined with the Levene test and by inspecting residual plots of fitted values. In the case of heteroscedasticity and non-normal distribution of the data, either a logarithmic or a Tukey transformation was applied to the data set. However, if the normality of the data and homogeneity of variance were not restored by the transformations, an equivalent nonparametric statistical test was selected. Spearman's correlation coefficient test was used to check the relationship between the measured background soil GHG fluxes and soil environmental controls. To determine the differences in mean soil GHG fluxes between treatments, a one-way ANOVA test was used with GHG species and treatments included in the model as response and predictor variables, respectively. To determine the effect of the added nutrients on soil GHG fluxes (CO₂, CH₄, and N₂O), soil CO₂ sources (heterotrophic and autotrophic), and soil environmental controls (water- filled pore space, soil temperature, and nitrates), LMEMs were employed. LMEMs effectively deal with temporal pseudo-replication (coming from repeated measurements) and, hence, safeguard against inflation of the degrees of freedom, which would significantly compromise the power of the statistical test. Added nutrients (treatments), seasons (wet and dry), CO₂ sources (autotrophic and heterotrophic), and phases (transitory and background) were included in the LMEMs as fixed effects, while sampling days and replicate plots were included

as random effects. Some of the LMEMs were extended to either include a variance function (to account for variation in the response variable per level of the fixed effect), a first-order temporal autoregressive process (to control for correlation between closely spaced measurements in time), or both. The extensions were included in the LMEMs on the premise that they improved the relative goodness of model fit based on the Akaike information criterion (AIC). All the statistical data analyses were performed using R 3.6.3 (R Development Core Team, 2019). Specifically, 'nlme' and 'car' packages were employed to run LMEMs and one-way ANOVA tests, respectively. Throughout the paper, statistical significance in all the tests was inferred if $p \leq 0.05$, and annual soil GHG fluxes were estimated through a trapezoidal interpolation on the measured monthly soil GHG fluxes.

2.4. Results

2.4.1. Soil physico-chemical characteristics, water-filled pore space, soil temperature, and nitrates

Soil characteristics did not significantly differ across plots; hence, the parameters presented in Table 2.1 represent the soil physico-chemical characteristics for the NME site.

Table 2.1. Soil physico-chemical properties in three depths and vegetation characteristics of the study site located in Budongo forest, north-western Uganda.

Soil physico-chemical properties	Soil depth (m)		
	0 - 0.10	0.10 - 0.30	0.30 - 0.50
Soil bulk density (g cm ⁻³)	1.2 ± 0.2	1.5 ± 0.2	1.3 ± 0.2
Soil pH (1:2.5)	6.4 ± 0.2	6.2 ± 0.2	6.0 ± 0.2
Soil total carbon (C) (kg C m ⁻²)	4.1 ± 0.0	3.1 ± 0.0	1.8 ± 0.0
Soil total nitrogen (N) (g N m ⁻²)	423 ± 1.0	387 ± 0.2	249 ± 0.6
Soil C/N ratio	9.5 ± 0.3	8.0 ± 0.3	7.2 ± 0.3
Sand (%)	55 ± 2	55 ± 2	49 ± 1
Silt (%)	27 ± 2	21 ± 1	14 ± 1
Clay (%)	18 ± 1	23 ± 1	38 ± 1
ECEC (mmol _c kg ⁻¹)	149 ± 8	76 ± 4	62 ± 4
Exchangeable aluminum (g Al m ⁻²)	0.10 ± 0.06	0.11 ± 0.15	0.14 ± 0.20
Exchangeable calcium (g Ca m ⁻²)	75.6 ± 4.10	39.0 ± 8.51	34.7 ± 8.59
Exchangeable magnesium (g Mg m ⁻²)	17.0 ± 0.90	12.3 ± 2.7	11.7 ± 1.0
Bray II extractable phosphorus (g P m ⁻²)	1.80 ± 0.20	1.01 ± 0.14	0.838 ± 0.159
Base saturation (%)	99 ± 1	97 ± 1	98 ± 1
Plant-available phosphorus (g P m ⁻²)	1.7 ± 0.0	-	-
Plant-available molybdenum (mg Mo m ⁻²)	14 ± 5.0	-	-
Vegetation characteristics (≥ 10 cm DBH)			
Forest type	Moist semi-deciduous tropical forest		
Most abundant tree species	Funtumia elastica, Celtis mildbraedii, Cynometra alexandri, Celtis zenkeri		
Stand height (m)	18.7 ± 0.1		
Mean basal area (m ² ha ⁻¹)	34.0 ± 1.0		
Tree density (trees ha ⁻¹)	621 ± 13		
N fixing trees at the site (trees ha ⁻¹)	~ 42		

Notes: DBH is the diameter at breast height. ECEC is the effective cation exchange capacity.

The soils have a high bulk density (specifically, 10 – 30 cm), slightly acidic pH, sandy texture, relatively high effective cation exchange capacity (ECEC), high base saturation (dominated by Ca and Mg), low level of plant-available phosphorus, and low C/N (Table 2.1). The water-filled pore space (WFPS) was significantly higher in the wet season (March to December; $55 \pm 1.0\%$) compared to the dry season (January to February; $43 \pm 1.7\%$; Fig. 2.2A; Fig. 2.3A; $p < 0.01$). WFPS was higher in N and N + P addition plots compared to the control plots both in the dry (N – $p = 0.02$; N + P – $p = 0.04$) and wet (N – $p = 0.02$; N + P – $p = 0.05$) seasons (Fig. 2.2A). Soil temperature varied minimally ($0.6\text{ }^{\circ}\text{C}$) across treatments and seasons (Fig. 2.2B), ranging between 20.1 and $21.4\text{ }^{\circ}\text{C}$ in the dry season and between 19.7 and $22.9\text{ }^{\circ}\text{C}$ in the wet season (Fig. 2.3B). Soil nitrate contents measured across all treatment plots were significantly larger in the dry season compared to the wet season (Fig. 2.2C; $p < 0.01$). Soil nitrate content from the N ($p = 0.01$) and N + P ($p = 0.02$) addition plots was significantly higher than the control plots in the wet season (Fig. 2.2C), but no significant difference was detected between the nutrient addition treatments and the control in the dry season (Fig. 2.2C). Strong nitrate peaks were observed in N and N + P addition plots in September 2019 and June 2020, shortly after fertilization (Fig. 2.3C).

2.4.2. Soil CO₂ fluxes

Soil CO₂ fluxes varied between 60 and $330\text{ mg C m}^{-2}\text{ h}^{-1}$ during the measurement period across all treatments. However, the highest CO₂ fluxes were measured in December at the interface between wet and dry seasons (Fig. 2.4A). Fertilization resulted in an immediate increase in CO₂ fluxes across all nutrient addition plots (N – 15% ; P – 14% ; N + P – 24%) in the transitory phase. However, this increase was only significant in the N + P plots (Fig. 2.5A; $p = 0.01$). There was no significant effect of fertilization on background CO₂ fluxes between nutrient addition treatments and the control plots (Fig. 2.5D). Similarly, no significant differences in the background CO₂ fluxes were detected between seasons, despite measuring marginally lower background CO₂ fluxes in the wet season compared to the dry season (Fig. 2.5D).

Additionally, no significant differences were detected between transitory and background CO₂ fluxes (Fig. 2.5A and D). Heterotrophic (microbial) CO₂ effluxes were significantly higher than the autotrophic (root) CO₂ effluxes (Fig. 2.6; $p < 0.01$) across all treatment plots, with microbes contributing about 3 times more to the total soil CO₂ effluxes compared to roots (Fig. 2.6; $p < 0.01$). Neither heterotrophic nor autotrophic respiration significantly differed between treatments (Fig. 2.6). Overall, there was a relatively low variability in annual CO₂ fluxes across treatments ($\text{CV} = 14.8 \pm 2.2\%$). The Spearman correlation coefficient indicated that background soil CO₂ fluxes did not correlate to any of the measured soil environmental controls (WFPS,

soil temperature, and nitrates) across all treatment plots (Fig. 2.7A–C).

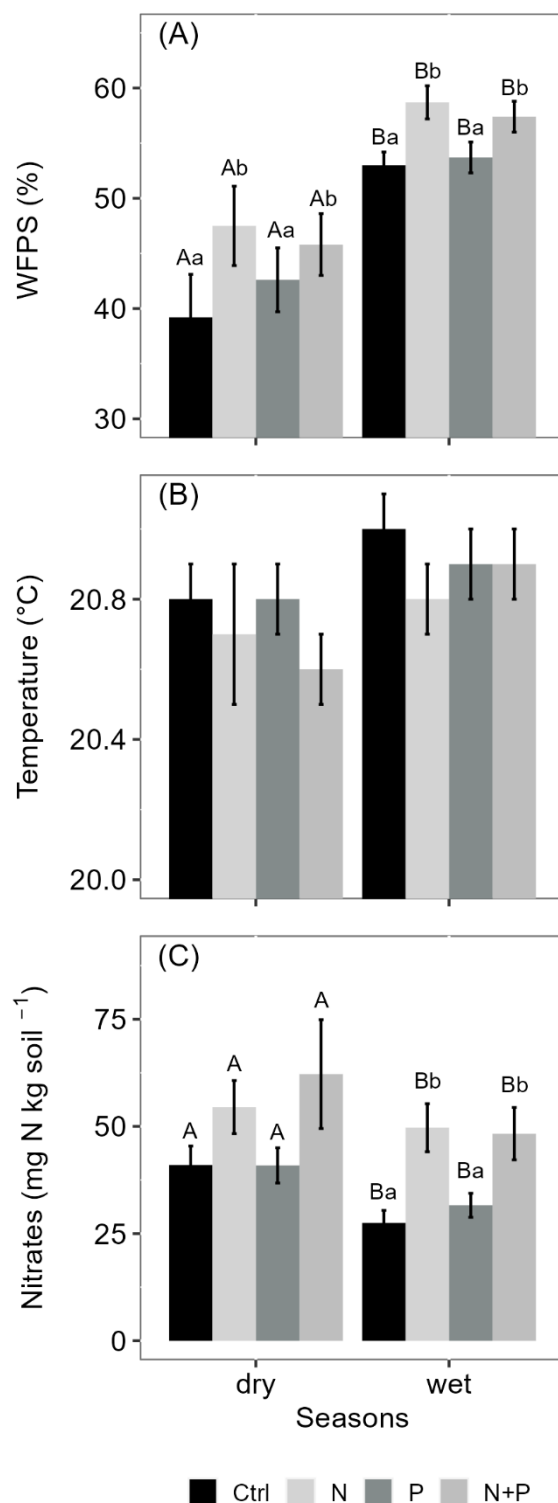


Figure 2.2. Mean (\pm standard error, SE, $n = 4$) WFPS (A), soil temperature (B), and nitrates (C) in the top 0.05 m of the control (Ctrl), nitrogen (N), phosphorus (P), and N + P plots of the nutrient manipulation experiment measured during the dry (January and February; monthly precipitation < 100 mm) and wet (March to December; monthly precipitation > 100 mm) seasons. Different lowercase letters indicate significant differences between treatments and the control, while different uppercase letters indicate significant differences between seasons (LMEMs; $p \leq 0.05$).

2.4.3. Soil CH₄ fluxes

Across all treatments, phases (transitory and background), and seasons, soil CH₄ fluxes varied between an uptake of -278 and a release of $77 \mu\text{g C m}^{-2} \text{h}^{-1}$. In the transitory phase, CH₄ consumption increased slightly but not significantly in the N (2%) and N + P (6%) plots. A larger but still not significant (marginal) increase was found in the case of P plots (54%; $p = 0.05$; Fig. 2.5B). Beyond 28 days from the time of fertilization, no significant difference in background soil CH₄ fluxes between treatments were detected in the dry season (Fig. 2.5E). However, a significantly higher background soil CH₄ consumption was measured in P plots in the wet season (Fig. 2.5E; $p = 0.01$). Soil CH₄ consumption in the dry season was, on average, 1.5 times larger than the wet season across all treatments (Fig. 2.5E; $p = 0.01$). Soil CH₄ uptake across all treatment plots measured during the transitory phase ($-39.0 \pm 3.7 \mu\text{g C m}^{-2} \text{h}^{-1}$) did not significantly differ from the CH₄ uptake in the background phase ($-42.8 \pm 3.4 \mu\text{g C m}^{-2} \text{h}^{-1}$; Fig. 2.5B and E).

Annual CH₄ uptake ranged between -2.7 and $-4.7 \text{ kg C ha}^{-1} \text{ yr}^{-1}$, with soils in all the treatment plots acting as net sinks for CH₄ (Table 2.2). The Spearman correlation coefficient test indicated that background CH₄ fluxes were strongly and positively correlated to WFPS (Fig. 2.7D), while soil temperature (Fig. 2.7E) and nitrates (Fig. 2.7F) were also significant but negatively correlated.

2.4.4. Soil N₂O fluxes

Soil N₂O fluxes across treatments, phases (transitory and background), and seasons varied between an uptake of -18 and a release of $499 \mu\text{g N m}^{-2} \text{h}^{-1}$. A strong increase in N₂O effluxes was measured immediately after fertilization (September and December 2019; April and June 2020; Fig. 2.4C) in all N addition plots, with increases of 445% in N plots ($p < 0.01$) and 455% in the N + P plots ($p < 0.01$) compared to the control plots in the transitory phase (Fig. 2.5C).

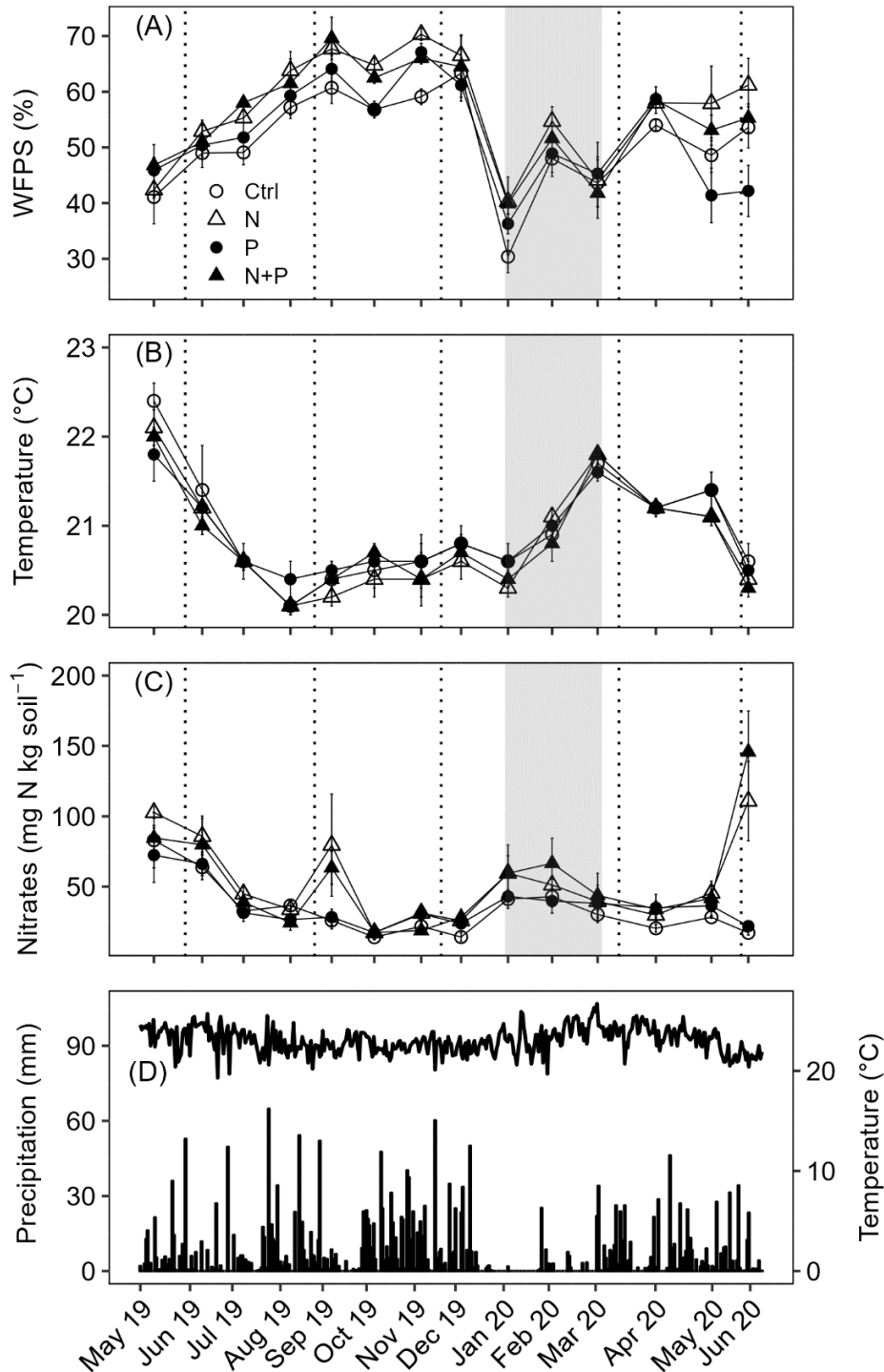


Figure 2.3. Mean (\pm standard error, SE, $n = 4$) WFPS (A), soil temperature (B), and nitrates (D) in the top 0.05 m measured monthly (May 2019 to June 2020) from control (Ctrl), nitrogen (N), phosphorus (P), and N + P plots of the nutrient manipulation experiment. Vertical lines indicate the timing of each split dose of N ($31.3 \text{ kg N ha}^{-1}$), P ($12.5 \text{ kg P ha}^{-1}$), and N ($31.3 \text{ kg N ha}^{-1}$) + P ($12.5 \text{ kg P ha}^{-1}$) fertilization every 3 months. The gray shaded rectangle (in A, B, and C) marks the beginning and end of the dry season (January and February; monthly precipitation < 100 mm), while panel (D) gives the daily precipitation (bars) and air temperature (line) between May 2019 and June 2020. Climatic data were obtained from a weather station installed at the Budongo Conservation Field Station, 2 km from the location of the nutrient manipulation experiment in the Budongo Central Forest Reserve, north-western Uganda.

The soil N₂O peaks in September 2019 and June 2020 (Fig. 2.4C) coincided with the peaking in soil nitrate concentrations (Fig. 2.3C). Background soil N₂O fluxes did not differ significantly between nutrient addition plots and the control plots both in the dry and wet seasons (Fig. 2.5F). Annual N₂O fluxes ranged between 1.8 and 4.8 kg N ha⁻¹ yr⁻¹, with soils in all the treatment plots acting as net sources of N₂O (Table 2.2). The Spearman correlation coefficient indicated that background soil N₂O fluxes were strongly and positively correlated to WFPS (Fig. 2.7G) in all treatment plots. The majority of the background soil N₂O fluxes higher than 15 µg N m⁻² h⁻¹ (constituting 74% of the average background soil N₂O fluxes) corresponded to WFPS greater than 49% (wetter conditions; Fig. 2.7G). Background soil N₂O fluxes negatively correlated to soil temperature (Fig. 2.7H) and nitrates (Fig. 2.7I) in all treatment plots.

Table 2.2. Mean (\pm standard error, SE, $n = 4$) soil GHG fluxes (CO₂, CH₄, N₂O) as well as annual soil GHG fluxes measured between May 2019 and June 2020 from control (Ctrl), nitrogen (N), phosphorus (P), and N + P plots of the nutrient manipulation experiment.

Treatment ^a	CO ₂ fluxes (mg C m ⁻² h ⁻¹)	Annual CO ₂ fluxes [†] (Mg C ha ⁻¹ yr ⁻¹)	CH ₄ fluxes (µg C m ⁻² h ⁻¹)	Annual CH ₄ fluxes [†] (kg C ha ⁻¹ yr ⁻¹)	N ₂ O fluxes (µg N m ⁻² h ⁻¹)	Annual N ₂ O fluxes [†] (kg N ha ⁻¹ yr ⁻¹)
Ctrl	164 ± 5.3 ^a	14.5 ± 0.6 ^a	-30.5 ± 4.9 ^a	-2.7 ± 0.4 ^a	20.5 ± 3.2 ^a	1.8 ± 0.3 ^a
N	186 ± 6.5 ^a	16.4 ± 0.9 ^a	-39.7 ± 4.4 ^a	-3.4 ± 0.4 ^a	50.2 ± 11 ^b	4.8 ± 1.5 ^b
P	186 ± 5.3 ^a	16.4 ± 1.0 ^a	-56.2 ± 3.8 ^b	-4.7 ± 0.7 ^b	21.8 ± 2.4 ^a	1.9 ± 0.3 ^a
N + P	197 ± 5.4 ^b	17.3 ± 0.8 ^b	-39.3 ± 6.3 ^a	-3.3 ± 0.7 ^a	53.8 ± 10 ^b	4.6 ± 0.4 ^b

Notes: ^aMeans followed by different lower-case letters indicate significant differences among treatments (One-way analysis of variance, $p \leq 0.05$); [†]Annual soil CO₂ fluxes, CH₄ fluxes, and N₂O fluxes were approximated by applying the trapezoid rule on time intervals between measured flux rates. The mean and annual soil GHG fluxes included both transitory and background flux measurements. Note: Transitory N₂O fluxes (measured within 28 days from fertilization) from N addition plots (N, N + P) were detrended to compensate for the absence of frequent measurements immediately after fertilization coming from sampling GHG fluxes monthly.

2.5. Discussion

2.5.1. Effect of nitrogen and phosphorus addition and soil environmental controls on soil CO₂ fluxes

The annual soil CO₂ effluxes from the control plots (Table 2.2) were lower than those measured from tropical forests in Thailand (Hashimoto *et al.*, 2004) and Hawaii (Townsend *et al.*, 1995), comparable to those from the Democratic Republic of Congo (Baumgartner *et al.*, 2020), Panama (Koehler *et al.*, 2009a; Pendall *et al.*, 2010), Brazil (Sousa Neto *et al.*, 2011), and Cameroon (Verchot *et al.*, 2020), and higher than those reported from Kenya (Wanyama *et al.*, 2019) and Indonesia (van Straaten *et al.*, 2011). The differences in soil CO₂ fluxes between the control plots in this study and studies done in other tropical forest sites may be due to differences in

soil environmental characteristics, e.g., soil C quality and quantity, soil temperature, and moisture availability at the respective sites (Nottingham *et al.*, 2015).

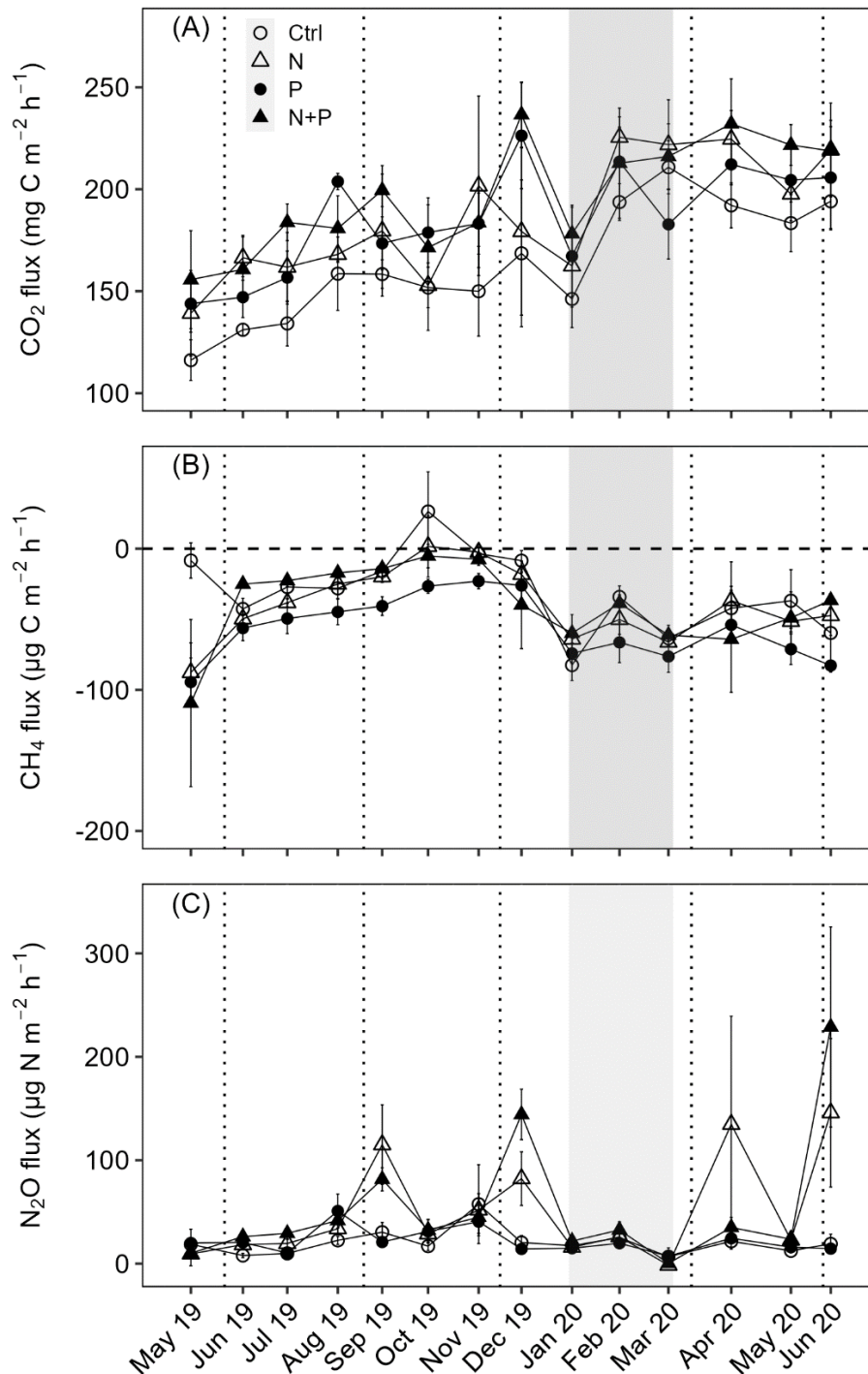


Figure 2.4. Mean (\pm standard error, SE, $n = 4$) soil CO₂ fluxes (A), CH₄ fluxes (B), and N₂O fluxes (C) measured monthly (between May 2019 and June 2020) from control (Ctrl), nitrogen (N), phosphorus (P), and N + P plots of the nutrient manipulation experiment. Vertical lines indicate the timing of each split dose of N (31.3 kg N ha⁻¹), P (12.5 kg P ha⁻¹), and N (31.3 kg N ha⁻¹) + P (12.5 kg P ha⁻¹) fertilization every 3 months. The gray-shaded rectangle marks the beginning and end of the dry season (January and February; monthly precipitation < 100 mm). Note: transitory N₂O fluxes (measured within 28 days from fertilization) from N addition plots (N and N + P) were detrended to compensate for the absence of frequent measurements immediately after fertilization coming from sampling GHG fluxes monthly.

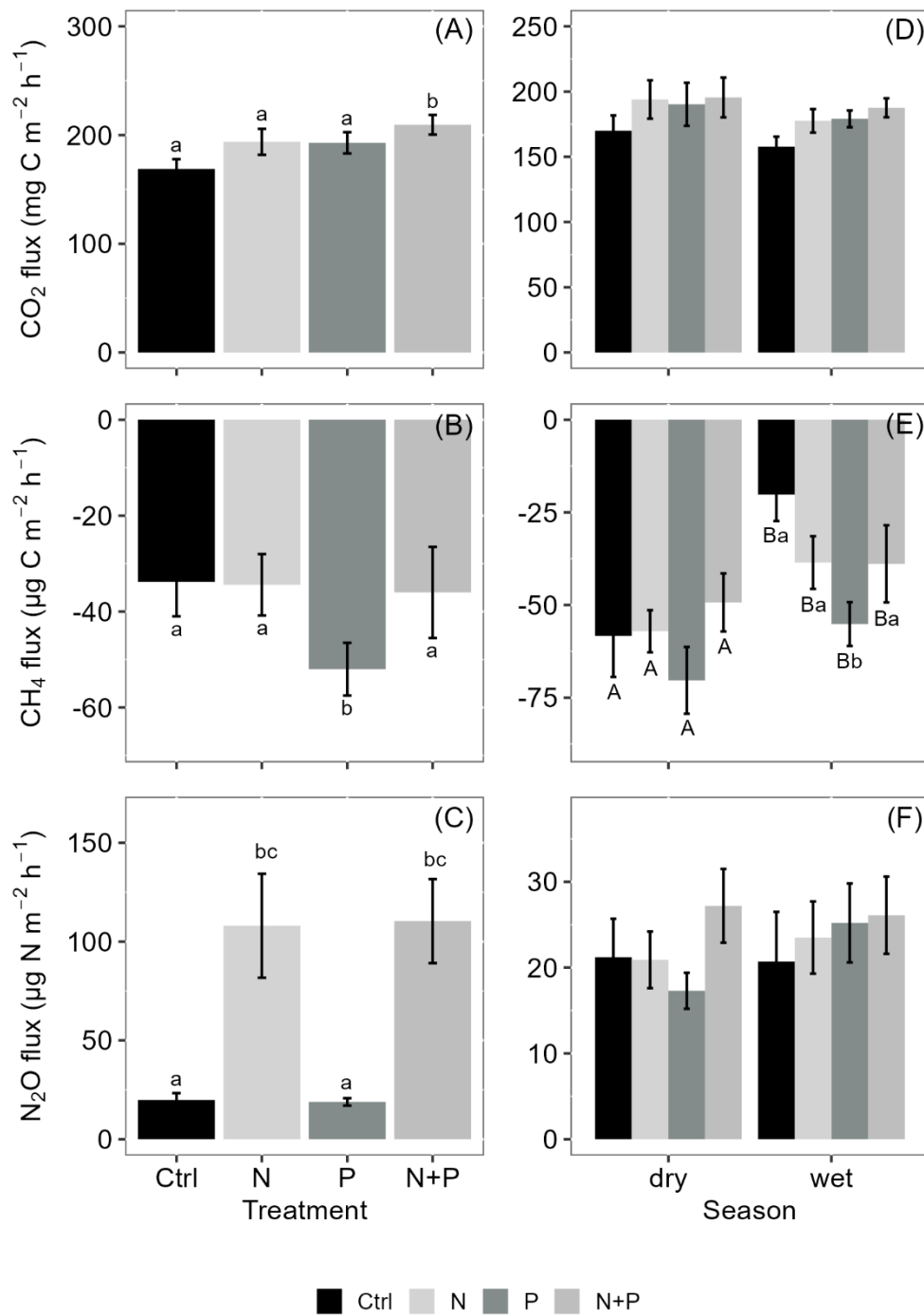


Figure 2.5. Mean (\pm standard error, SE, $n = 4$) soil CO₂ fluxes (A, D), CH₄ fluxes (B, E), and N₂O fluxes (C, F) from the control (Ctrl), nitrogen (N), phosphorus (P), and N + P plots of the nutrient manipulation experiment. Column 1 (A–C) includes only fluxes measured during the transitory phase (0–28 days after fertilization), and all the transitory fluxes were in the wet season (monthly precipitation > 100 mm). Column 2 (D–F) includes only background-level fluxes (fluxes measured more than 28 days after fertilization). Different lowercase letters indicate significant differences between nutrient addition treatments and the control, while different uppercase letters indicate significant differences between seasons (linear mixed effects models; $p \leq 0.05$). Note: transitory N₂O fluxes (measured within 28 days from fertilization) from N addition plots (N and N + P) were detrended to compensate for the absence of frequent measurements immediately after fertilization coming from sampling GHGs monthly.

The alleviation of nutrient limitations on soil biological activity (in microbial communities and root respiration) through fertilizer addition was particularly reflected by the significant increase in transitory CO₂ effluxes following the addition of N and P together (Fig. 2.5A). The transitory phase (< 28 days from fertilization) is the period where the addition of nutrients (N, P, and N + P) is expected to result in a large pulse of microbial activities. However, the fact that the increase in soil CO₂ effluxes was significant only in plots where N and P were added simultaneously (N + P) suggests a possible co-limitation between N and P on soil biological activity (Bréchet *et al.*, 2019). These results seemingly align with the proposed multiple-element limitation concept, which suggests a strong response in microbial-mediated processes upon the supply of limiting nutrients (Fanin *et al.*, 2015). Furthermore, the results likely indicate that some soil respiration sources may respond positively to N addition (Yan *et al.*, 2017), while others may respond positively to P addition (Ma *et al.*, 2020), yielding an overall additive response when added together. An increase in soil CO₂ effluxes following the simultaneous addition of N and P has also been reported in studies like Bréchet *et al.* (2019), and Soong *et al.* (2018) from Panamanian tropical forests.

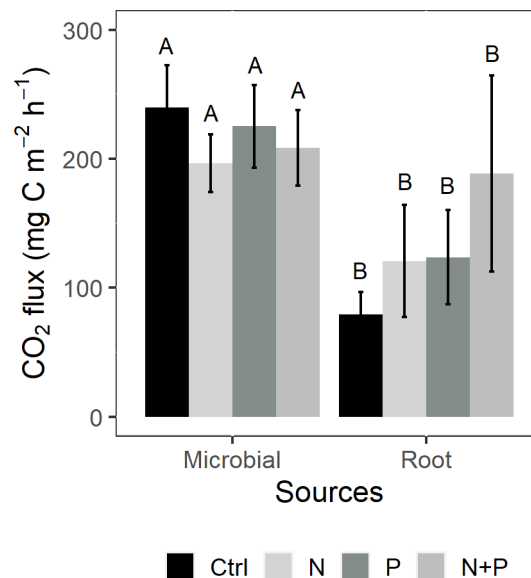


Figure 2.6. Mean (\pm standard error, SE, $n = 4$) soil CO₂ flux from the control (Ctrl), nitrogen (N), phosphorus (P), and N + P plots of a trenching treatment separated into microbial and root sources. Different upper-case letters indicate significant differences between microbial and root contribution to total CO₂ efflux (linear mixed effects models; $p \leq 0.05$).

In contrast, the lack of significant treatment effects on background soil CO₂ efflux (Fig. 2.5A and D) and its different components (heterotrophic and autotrophic; Fig. 2.6) may suggest that numerous counteracting processes could be happening at the same time, hence masking treatment effects. Some studies have, for instance, demonstrated that the addition of N subdues exoenzymes (Li *et al.*, 2018), decreases microbial biomass (Burton *et al.*, 2004; Hicks *et al.*, 2019),

increases net primary productivity (Adamek *et al.*, 2009), and reduces fine root biomass (Cusack *et al.*, 2011), while other studies have reported that P addition increases soil organic matter decomposition in tropical forest ecosystems (Cleveland & Townsend, 2006).

The possibility of counteracting processes at the experimental site is further exemplified by the lack of a relationship between all the measured soil environmental controls (soil temperature, nitrates, and soil moisture) and background CO₂ effluxes (Fig. 2.7A–C). Although these results are consistent with the findings by Baumgartner *et al.* (2020) in the Congo Basin, they contrast several GHG flux studies located in tropical forests that have reported a strong correlation between CO₂ effluxes and soil moisture (van Straaten *et al.*, 2011; Matson *et al.*, 2017 p. 201). For this experimental site, it could be that the minimal temporal fluctuation in soil temperature (Fig. 2.2B), together with the fact that water-filled pore space was mostly > 40% (Fig. 2.2A) during the sampling campaign dampened the effect of soil temperature and moisture on soil CO₂ fluxes.

2.5.2. Effect of nitrogen and phosphorus addition and soil environmental controls on soil CH₄ fluxes

The annual soil CH₄ fluxes from the control plots (Table 2.2) were at the upper end of the CH₄ fluxes measured in lowland tropical forests (Veldkamp *et al.*, 2013; Zheng *et al.*, 2016a; Aronson *et al.*, 2019), and at the lower end of those measured in (sub-)montane tropical forest ecosystems (Yan *et al.*, 2008; Sousa Neto *et al.*, 2011). The difference in soil texture and soil moisture regimes between this experimental site and the other study sites might explain why the CH₄ uptake at the respective sites was different. It is recognized that soil physical properties, particularly texture (Sousa Neto *et al.*, 2011), along with soil moisture content directly control the entry and diffusivity of CH₄ from the atmosphere to the oxidative sites in the soil (Veldkamp *et al.*, 2013).

In this experiment, the significantly higher CH₄ consumption from the P addition plots compared to the control during both the transitory and background periods (Fig. 2.5B and E) is attributed to the alleviation of P limitations affecting methanotrophic activity. Similar findings were reported by Zhang *et al.* (2011) and Yu *et al.* (2017) but contrasted those of Bréchet *et al.* (2019) and Zheng *et al.* (2016). It is worth noting that, although all these studies were located in tropical forests, they differed fundamentally in their experimental designs, the type and amount of fertilizers applied, and the frequency of fertilizer application, which could have influenced the reported CH₄ uptake rates at the respective sites.

The lack of a response in background CH₄ consumption following N fertilization (Fig. 2.5E) is

likely because there were contrasting ecosystem responses to the N addition. On the one hand, the addition of nitrogen significantly increased soil-water-filled pore space in comparison to the control (Fig. 2.2A; possibly as a result of reduced fine root biomass; Cusack *et al.*, 2011), which could have resulted in a decrease in methane uptake. On the other hand, the negative correlation between nitrates and background CH₄ fluxes (Fig. 2.7F) indicates that increases in soil nitrate content should increase CH₄ uptake. Additionally, the lack of a clearer signal in background CH₄ uptake may have something to do with the high variability in the measured CH₄ fluxes (CV = $97 \pm 58\%$) potentially caused by localized termite activity (Brune, 2014; Nauer *et al.*, 2018).

2.5.3. Effect of nitrogen and phosphorus addition and soil environmental controls on soil N₂O fluxes

The annual soil N₂O fluxes from the control plots (Table 2.2) were at the higher end of those measured in (sub-) montane tropical forests (Arias-Navarro *et al.*, 2017 p.; Gütlein *et al.*, 2018; Iddris *et al.*, 2020) and at the lower end of those measured in lowland tropical forest sites (e.g., Koehler *et al.*, 2009). This may either be due to the differences in soil N cycling rates (Koehler *et al.*, 2009b) or the differences in the spatial abundance of leguminous trees at the respective sites (Xu *et al.*, 2020). The immediate flush of N₂O following fertilization (in the transitory phase), both in the N and N + P addition plots (Fig. 2.4C; Fig. 2.5C), is due to the increase in soil N concentrations beyond microbial immobilization and plant N needs (Davidson *et al.*, 2000a p. 200), which is typical of an open or leaky N cycle (Koehler *et al.*, 2009b). Contrary to Kaspari *et al.* (2007) and Koehler *et al.* (2009), sustained N fertilization did not trigger a significant response in background soil N₂O fluxes from N addition plots (Fig. 2.5F). This was unexpected, but given the rapid drainage at the site (sandy texture; Table 2.1), there could have been a substantial loss of added N via leaching, which possibly rid the ecosystem of excess nitrates (Lohse & Matson, 2005; Martinson *et al.*, 2013). Notably, sustained P addition did not result in increased background N₂O fluxes (Fig. 2.5F), which contrasts the findings by Mori *et al.* (2017), who reported that P availability opens up the N cycle by stimulating mineralization of soil organic matter, releasing excess N that is lost as N₂O emissions. At this study site, it could be that either the amount of P added in the experiment was not sufficient to trigger a response in background soil N₂O fluxes or P is not a limiting nutrient for N₂O fluxes given the relatively high pH of the site (Table 2.1).

Unexpectedly, nitrates correlated negatively to background N₂O fluxes (Fig. 2.7I), yet many studies (e.g., Corre *et al.*, 2014; Zhang *et al.*, 2020) have found that nitrates and N₂O fluxes were positively correlated. The likely explanation for such a relationship is the transformation of N₂O to N₂ under wet conditions, which further reduced the amount of nitrates in soil (Matson

et al., 2017). Despite the minimal influence of seasonality on background N₂O fluxes (Fig. 2.5F), a strong positive correlation between background N₂O fluxes and WFPS was observed (Fig. 2.7G), which conforms to the explanation given by the conceptual hole in the pipe (HIP) model.

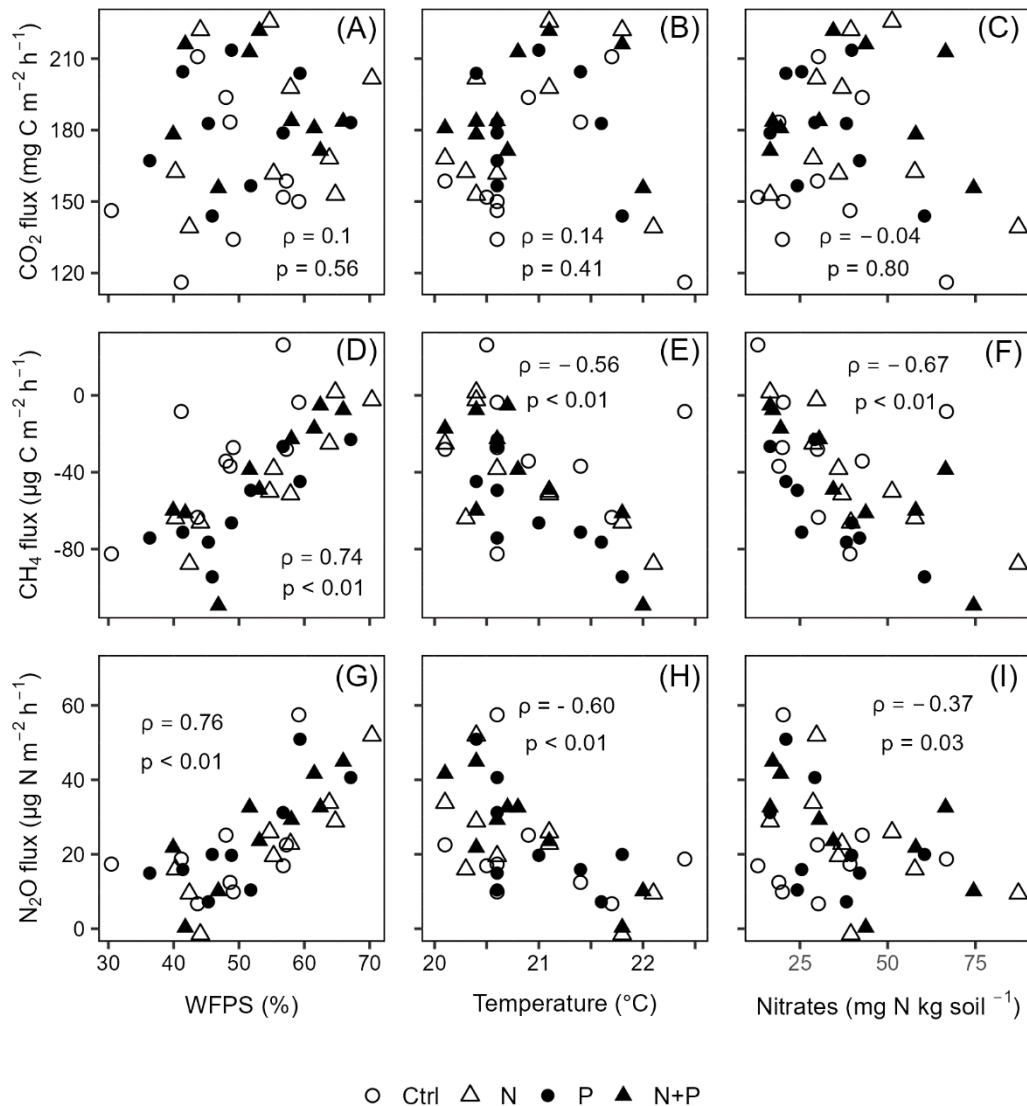


Figure 2.7. The Spearman correlation coefficient between mean background CO₂ (A–C), CH₄ (D–F), and N₂O (G–I) fluxes and WFPS (column 1), soil temperature (column 2), and nitrates (column 3) using monthly measurement means of four replicate treatment plots (i.e., control (Ctrl), nitrogen (N), phosphorus (P), and N + P) taken between May 2019 and June 2020 ($p \leq 0.05$; $n = 16$; i.e., four replicate plots in each of the four treatments). ρ is Spearman's correlation coefficient.

The HIP model places soil aeration status (approximated by WFPS) second to N availability in controlling soil N₂O fluxes. Soil aeration not only directly controls oxygen entry into the soil but also determines how N₂O is produced (denitrification or nitrification) and transported out of the soil (Davidson *et al.*, 2000a). Whereas there seems to be a balance between the denitrifi-

cation and nitrification process at this forest site (given that majority of the measurements corresponded to WFPS of $\leq 60\%$; Fig. 2.7G), the considerable N_2O fluxes at higher WFPS values ($\geq 60\%$; Fig. 2.7G) seem to suggest that denitrification is more dominant than nitrification in producing N_2O in these biomes.

2.6. Conclusion

Nutrient manipulation studies premised in tropical forests are crucial to understanding how these understudied yet very important sinks and sources of soil GHGs subtly respond to changes in soil macronutrient availability. N fertilization (N and N + P) significantly increased N_2O fluxes immediately after fertilization (transitory phase) but had no significant effect on background N_2O fluxes, which might occur if the system would gain N over longer periods. Against our expectations, neither background CO_2 effluxes nor CH_4 uptake decreased following the addition of N, indicating neither a negative effect of a potential surplus of soil N on root and microbial respiration nor a negative effect on methanotrophs. CO_2 effluxes even showed a significant increase during the transitory phase following N and N + P fertilization. However, this effect was only significant for N + P addition, indicating some N and P co-limitation. An increase in CH_4 uptake was found both shortly and after sustained P fertilization, supporting our second hypothesis which suggested that lifting the P limitation on soil methanotrophs would significantly increase CH_4 consumption. Surprisingly, both transitory and background N_2O and CO_2 fluxes (including the different components) were not significantly affected by P fertilization. Overall, the results from this first nutrient manipulation GHG flux study from a wet African tropical forest site, in general, indicate our limited knowledge about the counteracting interactions between N and P inputs and GHG fluxes from different tropical forest ecosystems. This confines any general conclusions and equally limits our ability to parametrize tropical forest ecosystems in Earth system models. Nevertheless, the contribution of tropical forest biomes to the global soil GHG budgets maybe disproportionately altered via potential future increases in N and P availability.

CHAPTER 3. SOIL GREENHOUSE GAS FLUXES FOLLOWING CONVERSION OF TROPICAL FORESTS TO FERTILIZER-BASED SUGARCANE SYSTEMS IN NORTH-WESTERN UGANDA

with minor editing differences, published as: Tamale, J., van Straaten, O., Hüppi, R., Turyagyenda, L.F., Fiener, P. and Doetterl, S. 2022. Soil greenhouse gas fluxes following conversion of tropical forests to fertilizer-based sugarcane systems in north-western Uganda. *Agriculture, Ecosystems, and Environment Journal*. 2022, 333, 1-13

3.1. Abstract

Tropical deforestation for fertilizer-based agriculture has greatly increased in the last decades resulting in significant greenhouse gas (GHG; carbon dioxide (CO₂), methane (CH₄), and nitrous oxide (N₂O)) emissions. Unfortunately, empirical studies on soil GHG fluxes from African deforestation hotspots are still limited, creating uncertainties in global GHG flux budgets. Therefore, we assessed how soil GHG fluxes along with their auxiliary controls (water-filled pore space (WFPS), temperature, and mineral nitrogen (N)) differed between the forest and sugarcane plantations. This assessment was based on monthly (forest) and intensive (sugarcane) GHG flux and auxiliary measurements between May 2019 and June 2020. Measurements were conducted in four reference forest plots and 12 sugarcane plots randomly assigned to three fertilization treatment groups (low, standard, and high), representing the fertilization gradient used by sugarcane farmers in Uganda. Despite the use of different fertilization rates as treatments for the sugarcane experiment, neither auxiliary controls nor soil GHG fluxes significantly differed among the treatments. Soil CO₂ effluxes were higher under sugarcane ($17.6 \pm 0.0 \text{ Mg C ha}^{-1} \text{ yr}^{-1}$) compared to the forest ($14.5 \pm 0.1 \text{ Mg C ha}^{-1} \text{ yr}^{-1}$; $p < 0.001$) because of the higher autotrophic respiration from the sugarcane's fine root biomass and the microbial decomposition of the sugarcane's larger soil organic carbon (SOC) stocks. Conversely, soil CH₄ uptake under sugarcane ($-1.1 \pm 0.0 \text{ kg C ha}^{-1} \text{ yr}^{-1}$) was three times lower than under forest ($-3.1 \pm 0.0 \text{ kg C ha}^{-1} \text{ yr}^{-1}$; $p < 0.001$), owing to the likely alteration of methanotroph abundance upon conversion. Likewise, soil N₂O emissions were smaller under sugarcane ($1.3 \pm 0.0 \text{ kg N ha}^{-1} \text{ yr}^{-1}$) compared to the forest ($1.8 \pm 0.0 \text{ kg N ha}^{-1} \text{ yr}^{-1}$; $p < 0.001$) because excess N from fertilizer addition in the sugarcane was either lost through leaching or taken up by the sugarcane crop. Only seasonal variability in WFPS, among the auxiliary controls, affected CH₄ uptake at both sites ($p < 0.001$) and soil CO₂ effluxes under sugarcane ($p = 0.018$). Noteworthy, soil N₂O fluxes from both sites were unaltered by the seasonality-mediated changes in auxiliary controls. All the results combined together demonstrate that even with the higher soil CO₂ effluxes under sugarcane compared to the forest, the sugarcane systems in the study area acted as a C sink because the SOC sequestration (a proxy for the uptake of CO₂) under sugarcane plantations of different ages far exceeded SOM mineralization. However, the higher SOC sequestration under sugarcane does not offset the initial significant loss in the above and belowground biomass C loss immediately after forest conversion. Moreover, the C sink under sugarcane can change if CO₂-equivalents related to N₂O and CH₄ fluxes are considered in the calculation of the sugarcane's C footprint.

3.2. Introduction

Tropical deforestation for fertilizer-intensive agriculture has increased greatly over the last decades and remains one of the greatest global environmental challenges of the 21st century because it contributes significantly to the emission of greenhouse gases (GHGs; Gibbs & Herold, 2007; Ciais *et al.*, 2014; Pearson *et al.*, 2017). In Uganda, approximately 60% of the forestland (~ 3 million hectares) has been lost to deforestation between 1990 and 2015 (NEMA, 2017), making this developing nation, one of the countries in tropical Africa that are currently faced with a deforestation crisis (Josephat, 2018). Deforested areas in Uganda are mostly allocated to large-scale sugarcane (*Saccharum officinarum*) cultivation and as a consequence, land area under fertilizer-based sugarcane cultivation has more than tripled in the past 20 years (Mwavu *et al.*, 2018). The expansion of the Ugandan sugarcane sector is largely premised on scaling up sugarcane production to match the per capita increase in sugar demand (currently at 12 kg sugar yr⁻¹; Johnston & Meyer, 2008), improve household incomes (Mwavu *et al.*, 2018), and provide feedstock for the emerging biofuel industry (Isabirye *et al.*, 2013). However, the impact of this land use shift on the temporal and spatial dynamics of the three main biogenic GHGs (carbon dioxide (CO₂), methane (CH₄), and nitrous oxide (N₂O)) is still poorly understood. Tropical deforestation together with the associated biomass burning is reported to not only set free significant amounts of C stored in the aboveground biomass (i.e., ~ 0.6 – 1.2 Gt C · yr⁻¹; Achard *et al.*, 2014) but also lead to long-term alterations in the soil-vegetation feedbacks (Runyan *et al.*, 2012). These in turn affect soil properties (particularly bulk density (BD), pH, soil organic carbon (SOC), effective cation exchange capacity (ECEC), base saturation (BS), and C: N ratio) that constrain the microbial production and consumption of the biogenic GHGs in the soil or at the soil-atmospheric interface (Veldkamp *et al.*, 2020). Further, it has been shown that the routine management operations practiced in cropland equally affect soil GHG fluxes (CO₂ (Oertel *et al.*, 2016), CH₄ (Dattamudi *et al.*, 2019), and N₂O fluxes (D'Haene *et al.*, 2008)). For instance, in many croplands, seedbed preparation, weeding, and harvesting operations are usually achieved through several tillage operations (Naseri *et al.*, 2020). Tillage, however, exposes the soil surface to higher temperatures resulting in increased organic matter decomposition and increased CO₂ emissions (Six *et al.*, 1998). Moreover, increased traffic of machinery over the fields (during the different tillage and field operations) compacts surface soils resulting in reduced diffusive entry of CH₄ from the atmosphere to the oxidative sites in the soil (Dexter, 2004). Besides tillage, many large-scale sugarcane production systems around the world rely on large doses of nitrogen (N- between 150 and 300 kg N ha⁻¹ yr⁻¹; Kostka *et al.*, 2009) and potassium (K- between 300 and 600 kg K ha⁻¹ yr⁻¹; Thorburn *et al.*, 2010), to maintain high yields

both in cane and ratoon fields (Thorburn *et al.*, 2005). However, high N fertilizer doses together with the warm and humid tropical environments where the sugarcane grows (Thorburn *et al.*, 2010) predispose the sugarcane fields to increased N₂O emissions (Dattamudi *et al.*, 2019). It has also been shown that excessive N fertilization inhibits methanotrophic CH₄ uptake due to the increased affinity of the NH₄⁺ ions for the oxidative sites on CH₄-monooxygenase (Veldkamp *et al.*, 2013). Little is known, however, about the effect of N fertilization on CO₂ effluxes from sugarcane fields. Management of sugarcane residues before harvesting of the cane stalks is another practice that has been reported to significantly affect GHG fluxes from sugarcane fields (Tavares *et al.*, 2018). Some sugarcane growers set fields on fire before harvesting to speed up harvesting operations (Blair, 2000) while others leave residues standing on the field after harvesting the stalks (also known as the green cane harvesting system—GCHS; Graham & Haynes, 2006) mainly to conserve soil moisture and replenish soil fertility (Robertson & Thorburn, 2007). On the one hand, burning of the residues leads to both increased N and P volatilization (Britts *et al.*, 2020) and higher CO₂ emissions from sugarcane fields (De Figueiredo & La Scala, 2011). On the other hand, GCHS increases C sequestration via increased C inputs to soil (Robertson & Thorburn, 2007) but these gains in SOC stocks are often offset by increased N₂O and CH₄ emissions from the unburnt fields (Dattamudi *et al.*, 2019). In Uganda, although nearly all sugarcane farmers leave residues standing on the fields and employ tillage operations at seedbed preparation and weeding, fertilizer application practices among these farmers can greatly differ due to financial reasons (Otieno *et al.*, 2019). The majority of the farmers typically apply a one-time standard fertilizer dose of urea ((NH₂)₂CO; 70 kg N ha⁻¹) mixed with muriate of potash (KCl; 23 kg K ha⁻¹) to the sugarcane fields during the growth cycle. However, there are still farmers that apply either less or more than the recommended standard fertilizer application rate. The different fertilizer application rates in combination with the tillage and residue management practices by farmers are expected to invariably affect soil GHG fluxes. However, there is still no concrete evidence on how replacing tropical forests with sugarcane managed under different fertilization regimes affects soil GHG fluxes, creating major uncertainties in our assessment of the role tropical land use change plays in the soil-atmospheric exchange of C and N. It was for this reason that we quantified soil GHG fluxes (CO₂, CH₄, and N₂O) along with their potential auxiliary controls (water-filled pore space (WFPS), temperature, and mineral N) from four reference forest plots and 12 replicate plots of a completely randomized design (CRD) experiment premised in a neighboring 20-year-old sugarcane plantation in north-western Uganda. In the following, it was hypothesized that tropical forest conversion for fertilizer-based sugarcane systems would result in:

1. Increased CO₂ emissions from the respective sugarcane CRD treatment plots compared to the reference forest plots (low input > standard input > high input > reference forest plots) coming from the continuous loss of forest SOC, until the soils under sugarcane reach a new equilibrium and the higher autotrophic respiration by the sugarcane fibrous roots.
2. Reduced CH₄ uptake in the respective sugarcane CRD treatment plots compared to the reference forest plots (high input < standard input < low input < reference forest plots) resulting from reduced methanotrophic activity under the heavily fertilized and compacted (from machinery traffic) sugarcane fields.
3. Increased N₂O emissions from the respective sugarcane CRD treatment plots compared to the reference forest plots (high input > standard input > low input > reference forest plots) attributed to N fertilization and increased mineralization of the retained crop residues.

3.3. Materials and methods

3.3.1. Study area

The study was conducted in north-western Uganda where large-scale deforestation for fertilizer-based sugarcane cultivation has been documented for several decades. The long-term mean annual temperature for the study area is about 25 °C while the annual precipitation is about 1700 mm (Lukwago *et al.*, 2020). Rainfall in the region follows a bimodal distribution pattern divided into two main wet seasons (March to May and August to November), and an extended (December to February) and short dry season (June to July; Lukwago *et al.*, 2020).

3.3.2. Experimental design

Two similar test sites with respect to altitude, topography, geology, soils, and climate were selected for the study (Appendix T.1). Site 1 (1°44'28.4" N, 31°32'11.0" E) represents the location of the nutrient manipulation experiment (NME) in the forest—Budongo Central Forest Reserve. The forest site characteristics as well as further details about the NME were reported by Manu *et al.* (2022). The present study builds on an earlier study conducted within the framework of the NME (Tamale *et al.*, 2021) to disentangle the effect of deforestation for fertilized sugarcane on soil GHG fluxes. In the present study, we compare the soil GHG fluxes measured from the untreated forest plots of the Tamale *et al.* (2021) study, here after referred to as reference forest plots, to the soil GHG fluxes measured from 12 replicate plots of a completely randomized design (CRD) experiment established in the neighboring sugarcane plantation (1°41'37.9" N, 31°30'6.3" E). The sugarcane CRD experiment plot dimensions (plot size: 40 m x 40 m, inner measurement core: 30 m x 30 m, and guard row: 40 m) were identical to those of the reference

forest plots. The CRD experiment consisted of a one-time standard fertilizer doze (70 kg N (as urea) + 23 kg K (as muriate of potash) ha⁻¹ growth cycle⁻¹), low fertilizer dose (0.5 times standard), and high fertilizer dose (1.5 times standard) as treatments. The fertilizer dozes used in the sugarcane CRD experiment represented a gradient of fertilizer application rates used by sugarcane farmers in this region (i.e., low, standard, and high). Each treatment was replicated four times, hence, the sugarcane CRD experiment consisted of 12 plots (n = 12, three treatments x four replications). The treatments were applied to the replicate plots of the CRD experiment on 14 May 2019. Inter-row weeding was done once every 2.5 months in the first eight months using a hand hoe, and none after the eighth month, since the sugarcane canopy had increased significantly to efficiently subdue the weeds. Additionally, the sugarcane fields hosting the CRD experiment were maintained as ratoon crops with residues returned to the fields after every harvest cycle.

3.3.3. Soil sampling and analysis

Soil physico-chemical characterization (i.e., BD, mineral N, OC, pH, and texture) over 1 m depth was done for both the forest and sugarcane sites before the start of soil GHG flux measurements. In the forest, soil samples were obtained from ten random locations within each of the four reference plots for the top 0.10 m depth. However, for depths between 0.10 and 1 m, soil samples were obtained outside the established reference forest plots to minimize disturbance to the soil microenvironment within these plots. For 0.10 – 0.50 m depth, soil samples were obtained from five random points within each of the 16 reconnaissance plots located at ~ 500 m from the current location of reference forest plots while for 0.50 – 1 m depth, soil samples were taken from 1 m pits dug in the inter plot spaces of the reference plots. At the sugarcane site, soil samples were obtained at three random locations within every established plot of the CRD experiment for three depths (0 – 0.10 m, 0.10 – 0.30 m, and 0.30 – 0.50 m), and from four pits (1 m x 1 m x 1.1 m) dug in the inter plot spaces of the established plots for the depths between 0.50 and 1.00 m. To have an indication, if the SOC stocks after 20 years of sugarcane cultivation had already approached a new C equilibrium, we also took soil samples in 50 - year-old ratoon plantations. These plantations were located about 1–2 km from the current location of the 20-year-old sugarcane plantations and both had similar soil types, climate, weed management, residue retention, and fertilization practices. Soil samples obtained from the same depth within a plot or pit were thoroughly mixed and about 500 g of the homogenized soil sample was air dried (~ 25 °C) and submitted to the University of Augsburg (Germany) and ETH Zurich (Switzerland) for analysis. Soil samples for C, N, and pH analyses were sieved to 2 mm before being

used in the analyses. Soil pH was measured on a 1:2.5 soil water suspension using a pH electrode. Soil BD was determined from the respective oven-dry soil sample masses (105 °C for 48 h) together with the Kopecky ring volume (volume = 251 cm³) used in obtaining the soil samples while considering the stone content. Soil C and N concentrations were determined using a C/N analyzer (Vario EL Cube CNS Elementar Analyzer, Germany). The respective soil C and N stocks of every depth interval per plot were calculated based on the soil BD measurements. At both sites (forest and sugarcane), the texture was determined using samples obtained from the profile pits for two depths, 0.10 m (for topsoil) and 0.50–0.60 m (for deeper soils) while textural analysis was done using a laser diffractometer (LS 13 320 Laser Diffraction Particle Size Analyzer, Beckman Coulter, United States of America).

3.3.4. Aboveground and belowground biomass determination

Aboveground biomass (AGB) was estimated for two tree diameter classes (1–10 cm and > 10 cm; Manu *et al.*, 2022) in the forest while in the sugarcane, only the maximum AGB at harvest was considered. Forest AGB was converted to C based on the widely accepted C fraction conversion factor for tropical forest biomass (0.50; Sarmiento *et al.*, 2005) while in the sugarcane, the AGB was converted to C using a C fraction factor of 0.43, determined with the C/N analyzer. Belowground biomass (BGB) in the sugarcane consisted of only living fine roots (diameter < 2 mm) given the fibrous nature of the sugarcane's root system, and was based on soil monoliths (measuring 0.20 m (*L*) x 0.20 m (*W*)) obtained from one face of every pit (described in sub section 3.3.3) following 0.10 m depth increments (*D*) down to 1 m. The obtained soil materials were thoroughly washed to isolate roots from the soil mass. The root samples were oven dried at 60 °C for 48 h at the National Agricultural Research Laboratories, Kampala, Uganda, and weighed to determine the root biomass per depth increment. However, in the forest, BGB consisted of both coarse (diameter > 2 mm) and fine (diameter < 2 mm) roots based on the pits (described in sub section 3.3.3). It is worth noting that whereas the pits provided a good estimate of the fine root biomass in the forest, they far underestimated the coarse root biomass because they were dug at a considerable distance away from the bases of big trees to minimize ecosystem disturbance. This consequently resulted in the exclusion of a significant proportion of coarse roots closest to big tree bases, creating a bias in the pit BGB data. To overcome this bias, we estimated the forest coarse roots from AGB using Eq. (3.1) proposed by Cairns *et al.* (1997) before summing it with fine roots determined from pits to obtain the forest BGB. Next, both the forest and sugarcane BGB were converted to C using a C fraction factor of 0.43 determined with a C/N analyzer.

$$BGB_{cf} = e^{(-1.0587+0.8836*\ln(AGB_f))} \quad (3.1)$$

where BGB_{cf} is the coarse root component of the forest BGB , expressed in kg dry matter ha⁻¹ while AGB_f is the aboveground biomass of the forest, expressed in kg dry matter ha⁻¹.

3.3.5. Soil greenhouse gas flux measurements, auxiliary measurements, flux calculation, and soil greenhouse gas flux budget estimation

Soil GHG flux measurements were conducted inside the inner measurement core (measuring 30 m x 30 m) of every plot in the forest (four) and sugarcane (twelve), with every core randomly installed with four chamber bases (made from a 250 mm PN10 PVC pipe, area = 0.044 m², and volume = ~ 12 L) at a depth of about 0.03 m. The installation of chamber bases was done nearly a month before the first gas sampling (May 2019), which together with leaving the chamber bases in place throughout the measurement period, ensured that any potential disturbances to the soil microenvironment under the chamber bases were minimized. Gas sampling was done on a plot-by-plot basis and completely random to ensure that any effects that the diurnal temperature changes may have on the measured soil GHG fluxes were minimized. A minute before the gas sampling started, all the chamber bases were fanned to ensure that the concentrations of the GHGs at the soil surface and the atmosphere immediately above the chamber were in equilibrium. Next, all the chamber bases in every plot were simultaneously covered with vented polyvinyl hoods (volume = 6.78 L) fitted with bulkheads (sampling ports). A composite gas sample (60 mL) was obtained at 3, 13, 23, and 33 min by drawing 15 mL of the gas sample from the individual chamber head airspaces and pooling them together at every time interval using the protocol of Arias-Navarro *et al.* (2013). Next, 40 mL of the composite gas sample was flushed through a 12 mL pre-evacuated Labco exetainer (Labco, UK) before transferring the remaining 20 mL into the exetainer and bringing it to an over-pressure. Soil GHG fluxes from the reference forest plots were measured monthly throughout the measurement period while for sugarcane, more intensive measurements were done in the first six months following fertilization before switching to monthly measurements for the remaining period of gas sampling. The intensive measurements aimed to capture the expected N₂O emission flush following fertilization in the sugarcane and were done as follows; a day before fertilization, 3-, 5-, 7-days after fertilization, weekly in the four weeks that followed fertilization, and then bi-weekly from the second to the sixth month after fertilization. In parallel to gas sampling, auxiliary controls (soil temperature, volumetric water content, and soil mineral N) were determined at 0.05 m depth in locations close to the respectively installed chamber bases. Soil temperature was measured using a digital thermometer (Greisinger GMH 3230, Germany) while volumetric water content was

determined using a calibrated Theta FDR probe (AT Delta-T Devices Limited, United Kingdom). Soil mineral N content (consisting of nitrate (NO_3^-) and ammonium (NH_4^+)) was determined using the RQflex®10 reflectometer (Merck, Germany). It is worth noting that the gas-sampling period (May 2019 to June 2020) was wetter than normal because the precipitation amounts received during this period far exceeded the long-term mean annual precipitation (36%; Appendix T.1). During the gas sampling campaign, batches of gas-filled exetainers were shipped to ETH Zürich, Switzerland, for analysis at the gas chromatograph (GC; Scion 456-GC Bruker, Germany). The GC has an auto-sampler and is equipped with a thermal conductivity detector (CO_2), flame ionization detector (CH_4), and an electron capture detector (N_2O). Soil CO_2 , CH_4 , and N_2O concentrations in the collected composite gas samples were determined by comparing the peak areas of the samples to the peak areas of a set of standards for the gases of interest. Soil CO_2 , CH_4 , and N_2O fluxes were determined using the "gasflxvis" scheme described in detail by Hüppi *et al.* (2018). Net soil GHG flux budgets for both the forest and sugarcane plantations were estimated for a 100-year time window by converting the annual soil GHG fluxes to CO_2 -equivalents ($\text{CO}_2\text{-eq}$) using factors of 1, 28, and 265 for CO_2 , CH_4 , and N_2O , respectively (IPCC, 2021).

3.3.6. Statistical analysis

Before conducting any statistical analyses, time series data on soil GHG fluxes and the auxiliary controls were divided into wet and dry seasons to understand how seasonality affects both the soil GHG fluxes and auxiliary controls. The wet season data included all sampling points where monthly precipitation was greater than 100 mm and the reverse was true for the dry season. It is worth noting that although both soil NH_4^+ and NO_3^- concentrations were monitored throughout the GHG sampling period, only the NO_3^- dataset is presented in the paper because the NH_4^+ concentration at both sites was mostly low and sometimes below the reflectometer detection limit. All the data were inspected for normality and homoscedasticity before running any of the parametric tests (particularly one-way analysis of variance (ANOVA) and linear mixed effects models (LMEMs)) using quantile-quantile plots and Shapiro test, and Levene test, respectively. In case the diagnostic plots or (and) tests revealed skewness of the data or heteroscedasticity, a Tukey transformation was applied to the data, followed by running the normality and homoscedasticity tests again. However, if after transformation, normality and homoscedasticity were not restored, an equivalent nonparametric statistical test was selected. These included the generalized linear mixed effects models (GLMMs), the spearman-rank correlation coefficient test, and the Kruskal–Wallis test. The GLMMs and LMEMs included the respective soil GHG fluxes (CO_2 , CH_4 , and N_2O) and auxiliary controls (WFPS, temperature, and mineral N) as response

variables, land use type (forest and sugarcane under different fertilization regimes) as the fixed effects, plot numbers and sampling days as random effects. In some cases, the LMEMs were extended to cater to heteroscedasticity and correlation between measurements taken at closely spaced intervals. Extension of the LMEMs was only done if it improved the relative goodness of fit of the model reflected by a lower Akaike information criteria value. Annual soil CO₂, CH₄, and N₂O fluxes were approximated through the application of a trapezoidal interpolation on the time intervals between measured soil GHG flux rates, assuming a constant daily flux rate. The differences in soil physico-chemical characteristics between the sugarcane and forest sites were checked with either one-way ANOVA or Kruskal-Wallis test. The respective ANOVA models included different soil properties as response variables and land use types as predictor variables. The spearman-rank correlation coefficient test was used to determine the relationship between the measured soil GHG fluxes and auxiliary controls. Throughout the paper, statistical analyses were done in R 3.6.3 (R Development Core Team, 2019) using the ‘*car*’ (ANOVA), ‘*nlme*’ (LMEMs), ‘*mass*’ (GLMMs), and inbuilt packages (for spearman-rank correlation coefficient test and Kruskal-Wallis test), with statistical significance for all the tests set at $p \leq 0.05$.

3.4. Results

3.4. 1. Auxiliary controls and soil greenhouse gas fluxes

Topsoil (measured at 0.05 m depth) WFPS, temperature, and NO₃⁻ did not significantly differ between the treatments of the sugarcane CRD experiment despite the application of varying quantities of N and K fertilizers (i.e., low, standard, and high) as treatments for the CRD experiment (Fig. 3.1; Table 3.1). Soil WFPS ranged between 6% and 72% in the sugarcane and between 24% and 69% in the forest. WFPS exhibited seasonal variability, with larger WFPS measured in the wet season compared to the dry season both in the forest (14%; Table 3.1; $p < 0.001$) and in the sugarcane (20%; Table 3.1; $p < 0.001$). Significantly higher WFPS was measured in the forest compared to the sugarcane both in the wet (13%; Table 3.1; $p < 0.001$) and in the dry season (18%; Table 3.1; $p < 0.001$). In contrast, there was a minimal to negligible variation in soil temperature (0.2 °C) in the forest across the wet and dry seasons (Fig. 3.1B; Table 3.1) compared to the sugarcane where the wet season soil temperature was 3.8 °C higher than the dry season (Fig. 3.1B; Table 3.1; $p < 0.001$). Forest NO₃⁻ concentrations in soil solution measured in the dry season were nearly twofold higher than in the wet season (Table 3.1; $p < 0.001$). However, under sugarcane, no significant differences in soil NO₃⁻ concentrations were detected between the wet and dry seasons despite measuring higher soil NO₃⁻ concentrations in the wet season compared to the dry season (Table 3.1). Overall, the forest had significantly larger soil

NO_3^- concentrations than the sugarcane both in the wet and dry seasons (Table 3.1; $p < 0.001$).

Table 3.1. Seasonal mean (\pm standard error, SE, $n = 4$) auxiliary controls (water-filled pore space (WFPS), soil temperature, and nitrate (NO_3^-)) and soil greenhouse gas fluxes (CO_2 , CH_4 , and N_2O) measured in the topsoil (at 0.05 m) from the reference forest plots and the sugarcane under different treatments (low, standard, and high).

Treatment /season	WFPS (%)	Soil temperature ($^{\circ}\text{C}$)	NO_3^- (mg N kg^{-1})	Daily CO_2 fluxes (mg C m^{-2} h^{-1})	Daily CH_4 fluxes ($\mu\text{g C m}^{-2}$ h^{-1})	Daily N_2O fluxes ($\mu\text{g N m}^{-2}$ h^{-1})	
Wet season							
Forest	$53.8 \pm 1.4^{\text{Aa}}$	$21.0 \pm 0.1^{\text{a}}$	$27.5 \pm 2.9^{\text{Aa}}$	$165 \pm 5^{\text{a}}$	$-31.2 \pm 3.3^{\text{Aa}}$	$19.9 \pm 3.7^{\text{a}}$	
Sugarcane	Low	39.8 ± 1.3	25.1 ± 0.4	7.1 ± 1.3	228 ± 5	-8.7 ± 2.3	6.2 ± 0.9
	Standard	42.8 ± 1.4	24.1 ± 0.3	10.5 ± 1.9	217 ± 7	-9.8 ± 2.2	7.3 ± 1.2
	High	40.1 ± 1.3	24.5 ± 0.4	8.2 ± 1.3	200 ± 5	-12.5 ± 1.9	5.7 ± 0.9
Mean ^a	$40.9 \pm 0.8^{\text{Ab}}$	$24.6 \pm 0.2^{\text{Ab}}$	$8.6 \pm 0.9^{\text{b}}$	$215 \pm 3^{\text{Ab}}$	$-10.3 \pm 1.2^{\text{Ab}}$	$6.4 \pm 0.6^{\text{b}}$	
Dry season							
Forest	$39.2 \pm 3.9^{\text{Ba}}$	$20.8 \pm 0.1^{\text{a}}$	$41.0 \pm 4.4^{\text{Ba}}$	$167 \pm 12^{\text{a}}$	$-60.2 \pm 8.0^{\text{Ba}}$	$20.9 \pm 4.5^{\text{a}}$	
Sugarcane	Low	20.8 ± 2.4	21.6 ± 0.3	0.0 ± 0.0	154 ± 7	-27.8 ± 5.6	0.9 ± 1.0
	Standard	22.5 ± 2.2	20.6 ± 0.4	0.6 ± 0.6	146 ± 6	-20.0 ± 10.2	1.7 ± 2.1
	High	20.1 ± 2.3	20.3 ± 0.4	2.1 ± 1.4	150 ± 10	-24.4 ± 2.3	1.8 ± 0.7
Mean ^a	$21.1 \pm 1.3^{\text{Bb}}$	$20.8 \pm 0.2^{\text{Ba}}$	$0.9 \pm 0.7^{\text{b}}$	$150 \pm 4^{\text{Bb}}$	$-24.0 \pm 3.8^{\text{Bb}}$	$1.5 \pm 0.8^{\text{b}}$	

^aMean (\pm standard error, SE, $n = 3$) of the treatments (i.e., low, standard, and high) of the CRD experiment in the sugarcane. Different lowercase letters indicate significant differences between the sugarcane and forest while different uppercase letters indicate significant differences between seasons within each land use ((Generalized) linear mixed-effects models with Tukey's HSD test at $p \leq 0.05$). Standard equals 70 kg N + 23 kg K ha^{-1} growth cycle⁻¹, low equals 0.5 times standard and high equals 1.5 times standard.

Similarly, soil GHG fluxes did not significantly differ among the treatments of the CRD experiment in the sugarcane (both in the wet and dry seasons), despite the application of varying fertilization rates as treatments for the CRD experiment (Table 3.1). During the measurement period (May 2019 to June 2020), daily soil CO_2 effluxes varied across space and time ranging between 67 and 386 mg C m^{-2} h^{-1} under sugarcane and between 78 and 240 mg C m^{-2} h^{-1} under forest. Interestingly, forest soil CO_2 effluxes were unaffected by seasonality (Table 3.1). However, under sugarcane, significantly higher CO_2 effluxes were measured in the wet season compared to the dry season (Table 3.1; $p < 0.001$). During the wet season, sugarcane soil CO_2 respiration was 1.3 times larger than the forest soil CO_2 respiration (Table 3.1; $p < 0.001$), while the reverse was found for the dry season (Table 3.1; $p = 0.018$). The highest soil CO_2 effluxes were measured in June 2019 for sugarcane and in March 2020 for the forest (Fig. 3.2A), with both periods representing a transition from either wet to dry season (sugarcane) or dry to wet season (forest), and were characterized by moderate WFPS (about 40%; Fig. 3.1A). Both forest and sugarcane soil CO_2 effluxes positively correlated to WFPS and soil temperature, although, these correlations were weak (Table 3.2; $p \leq 0.05$; $r < 0.5$). In contrast, soil CO_2 effluxes from both the forest and sugarcane were negatively correlated to NO_3^- , and both relationships were similarly weak (Table 3.2; $p \leq 0.05$; $r < 0.5$). Soil CH_4 fluxes exhibited both a high spatial and temporal variability. Spatially, soil CH_4 uptake varied between an uptake of $-94.5 \mu\text{g C m}^{-2}$ h^{-1} and emission of $15.4 \mu\text{g C m}^{-2}$ h^{-1} under forest, and an uptake of $-128.7 \mu\text{g C m}^{-2}$ h^{-1} and a

release of $80.4 \mu\text{g C m}^{-2} \text{h}^{-1}$ under sugarcane throughout the measurement period.

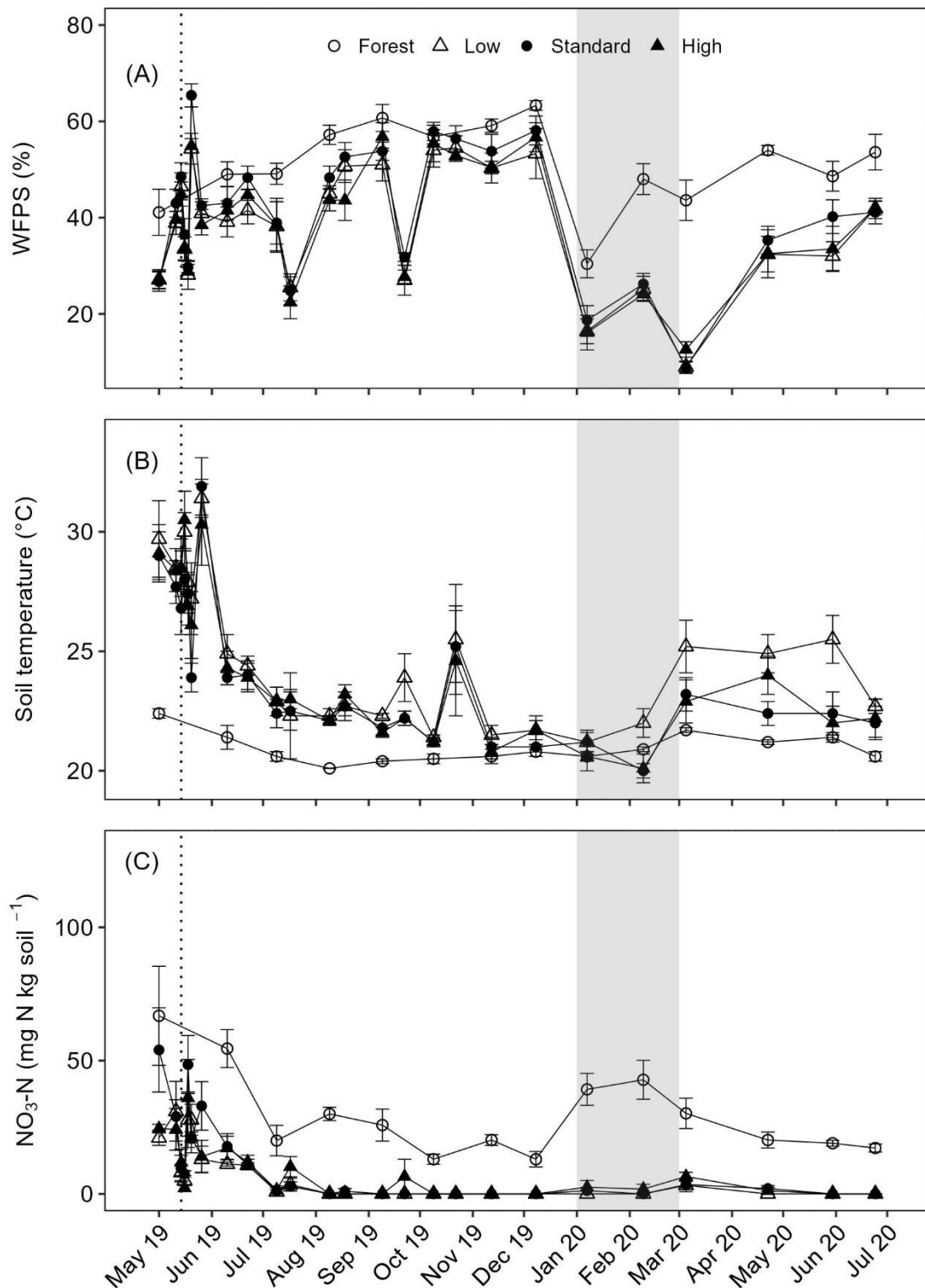


Figure 3.1. Mean (\pm standard error, SE, $n = 4$) water-filled pore space (WFPS; A), soil temperature (B), and nitrate (NO_3^-) content (C) measured at 0.05 m (May 2019 to June 2020) from the reference forest plots and the replicate treatment plots in the 20-year-old sugarcane plantation. The mean WFPS, soil temperature, and NO_3^- content result from four plots per treatment for every sampling time. The dashed vertical line indicates the application of urea and muriate of potash fertilizers in the sugarcane plots. The gray shaded rectangle (A-C) indicates the start and end of the dry period (monthly precipitation ≤ 100 mm). Standard equals $70 \text{ kg N} + 23 \text{ kg K ha}^{-1}$ growth cycle⁻¹, low equals 0.5 times standard and high equals 1.5 times standard

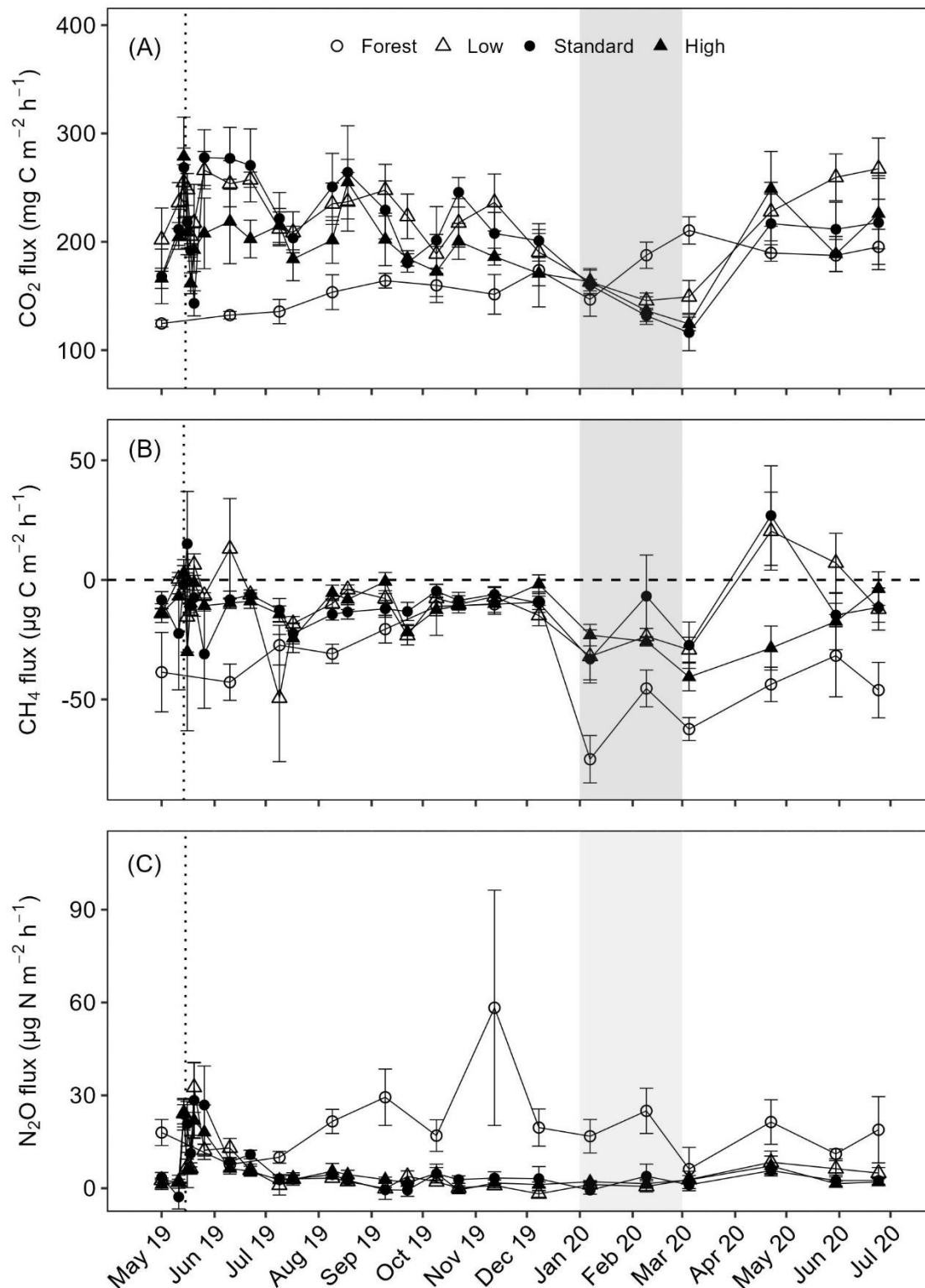


Figure 3.2. Mean (\pm standard error, $n = 4$) soil CO₂ (A), CH₄ (B), and N₂O fluxes (C) measured between May 2019 and June 2020 from the forest and the sugarcane plots. The mean soil GHG fluxes result from measurements of four plots per treatment for every sampling time point. The dashed vertical line indicates the application of urea and muriate of potash fertilizers in the sugarcane. The gray shaded rectangle (A-C) indicates the start and end of the dry period (monthly precipitation ≤ 100 mm). Standard equals 70 kg N + 23 kg K ha⁻¹ growth cycle⁻¹, low equals 0.5 times standard and high equals 1.5 times standard.

Temporally, soil CH₄ uptake measured in the dry season was two times higher than the soil CH₄ uptake measured in the wet season, both under forest (Fig. 3.2B; Table 3.1; $p = 0.003$) and under sugarcane (Fig. 3.2B, Table 3.1; $p < 0.001$). Although 5% and 17% of the measured CH₄ fluxes from the forest and sugarcane, respectively, were emissions, the soils at the two sites remained net sinks of CH₄ both in the dry and wet seasons (Table 3.1).

Table 3.2. Spearman-rank correlation coefficients (r) between soil CO₂ fluxes ($\text{mg C m}^{-2} \text{h}^{-1}$), soil CH₄ fluxes ($\mu\text{g C m}^{-2} \text{h}^{-1}$), soil N₂O fluxes ($\mu\text{g N m}^{-2} \text{h}^{-1}$), and auxiliary controls (WFPS (%), soil temperature (°C), nitrate (NO₃⁻; mg N kg soil^{-1})) measured at 0.05 m depth from the reference forest and sugarcane. The spearman-rank correlation coefficients were calculated using means of the four reference forest plots and 12 replicate treatment plots in the sugarcane-based on daily, weekly, biweekly and monthly measurements in the sugarcane and only monthly measurements in the forest.

Land use	Variable	WFPS	Soil temperature	NO ₃ ⁻
Forest	CO ₂ flux	0.11	0.08	-0.37
	CH ₄ flux	0.78**	-0.40	-0.51
	N ₂ O flux	0.59*	-0.47	-0.08
Sugarcane	CO ₂ flux	0.38	0.31	-0.08
	CH ₄ flux	0.68**	0.10	-0.14
	N ₂ O flux	0.10	0.49*	0.40*

Significance codes: '**' $p \leq 0.01$; and '*' $p \leq 0.05$

Forest soils were stronger net sinks of CH₄ than the sugarcane soils across the dry and wet seasons (Fig. 3.2B, Table 3. 1; $p < 0.001$). At both sites, soil CH₄ uptake not only strongly and positively correlated to WFPS (Table 3.2; $p \leq 0.01$; $r > 0.5$) but also weakly and negatively correlated to NO₃⁻ (Table 3.2; $p \leq 0.05$; $r < 0.5$). There were, however, counteracting and weak responses of soil CH₄ uptake to temperature at the two sites (Table 3.2; $p \leq 0.05$; $r < 0.5$), namely negative and positive correlations to temperature in the forest and sugarcane, respectively (Table 3.2). Soil N₂O fluxes were equally highly variable in space and time ranging between an uptake of $-1.5 \mu\text{g N m}^{-2} \text{h}^{-1}$ and a release of $172 \mu\text{g N m}^{-2} \text{h}^{-1}$ under forest and between an uptake of $-12.2 \mu\text{g N m}^{-2} \text{h}^{-1}$ and a release of $61.5 \mu\text{g N m}^{-2} \text{h}^{-1}$ under sugarcane. Although fertilization in the sugarcane resulted in slightly elevated soil N₂O fluxes in the week that followed fertilization (reaching magnitudes of $61.5 \mu\text{g N m}^{-2} \text{h}^{-1}$), soil N₂O fluxes were mostly low for the greater part of the sampling period (Appendix F.1, Fig. 3.2C). Hence, the soils under sugarcane cultivation were a weaker source of N₂O compared to the forest soils (Table 3.1, Table 3.3), which were significant emitters of N₂O both in the wet and dry season (Fig. 3.2C, Table 3.1, Table 3.3; $p < 0.001$). Neither the forest nor the sugarcane soil N₂O fluxes showed a clear seasonal pattern (Fig. 3.2C, Table 3.1). Soil N₂O fluxes were positively correlated to WFPS at the two sites, however, this relationship was only strong for the forest (Table 3.2; $p \leq 0.05$; $r > 0.5$). Soil N₂O fluxes were negatively and positively correlated to temperature under forest and sugarcane, re-

spectively (Table 3.2; $p \leq 0.05$; $r < 0.5$). Similarly, Soil N₂O fluxes were negatively and positively correlated to the NO₃⁻ under forest and sugarcane, respectively (Table 3.2; $p \leq 0.05$; $r < 0.5$).

Table 3.3. Annual soil GHG fluxes between May 2019 and June 2020 from the reference forest and sugarcane plantations.

Land use	Annual soil GHG fluxes			Annual soil GWP			Net soil GWP
	CO ₂ flux (Mg C ha ⁻¹ yr ⁻¹)	CH ₄ flux (kg C ha ⁻¹ yr ⁻¹)	N ₂ O flux (kg N ha ⁻¹ yr ⁻¹)	CO ₂	CH ₄	N ₂ O	CO ₂ -eq (Mg CO ₂ -eq ha ⁻¹ yr ⁻¹)
Forest	14.5 ± 0.1 ^a	-3.1 ± 0.0 ^a	1.8 ± 0.0 ^a	14.5 ± 0.1	-0.09 ± 0.0	0.5 ± 0.0	14.9 ± 0.1
Sugarcane	17.6 ± 0.0 ^b	-1.1 ± 0.0 ^b	0.3 ± 0.0 ^b	17.6 ± 0.0	-0.03 ± 0.0	0.1 ± 0.0	17.7 ± 0.0

Notes: The presented values are means with standard errors (SE). Means followed by different lower-case letters indicate significant differences in the annual soil GHG flux between the forest and sugarcane (ANOVA with Tukey's HSD test or Kruskal-Wallis with a multiple-comparison extension test at $p \leq 0.05$). The annual soil GHG fluxes were based on four reference plots in the forest (\pm SE; $n = 4$) and 12 replicate plots in the sugarcane (\pm SE; $n = 12$). GWP means net global warming potential.

3.4.2. Carbon stocks in biomass and soil

The forest stored more C in its AGB compartments compared to the fertilized sugarcane (Fig. 3.3A). Fertilization under sugarcane resulted in increased AGB along the fertilizer intensification gradient (low < standard < high), but significant differences were only detected between high and low fertilization regimes (Fig. 3.3A). The BGB was also much higher in the case of the forest than the sugarcane (Fig. 3.3B). However, focussing on fine roots, the sugarcane produced significantly higher stocks for all evaluated soil depths (Fig. 3.3C). Interestingly, the mean SOC stocks (0–1 m) for all sugarcane plots were significantly higher compared to the mean of all forest plots (26%; Fig. 3.3D). The largest difference in SOC stocks between sugarcane and forest plots was found for the 0.10–0.30 m depth, with a nearly twofold increase in the SOC stocks under sugarcane compared to under forest for this depth (Appendix T.2). Even higher SOC stocks were found for older plantations (45%; Fig. 3.3D).

3.5. Discussion

3.5.1. Soil greenhouse gas flux dynamics in the reference forest and sugarcane plantations

In this study, soil GHG flux measurements from both the forest and neighboring sugarcane plantations indicate that tropical forest conversion to fertilized sugarcane increases soil CO₂ effluxes (Table 3.1; Table 3.3), decreases soil CH₄ uptake (Table 3.1; Table 3.3), and significantly affects soil N₂O emissions shortly after fertilization (Appendix F.1). The increase in soil CO₂ effluxes under sugarcane relative to the forests is consistent with our first hypothesis and agrees with studies that reported significantly larger soil CO₂ effluxes from cropland compared

to the reference forest (Kim & Kirschbaum, 2014; Aryal *et al.*, 2018; Aini *et al.*, 2020), but contrasts those that reported a decrease in soil respiration following tropical land-use change (Wanyama *et al.*, 2019; Verchot *et al.*, 2020). We measured significantly larger soil CO₂ effluxes from the sugarcane than the forest because of the higher soil C input (via the decay and decomposition of the dense fine root biomass) under sugarcane compared to the forest (Fig. 3.3C).

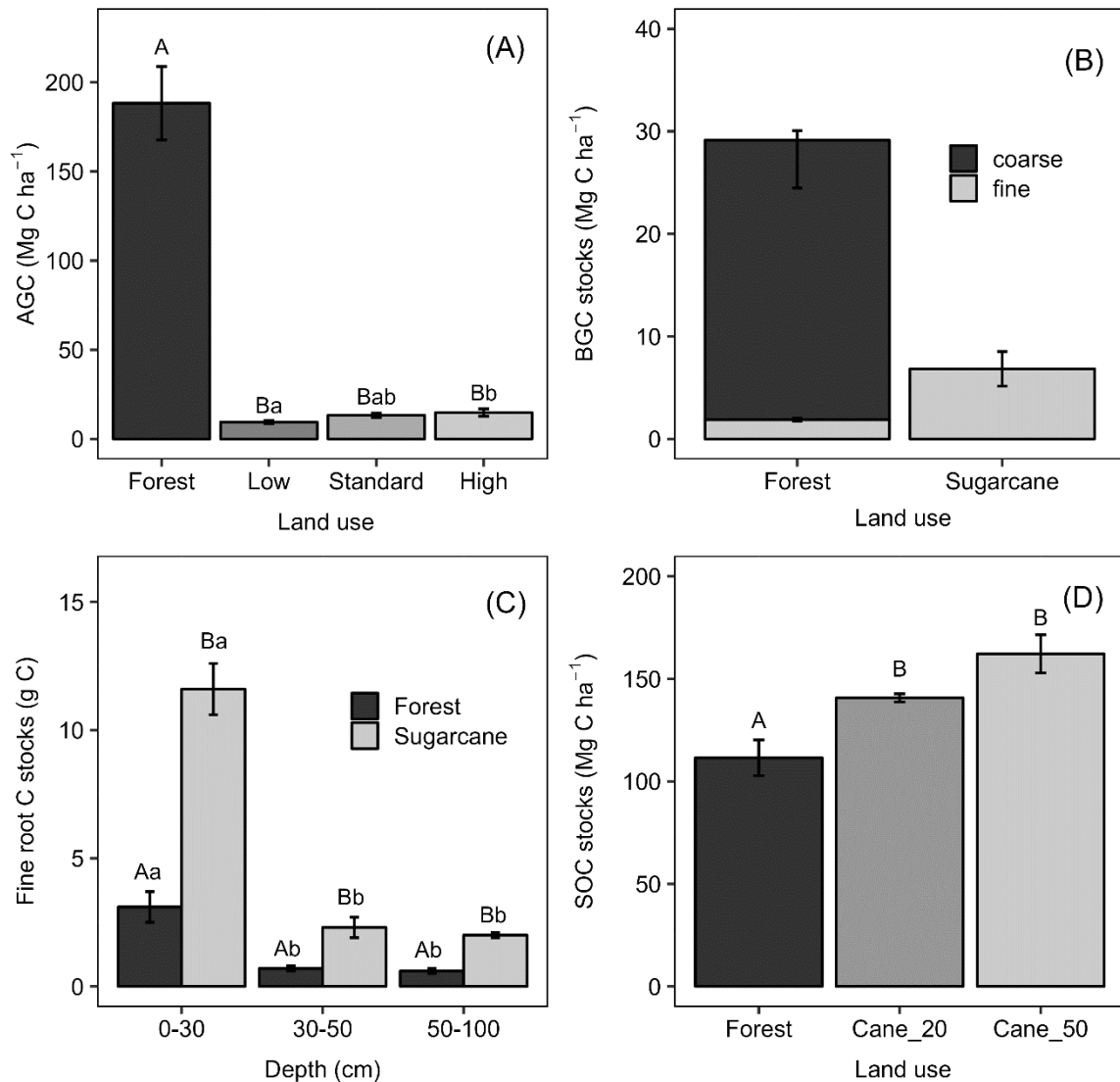


Figure 3.3. Mean (\pm standard error, SE, $n = 4$) aboveground biomass (AGB; A), belowground biomass (BGB; B), fine root (C), and soil organic carbon stocks to 1 m depth (SOC; D). Different uppercase letters indicate significant differences between the forest and sugarcane sites while different lowercase letters indicate significant differences either between the sugarcane treatments (Fig. 3.3A) or different soil depths (Fig. 3.3C). Low, standard, and high (Fig. 3.3A) refer to the fertilization treatments of the sugarcane plots. Standard equals 70 kg N + 23 kg K ha⁻¹ growth cycle⁻¹, low equals 0.5 times standard and high equals 1.5 times standard. Cane_20 and Cane_50 in Fig. 3.3D stand for 20- and 50-year-old sugarcane fields, respectively.

SOC stocks and soil respiration are known to follow first-order kinetics (Menichetti *et al.*, 2019; Riggers *et al.*, 2021), hence higher C input to soil would likely result in higher soil respiration rates (La Scala Jr. *et al.*, 2009). Additionally, plowing operations in the sugarcane plantations will have exposed the larger SOC stocks to microbial decomposition, especially in the wet season when the soil conditions were warm and moist leading to increased soil CO₂ effluxes (Table 3.1). Reinsch *et al.* (2018) found significantly higher soil respiration rates from plowed grassland plots compared to the control swards, and they attributed this to the increased decomposition of the native soil organic matter in the plowed fields, and the fact that plowing was done at a time when large amounts of plant residues were standing on the fields. Similarly, we observed that not only did sugarcane farmers in north-western Uganda retain substantial amounts of residues on their fields (14.6 Mg C ha⁻¹ yr⁻¹; Fig. 3.4), but also carried out all tillage operations related to weeding at the time when a significant proportion of residues from the previous crop was still present on the fields, leading to higher soil CO₂ effluxes. Furthermore, we postulate that fertilization under sugarcane will have enhanced root activity resulting in increased autotrophic respiration by the sugarcane roots (Sun *et al.*, 2017; Paradiso *et al.*, 2019) and increased production of root exudates, which concomitantly stimulated microbial consumption of organic acids in the rhizosphere (Fujii *et al.*, 2021).

Surprisingly, in this study, the response of soil CO₂ effluxes to seasonal changes in soil moisture or temperature seemed ecosystem dependent. For instance, under sugarcane, soil CO₂ effluxes measured during the wet season were significantly higher than in the dry season (Table 3.1), mainly because of the higher soil temperatures and moisture for the wet season compared to the dry season (Table 3.1). However, under forest, soil CO₂ effluxes were unaffected by seasonality-mediated changes in auxiliary controls (Table 3.1), and we attribute this to the negligible fluctuation in soil temperature throughout the measurement period (Tamale *et al.*, 2021). Furthermore, despite WFPS varying significantly between the dry and wet seasons, it also remained within the optimal range for soil microbial activity (35–45%; Fig. 3.1A; Hall *et al.*, 2013; van Straaten *et al.*, 2019), hence did not affect soil CO₂ effluxes as previously reported by Davidson *et al.* (2000), van Straaten *et al.* (2011), and Itoh *et al.* (2012). The conversion of the tropical forests to sugarcane fields, not only reduced the CH₄ uptake strength of the sugarcane soils (Table 3.1; Table 3.3) but also turned them into a CH₄ source under wet conditions (Fig. 3.2B). These findings confirm the second hypothesis and agree with studies where forest conversion to cropland resulted in lower soil CH₄ uptake (Petitjean *et al.*, 2019; Verchot *et al.*, 2020). Usually, the decline in soil CH₄ uptake in croplands is typically associated with heavy N fertilization

(Oertel *et al.*, 2016; Chen *et al.*, 2021) and increased compaction of topsoil due to heavy machinery (Tullberg *et al.*, 2018; Veldkamp *et al.*, 2020; Drewer *et al.*, 2021). However, we found the contrary. Firstly, N fertilization in the sugarcane did not affect soil CH₄ uptake, probably because the sugarcane soil NH₄⁺ concentrations were too low to interfere with the functioning of methanotrophs. These findings, however, contrast studies that reported either a stimulation (Liu & Greaver, 2009; Shang *et al.*, 2011) or inhibition effect of N fertilization on soil CH₄ uptake (Ding *et al.*, 2004; Dalal *et al.*, 2008; Aronson & Helliker, 2010). Secondly, frequent plowing in the sugarcane fields did not significantly increase the soil BD there compared to the undisturbed forest. Instead, we measured significantly higher soil BD in the top 30 cm of the reference forest plots (Appendix T.2) than in the sugarcane plots. Even then, both the higher BD (Appendix T.2) and the greater WFPS of the forest soils surprisingly did not translate to significantly higher CH₄ production (Table 3.1; Table 3.3). We suspect that this was because: (1) of the slightly coarser texture of the forest topsoil compared to the sugarcane (Appendix T.2) and (2) that the conversion to sugarcane may have altered the abundance of methanotrophs in the sugarcane soils lowering their CH₄ oxidation potential. With respect to the latter, Täumer *et al.* (2021) found a higher abundance of Alphaproteobacteria microbial communities in the temperate forest than in the neighboring grasslands, and as a consequence, forest soils sequestered more CH₄ than the grasslands. We measured higher soil CH₄ uptake in the dry season than in the wet season at both sites (Fig. 3.2B, Table 3.1), highlighting the dependence of soil CH₄ uptake on WFPS in well-aerated upland tropical soils (Oertel *et al.*, 2016; Wanyama *et al.*, 2019; Tamale *et al.*, 2021).

Contrary to the third hypothesis, fertilization in the sugarcane only resulted in the expected soil N₂O flush shortly after fertilization (Appendix F.1) but did not result in significant differences in soil N₂O fluxes among the treatments of the sugarcane CRD experiment. Equally unexpected was the significantly lower soil N₂O fluxes from the fertilized sugarcane plots compared to the reference forest (Table 3.1; Table 3.3). While the soil N₂O flush shortly after fertilization in our study (Appendix F.1) was consistent with the findings of Allen *et al.* (2010) and Wang *et al.* (2016) conducted in the Australian sugarcane fields, we measured much lower annual soil N₂O fluxes compared to Allen *et al.* (2010) and Wang *et al.* (2016). We postulate that this was due to the much higher N fertilization rates used in these studies (80–200 kg N ha⁻¹) compared to our study (35–105 kg N ha⁻¹). Besides the disparity in fertilization rates among these studies, we also attribute the unexpectedly low soil N₂O fluxes from our fertilized sugarcane fields to the likely leaching of the added N fertilizer (given the sandy texture of the soils; Appendix T.2) or its immediate uptake by the vigorously growing sugarcane crop potentially reducing N₂O

emissions. The latter was indeed corroborated by the measured increase in the aboveground biomass along the fertilizer intensification gradient (low < standard < high; Fig. 3.3A), potentially explaining why both the sugarcane soil NO_3^- contents and N_2O fluxes remained significantly lower than the forest (Fig. 3.1C, Fig. 3.2C, Table 3.1). Furthermore, we suspect that surface application of urea fertilizers without subsequent incorporation into the soil likely exposed the added N fertilizers to ammonia volatilization thereby removing excess N for de (nitrification) processes. Separate studies by Schwenke *et al.* (2014) and Li *et al.* (2015) reported a 30% loss of the added N fertilizers to ammonia volatilization and attributed this to the surface placement of these N fertilizers. Although the hole-in-the-pipe conceptual model suggests that soil N_2O fluxes are limited by both soil water content and N availability (Davidson & Verchot, 2000), soil N_2O fluxes from both the forest and sugarcane fields did not respond to seasonal variation in WFPS and soil NO_3^- contents (Table 3.1). We think that this was due to counteracting responses in both soil WFPS and nitrate contents during the wet and dry seasons in the forest. It is evident that soil WFPS increased during the wet season and declined during the dry season while soil NO_3^- content declined during the wet season and increased during the dry season (Fig. 3.1A, Table 3.1). However, under sugarcane, background soil NO_3^- contents were consistently too low throughout the measurement period (Fig. 3.1C) to significantly affect N_2O fluxes (Fig. 3.2C). Notably, however, the measured soil N_2O fluxes under sugarcane positively correlated to both WFPS and soil nitrate content (Table 3.2) as similarly reported by Butterbach-Bahl *et al.* (2013) and Davidson & Verchot (2000).

3.6. Conclusion

Tropical deforestation is assumed to represent a significant anthropogenic source of soil-borne GHG emissions. However, soil GHG flux estimates for the deforestation hotspots in tropical Africa are still limited. It was for this reason that we measured soil GHG fluxes along with their potential auxiliary controls from four reference forest plots and 12 replicate plots of a CRD experiment in the 20- year-old sugarcane plantation in north-western Uganda. Despite the use of different fertilizer application rates (low, standard, and high) as treatments for the sugarcane CRD experiment, no significant differences were detected in both the auxiliary controls and soil GHG fluxes among the CRD treatments. This was because, the applied fertilizers were immediately taken up by the vigorously growing sugarcane crop, which is also consistent with the measured increase in the sugarcane aboveground biomass along the fertilizer intensification gradient (low < standard < high). Soil CO_2 effluxes were larger in the sugarcane fields compared to the native forest because of the likely exposure of the sugarcane's surprisingly larger SOC

stocks to microbial decomposition and the increased autotrophic respiration from its high fine root biomass. The forest soils were a stronger net sink of CH₄ than the sugarcane soils despite them (forest soils) having both higher bulk densities and larger water-filled pore space (WFPS). Although there was a marginal increase in both the soil NO₃⁻ content and N₂O emissions in the two weeks that followed fertilization in the sugarcane, this never matched the already stronger net release of N₂O from the forest soils given their inherently larger N cycling rates. Only seasonal variability in WFPS, among the auxiliary controls, affected CH₄ uptake at both sites and soil CO₂ effluxes in the sugarcane. Noteworthy, soil N₂O fluxes from both sites were unaltered by seasonality. Overall, the study highlights that even in the case of increased SOC sequestration under the sugarcane fields (as indicated in this study) and the lower N₂O emissions compared to the forest sites, the forest-sugarcane conversion leads to a substantial C loss to the atmosphere. This is because such a land use shift results in an immediate loss of a significant amount of C stored both in the above and belowground biomass of the forest, followed by increased emission of CO₂ (soil respiration, fertilizer use, and harvest) and reduced uptake of CH₄ under sugarcane on the long term.

**CHAPTER 4. IMPACT OF UREA FERTILIZATION
RATES ON NITROGEN DYNAMICS, PRODUCTIVITY,
AND PROFITABILITY FROM UGANDAN
SUGARCANE PLANTATIONS**

with minor editing differences, submitted as: Tamale, J., Nasta, P., Hutson, J., Turyagyenda, L.F., van Straaten, O., Doetterl, S., and Fiener, P. 2023. Impact of urea fertilization rates on nitrogen dynamics, productivity, and profitability from Ugandan sugarcane plantations. *Soil Use and Management Journal* (SUM-2023-107).

4.1. Abstract

Sugarcane is the primary source of sugar and biofuel for many (sub) tropical economies. However, its production heavily relies on large nitrogen (N) doses, which often exceed the crop N requirements resulting in groundwater contamination and increased soil carbon footprints. In this respect, we setup a completely randomized design experiment (covering 5.6-hectares) in a ratoon sugarcane plantation in north-western Uganda to investigate N dynamics, productivity, and profitability under sugarcane plantations. A total of twelve 40 × 40 m experimental plots were established with three fertilization treatments (low, 35 kg N ha⁻¹; standard, 70 kg N ha⁻¹; high, 105 kg N ha⁻¹) and four replications. In every treatment plot, we determined: (1) N leaching losses based on drainage fluxes estimated with the water subroutine of the Leaching Estimation and Chemistry Model (LEACHM) and leachate N concentrations measured by suction cup lysimeters installed at the soil depth of 90 cm; (2) soil nitrous oxide (N₂O) fluxes using static vented chambers and gas chromatograph; and (3) field fresh weight (FFW), which, was used to obtain partial factor productivity and return on investment. First, our findings highlight that it was feasible to apply three out of five pedotransfer functions (PTFs) to estimate soil hydraulic properties for our test site, even though these PTFs were developed in Europe and North America. Second, N leaching fluxes marginally increased when low (1.7 ± 0.6 kg N ha⁻¹) and standard (3.4 ± 0.7 kg N ha⁻¹) N fertilization rates were used but significantly increased (14.2 ± 2.2 kg N ha⁻¹; $p \leq 0.001$) when the standard N rate was exceeded. Third, the measured soil N₂O emissions were unaffected by N fertilization. Fourth, there was a non-significant response of FFW to increasing N rates (low; 124 ± 12 Mg FFW ha⁻¹ < standard; 171 ± 16 Mg FFW ha⁻¹ < high; 192 ± 27 Mg FFW ha⁻¹), despite a significant to a marginal increase in crop N uptake between low and standard N rates and at higher-than-standard N rate, respectively. The study findings suggest that: (i) surpassing the standard N rate for sugarcane would not be economically viable since it would only marginally increase FFW at the expense of groundwater quality, especially in shallow aquifers; (ii) and despite demonstrating that sugarcane cultivation can still be profitable at lower-than-standard N rates since part of the N requirement is met by mineralizing the high soil organic carbon (SOC) stocks in sugarcane fields, it remains unreconciled from this short-term study, whether reducing N rates below the standard N rate will not counterintuitively lower SOC stocks in the long term. The high SOC stocks under sugarcane reflect the long-term carbon input dynamics obtained with the standard N rates.

4.2. Introduction

Sugarcane (*Saccharum officinarum*) is an important source of sugar (Singh *et al.*, 2008; Brumbley *et al.*, 2008; de Morais *et al.*, 2015) and biofuel (Carmo *et al.*, 2013; Mello *et al.*, 2014) in many (sub) tropical countries and accounts for nearly 1.75% (26.5 million hectares) of the world's arable land area (Leff *et al.*, 2004). The ongoing debate on energy production suggests that the global dependency on fossil fuels and the associated greenhouse gas (GHG) emissions to the atmosphere can be significantly reduced if the bioenergy potential of crops like sugarcane is efficiently harnessed in large plantations (Popp *et al.*, 2014; Bordonal *et al.*, 2018). However, the shift from fossil fuel to bioenergy requires massive crop biomass production, which is mostly achieved through nitrogen (N) fertilization, with application rates ranging between 60 and 400 kg N ha⁻¹ yr⁻¹ for both freshly established and ratoon sugarcane crops (Stewart *et al.*, 2006; Meyer & Antwerpen, 2010; Robinson *et al.*, 2011; Tamale *et al.*, 2022). Nonetheless, these rates often exceed standard crop N requirements even in the case of the deeply weathered and nutrient-poor Ferralsols (where most sugarcane crops are grown; Cherubin *et al.*, 2015), resulting in significant N losses to the environment and atmosphere (Tilman *et al.*, 2002; Robinson *et al.*, 2011).

One pathway through which N is lost from fertilizer-based sugarcane systems is nitrate (NO₃⁻) leaching (Stewart *et al.*, 2006; Ghiberto *et al.*, 2011; Thorburn *et al.*, 2011; Blum *et al.*, 2013), a process involving movement of applied N to the groundwater (Zhou *et al.*, 2016; Ju & Zhang, 2017; Bijay-Singh & Craswell, 2021). Hence, N leaching represents both a serious contamination problem for drinking water and a large economic loss for these agricultural systems (Bijay-Singh & Craswell, 2021). It is for this reason that the last three decades have seen a surge in concerted scientific investigations to better understand the factors that underpin N leaching dynamics in fertilized sugarcane systems across tropical and subtropical regions (e.g., Japan; Okamoto *et al.*, 2021, Australia; Stewart *et al.*, 2006; Thorburn *et al.*, 2011; Brazil; Ghiberto *et al.*, 2011; Blum *et al.*, 2013). These efforts included: (1) the use of tracers (such as ¹⁵N-enriched fertilizer; Meier *et al.*, 2006; Ghiberto *et al.*, 2009) to quantify N loss via deep percolation, and (2) the evaluation of process-based models (e.g., Leaching Estimation and Chemistry Model, LEACHM; Hutson, 2003, Agricultural Production Systems simulator, APSIM; Holzworth *et al.*, 2014, HYDRUS; Šimůnek *et al.*, 2008) for simulating water fluxes and/or N transport in the vadose zone under fertilized sugarcane (Thorburn *et al.*, 2011; Shishaye, 2015). N leaching models require data on climate, crop phenology and characteristics, depth to the water table, and soil hydraulic properties (namely, the soil water retention function and hydraulic conductivity function).

However, data scarcity in some sugarcane-growing regions, especially sub-Saharan Africa, makes applying such models nearly impossible. For data-poor regions like sub-Saharan Africa, the use of pedotransfer functions (PTFs) to estimate the soil water retention function and hydraulic conductivity function from readily available basic soil physical and chemical properties (i.e., grain size distribution, soil bulk density, and organic carbon) is highly recommended (Van Looy *et al.*, 2017; Nasta *et al.*, 2021). Unfortunately, the basic physical and chemical soil properties' data are also lacking over most parts of the tropics (including sub-Saharan Africa), thereby limiting the applicability of N leaching models. Hence, the scale of the N leaching problem under fertilized sugarcane systems in sub-Saharan Africa is, to date, poorly understood. Yet, sub-Saharan Africa accounts for about 4% of the world's sugarcane production (Tyler, 2008) and is poised for future sugarcane expansion given the low production costs, high production potential, access and proximity to European markets, as well as high abundance of arable land (Hess *et al.*, 2016).

Besides N leaching, the application of inorganic N fertilizers at the soil surface without incorporation into the soil has been reported to result in significant N losses to the atmosphere via ammonia volatilization and is estimated to account for about 30% loss in the applied N fertilizers for most croplands (Schwenke *et al.*, 2014; Li *et al.*, 2015). Most sugarcane farmers across the (sub) tropics attempt to mitigate the expected ammonia volatilization by applying N fertilizer in bands (Prasertsak *et al.*, 2002; Skocaj *et al.*, 2013). However, this practice remains unpopular among sub-Saharan African sugarcane farmers who mainly apply N fertilizers at the surface without incorporation into the soil (Tamale *et al.*, 2022), predisposing their fields to increased ammonia volatilization. At the same time, sugarcane plantations, by virtue of the wet and humid tropical environments in combination with the relatively high N inputs, are considered significant anthropogenic sources of nitrous oxide (N₂O; Allen *et al.*, 2010; Wang *et al.*, 2016; Dattamudi *et al.*, 2019). This greenhouse gas has a larger radiative forcing relative to carbon dioxide (Forster *et al.*, 2007) and a strong depleting effect on stratospheric ozone (Ravishankara *et al.*, 2009). It is estimated that nearly 2.2 kg N₂O-N ha⁻¹ yr⁻¹ is released globally from sugarcane plantations (Yang *et al.*, 2021). However, such estimates still suffer from considerable uncertainty because their derivation is primarily premised on studies conducted in Australia (Allen *et al.*, 2010; Wang *et al.*, 2016) and Brazil (e.g., Carmo *et al.*, 2013; Soares *et al.*, 2015), with little to no representation of sub-Saharan Africa. Tamale *et al.* (2022) recently conducted year-round soil greenhouse gas measurements (including N₂O fluxes) in Ugandan sugarcane plantations.

Despite the N losses, the sugarcane crop still recovers a proportion of the applied N in its biomass. However, the N recovery rates under sugarcane plantations are not fully reconciled with some studies reporting values between 20 and 40% (Meyer *et al.*, 2007; Antille & Moody, 2021) while others reported values between 60 and 70% (Franco *et al.*, 2011; Furtado da Silva *et al.*, 2020). Consequently, N budgets, N utilization efficiency (also known as partial factor productivity), and the return on investment under sugarcane remain poorly understood especially in the case of sub-Saharan Africa where studies on N dynamics, productivity, and profitability in sugarcane plantations are rare. Hence, we conducted a study in a 5.6-hectare (ha) ratoon sugarcane field located in north-western Uganda with the following objectives:

1. To evaluate the feasibility of using the five-well-established PTFs developed in Europe, North America, and Brazil to predict the soil water retention function and hydraulic conductivity function for Ugandan Ferralsols.
2. To determine the effect of increasing N rates (low, standard, high) on N dynamics (soil N leaching flux, soil N₂O fluxes, crop N uptake, and soil N balance).
3. To determine whether fertilizing below or above the standard N fertilization rates results in incremental productivity and profitability benefits for sugarcane farmers.

4.3. Materials and methods

4.3.1. Study area description and available datasets

The study was carried out in a 5.6 ha ratoon sugarcane field in Kanyege, north-western Uganda (1°41'37.9" N, 31°30'6.3" E, 1062 m a.s.l). The area is covered with large-scale sugarcane farms that supply raw materials to Kinyara Sugar Works Limited, the second-largest sugar processing company in Uganda. Atmospheric and weather data were obtained from: (1) an ATMOS 41 weather station (METER Group Inc, USA, www.metergroup.com) installed 2 m above the ground in an open area at the study site. The weather station recorded precipitation, air temperature, wind speed, air relative humidity, and net solar radiation at 15-minute intervals between May 1, 2019, and June 30, 2020; (2) a weather station operated and maintained by the Uganda National Meteorological Authority (UNMA) located at 1°41'8.7", 31°43'5.7", 1146 m a.s.l about 27 km from the study site. We used data from the UNMA weather station for the period January 1 to April 30, 2019, before the installation of the ATMOS 41 weather station at the study site. UNMA weather data was recorded at an hourly temporal resolution. Potential evapotranspiration (ET_p) was estimated with the Penman-Monteith equation (Allen *et al.*, 1998; Batsukh *et al.*, 2021) using wind speed, air relative humidity, net solar radiation, and minimum and maximum temperature data from ATMOS 41 and UNMA weather stations. Mean annual

rainfall over the study region is about 1700 mm and is distributed in two wet seasons (March to May and August to November) separated by an extended dry season between December and February and a short dry season in June and July (Lukwago *et al.*, 2020). The mean annual temperature is approximately 25 °C. The soils in the study area are well-drained and deeply weathered (Tamale *et al.*, 2022) and are classified as Petroplinthic/Pisoplinthic Rhodic Ferralsols (IUSS Working Group WRB, 2015). These soils were mainly formed from the weathering of the Precambrian basement complex parent material consisting of granites and gneisses (Lehto *et al.*, 2014). The static depth of the groundwater table ranges between 13 and 30 m below ground level over the Masindi region (Nanteza *et al.*, 2016). The study area has an undulating topography with slope gradients mostly less than 10% and ridge crests reaching a maximum altitude of 1150 m a.s.l (Conlong & Mugalula, 2001).

4.3.2. Experimental design

The study follows the analysis of a completely randomized design (CRD; Tamale *et al.*, 2022) experiment established at the beginning of April 2019 in a ratoon sugarcane field in Kanyege, north-western Uganda (Fig. 4.1A-B). The CRD experiment consisted of twelve treatment plots laid out in a 5.6-hectare sugarcane field. Each treatment plot measured 40 m x 40 m, had an inner measurement core of 30 m x 30 m to avoid boundary effects, and was separated from adjacent plots by a 40 m guard row to prevent spillover of treatments (Fig. 4.1B). The twelve experimental plots reflect three N fertilizer treatments (low, standard, and high N applications) replicated four times (n=12; three treatments x four replications). The standard fertilizer rate (SFR) was 70 kg N ha⁻¹ applied as urea, (NH₂)₂CO per crop growth cycle, while low and high N fertilizer rates refer to 0.5 and 1.5 times SFR, respectively. The fertilizers were applied to all treatment plots on May 14, 2019 (at about 3 months from sprouting), following standard practice by sugarcane farmers in the region (i.e., one-time N application at the surface without incorporation into the soil). Inter- and intra-row weeding was done three times during the first eight months following sprouting, by which time the canopy was sufficient to subdue emerging weeds. The experimental activities illustrated in Fig. 4.1 are explained in detail in sections 2.3-2.6.

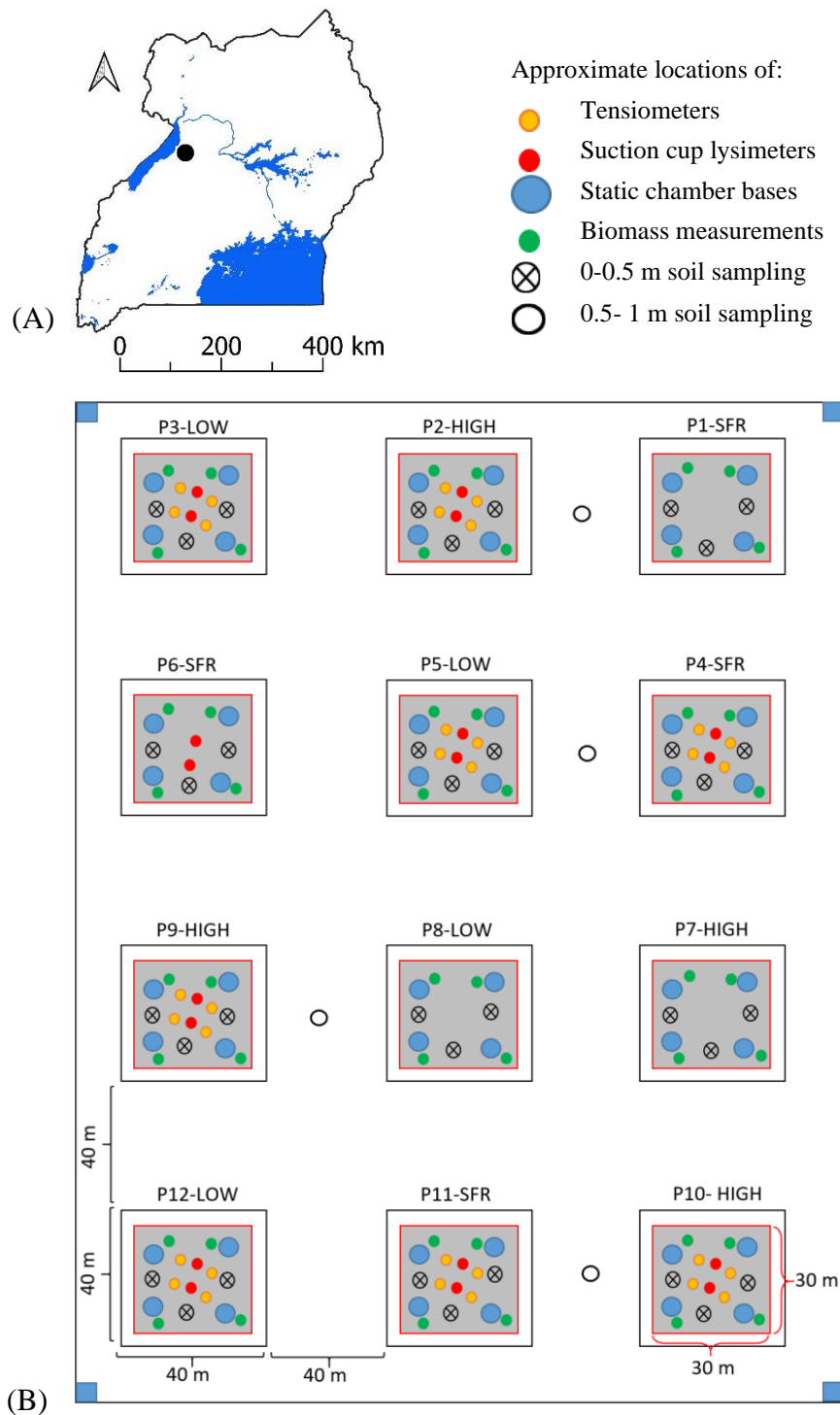


Figure 4.1. (A) Geographic location of the study area (black dot) in the north-western part of Uganda, (B) sketch of the completely randomized design (CRD) experiment set up in a 5.6 ha field. The CRD experiment consisted of 12 treatment plots (measuring 40 m × 40 m) in which soil matric potential, nitrate concentrations, and soil nitrous oxide fluxes, were measured using tensiometers (yellow circles), suction cup lysimeters (red circles), and static chamber bases (blue circles), respectively, under standard (SFR; 70 kg ha⁻¹), low (0.5 times SFR), and high (1.5 times SFR) nitrogen (N) applications. The plots are labelled by reporting plot (P) number and four replications of N applications (LOW, SFR, HIGH). Biomass measurements (green circles) and soil sampling between 0 and 0.5 m (black crossed circle) were carried out in each treatment plot, while deep soil sampling (0.5 – 1.0 m; empty black circles) are located between the treatment plots.

4.3.3. Soil sampling

Disturbed and undisturbed soil samples were collected from three random locations in every replicate plot at three depths (0-10, 10-30, 30-50 cm; crossed circles in Fig. 4.1B) and from deeper soil layers (50-100 cm; empty circles in Fig. 4.1B) in four pits dug in the guard row spaces. The sampling depths reflect the vertical variability of the soil profiles in which four soil layers were identified (Ap, A, Bs₁, and Bs₂; Fig 4.2). The disturbed soil samples were used for determining sand (Sa), silt (Si), clay (Cl), and soil organic carbon (SOC) content. Grain size distribution was determined using the sieving technique for the sand-sized particles (effective diameter from 2.0 mm to 0.50 mm) and the hydrometer method for the clay-sized particles (effective diameter less than 0.002 mm; Gee & Or, 2002).

Table 4.1. Mean (\pm standard error, SE, $4 \leq N \leq 36$) basic soil physical and chemical properties at the soil depths of 0-10, 10-30, 30-50, and 50-100 cm based on measurements done at the experimental site (N denotes the number of soil samples). ρ_b , Sa, Si, Cl, SON, and SOC indicate soil bulk density, sand, silt, clay, soil organic nitrogen, and soil organic carbon, respectively.

Soil physico-chemical properties	Soil depth (cm)			
	0-10	10-30	30-50	50-100
ρ_b (g cm ⁻³)	1.08 \pm 0.02	1.24 \pm 0.02	1.20 \pm 0.03	1.14 \pm 0.03
Sa (%)	52 \pm 2.2	47 \pm 2.5	33 \pm 1.5	29 \pm 0.4
Si (%)	21 \pm 2.4	18 \pm 2.0	13 \pm 1.3	15 \pm 5.4
Cl (%)	27 \pm 1.1	35 \pm 0.8	54 \pm 1.5	56 \pm 5.3
pH H ₂ O (1:2.5)	5.5 \pm 0.1	5.5 \pm 0.1	5.5 \pm 0.0	5.4 \pm 0.1
SON (%)	0.18 \pm 0.0	0.14 \pm 0.0	0.09 \pm 0.0	0.06 \pm 0.0
SOC (%)	2.7 \pm 0.1	2.0 \pm 0.0	1.1 \pm 0.0	0.6 \pm 0.0
C/N	14.8 \pm 0.12	14.3 \pm 0.13	11.7 \pm 0.12	10.0 \pm 0.13
SON stocks (Mg N ha ⁻¹)	1.94 \pm 0.04	3.39 \pm 0.04	2.26 \pm 0.05	3.67 \pm 0.09
SOC stocks (Mg C ha ⁻¹)	28.8 \pm 0.7	48.6 \pm 0.8	26.4 \pm 0.8	36.6 \pm 0.6

The textural class of each soil sample was determined using the United States Department of Agriculture (USDA) classification and is coarse-textured (sandy clay to sandy clay loam) in the surface layers (0-30 cm) and predominantly fine textured (clay) in the subsurface layers (30-100 cm; Table 4.1). SOC and soil organic nitrogen (SON) were determined with a C/N elemental analyzer (vario EL cube; Elementar Analysis Systems GmbH, Hanau, Germany). Soil pH H₂O (1:2.5) was measured using a pH meter. The undisturbed soil samples were used to measure the soil bulk density, ρ_b (g cm⁻³), defined as the oven-dry mass (48 hours at 105 °C) per bulk volume (Kopecky ring, 251 cm³). SON and SOC were multiplied by ρ_b to obtain SON- and SOC-stocks, respectively, while accounting for stone content.

4.3.4. Nitrogen leaching estimation

4.3.4.1. Soil pore water sampling and nitrate concentration measurements

Before installation of the suction cup lysimeters (outside diameter = 22 mm, interior diameter = 16 mm, wall thickness = 3 mm; MMM tech support GmbH & Co. KG, Germany; www.mmm-

tech.de/en/lysimeter/lys), we measured the effective rooting depth (z_R) for the sugarcane crop ($z_R = 60$ cm), which is the soil depth containing most plant roots (i.e., > 90%). Eighteen suction cup lysimeters were installed in nine treatment plots (one pair x 9 plots; red circles in Fig. 4.1B) to sample pore water; however, two suction cup lysimeters installed in plot 6 (P6-SFR) malfunctioned, and we were unable to sample soil water from this plot. The suction cup lysimeters were installed two weeks before the first water sampling to ensure minimal alteration of biochemical processes near the suction cup lysimeters. To capture the expected variability in soil water content due to crop root uptake, we installed one suction cup lysimeter in the inter-row space while the other one was installed in the intra-row space. The installation depth was 90 cm, well below z_R . A day before sampling, we applied a 40 kPa suction to the lysimeter using a hand vacuum pump for 24 hours to collect adequate volumes of soil water. On the sampling day, the suction was released, and the solution was collected from the lysimeter shaft using an airtight syringe. The collected water from the two-suction cup lysimeters in a plot was transferred to a pre-labeled plastic bottle and mixed thoroughly for about 30-60 seconds to obtain a homogeneous water sample for every plot. Each homogenized water sample was analyzed for nitrate (NO_3^-) concentrations using a portable RQflex® 10 reflectometer test kit (Merck, Germany) equipped with a specific bar code and test strips (detection range: 0.3 – 90 mg N/L). Soil pore water sampling and N leachate concentration determination were done once every two weeks for most of the sampling period. However, measurements were more frequent during the first month following fertilization (one day before fertilization, three and five days after fertilization, and then once a week until the end of the first month) to capture the expected NO_3^- flush in percolating water following N application. Next, we used a trapezoidal interpolation on the measured N concentrations in percolating water to estimate the daily N concentrations.

4.3.4.2. Soil matric potential measurements

Soil matric potential was measured two to four times a month using two pairs of tensiometers (outer diameter = 16 mm, inner diameter = 12 mm; MMM tech support GmbH & Co. KG, Germany; www.mmm-tech.de/en/lysimeter/lys) installed at 60 and 90 cm depth in 8 of the 12 replicate plots of the CRD experiment. Hence, 32 tensiometers were installed at the study site (yellow circles in Fig. 4.1B).

4.3.4.3. Soil water drainage flux modeling and nitrogen leaching loss estimation

Soil water drainage fluxes were estimated using the water subroutine of the Leaching Estimation and Chemistry Model (LEACHM; Hutson, 2003) by simulating the water flow across a 1-m-deep layered soil profile representative of the 5.6 ha experimental area. The one-dimensional

transient vertical water flow across the soil profile was modeled via a numerical solution of Richards' equation:

$$\frac{\partial \theta}{\partial t} = \frac{\partial}{\partial z} \left[K(\theta) \frac{\partial H}{\partial z} \right] - U(z, t) \quad (4.1)$$

where θ is the volume fraction of water ($\text{cm}^3 \text{cm}^{-3}$), t is time (d), z is depth (cm), K is unsaturated hydraulic conductivity (cm d^{-1}), H is the hydraulic head (the sum of the pressure and gravitational soil water potential, cm), and U is the sink term representing absorption of water by plants (d^{-1}). The root distribution was assumed to be uniform throughout the root zone ($z_R=60$ cm; Fig. 4.2). The surface boundary conditions were specified as precipitation (P), potential evaporation (E), and transpiration (T), while the bottom boundary condition was specified as free drainage (D) (Fig. 4.2). Hydraulic equilibrium was specified as the initial condition across the 1-m- deep soil profile (Fig. 4.2).

SWRF was described using the van Genuchten (1980) equation which relates the degree of saturation, S_e (-), to soil matric potential, ψ (cm):

$$S_e(\psi) = \frac{\theta - \theta_r}{\theta_s - \theta_r} = \frac{1}{(1 + |\alpha \psi|^n)^{(1-1/n)}} \quad (4.2)$$

where θ_r ($\text{cm}^3 \text{cm}^{-3}$) and θ_s ($\text{cm}^3 \text{cm}^{-3}$) are the residual and saturated volumetric water contents, α (cm^{-1}), and n ($= 1/(1-m)$), dimensionless) are empirical shape parameters of the soil water retention function.

According to van Genuchten (1980), the hydraulic conductivity function is defined as:

$$K(S_e) = K_s S_e^\tau \left[1 - (1 - S_e^m)^m \right]^2 \quad (4.3)$$

where K_s (cm d^{-1}) is the saturated hydraulic conductivity, τ (-) is the tortuosity parameter usually assumed as either 0.5 (Mualem, 1976) or -1 (Schaap & Leij, 2000; Schaap *et al.*, 2001).

The soil hydraulic parameters (θ_r , θ_s , α , n , and K_s) in each soil layer were estimated from the spatial-average values of S_a , S_i , Cl , and ρ_b (Table 4.1) using five well-known PTFs developed in North America, Europe, and Brazil. These PTFs included: (1) Rawls *et al.* (1982), (2) ROSETTA (Schaap *et al.*, 2001), (3) Tomasella and Hodnett (1998), (4) Weynants *et al.* (2009), (5) Wösten *et al.* (1999), hereafter, denoted as RAWLS82, ROSETTA, T&H98, WEY09, and WOS99, respectively. Appendix T.3 lists the equations of five PTFs (RAWLS82, ROSETTA, T&H98, WEY09, and WOS99) used to estimate the soil hydraulic parameters (θ_r , θ_s , α , n , and

K_s) featuring in the van Genuchten's soil water retention function and hydraulic conductivity function (Appendix F.2; and Appendix F.3).

Hence, we obtained five numerical simulations based on the five PTFs listed above. Next, we evaluated the performance of the five PTFs by comparing the match between simulated (PTF-based) and measured matric potentials using: (1) the coefficient of determination (R^2), (2) index of agreement (d), (3) Nash-Sutcliffe efficiency (NSE), and (4) root mean square error (RMSE) indices. Optimal prediction is obtained with a value equal to zero for RMSE and equal to one for R^2 , d, and NSE. Measured and simulated values of soil matric potential on March 04, and March 09, 2020, were ignored because these measurements were close to the tensiometer's detection limit. Finally, the daily drainage flux was assumed as the mean of the daily drainage fluxes obtained with the best-performing PTFs. Therefore, the daily N leaching fluxes under different treatments were obtained by multiplying the mean daily drainage flux (simulated in LEACHM) by the interpolated daily N concentrations (measured with suction cup lysimeters).

4.3.5. Soil nitrous oxide flux measurements

Soil nitrous oxide (N_2O) flux measurements from the respective treatments of the CRD experiment were reported in an earlier study (Tamale *et al.*, 2022). Briefly, these were measured by randomly installing, a month prior to sampling (April 2019), four static PVC chamber bases (area = 0.044 m², volume = ~ 12 L) at the soil surface (~ 0.03 m) within the inner measurement core of every treatment plot (blue circles in Fig. 4.1B). On the sampling day, all chamber bases in every plot were covered with polyvinyl hoods (volume = 6.78 L) to obtain a pooled gas sample at each of four time intervals (3, 13, 23, and 33 min) using the approach proposed by Arias-Navarro *et al.* (2013). A total of 1200 pooled gas samples were obtained over the sampling period (14 months), stored in pre-evacuated airtight 12 mL Labco Exetainer® glass vials (Labco Ltd, Lampeter, United Kingdom) and transferred to the Soils laboratory of ETH Zürich, Switzerland, where GHG concentrations in the obtained gas samples were analyzed with gas chromatography (GC; Scion 456-GC Bruker, Germany). Soil N_2O fluxes were calculated based on the Hüppi *et al.* (2018) “gasflxvis” scheme implemented using an online Soil GHG flux shiny tool (<https://sae-interactive-data.ethz.ch/gasflxvis/>).

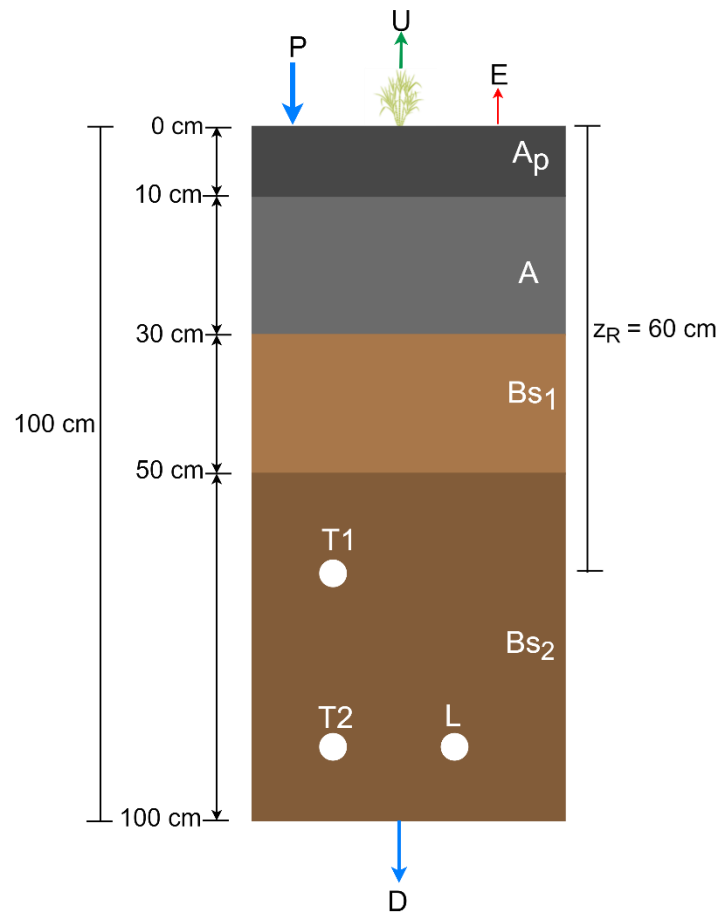


Figure 4.2. Sketch of the 1-m-deep soil profile composed of four soil layers (A_p , A , Bs_1 , Bs_2 corresponding to 0-10 cm, 10-30 cm, 30-50 cm, and 50-100 cm soil depths, respectively). Precipitation (P) and evaporation (E) occur at the soil surface. At the same time, the sink term U controls the transpiration through the roots in the root zone ($z_R=60$ cm), and water moves down across the bottom of the soil profile through drainage (D). $T1$ and $T2$ are the observation nodes ($z=60$ cm and $z=90$ cm) at which simulated and measured matric potential values were compared to test pedotransfer function performance.

4.3.6. Field fresh weight, crop nitrogen uptake, and soil nitrogen balance

We harvested four random 1 m x 1 m quadrants in every treatment plot of the CRD experiment after 16 months (green circles in Fig. 4.1B) and weighed the field fresh weight from every quadrant to determine biomass. Note that our field fresh weight data only represents biomass/yield from sugarcane fields with minimal sprouting failures.

Crop N uptake was estimated by multiplying the mean dry biomass by its N content determined from the C/N Analyzer (vario EL cube; Elementar Analysis Systems GmbH, Hanau, Germany) at the University of Augsburg, Germany.

Next, we quantified the tradeoff between N gains and losses under the different CRD treatments. The N gains included: (1) N mineralization from soil organic matter (SOM; R. H. McKenzie, personal communication, February 23, 2017), (2) wet N deposition over the study area (Manu *et al.*, 2022), and (3) one-time fertilizer dose of N following low, standard, and high

application rates as described above in section 2.2. The N losses included: soil N₂O emissions, plant N uptake, N leaching, and other N losses (potentially ammonia volatilization).

4.3.7. Partial factor productivity and return on investment

Partial factor productivity was estimated by dividing the field fresh weight from the respective CRD treatment plots by their corresponding N fertilizer rates. Next, we obtained data on the factory price of sugarcane field fresh weight (Uganda shillings, UGX) and the market price of urea fertilizers for the years 2018 through 2022 (UGX) from Masindi Sugarcane Growers' Association and the respective prices were converted to US dollars using the average exchange rate for the period 2018-2022 from the world bank website (<https://data.worldbank.org>). We then determined the return on investment as the ratio of the income generated from the sale of sugarcane field fresh weight for every US dollar spent on procuring fertilizers across the years 2018 to 2022.

4.3.8. Statistical analysis

Differences in soil N leaching flux, plant N uptake, soil N₂O emissions, field fresh weight, and partial factor productivity among the CRD treatments were analyzed using univariate analysis of variance (ANOVA) followed by the post hoc Tukey's honestly significant difference (HSD) test for multiple comparison between treatment groups. Before running ANOVA, we checked whether all the response variables were normally distributed based on quantile-quantile (QQ) plots and Shapiro tests and if their respective variances were homogeneous based on the Levene test. If the tests revealed non-normal distribution and heteroscedasticity of the data, we applied a Tukey transformation to the data and repeated the normality and homoscedasticity tests for a second time. All the statistical analyses were done in R 3.6.3 (R Development Core Team, 2022) using the '*rcompanion*' package for the normality and homoscedasticity check as well as the Tukey transformation, and the '*car*' package for the univariate ANOVA and posthoc Tukey's HSD tests.

4.3.9. Description of the methodology

Briefly, the study consists of three interconnected parts. Part 1 (blue box in Fig. 4.3) entails the simulation of daily drainage fluxes across a 1-m-deep layered soil profile representative for the study area using the water subroutine of LEACHM based on: potential evapotranspiration (ET_p), precipitation (P), crop characteristics, and PTF-derived soil hydraulic properties. We obtained five simulations in LEACHM using five PTFs, and the daily drainage flux was assumed to be the mean of the daily drainage fluxes obtained with the best-performing PTFs. Part two (red box in Fig. 4.3) comprises the N dynamics (N gains (in brown) and losses (in purple))

under sugarcane. The soil N gains include N fertilization, wet N deposition in precipitation (Manu *et al.*, 2022), and N addition through SOM mineralization based on eq. (4.4) (R. H. McKenzie, personal communication, February 23, 2017; Fig. 4.3).

$$\text{soil } N_{\min} = 3 - 1.6544 * SOM + 0.7119 * (SOM)^2, R = 0.77 \quad (4.4)$$

where $\text{soil } N_{\min}$ is soil nitrogen mineralization

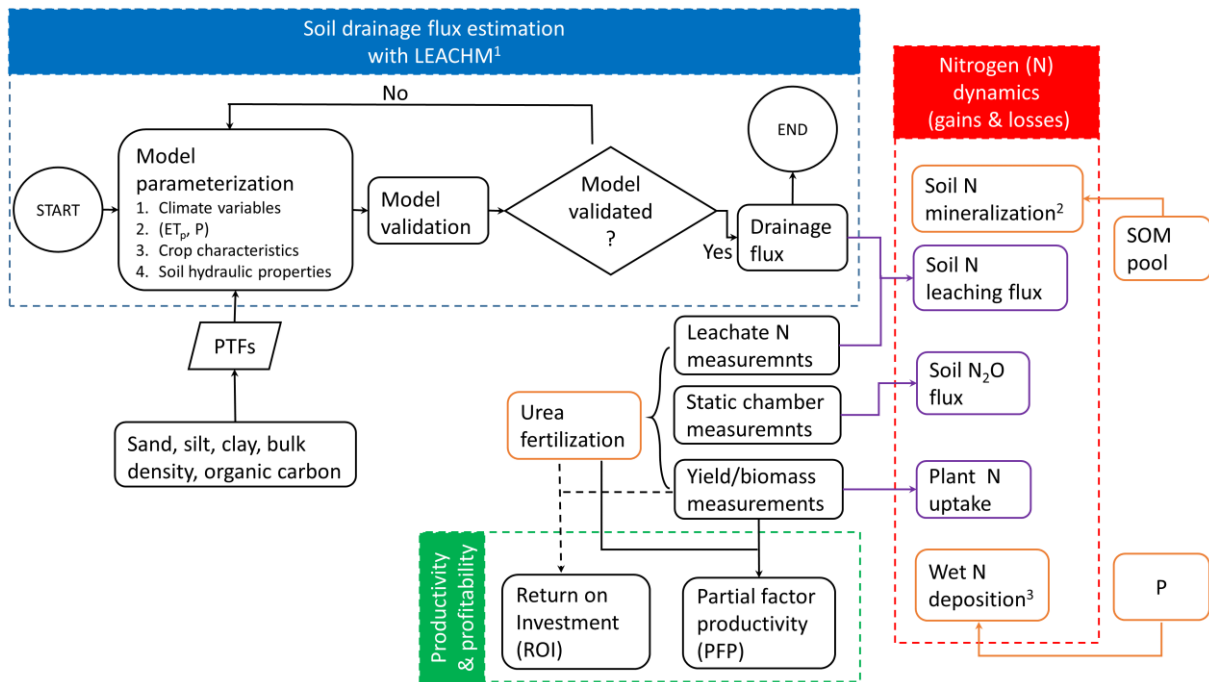


Figure 4.3. Flow chart of the methodology underpinning the study comprising of ¹drainage flux estimated with water subroutine of the Leaching Estimation and Chemistry Model (LEACHM; blue box; Hutson, 2003); nitrogen dynamics estimation (red box); and productivity and profitability assessment (green box). *P* denotes precipitation, and ET_p means potential evapotranspiration estimated with the Penman-Monteith method (Allen *et al.*, 1998). PTFs means pedotransfer functions (RAWLS82, ROSETTA, T&H98, WEY09, and WOS99) used to estimate the soil hydraulic properties in each soil layer in the 1-m-deep soil profile. N_2O and SOM denote nitrous oxide emissions and soil organic matter, respectively. ²Soil N mineralization was estimated from SOM using an empirical relationship proposed by R. H. McKenzie, personal communication, February 23, 2017. ³Wet N deposition in precipitation estimated by (Manu *et al.*, 2022). Brown boxes and arrows represent N gains, while purple boxes and arrows represent N losses.

N losses include: soil N leaching flux derived from the estimated drainage flux (in LEACHM; Hutson, 2003) and the measured leachate N concentrations, soil N_2O emissions obtained from static chamber measurements and gas chromatography, and plant N uptake obtained from dry biomass and its N content. Part three (green box in Fig. 4.3) aims at determining the productivity and profitability of sugarcane plantations at increasing urea fertilization rates. This part mainly comprises two components: partial factor productivity and return on investment. Partial factor productivity is field fresh weight per unit kg of N added, while return on investment is the revenue gained (USD) for every USD spent on urea fertilizers.

4.4. Results

4.4.1. Soil nitrogen dynamics at increasing nitrogen fertilization rates

4.4.1.1. Estimation of the soil water retention and hydraulic conductivity function

Table 4.2 reports the soil hydraulic parameters (θ_r , θ_s , α , n , and K_s) featuring in van Genuchten's soil water retention and hydraulic conductivity functions and used to determine soil water fluxes in LEACHM. All the five PTFs predicted soil hydraulic parameter values that ranged between 0 and 0.108 $\text{cm}^3 \text{cm}^{-3}$ for θ_r , 0.450 and 0.555 $\text{cm}^3 \text{cm}^{-3}$ for θ_s , 0.011 and 0.630 cm^{-1} for α , 1.079 and 1.419 for n . Regarding hydraulic conductivity function, all five evaluated PTFs predicted K_s values ranging between 6 and 109 cm d^{-1} for the topsoil layer (0-10 cm) and between 3 and 155 cm d^{-1} for the subsurface layers (10-100 cm; Table 4.2).

Table 4.2. Soil hydraulic parameters (residual water content (θ_r), saturated water content (θ_s), SWRF shape parameters (α and n), and saturated hydraulic conductivity (K_s) at the soil depths of 0-10, 10-30, 30-50 and 50-100 cm) estimated by five pedotransfer functions (PTFs; RAWLS82, ROSETTA, T&H98, WEY09, and WOS99).

PTF	Soil hydraulic parameters	Soil depth (cm)			
		0-10	10-30	30-50	50-100
RAWLS82	θ_r ($\text{cm}^3 \text{cm}^{-3}$)	0	0	0	0
	θ_s ($\text{cm}^3 \text{cm}^{-3}$)	0.459	0.461	0.515	0.538
	α (cm^{-1})	0.060	0.067	0.022	0.016
	n (-)	1.157	1.129	1.100	1.105
	K_s (cm d^{-1})	81.0	100.0	11.7	6.7
ROSETTA	θ_r ($\text{cm}^3 \text{cm}^{-3}$)	0.081	0.088	0.106	0.108
	θ_s ($\text{cm}^3 \text{cm}^{-3}$)	0.519	0.491	0.530	0.552
	α (cm^{-1})	0.017	0.019	0.024	0.024
	n (-)	1.419	1.376	1.282	1.281
	K_s (cm d^{-1})	69.7	34.8	32.3	38.6
T&H98	θ_r ($\text{cm}^3 \text{cm}^{-3}$)	0	0	0	0
	θ_s ($\text{cm}^3 \text{cm}^{-3}$)	0.515	0.501	0.503	0.512
	α (cm^{-1})	0.397	0.448	0.630	0.450
	n (-)	1.160	1.138	1.096	1.093
	K_s (cm d^{-1})	101	112	155	111
WEY09	θ_r ($\text{cm}^3 \text{cm}^{-3}$)	0	0	0	0
	θ_s ($\text{cm}^3 \text{cm}^{-3}$)	0.494	0.478	0.509	0.521
	α (cm^{-1})	0.016	0.015	0.011	0.011
	n (-)	1.167	1.134	1.083	1.079
	K_s (cm d^{-1})	6.17	5.12	3.07	2.99
WOS99	θ_r ($\text{cm}^3 \text{cm}^{-3}$)	0	0	0	0
	θ_s ($\text{cm}^3 \text{cm}^{-3}$)	0.528	0.487	0.517	0.545
	α (cm^{-1})	0.047	0.052	0.023	0.015
	n (-)	1.157	1.109	1.099	1.114
	K_s (cm d^{-1})	109	20	11	13

Evaluation of the performance of the five PTFs was based on the comparison between simulated and measured soil matric potential values at $z = 60$ cm and $z = 90$ cm (Fig. 4.4). RAWLS82, ROSETTA, and WOS99 PTFs estimated soil matric potentials that closely matched the measured matric potentials (Fig. 4.4 A-J; Appendix F.5). These PTFs (RAWLS82, ROSETTA, and

WOS99) obtained the lowest RMSEs (58-121 cm; Fig. 4.4A-D, I-J) and the highest R^2 (0.44-0.91; Fig. 4.4A-D, I-J) and d (0.67-0.89; Fig. 4.4A-D, I-J) indices. In addition, their NSE values ranged between 0 and 1 at the soil depth of 60 cm and between -0.71 and 0 at the soil depth of 90 cm (Fig. 4.4A-D, I-J). On the contrary, soil matric potential estimated by T&H98 and WEY09 PTFs poorly matched observed matric potential values. As a result, these PTFs (T&H98 and WEY09) obtained the lowest performance indicated by high RMSEs (127-309 cm), low R^2 (0.12-0.82), and d (0.22-0.79) (Fig. 4.4E-H), and more negative NSE values in comparison to RAWLS82, ROSETTA, and WOS99 PTFs (Fig. 4.4A-J).

Given the above-mentioned performance metrics, we derived the mean annual water balance components (runoff, drainage, evaporation, transpiration, and storage; Table 4.3; Appendix F.4) based on RAWLS82, ROSETTA, and WOS99 PTFs. Accordingly, we estimated that on average, drainage, surface evaporation, and transpiration represented 41%, 24%, and 35% respectively, of the precipitation (2,572 mm) while runoff and deep storage were negligible (0-0.7%; Table 4.3).

Table 4.3. Mean soil water balance components (runoff, drainage, evaporation, transpiration, and storage) from January 2019 and Jun 2020 based on RAWLS82, ROSETTA, and WOS99 PTFs.

PTF	Runoff (mm)	Drainage (mm)	Evaporation (mm)	Transpiration (mm)	Storage (mm)
RAWLS82	0	1102	548	892	30
ROSETTA	0	1069	611	892	0
WOS99	0	1108	550	892	22
Mean (\pm standard error, SE, N = 3)	0 \pm 0	1093 \pm 12	570 \pm 20	892 \pm 0.0	17 \pm 9

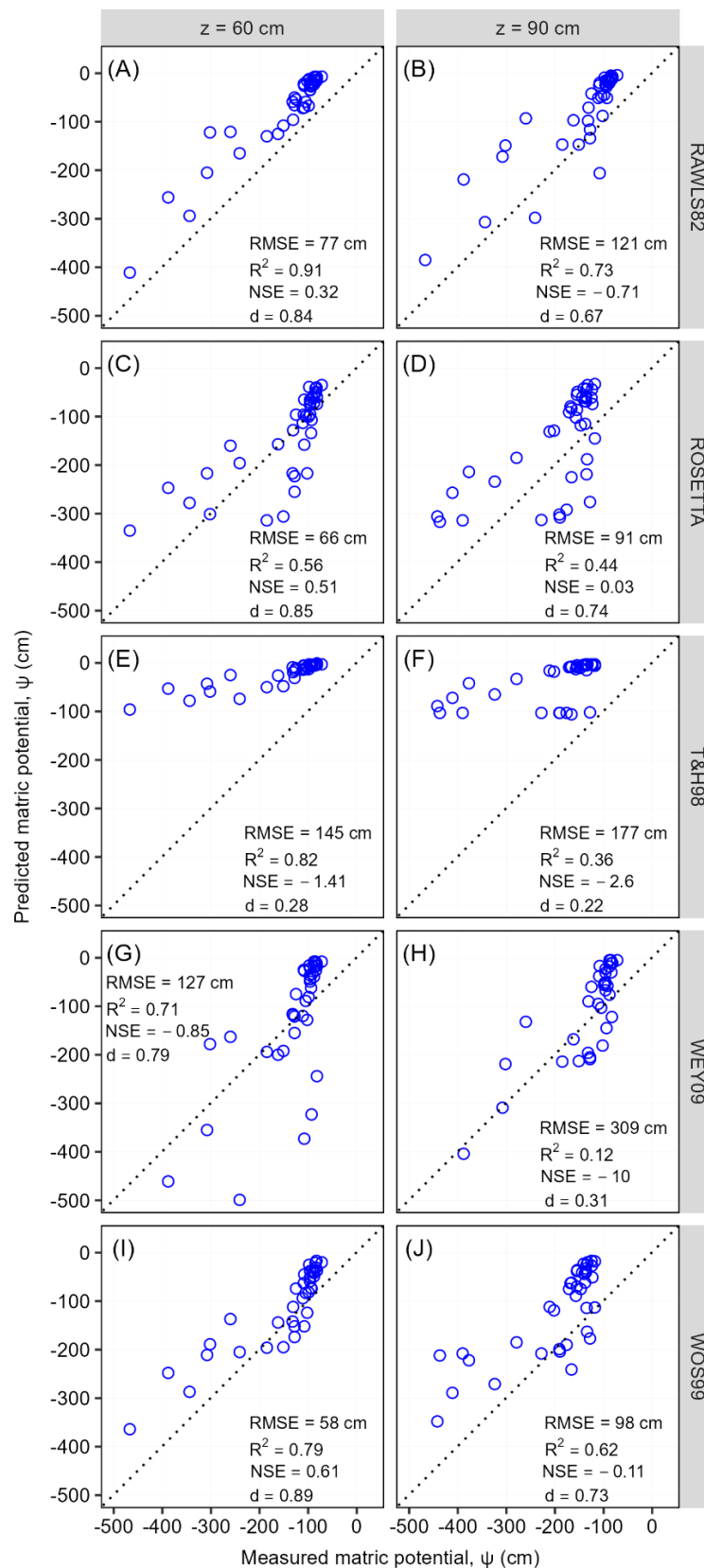


Figure 4.4. Predicted and measured soil matric potential based on RAWLS82 (A and B), ROSETTA (C and D), T&H98 (E and F), WEY09 (G and H), and WOS99 (I and J) pedotransfer functions at soil depths of 60 and 90 cm. The corresponding root mean square error (RMSE), coefficient of determination (R^2), Nash Sutcliffe efficiency (NSE), and index of agreement (d) are reported in each subplot.

4.4.1.2. Nitrogen leaching flux, soil nitrous oxide emissions, plant nitrogen uptake, and nitrogen balance

N leaching fluxes estimated by multiplying soil water drainage fluxes from the water subroutine of LEACHM and the measured soil solution N concentration from the suction cup lysimeters show that addition of N fertilizers at different rates (low, standard, and high) resulted in varying N leaching fluxes across space (Fig. 4.5A) and time (Fig. 4.6A). Mean annual N leaching flux measured from the low (1.7 ± 0.6 kg N ha⁻¹; Fig. 4.5A) and standard (3.4 ± 0.7 kg N ha⁻¹; Fig. 4.5A) treatment plots were comparable ($p \leq 0.05$) but both significantly lower than the mean annual N leaching flux measured from high treatment plots (14.2 ± 2.2 kg N ha⁻¹; $p \leq 0.001$; Fig. 4.5A). N leaching fluxes at 90 cm in all treatments peaked around the third- and eighth-week following fertilization (Fig. 4.6A), periods that corresponded to the largest rainfall amounts following fertilization (Fig. 4.6B). The N leaching fluxes thereafter declined to background levels (Fig. 4.6A) for the rest of the sampling period in all treatment plots except in the high fertilization treatment plots where relatively weak N leaching pulses were observed in the 17th and 21st weeks (Fig. 4.6A).

Interestingly, fertilization did not alter the magnitude of soil N₂O emissions since we measured comparable soil N₂O emissions across all treatment plots of the CRD experiment (~ 0.2 - 0.3 kg N ha⁻¹ yr⁻¹; Fig. 4.5B).

The mean N uptake under the low fertilization regime (61.9 ± 5.8 kg N ha⁻¹ yr⁻¹) was significantly lower than under standard (84.9 ± 9.4 kg N ha⁻¹ yr⁻¹) and high (93.5 ± 13.6 kg N ha⁻¹ yr⁻¹) fertilization regimes (Fig. 5C). Interestingly, fertilizer doses higher than the standard N fertilization rate resulted in only marginal and non-significant increases in plant N uptake for the high fertilization plots in comparison to the standard ones (Fig. 5C).

Available soil N added via urea fertilization (35 - 105 kg N ha⁻¹), soil N mineralization (34 kg N ha⁻¹), and wet N deposition (8.5 kg N ha⁻¹) was similarly distributed across treatments into plant N uptake, N leaching, soil N₂O emissions, and other N losses unquantified in this study (Fig. 4.5D). Plant (biomass) N uptake, N leaching, soil N₂O emissions, and other N losses represented ~ 60 - 75% , 2.1 - 9.3% , ~ 0.2 - 0.4% , and ~ 20 - 30% of the available soil N, respectively (Fig. 4.5D).

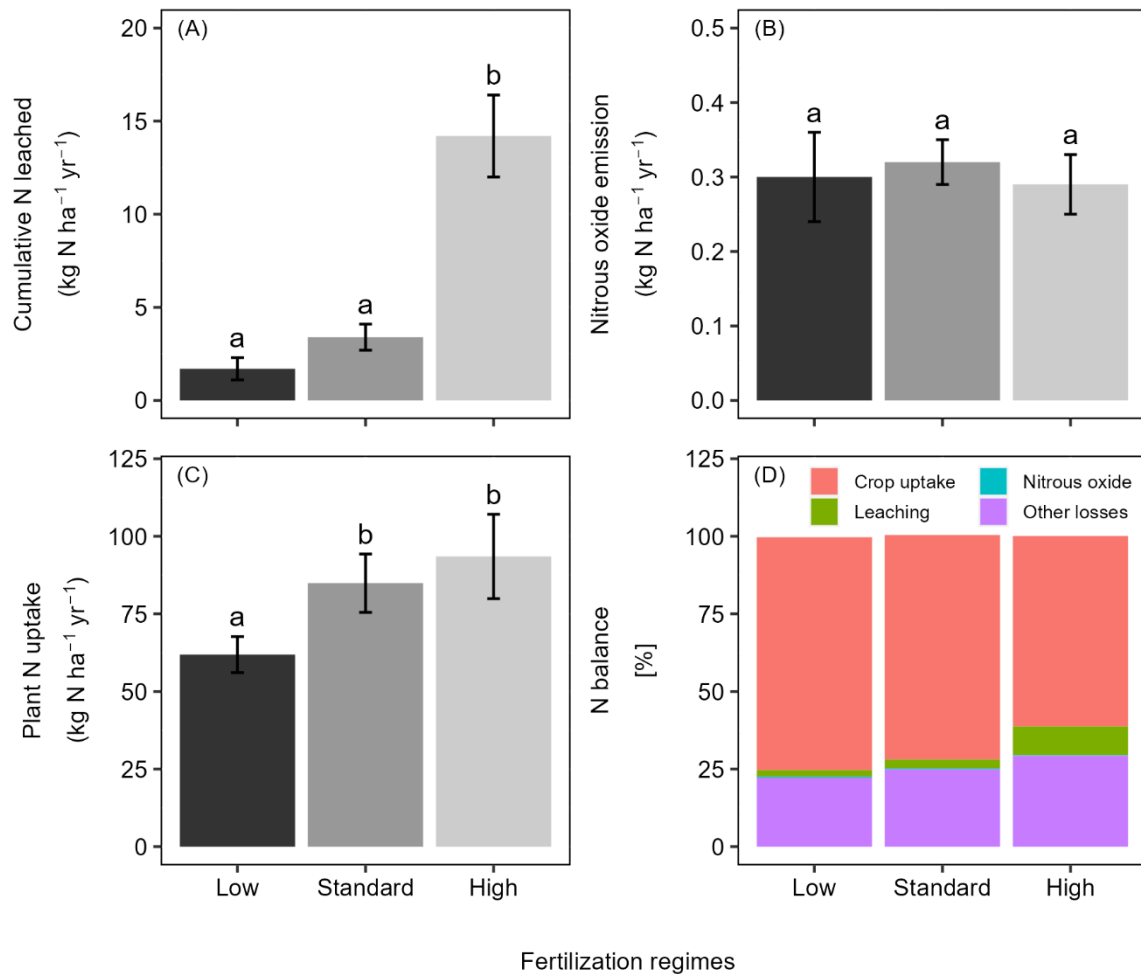


Figure 4.5. Mean (\pm standard error, SE) annual N leached (A), nitrous oxide emissions (B), plant N uptake (C), and the N balance (D) under low, standard, and high fertilization regimes. The value of nitrous oxide emissions and plant N uptake in panels A and B are means of four plots ($n = 4$), while for N leached, the mean N concentrations were obtained from two suction cup lysimeters installed in three of the four plots for low, standard, and high treatments ($n = 3$) and mean drainage fluxes based on three best performing pedotransfer functions (RAWLS82, ROSETTA, and WOS99). The N balance in panel D shows how N mineralized from soil organic matter, applied N, and natural N fertilization via wet deposition is distributed among the respective N pools under different treatments. Lowercase letters in panels A, B, and C indicate significant differences between treatments (ANOVA with Tukey's HSD test with a multiple-comparison extension test at $p \leq 0.05$).

4.4.1.3. Productivity and profitability of sugarcane cultivation at increasing nitrogen rates

The productivity (field fresh weight and partial factor productivity) and profitability (return on investment) indices are presented in Fig. 4.7. Field fresh weight increased with an increase in N fertilizer rate (low, 124 ± 12 Mg FFW ha⁻¹ yr⁻¹ < standard, 171 ± 16 Mg FFW ha⁻¹ yr⁻¹ < high, 192 ± 27 Mg FFW ha⁻¹ yr⁻¹; Fig. 4.7A), however, no significant differences in the mean field fresh weight were detected among treatments (Fig. 4.7A; $p = 0.057$). With respect to partial

factor productivity, utilization of the applied fertilizer was significantly higher at low N fertilization rates (3.5 ± 0.4 Mg FFW ha^{-1} kg N ha^{-1} ; Fig. 4.7B; $p \leq 0.001$) in comparison to both the standard (2.4 ± 0.2 Mg FFW ha^{-1} kg N ha^{-1}) and higher N fertilization rates (1.8 ± 0.3 Mg FFW ha^{-1} kg N ha^{-1}).

Contrary to the marginal increment in field fresh weight along the fertilizer intensification gradient (low < standard < high; Fig. 4.7A), return on investment declined by ~28-40% when N fertilization rates were increased from low to standard and by ~20-30% when N fertilization rates exceeded the standard, especially in the period between 2018 and 2020 (Fig. 4.7C). However, in the period between 2021 and 2022, when the market price of fertilizer increased nearly fourfold against the inelastic factory price for field fresh weight, return on investment almost shrunk to zero even at the lowest N fertilization rate (Fig. 4.7C).

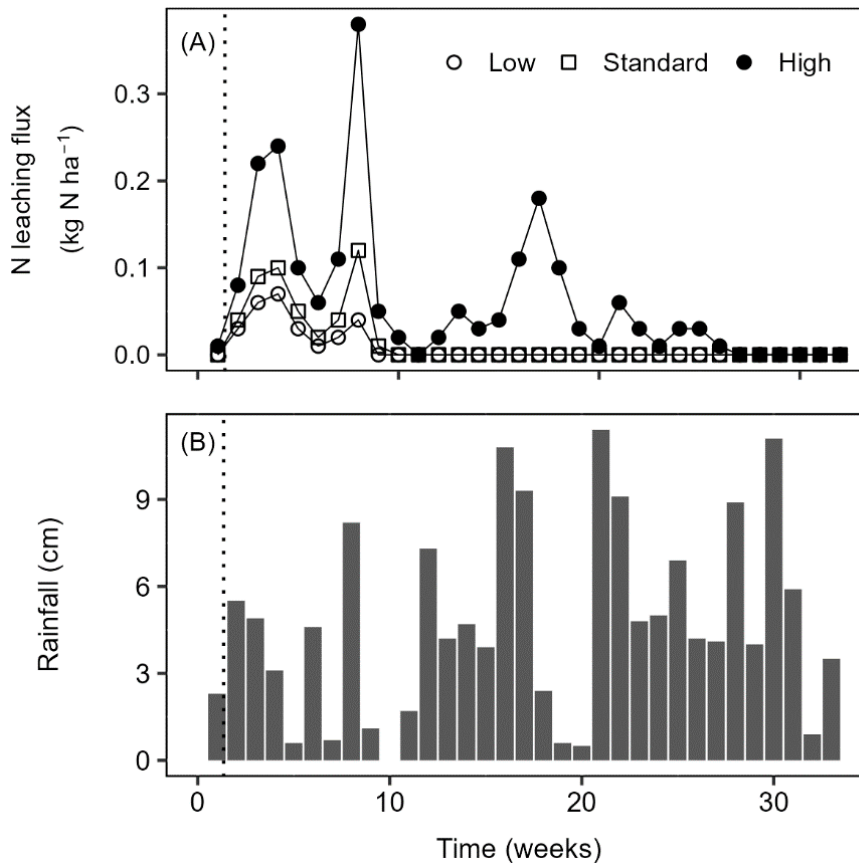


Figure 4.6. (A) Mean weekly N leaching flux from low, standard, and high fertilization regimes and (B) weekly rainfall sums between April and December 2019. The vertical dotted line indicates the timing of a single-dose fertilizer application in the treatment plots.

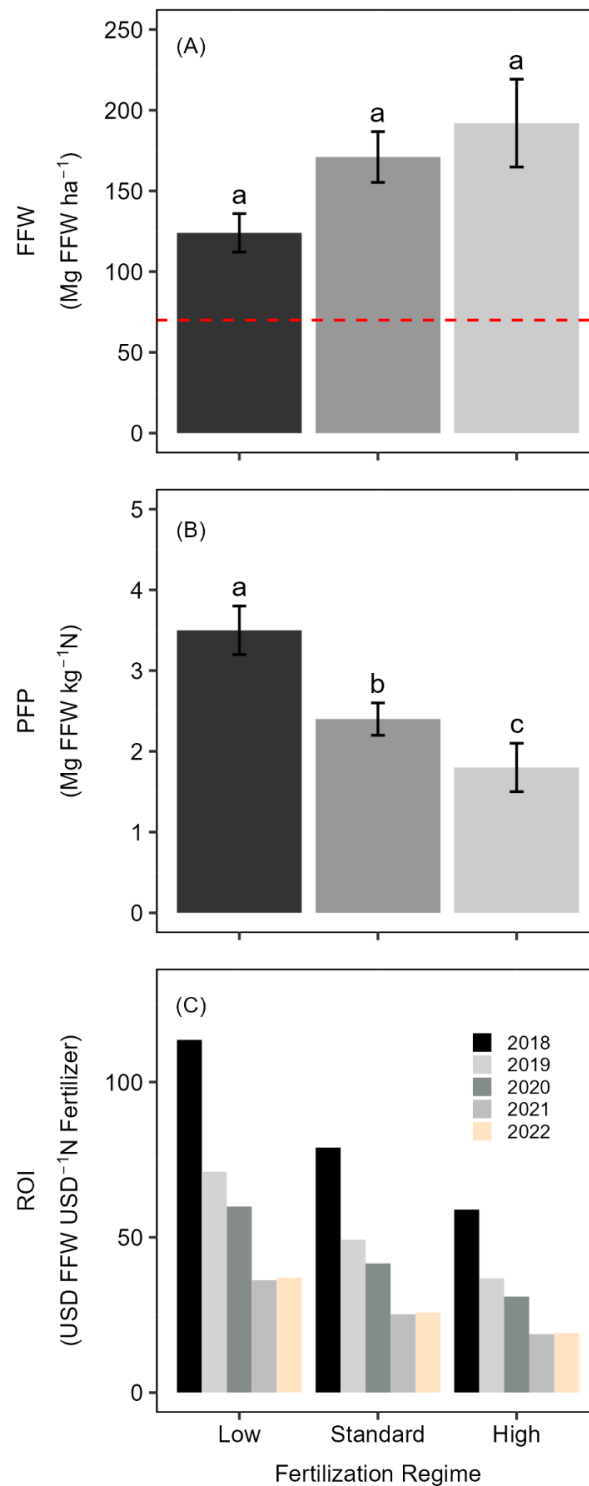


Figure 4.7. Mean (\pm standard error, SE, $n = 4$) yield expressed as field fresh weight (FFW; A), partial factor productivity (PFP; B), and return on investment (ROI; C), along the fertilizer intensification gradient (low, standard, and high). Lowercase letters in panels A, B, and C indicated significant differences between treatments (ANOVA with Tukey's HSD test with a multiple-comparison extension test at $p \leq 0.05$). The dotted horizontal red line in panel A indicates the minimum acceptable FFW from sugarcane ratoon fields in north-western Uganda, below which sugarcane fields are plowed down and new ones established (based on Masindi Sugarcane Farmers' Association).

4.5. Discussion

4.5.1. Performance of pedotransfer functions in the estimation of the soil hydraulic properties of Ferralsols

The N leaching part of the study was based on the simulation of water flux in the soil-plant-atmosphere continuum in LEACHM. However, knowledge of soil water retention function and hydraulic conductivity function was needed as it represents a fundamental prerequisite for both numerical solution of the Richards' equation and reliable simulations of drainage fluxes (Dane & Clarke Topp, 2002). Direct measurements of soil hydraulic properties entail large-scale field campaigns to collect soil samples and laboratory experiments, which are often tedious, labor-intensive, and time-consuming (Gijssman *et al.*, 2002; Nasta *et al.*, 2021). Moreover, relatively small soil samples may not replicate the water dynamics in a layered soil profile. Therefore, optimizing soil hydraulic parameters via inverse modeling is commonly used and involves minimizing the discrepancy between simulated and observed soil water content and soil matric potential values at different soil depths (Vrugt & Dane, 2005). However, multiple environmental sensors need to be installed and connected to a router that receives data at high temporal resolution from each probe node and transfers them to the coordinator, which streams the information to an internet server. This system enables the storage of a large amount of data but requires dedicated technicians and a considerable investment in hardware and software (Guelouz *et al.*, 2020), which are often missing in most parts of sub-Saharan Africa. Hence, under these circumstances, we opted to estimate the soil hydraulic parameters from readily available soil physical data using well-established PTFs (Van Looy *et al.*, 2017).

Three (RAWLS82, ROSETTA, and WOS99) of the five PTFs trained in the northern hemisphere under temperate climate conditions led to satisfactory model performance based on the comparison between simulated and observed soil matric potential values at soil depths of 60 and 90 cm (Fig. 4.4A-D, I-J). Surprisingly, T&H98 and WEY09 PTFs obtained the lowest performance (Fig. 4.4E-H), despite the former PTF being trained and validated on Brazilian Ferralsols, which are physically, mineralogically, and morphologically similar to the soils at our test site. Several potential explanations exist for this mismatch and the overall variability in the performance observed among PTFs: (i) performance of PTFs is linked to the pedological origin of the soil upon which it was developed and not necessarily the soil type (Minasny *et al.*, 1999); hence, application of PTFs beyond their pedological origin is often challenging (Gijssman *et al.*, 2002); (ii) the methods of particle size analyses (particularly pretreatment and dispersion of soils) are poorly defined, yet, this is particularly important for iron-rich soils (Ferralsols) in

which aggregates tend to be very stable and resistant to dispersion; (iii) the measurement of soil organic matter is influenced by the presence of calcite and stone sized particles.

4.5.2. Effect of increasing urea fertilization rates on nitrogen dynamics, productivity, and profitability of sugarcane

In this study, the sugarcane crops recovered between 60-75% of the available soil N in their aboveground biomass (Fig. 4.5D) with significant to marginal increases in crop N uptake measured along the fertilizer intensification gradient (Fig. 4.5C). Our findings on N recovery in sugarcane aboveground biomass contrast several previous studies that reported a much lower crop N uptake for sugarcane (i.e. between 28 and 55%; Tilman *et al.*, 2002; Vieira-Megda *et al.*, 2015; Vennila *et al.*, 2021). However, our findings are in agreement with the wide recognition that the N recovered in crop biomass is always much lower than what is added to the soil through SOM mineralization, wet N deposition, and N fertilization due to inevitable losses via N leaching (Blum *et al.*, 2013), N₂O emissions (Dattamudi *et al.*, 2019), and ammonia volatilization (Schwenke *et al.*, 2014). For our study, losses to N₂O emissions were very minimal for all the treatments (Fig. 4.5B), and so were the losses to N leaching except for the high N fertilization rates where leaching losses were substantial (Fig. 4.5A). Additionally, despite not measuring ammonia volatilization in our study, we still suspect that the 25-40 % unaccounted for losses in our respective sugarcane N budgets (Fig. 4.5D) might be the result of ammonia volatilization. As is the practice in north-western Uganda, we placed the urea fertilizers at the surface without incorporation into the soil, which likely predisposed the N fertilizers to increased ammonia volatilization. Schwenke *et al.* (2014) reported that nearly 30% of the applied N fertilizer was lost to ammonia volatilization when the N fertilizers were placed at the surface without incorporation in Australian cereal fields.

Field fresh weight marginally increased with higher urea fertilization rates, while partial factor productivity and return on investment significantly declined along the fertilizer intensification gradient (low > standard > high; Fig 4.7A-C). We postulate that the increase in mean field fresh weight at increasing urea fertilization rates was likely because N availability has been shown to stimulate photosynthetic traits of sugarcane such as chlorophyll content, stomatal conductance, leaf area, specific leaf nitrogen content, and photosynthetic rate as well as plant height and total leaves (Lofton & Tubaña, 2015; Dinh *et al.*, 2017), all of which led to increased biomass production. What is, however, surprising in our study is the fact that N-mediated increases in field fresh weight were only marginal contrary to previous studies that reported a significant increase in sugarcane field fresh weight following larger N doses (Lofton & Tubaña, 2015; Boschiero *et*

al., 2020). We think that the modest increment in field fresh weight along the fertilization intensification gradient at our study site was because part of the sugarcane N requirements was met through mineralization of the fairly high SOM stocks (34 kg N ha^{-1}) coupled with the addition of N via wet deposition (8.5 kg N ha^{-1} ; Manu *et al.*, 2022) thus dampening the responsiveness of sugarcane field fresh weight to large N doses. Similarly, Otto *et al.* (2016) found none to moderate responsiveness of sugarcane field fresh weight to N fertilization in nearly 34 of the 45 established experimental trials in Brazil. They attributed this to the sufficient supply of N from the mineralization of the SOM stocks.

It is important to highlight that on the one hand, our field fresh weight estimates from all the treatments (low, standard, and high; $124\text{-}192 \text{ Mg ha}^{-1}$) were comparable to those reported by (Tayade *et al.*, 2020) ($\sim 180 \text{ Mg ha}^{-1}$) and on the other hand, were mostly on the upper end ($30\text{-}150 \text{ Mg ha}^{-1}$) of those reported by Yadav (2004), Lofton & Tubaña (2015) and Premalatha *et al.* (2016). Two possible explanations exist for the higher field fresh weight estimates in our study. (i) It is likely that N fertilization increased millable canes, cane length, girth, and weight along the fertilizer intensification gradient, as similarly suggested by Tayade *et al.* (2020). (ii) It could also be that despite randomizing the biomass measurements in every treatment plot, we still inadvertently underrepresented sprouting failures increasing the variability in our biomass estimates. Stubble bud sprouting failures in ratoon cane fields (due to pests, diseases, and mechanical damage) have been shown to result in low shoot populations and reduced cane yields (Jain *et al.*, 2007; Shukla *et al.*, 2009). Our findings demonstrated that provided sprouting failures in the ratoon fields are minimized, for instance through gap filling. In consequence, farmers in north-western Uganda can potentially realize the minimum acceptable yield threshold of $70 \text{ Mg FFW ha}^{-1}$ even at lower-than-standard fertilization rates (Fig. 4.7A).

Partial factor productivity is an integrative index that quantifies the total economic output of the respective fertilization regimes relative to the utilization of the applied N (Antille & Moody, 2021). A perusal of the data on partial factor productivity revealed a decline in the estimated partial factor productivity along a fertilizer intensification gradient (Fig. 4.7B). The declining partial factor productivity at increasing N rates has also been previously reported by Premalatha *et al.* (2016) in Indian sugarcane fields as well as Thorburn *et al.* (2013, 2017) in Australian sugarcane fields. The higher partial factor productivity at low N doses reflects better utilization of the applied N fertilizer resulting from a much higher physiological efficiency of the sugarcane crop under N-limited conditions (Suman *et al.*, 2007). Nonetheless, the partial factor productivity estimates for the respective fertilization regimes were still on the upper end of the

worldwide partial factor productivity ranges for sugarcane (0.25-0.9 Mg FFW kg⁻¹ N; Thorburn *et al.*, 2013) mainly because partial factor productivity was a derivative of the much higher field fresh weight. Notwithstanding, return on investment—the economic analysis of the profitability of the different fertilization regimes, followed a comparable trend as seen with partial factor productivity (Fig. 4.7C). However, it is worth highlighting that during the years when the market price of fertilizers increased fourfold against a stagnant factory price of field fresh weight, application of fertilizers, even at the lowest N rate only resulted in extremely small to no return on investment margins (Fig. 4.7C).

4.6. Conclusion

In this study, we investigated the effect of increasing urea fertilization rates on nitrogen dynamics, productivity, and profitability of sugarcane plantations established on Ferralsols in north-western Uganda. We established a completely randomized design experiment subject to three N fertilization rates (low, standard, and high) as treatments and four replications. In every replicate plot, we determined: (i) N leaching fluxes by integrating estimates of soil water drainage fluxes (from the best-performing PTFs) and measured nitrate concentrations in percolating water sampled with suction cup lysimeters; (ii) soil N₂O fluxes using static chambers and gas chromatograph; and (iii) sugarcane field fresh weight (yield) by harvesting four random 1 m rows. Our results show that sugarcane field fresh weight increased with increasing urea rates though the field fresh weight increment was insignificant. Additionally, we demonstrated that determining N leaching flux in the data-poor sub-Saharan region could inexpensively benefit from PTFs trained in North America or Europe.

Furthermore, N leaching fluxes marginally increased when low to standard N rates were used but significantly increased when the standard N rate was exceeded. Lastly, soil N₂O emissions were unaffected by N fertilization. All the findings from this study highlight that the standard N rate is the most economically viable and profitable fertilization regime for sugarcane production in Uganda since higher N rates lead to only marginal increases in sugarcane yields at the expense of groundwater quality in shallow aquifers. Additionally, we showed that provided the inherently high SOM levels in the sugarcane fields are maintained through residue retention combined with minimizing sprouting failures through gap filling, sugarcane cultivation can still be feasibly profitable at lower-than-standard N fertilization rates. This is because field fresh weight at low N rates exceeded the minimum acceptable yield threshold of 70 Mg FFW ha⁻¹ set by farmers in north-western Uganda. What remains unclear from this short-term study, however, is if lowering N rates below the standard N rate will not counterintuitively lower SOC

stocks in the long term since the measured high SOC stocks under sugarcane reflect the long-term C input dynamics obtained with the standard N rates.



CHAPTER 5. SYNTHESIS

5.1. Main findings

The main aim of the PhD thesis was to discern the regulation effect that nutrient availability has on soil GHG fluxes and N leaching losses in a nutrient-limited tropical forest and an intensively fertilized sugarcane plantation in north-western Uganda. Specifically, it focused on how: (i) nutrient limitations regulate soil GHG fluxes from tropical forests; (ii) deforestation for sugarcane cultivation alters soil GHG fluxes; and (iii) urea fertilization affects N dynamics (crop N recovery, soil N leaching, and soil N₂O emissions), productivity and profitability under sugarcane. Therefore, a factorial nutrient manipulation experiment (NME) was setup in the tropical forest comprising of N, P, N+P, and the control treatments and a completely randomized design (CRD) experiment in the proximally neighboring sugarcane plantation comprising of a fertilizer intensification gradient of the commonly used N and K application rates (low, standard, high) as treatments.

In the first part of the PhD thesis, the tropical forest responses to changes in soil macronutrient dynamics in the context of increasing N and P deposition rates over the African tropical regions were assessed. It was found that soil N₂O fluxes significantly increased in the first 28 days following N addition (N or N+P) because N fertilization likely increased available soil N beyond microbial and plant needs leaving excess N to (de)nitrification. Surprisingly, sustained N fertilization did not affect background soil N₂O fluxes measured more than 28 days from fertilization. CH₄ consumption was marginally increased immediately after P fertilization (0-28 days) and significantly in the long-term (> 28 days after fertilization) because P availability likely enhanced methanotrophic activity. Soil CO₂ effluxes immediately increased in plots that received a combined dose of N and P (N+P) in comparison to the control reflecting a possible co-limitation of N and P availability on soil respiration in tropical forests. Despite the fertilizer rates used in this study not exactly mimicking the natural N and P deposition rates, the findings potentially suggest that the increasing N and P deposition rates over the tropical regions will likely alter tropical forest contribution to global GHG flux budgets. Hence, N and P deposition is most likely to be an important consideration in constraining tropical and global GHG flux budgets.

Using the SOC stocks and soil GHG fluxes measured from the control plots of the forest NME study in combination with the SOC stocks and soil GHG fluxes measured from the respective treatment plots (low, standard, and high rates) of the sugarcane CRD experiment, it was assessed how deforestation for sugarcane affected soil GHG flux budgets. Soil CO₂ fluxes were significantly higher under sugarcane compared to forest resulting from the higher autotrophic

respiration by the sugarcane's larger fine root biomass coupled with microbial decomposition of the sugarcane's larger SOC stocks. Sugarcane soils, however, consumed significantly lower CH₄ amounts compared to forest soils because the shift in land use likely resulted in alteration of methanotrophic abundance. Surprisingly, despite application of N fertilizers in the sugarcane, soil N₂O fluxes under sugarcane were significantly lower than the forest which is attributed to increased N recovery in the sugarcane biomass as well as N leaching losses to deep percolation. All the results combined demonstrate that even with the higher soil CO₂ effluxes under sugarcane compared to the forest, the increase in SOC sequestration in the sugarcane plantations of the different ages relative to the native forest, suggests that sugarcane systems in the study area acted as a C sink since the uptake of CO₂ (approximated from SOC sequestration) far exceeds SOM mineralization. However, SOC sequestration under sugarcane does not offset the initial significant loss in the above and belowground biomass C loss immediately after forest conversion. Moreover, the C sink under sugarcane can change if CO₂-equivalents related to N₂O and CH₄ fluxes are considered in the calculation of the sugarcane's C footprint.

Lastly, the effect of urea fertilization rates on N dynamics, productivity, and profitability under sugarcane was assessed using soil N₂O emissions from the different sugarcane CRD experimental treatment plots (low, standard and high N rates) in combination with the measurements on N allocation in sugarcane biomass and modelling of N leaching rates. However, the determination of N leaching rates as part of the N dynamics was limited by the lack of measurements on soil hydraulic characteristics for the study test site. This challenge was overcome by testing a suite of American, Brazilian, and European pedotransfer functions (PTFs) for their suitability in determining the soil water retention and hydraulic conductivity function for the study test site in Uganda. Hence, it was demonstrated that some PTFs were robust enough to be used outside their training and validation areas with a satisfactory degree of accuracy. N leaching fluxes marginally increased when N rates were increased from low to standard but significantly when the N rates exceeded the standard rate. N losses via soil N₂O emissions were negligible across the fertilizer intensification gradient. Additionally, a non-significant response of sugarcane yield to N fertilization was measured despite a significant to marginal increase in crop N uptake between low and standard N rates and at N rates higher than the standard, respectively. In the third study, it was demonstrated that surpassing the standard N rate for sugarcane in north-western Uganda would be less economically viable since it would only marginally increase yields at the expense of increased N loads in groundwater. Additionally, despite demonstrating that sugarcane cultivation can still be profitable at lower-than-standard N rates since part of the N requirement is met by mineralizing the high soil organic matter levels in sugarcane

fields, it remains unreconciled from this short-term study whether reducing N rates below the standard N rate will not counterintuitively lower SOC stocks in the long term. The high SOC stocks under sugarcane reflect the long-term C input dynamics obtained with the standard N rates.

5.2. How different are tropical forests from high-latitude forests in their soil greenhouse gas flux response to changes in nutrient dynamics?

Up until now, the discourse about forest soil GHG flux response to changes in nutrient dynamics has been largely centered around findings from high-latitude forest biomes (i.e., temperate forests; Bowden *et al.*, 1991; Ambus & Robertson, 2006 and boreal forests; Matson *et al.*, 2009; Rütting *et al.*, 2021) because tropical forest NME studies remain rare. Notwithstanding, emerging evidence from the tropics now shows that tropical forests are strikingly different from their temperate and boreal forest counterparts in their soil GHG flux response to changes in the inherent soil nutrient dynamics. Chapter two of this study brings forth new insights that partially or fully reinforce the emerging evidence from the tropics.

For instance, it was found that addition of N (N or N+P) at the N saturated tropical forest site located in mid-latitude Africa resulted in increased soil N₂O fluxes immediately (0-28 days) after N fertilization corroborating findings of Koehler *et al.* (2009), Corre *et al.* (2014), and Wang *et al.* (2014). Even if a spike in background soil N₂O fluxes was not measured after sustained fertilization at this tropical site during the two years of N addition, it is still postulated that continuing the fertilization activities for longer periods (e.g., over five years) would likely yield comparable responses in background soil N₂O fluxes as those reported by Hall & Matson (1999) and Koehler *et al.* (2009). The immediate and long term increase in soil N₂O fluxes following fertilization is attributed to the leaky nature of the N cycle in old-growth tropical forests predisposing them to increased soil N₂O losses (Hall & Matson, 1999; Koehler *et al.*, 2009b). Conversely, in N-limited temperate and boreal forests, N is retained to support forest productivity, species composition, and diversity (Högberg *et al.*, 2017; Zhang *et al.*, 2022). Hence, in such forest biomes, increases in soil N availability only result in a slow and delayed response in soil N₂O fluxes (Magill *et al.*, 1997; Gundersen *et al.*, 1998). Indeed, this is corroborated by the minimal to no effect of N addition on soil N₂O fluxes even in temperate and boreal forest experimental setups where the applied N fertilization rates (> 125 kg N ha⁻¹ yr⁻¹) exceeded those used in this experiment (Boden *et al.*, 1991; Ambus & Robertson, 2006; Matson *et al.*, 2009; Rütting *et al.*, 2021).

Contrary to the widely reported inhibition effect of N addition on CH₄ uptake in temperate forest soils (Stuedler *et al.*, 1989; Gullledge *et al.*, 2004; Yang *et al.*, 2017), no indication that N availability limited soil methanotrophic activity was found at this N saturated old-growth tropical forest site both on the short- and long-term. Instead, it was P addition that stimulated soil methanotrophic activity immediately and after prolonged P addition. While the effect of P on soil methanotrophic activity in tropical forests has been partly linked to P availability increasing root water uptake and the concomitant increase in aerobic sites for soil CH₄ consumption (Zhang *et al.*, 2011), the water filled pore space data from the P plots does not support this line of thought. Notwithstanding, the regulation effect of P on soil methanotrophic activity in both tropical and high latitude forests is far from being reconciled because studies on P limitation of CH₄ uptake are still limited in both biomes.

Contrary to the temperate and boreal forests which grow on young soils rich in P (Finzi, 2009; Vadeboncoeur, 2010; Allen *et al.*, 2020), it was expected that soil CO₂ effluxes from this P-limited tropical forest would respond positively to lifting of the P limitation on the autotrophic and heterotrophic components of soil respiration. This is because, like for all tropical forests, the test site too had low soil P levels attributed to heavy fixation of the rock derived P by the low weatherable minerals (Halloysites and Kaolinites), and oxides and hydroxides of iron and aluminium prevalent in these soils (Martinelli *et al.*, 1999; Dalling *et al.*, 2016; Wright *et al.*, 2018; Wright, 2019). This hypothesis was, however, partially confirmed since N+P instead of P addition plots showed a positive response to increases in P availability shortly after fertilization (0-28 days). This study, thus, reinforces earlier evidence that soil respiration in tropical forests is co-limited by N and P availability with some soil respiration components responding positively to N addition and others to P availability yielding an overall additive effect than when N or P are added alone (Barantal *et al.*, 2012; Fanin *et al.*, 2015, 2016; Bréchet *et al.*, 2019). Therefore, both the study findings and those of Barantal *et al.* (2012), Fanin *et al.* (2015), and Bréchet *et al.* (2019), highlight the need for NME studies to evaluate the combined effect of N and P on tropical forest ecosystem functioning. The multiple-nutrient limitation concept, has for long been centred around the nutrient-rich high latitude forest ecosystems (Elser *et al.*, 2007; Vadeboncoeur, 2010), yet emerging evidence now shows that that this concept could potentially extend to tropical forests (Bréchet *et al.*, 2019).

5.3. How will increasing nitrogen and phosphorus deposition rates over the tropics affect tropical forest soil greenhouse gas fluxes?

While the NME experiment in chapter two of this study was established to investigate how nutrient limitations constrain soil GHG fluxes, it also sheds valuable insights on how anthropogenic nutrient inputs (through deposition) may affect future soil GHG fluxes from African tropical forests and other tropical sites with a similarly pronounced rainfall seasonality as well as specific soil and vegetation characteristics (Table 2.1). Nutrient depositions are often highest immediately after the onset of the rainy season (Wang *et al.*, 2020), especially due to aerosol deposition following burning activities associated with deforestation during the dry season (Giglio *et al.*, 2006; Roberts *et al.*, 2009). Accordingly, it is suspected that the increased N inputs during this short time may yield similar responses to those observed in the transitory period measured at this study site, namely N₂O flushes when reactive nitrogen enters the soil. Although N additions did not elicit a positive N₂O response during the background period, it is quite likely that our fertilization activities (from year 1 to year 2 of the study) had not gone on for long enough to simulate chronic long-term N additions. A study conducted by Koehler *et al.* (2009) in Panama showed that 11 years of chronic N addition significantly increased both transitory and background soil N₂O emissions. In addition, this study shows that future increases in P deposition over tropical forests may significantly increase the CH₄ sink capacity of tropical forest soils. Also, it was interesting to observe that the addition of N and P simultaneously resulted in increased CO₂ effluxes immediately after fertilization, likely suggesting a co-limitation of N and P on soil respiration. This means that future increases in the deposition of N- and P-rich ashes (from biomass burning) might result in significant soil CO₂ emissions from these biomes, while it is unclear if this is compensated via an increase in photosynthetic CO₂ uptake, as indicated by Cernusak *et al.* (2013). In this context, it is important to note that it has been demonstrated by Barkley *et al.* (2019) that P derived from biomass burning aerosols is more soluble than the P from dust aerosols; hence, the former would have an immediate impact on ecosystem processes.

5.4. How does forest-sugarcane conversion drive global change?

Findings of chapter three of this study highlight how deforestation for sugarcane cultivation results in a large immediate release of C stored in forest aboveground biomass as much of the standing biomass is cut down or burnt (172 Mg C ha⁻¹; Fig. 5.1). This is subsequently followed by the gradual decomposition of forest belowground biomass in the years after forest clearing

(22.4 Mg C ha⁻¹; Fig. 5.1). Once converted to sugarcane, soil CH₄ uptake rapidly declines relative to the forest (Table 3.3). At the same time, C is sequestered by the growing sugarcane, but this sequestration is short-lived as it is again released to the atmosphere (14.6 Mg C ha⁻¹ yr⁻¹; Fig. 5.1) when the sugarcane is harvested (at about 18 months) and processed.

Equally remarkable though unexpected, are the significantly larger SOC stocks in both the 20- and 50-year-old sugarcane plantations compared to the forest (Fig. 3.3D). It was expected that SOC stocks would decline after deforestation because there will be reduced litter input to soils (Guo & Gifford, 2002). Further, the warmer soil temperatures and tillage activities (to 30 cm) in sugarcane will certainly have increased the vulnerability of both the old and new SOC stocks to microbial decomposition (Six *et al.*, 1998). Instead, a 26-44% increase in SOC stocks was measured in the sugarcane plantations in comparison to the forest (Fig. 3.3D). On one hand, it is suspected that the net SOC accumulation in sugarcane reflected: (i) slower leaf litter decomposition rates because sugarcane leaves have a higher C/N ratio than the forest litter, and (ii) increased root productivity will result in the increased allocation of C to the root network (Anderson-Teixeira *et al.*, 2013). On the other hand, the 15% difference in SOC stocks (21.5 Mg C ha⁻¹; Fig. 3.3D) between the 20- and 50-year-old sugarcane plantations likely suggests that the SOC stocks under sugarcane were not yet in equilibrium. These results imply that the SOC stocks in sugarcane may take several decades after deforestation before they reach a new SOC equilibrium, which contrasts some studies that reported 10–20 years for the equilibration of SOC stocks under converted land uses (de Blécourt *et al.*, 2013; van Straaten *et al.*, 2015). However, due to the lack of other constraining data to identify the source and age of C in soil along the conversion gradient, it is hard to verify this interpretation. It is equally possible that the results of increasing SOC stocks are not related to C increases after conversion to sugarcane, but rather selective preservation of forest SOC on low-fertility agricultural fields (Cadisch *et al.*, 1996).

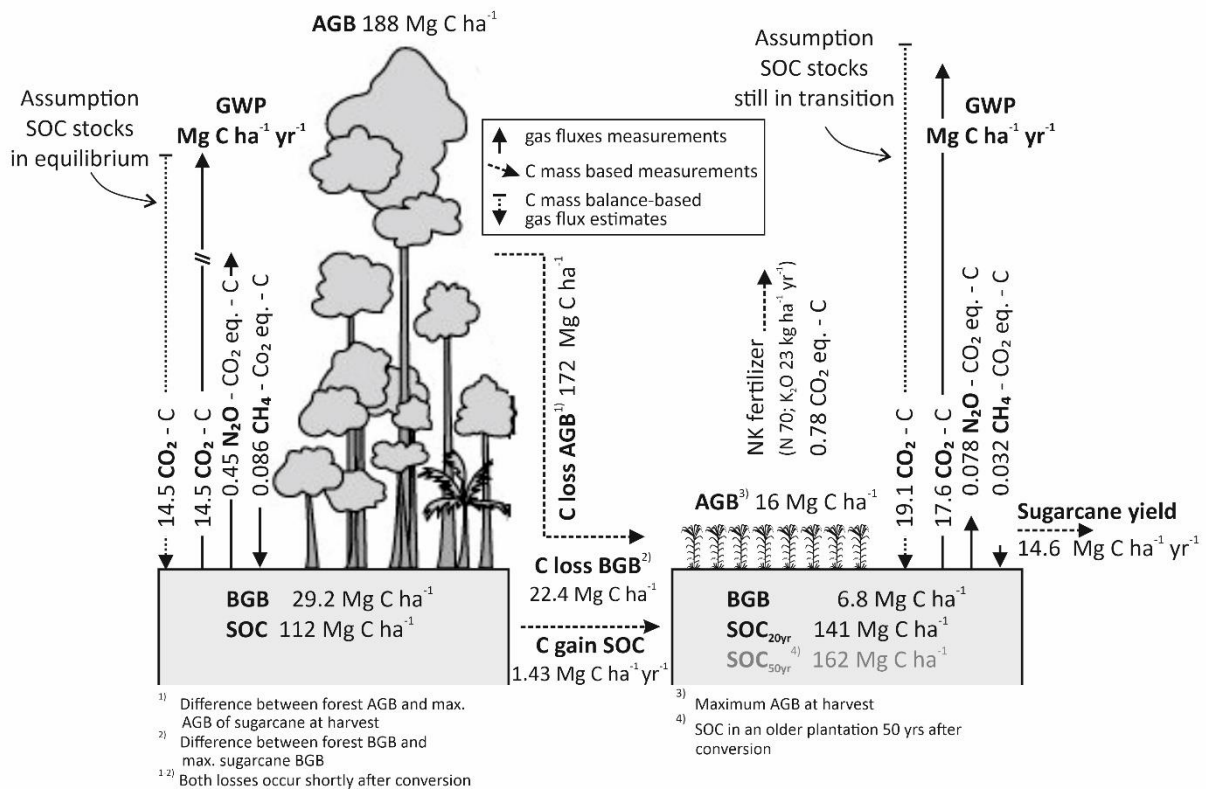


Figure 5.1. Schematic illustration of the implication of forest replacement with fertilizer-based sugarcane production on the net ecosystem C fluxes. AGB is aboveground biomass, BGB is belowground biomass, SOC_{20 yr} and SOC_{50 yr} are the soil organic carbon stocks in the sugarcane fields after 20 and 50 years of establishment (deforestation), respectively. The fertilizer application rates, maximum AGB, and yield for the sugarcane system represent a typical standard sugarcane system (i.e., Standard equals 70 kg N + 23 kg K ha⁻¹ growth cycle⁻¹) in north-western Uganda.

5.5. Implications for nutrient management under sugarcane

Fertilizing above the standard N rate for sugarcane (70 kg N ha⁻¹) is not uncommon among sugarcane farmers in north-western Uganda because there is a wide perception that higher N fertilizer rates normally translate to higher yields compared to when standard N rates or lower N rates are used. Findings of chapter four of this study cast doubt on this line of thinking. Despite sugarcane field fresh weight increasing along the fertilizer intensification gradient (low N rate < standard N rate < high N rate), the increase was not significant. Profitability under sugarcane, is in part, a tradeoff between the cost of fertilizer inputs and amount of harvested field fresh weight. However, the prices of fertilizers in Uganda and across Africa have been and remain very volatile against inelastic prices of sugarcane field fresh weight. For instance, in the past five years, the price of fertilizer (per kg N) increased by almost fourfold against a constant price of biomass (per ton of field fresh weight) shrinking the profit margins even at the lowest

fertilization rates due to the high cost of fertilizers (Fig. 4.7C). Interestingly, the barrier to profitability created by increase and or fluctuations in the price of fertilizers can be overcome by effectively tapping into the inherent potential of the sugarcane soils to release adequate levels of limiting nutrients for crop growth from SOM rather than heavily relying on expensive nutrient sources. Our findings show that the sugarcane soils at our site are rich in SOM (Fig. 3.3 D) and can potentially release nearly 34 kg N ha yr⁻¹ through mineralization processes (Fig. 4.3). Therefore, maintaining high levels of SOM in sugarcane fields combined with addressing the challenge of sprouting failures evident across most sugarcane fields (through gap filling) in north-western Uganda would likely help sugarcane farmers in this sub-Saharan country close the yield gap without heavily investing in fertilizer inputs which increase N loads in the ground water resources. It, however, remains unreconciled from this short-term study whether reducing N rates below the standard N rate will not counterintuitively lower SOC stocks in the long term. The high SOC stocks under sugarcane reflect the long-term C input dynamics obtained with the standard N rates.

5.6. General conclusion and outlook

This PhD study is one of the pioneer studies to disentangle the regulation effect that soil macronutrient availability has on soil GHG fluxes from tropical forests, unravel how conversion of forest to sugarcane would affect soil GHG budgets, and shed valuable insights on nutrient use efficiency under sugarcane plantations managed with different fertilization rates. The most important findings are:

- (i) Nutrient availability disproportionately altered soil GHG fluxes from the tested old-growth tropical forest immediately (0-28 days) and after (> 28 days) sustained nutrient additions. Soil N₂O emissions significantly increased shortly after addition of N and N+P suggesting that N availability in N addition plots exceeded microbial and plant N demands resulting in significant nitrification and denitrification losses. Soil respiration significantly increased shortly after addition of N and P together suggesting a possible co-limitation of N and P on soil respiration. Soil CH₄ uptake was significantly larger in P addition plots compared to the control suggesting a positive effect of P availability on soil methanotrophs;
- (ii) Forest conversion to sugarcane resulted in an immediate significant loss of native forest C coming from the cutting and burning of aboveground biomass and increased decay of the belowground biomass. After conversion, sugarcane, being a highly productive C₄ crop, sequestered significant amounts of atmospheric CO₂ via photosynthesis which was then allocated to the soil C pool through the decay of fine root biomass and routinely retained

residues. Indeed, SOC stocks under sugarcane plantations were significantly higher than under forest with the build-up of SOC stocks under the sugarcane being influenced by the time since conversion. The increase in soil C sequestration with plantation age is corroborated by the significantly higher SOC stocks in the 50-year-old sugarcane plantations compared to the 20-year-old-sugarcane plantations. The SOC stocks buildup in sugarcane plantations of different ages (20 and 50 years) suggests sugarcane system as a C sink, but this does not offset the initial significant loss of forest above and belowground C following conversion. Moreover, the C sink under sugarcane can change if the CO₂-equivalents of N₂O and CH₄ are considered.

- (iii) There was a slight increase in field fresh weight along the fertilizer intensification gradient (low > standard > high), but this was not statistically significant due to the large variability in yield. Interestingly, it was demonstrated that farmers could still attain the minimum acceptable field fresh weight even at lower-than-standard N rates because part of the plant N requirement is likely met through the mineralization of the inherently high SOM levels under sugarcane. It was estimated that sugarcane soils potentially released nearly 34 kg N ha⁻¹ of the plant N requirement through mineralization. However, even though these findings seemingly offer promising prospects on obtaining the minimum acceptable sugarcane yields (70 ton FFW /ha) at lower-than-standard N rates, it remains unclear from this short-term study, if lowering N rates below the standard N rate will not counterintuitively lower SOC stocks in the long term. This is because the measured high SOC stocks under sugarcane reflect the long-term C input dynamics obtained with the standard N rates.

This PhD study is the first to measure soil GHG fluxes and N dynamics from an African native tropical forest and sugarcane plantation over a period of fourteen months. Evidently, more studies are needed to: (i) discern how lifting of macronutrient limitations would affect different microbial communities that mediate the magnitudes and rates of the measured soil GHG fluxes from African tropical forests; (ii) improve our mechanistic understanding of the regulation effect of P on methanotrophic activity; (iii) elucidate how changes in N and P availability affects nitrification and denitrification processes as well as the autotrophic and heterotrophic components of soil respiration; (iv) unravel how deforestation for high value crops or conversion of cropland back to forest affects C dynamics; (v) and improve constraining N budgets in tropical agroecosystems by improving N leaching estimates.

REFERENCES

- de los A. Portocarrero, R. & Acreche, M.M. 2013. Nitrate Leaching in an Argiudoll Cultivated with Sugarcane. *Sugar Tech*, 16, 1–4.
- Achard, F., Beuchle, R., Mayaux, P., Stibig, H., Bodart, C., Brink, A., Carboni, S., Desclée, B., Donnay, F., Eva, H.D., Lupi, A., Raši, R., Seliger, R. & Simonetti, D. 2014. Determination of tropical deforestation rates and related carbon losses from 1990 to 2010. *Global Change Biology*, 20, 2540–2554.
- Adamek, M., Corre, M.D. & Hölscher, D. 2009. Early effect of elevated nitrogen input on above-ground net primary production of a lower montane rain forest, Panama. *Journal of Tropical Ecology*, 25, 637–647.
- Aini, F.K., Hergoualc’h, K., Smith, J.U., Verchot, L. & Martius, C. 2020. How does replacing natural forests with rubber and oil palm plantations affect soil respiration and methane fluxes? *Ecosphere*, 11, 1–20.
- Allen, K., Fisher, J.B., Phillips, R.P., Powers, J.S. & Brzostek, E.R. 2020. Modeling the Carbon Cost of Plant nitrogen and phosphorus uptake across temperate and tropical forests. *Frontiers in Forests and Global Change*, 3, 1–12.
- Allen, D.E., Kingston, G., Rennenberg, H., Dalal, R.C. & Schmidt, S. 2010. Effect of nitrogen fertilizer management and waterlogging on nitrous oxide emission from subtropical sugarcane soils. *Agriculture, Ecosystems & Environment*, 136, 209–217.
- Allen, G.R., Pereira, S.L., Raes, D. & Smith, M. 1998. *Crop evapotranspiration-Guidelines for computing crop water requirements-FAO Irrigation and drainage paper 56*. Food and Agriculture Organization, Rome, Italy.
- Altpeter, F. & Oraby, H. 2010. Sugarcane. In: *Genetic modification of plants* (eds. Kempken, F. & Jung, C.), pp. 453–472. Springer Berlin Heidelberg, Berlin, Heidelberg.
- Ambus, P. & Robertson, G.P. 2006. The effect of increased N deposition on nitrous oxide, methane and carbon dioxide fluxes from unmanaged forest and grassland communities in Michigan. *Biogeochemistry*, 79, 315–337.

-
- Amigun, B., Musango, J.K. & Stafford, W. 2011. Biofuels and sustainability in Africa. *Renewable and Sustainable Energy Reviews*, 15, 1360–1372.
- Amigun, B., Sigamoney, R. & von Blottnitz, H. 2008. Commercialisation of biofuel industry in Africa: A review. *Renewable and Sustainable Energy Reviews*, 12, 690–711.
- Anderson-Teixeira, K.J., Masters, M.D., Black, C.K., Zeri, M., Hussain, M.Z., Bernacchi, C.J. & DeLucia, E.H. 2013. Altered belowground carbon cycling following land-use change to perennial bioenergy crops. *Ecosystems*, 16, 508–520.
- Antille, D.L. & Moody, P.W. 2021. Nitrogen use efficiency indicators for the Australian cotton, grains, sugar, dairy and horticulture industries. *Environmental and Sustainability Indicators*, 10, 1–10.
- Antunes, F.A.F., Chandel, A.K., Terán-Hilares, R., Milessi, T.S.S., Travalía, B.M., Ferrari, F.A., Hernandez-Pérez, A.F., Ramos, L., Marcelino, P.F., Brumano, L.P., Silva, G.M., Forte, M.B.S., Santos, J.C., Felipe, M.G.A. & da Silva, S.S. 2019. Biofuel production from sugarcane in Brazil. In: *Sugarcane biofuels* (eds. Khan, M.T. & Khan, I.A.), pp. 99–121. Springer International Publishing, Cham.
- Arias-Navarro, C., Díaz-Pinés, E., Kiese, R., Rosenstock, T.S., Rufino, M.C., Stern, D., Neufeldt, H., Verchot, L.V. & Butterbach-Bahl, K. 2013. Gas pooling: A sampling technique to overcome spatial heterogeneity of soil carbon dioxide and nitrous oxide fluxes. *Soil Biology and Biochemistry*, 67, 20–23.
- Arias-Navarro, C., Díaz-Pinés, E., Zuazo, P., Rufino, M.C., Verchot, L.V. & Butterbach-Bahl, K. 2017. Quantifying the contribution of land use to N₂O, NO and CO₂ fluxes in a montane forest ecosystem of Kenya. *Biogeochemistry*, 134, 95–114.
- Armour, J.D., Nelson, P.N., Daniells, J.W., Rasiah, V. & Inman-Bamber, N.G. 2013. Nitrogen leaching from the root zone of sugarcane and bananas in the humid tropics of Australia. *Agriculture, Ecosystems & Environment*, 180, 68–78.
- Aronson, E.L., Dierick, D., Botthoff, J.K., Oberbauer, S., Zelikova, T.J., Harmon, T.C., Rundel, P., Johnson, R.F., Swanson, A.C., Pinto-Tomás, A.A., Artavia-León, A., Matarrita-Carranza, B. & Allen, M.F. 2019. ENSO-influenced drought drives methane flux dynamics

- in a tropical wet forest soil. *Journal of Geophysical Research: Biogeosciences*, 124, 2267–2276.
- Aronson, E.L. & Helliker, B.R. 2010. Methane flux in non-wetland soils in response to nitrogen addition: a meta-analysis. *Ecology*, 91, 3242–3251.
- Artaxo, P., Rizzo, L.V., Brito, J.F., Barbosa, H.M.J., Arana, A., Sena, E.T., Cirino, G.G., Bastos, W., Martin, S.T. & Andreae, M.O. 2013. Atmospheric aerosols in Amazonia and land use change: from natural biogenic to biomass burning conditions. *Faraday Discussions*, 165, 1–33.
- Aryal, D., Morales Ruiz, D., Tondopó Marroquín, C., Pinto Ruiz, R., Guevara Hernández, F., Venegas Venegas, J., Ponce Mendoza, A., Villanueva López, G., Casanova Lugo, F., Rodríguez Larramendi, L., Ley de Coss, A., Hernández López, A., Medina Jonapá, F., Velázquez Sanabria, C., Alcudia Aguilar, A. & Euán Chi, I. 2018. Soil Organic Carbon Depletion from Forests to Grasslands Conversion in Mexico: A Review. *Agriculture*, 8, 1–15.
- Barantal, S., Schimann, H., Fromin, N. & Hättenschwiler, S. 2012. Nutrient and carbon limitation on decomposition in an Amazonian moist forest. *Ecosystems*, 15, 1039–1052.
- Barkley, A.E., Prospero, J.M., Mahowald, N., Hamilton, D.S., Poppendorf, K.J., Oehlert, A.M., Pourmand, A., Gatineau, A., Panechou-Pulcherie, K., Blackwelder, P. & Gaston, C.J. 2019. African biomass burning is a substantial source of phosphorus deposition to the Amazon, Tropical Atlantic Ocean, and Southern Ocean. *Proceedings of the National Academy of Sciences*, 116, 16216–16221.
- Batsukh, K., Zlotnik, V.A., Suyker, A. & Nasta, P. 2021. Prediction of biome-specific potential evapotranspiration in Mongolia under a scarcity of weather data. *Water*, 13, 1–20.
- Baumgartner, S., Barthel, M., Drake, T.W., Bauters, M., Makelele, I.A., Mugula, J.K., Summerauer, L., Gallarotti, N., Cizungu Ntaboba, L., Van Oost, K., Boeckx, P., Doetterl, S., Werner, R.A. & Six, J. 2020. Seasonality, drivers, and isotopic composition of soil CO₂ fluxes from tropical forests of the Congo Basin. *Biogeosciences*, 17, 6207–6218.
- Bauters, M., Verbeeck, H., Rütting, T., Barthel, M., Bazirake Mujinya, B., Bamba, F., Bodé, S., Boyemba, F., Bulonza, E., Carlsson, E., Eriksson, L., Makelele, I., Six, J., Cizungu

-
- Ntaboba, L. & Boeckx, P. 2019. Contrasting nitrogen fluxes in African tropical forests of the Congo Basin. *Ecological Monographs*, 89, 1–17.
- Bédard, C. & Knowles, R. 1989. Physiology, biochemistry, and specific inhibitors of CH₄, NH₄⁺, and CO oxidation by methanotrophs and nitrifiers. *Microbiological Reviews*, 53, 68–84.
- Bijay-Singh & Craswell, E. 2021. Fertilizers and nitrate pollution of surface and ground water: an increasingly pervasive global problem. *SN Applied Sciences*, 3, 1–24.
- Blair, N. 2000. Impact of cultivation and sugar-cane green trash management on carbon fractions and aggregate stability for a Chromic Luvisol in Queensland, Australia. *Soil and Tillage Research*, 55, 183–191.
- de Blécourt, M., Brumme, R., Xu, J., Corre, M.D. & Veldkamp, E. 2013. Soil carbon stocks decrease following conversion of secondary forests to rubber (*Hevea brasiliensis*) plantations (B Bond-Lamberty, Ed.). *PLoS ONE*, 8, 1–9.
- Blum, J., Melfi, A.J., Montes, C.R. & Gomes, T.M. 2013. Nitrogen and phosphorus leaching in a tropical Brazilian soil cropped with sugarcane and irrigated with treated sewage effluent. *Agricultural Water Management*, 117, 115–122.
- Bobbink, R., Hicks, K., Galloway, J., Spranger, T., Alkemade, R., Ashmore, M., Bustamante, M., Cinderby, S., Davidson, E., Dentener, F., Emmett, B., Erisman, J.-W., Fenn, M., Gilliam, F., Nordin, A., Pardo, L. & De Vries, W. 2010. Global assessment of nitrogen deposition effects on terrestrial plant diversity: a synthesis. *Ecological Applications*, 20, 30–59.
- Bodelier, P.L.E. & Laanbroek, H.J. 2004. Nitrogen as a regulatory factor of methane oxidation in soils and sediments. *FEMS Microbiology Ecology*, 47, 265–277.
- Bodelier, P.L. & Steenbergh, A.K. 2014. Interactions between methane and the nitrogen cycle in light of climate change. *Current Opinion in Environmental Sustainability*, 9–10, 26–36.
- Bolinder, M.A., Angers, D.A., Giroux, M. & Laverdière, M.R. 1999. Estimating C inputs retained as soil organic matter from corn (*Zea mays* L.). *Plant and Soil*, 215, 85–91.

-
- Bordonal, R. de O., Carvalho, J.L.N., Lal, R., de Figueiredo, E.B., de Oliveira, B.G. & La Scala, N. 2018. Sustainability of sugarcane production in Brazil. A review. *Agronomy for Sustainable Development*, 38, 1–23.
- Boschiero, B.N., Mariano, E., Torres-Dorante, L.O., Sattolo, T.M.S., Otto, R., Garcia, P.L., Dias, C.T.S. & Trivelin, P.C.O. 2020. Nitrogen fertilizer effects on sugarcane growth, nutritional status, and productivity in tropical acid soils. *Nutrient Cycling in Agroecosystems*, 117, 367–382.
- Bowden, R.D., Melillo, J.M., Steudler, P.A. & Aber, J.D. 1991. Effects of nitrogen additions on annual nitrous oxide fluxes from temperate forest soils in the northeastern United States. *Journal of Geophysical Research*, 96, 1–8.
- Bréchet, L., Courtois, E.A., Saint-Germain, T., Janssens, I.A., Asensio, D., Ramirez-Rojas, I., Soong, J.L., Van Langenhove, L., Verbruggen, E. & Stahl, C. 2019. Disentangling Drought and Nutrient effects on soil carbon dioxide and methane fluxes in a tropical forest. *Frontiers in Environmental Science*, 7, 1–13.
- Britts, T.H.C., Silva, W.G. da & Abrita, M.B. 2020. The sugarcane growth in the Municipality of Rio Brillhante-ms and the environmental impacts caused by burning straw of the sugarcane (2001 to 2010). *Revista Cerrados*, 14, 58–76.
- Brooks, R.H. & Corey, A.T. 1964. Hydraulic properties of porous media and their relation to drainage design. *Transactions of the ASAE*, 7, 0026–0028.
- Brumbley, S.M., Snyman, S.J., Gnanasambandam, A., Joyce, P., Hermann, S.R., da Silva, J.A.G., McQualter, R.B., Wang, M.-L., Egan, B.T., Paterson, A.H., Albert, H.H. & Moore, P.H. 2008. Sugarcane. In: *Compendium of Transgenic Crop Plants* (eds. Kole, C. & Hall, T.C.), pp. 1–58. John Wiley & Sons, Ltd, Chichester, UK.
- Brumme, R. & Borcken, W. 1999. Site variation in methane oxidation as affected by atmospheric deposition and type of temperate forest ecosystem. *Global Biogeochemical Cycles*, 13, 493–501.
- Brune, A. 2014. Symbiotic digestion of lignocellulose in termite guts. *Nature Reviews Microbiology*, 12, 168–180.

- Burton, A.J., Pregitzer, K.S., Crawford, J.N., Zogg, G.P. & Zak, D.R. 2004. Simulated chronic NO_3^- deposition reduces soil respiration in northern hardwood forests. *Global Change Biology*, 10, 1080–1091.
- Butterbach-Bahl, K., Baggs, E.M., Dannenmann, M., Kiese, R. & Zechmeister-Boltenstern, S. 2013. Nitrous oxide emissions from soils: how well do we understand the processes and their controls? *Philosophical Transactions of the Royal Society B: Biological Sciences*, 368, 1–13.
- Butterbach-Bahl, K., Kesik, M., Miehle, P., Papen, H. & Li, C. 2004a. Quantifying the regional source strength of N-trace gases across agricultural and forest ecosystems with process based models. *Plant and Soil*, 260, 311–329.
- Butterbach-Bahl, K., Kiese, R. & Liu, C. 2011. Measurements of biosphere–atmosphere exchange of CH_4 in terrestrial ecosystems. In: *Methods in Enzymology*, pp. 271–287. Elsevier.
- Butterbach-Bahl, K., Kock, M., Willibald, G., Hewett, B., Buhagiar, S., Papen, H. & Kiese, R. 2004b. Temporal variations of fluxes of NO , NO_2 , N_2O , CO_2 , and CH_4 in a tropical rain forest ecosystem. *Global Biogeochemical Cycles*, 18, 1–11.
- Cadisich, G., Imhof, H., Urquiaga, S., Boddey, R.M. & Giller, K.E. 1996. Carbon turnover ($\delta^{13}\text{C}$) and nitrogen mineralization potential of particulate light soil organic matter after rain-forest clearing. *Soil Biology and Biochemistry*, 28, 1555–1567.
- Cai, H., Dunn, J.B., Wang, Z., Han, J. & Wang, M.Q. 2013. Life-cycle energy use and greenhouse gas emissions of production of bioethanol from sorghum in the United States. *Biotechnology for Biofuels*, 6, 1–15.
- Cairns, M.A., Brown, S., Helmer, E.H. & Baumgardner, G.A. 1997. Root biomass allocation in the world's upland forests. *Oecologia*, 111, 1–11.
- Cantarella, H., Trivelin, P.C.O., Contin, T.L.M., Dias, F.L.F., Rossetto, R., Marcelino, R., Coimbra, R.B. & Quaggio, J.A. 2008. Ammonia volatilisation from urease inhibitor-treated urea applied to sugarcane trash blankets. *Scientia Agricola*, 65, 397–401.
- Carmo, J.B. do, Filoso, S., Zotelli, L.C., de Sousa Neto, E.R., Pitombo, L.M., Duarte-Neto, P.J., Vargas, V.P., Andrade, C.A., Gava, G.J.C., Rossetto, R., Cantarella, H., Neto, A.E. &

-
- Martinelli, L.A. 2013. Infield greenhouse gas emissions from sugarcane soils in Brazil: effects from synthetic and organic fertilizer application and crop trash accumulation. *GCB Bioenergy*, 5, 267–280.
- de Carvalho, A.M., de Oliveira, A.D., Coser, T.R., de Sousa, T.R., de Lima, C.A., Ramos, M.L.G., Malaquias, J.V., Gonçalves, A.D.M. de A. & Ribeiro Júnior, W.Q. 2021. N₂O emissions from sugarcane fields under contrasting watering regimes in the Brazilian savannah. *Environmental Technology & Innovation*, 22, 1–11.
- Cernusak, L.A., Winter, K., Dalling, J.W., Holtum, J.A.M., Jaramillo, C., Körner, C., Leakey, A.D.B., Norby, R.J., Poulter, B., Turner, B.L. & Wright, S.J. 2013. Tropical forest responses to increasing atmospheric CO₂: current knowledge and opportunities for future research. *Functional Plant Biology*, 40, 531–551.
- Chalco Vera, J., Erazzú, L. & Acreche, M. 2019. Effects of sugarcane trash burning and nitrogen fertilization on soil-carbon balances in Argentina. *Proceedings of the International Society of Sugar Cane Technologists*, 30, 1172–1178.
- Chalco Vera, J., Valeiro, A., Posse, G. & Acreche, M.M. 2017. To burn or not to burn: The question of straw burning and nitrogen fertilization effect on nitrous oxide emissions in sugarcane. *Science of The Total Environment*, 587–588, 399–406.
- Chapman, L.S., Haysom, M.B.C. & Saffigna, P.G. 1994. The recovery of ¹⁵N from labelled urea fertilizer in crop components of sugarcane and in soil profiles. *Australian Journal of Agricultural Research*, 45, 1577–1585.
- Chapuis, R.P. 2012. Predicting the saturated hydraulic conductivity of soils: a review. *Bulletin of Engineering Geology and the Environment*, 71, 401–434.
- Chen, J., Feng, M., Cui, Y. & Liu, G. 2021. The impacts of nitrogen addition on upland soil methane uptake: A global meta-analysis. *Science of The Total Environment*, 795, 1–9.
- Chen, D., Zhou, L., Rao, X., Lin, Y. & Fu, S. 2010. Effects of root diameter and root nitrogen concentration on in situ root respiration among different seasons and tree species. *Ecological Research*, 25, 983–993.

-
- Cherubin, M.R., Franco, A.L.C., Cerri, C.E.P., Oliveira, D.M. da S., Davies, C.A. & Cerri, C.C. 2015. Sugarcane expansion in Brazilian tropical soils—Effects of land use change on soil chemical attributes. *Agriculture, Ecosystems & Environment*, 211, 173–184.
- Cherubin, M.R., Oliveira, D.M. da S., Feigl, B.J., Pimentel, L.G., Lisboa, I.P., Gmach, M.R., Varanda, L.L., Morais, M.C., Satiro, L.S., Popin, G.V., Paiva, S.R. de, Santos, A.K.B. dos, Vasconcelos, A.L.S. de, Melo, P.L.A. de, Cerri, C.E.P. & Cerri, C.C. 2018. Crop residue harvest for bioenergy production and its implications on soil functioning and plant growth: A review. *Scientia Agricola*, 75, 255–272.
- Ciais, P., Dolman, A.J., Bombelli, A., Duren, R., Pregon, A., Rayner, P.J., Miller, C., Gobron, N., Kinderman, G., Marland, G., Gruber, N., Chevallier, F., Andres, R.J., Balsamo, G., Bopp, L., Bréon, F.-M., Broquet, G., Dargaville, R., Battin, T.J., Borges, A., Bovensmann, H., Buchwitz, M., Butler, J., Canadell, J.G., Cook, R.B., DeFries, R., Engelen, R., Gurney, K.R., Heinze, C., Heimann, M., Held, A., Henry, M., Law, B., Luysaert, S., Miller, J., Moriyama, T., Moulin, C., Myneni, R.B., Nussli, C., Obersteiner, M., Ojima, D., Pan, Y., Paris, J.-D., Piao, S.L., Poulter, B., Plummer, S., Quegan, S., Raymond, P., Reichstein, M., Rivier, L., Sabine, C., Schimel, D., Tarasova, O., Valentini, R., Wang, R., van der Werf, G., Wickland, D., Williams, M. & Zehner, C. 2014. Current systematic carbon-cycle observations and the need for implementing a policy-relevant carbon observing system. *Biogeosciences*, 11, 3547–3602.
- Cleveland, C.C., Reed, S.C. & Townsend, A.R. 2006. Nutrient regulation of organic matter decomposition in a tropical rain forest. *Ecology*, 87, 492–503.
- Cleveland, C.C. & Townsend, A.R. 2006. Nutrient additions to a tropical rain forest drive substantial soil carbon dioxide losses to the atmosphere. *Proceedings of the National Academy of Sciences*, 103, 10316–10321.
- Conant, R.T., Ryan, M.G., Ågren, G.I., Birge, H.E., Davidson, E.A., Eliasson, P.E., Evans, S.E., Frey, S.D., Giardina, C.P., Hopkins, F.M., Hyvönen, R., Kirschbaum, M.U.F., Lavelle, J.M., Leifeld, J., Parton, W.J., Megan Steinweg, J., Wallenstein, M.D., Martin Wetterstedt, J.Å. & Bradford, M.A. 2011. Temperature and soil organic matter decomposition rates - synthesis of current knowledge and a way forward. *Global Change Biology*, 17, 3392–3404.

-
- Conlong, D.E. & Mugalula, A. 2001. Eldana saccharina (Lep: Pyralidae) and its parasitoids at Kinyara sugar works, Uganda. *Proceedings of the South African Sugar Technologists' Association*, 75, 183–185.
- Corre, M.D., Sueta, J.P. & Veldkamp, E. 2014. Nitrogen-oxide emissions from tropical forest soils exposed to elevated nitrogen input strongly interact with rainfall quantity and seasonality. *Biogeochemistry*, 118, 103–120.
- Corre, M.D., Veldkamp, E., Arnold, J. & Wright, S.J. 2010. Impact of elevated N input on soil N cycling and losses in old-growth lowland and montane forests in Panama. *Ecology*, 91, 1715–1729.
- Cusack, D.F., Silver, W.L., Torn, M.S., Burton, S.D. & Firestone, M.K. 2011. Changes in microbial community characteristics and soil organic matter with nitrogen additions in two tropical forests. *Ecology*, 92, 621–632.
- Dalal, R.C., Allen, D.E., Livesley, S.J. & Richards, G. 2008. Magnitude and biophysical regulators of methane emission and consumption in the Australian agricultural, forest, and submerged landscapes: a review. *Plant and Soil*, 309, 43–76.
- Dalling, J.W., Heineman, K., Lopez, O.R., Wright, S.J. & Turner, B.L. 2016. Nutrient availability in tropical rain forests: The paradigm of phosphorus limitation. In: *Tropical Tree Physiology* (eds. Goldstein, G. & Santiago, L.S.), pp. 261–273. Springer International Publishing, Cham.
- Dane, J.H. & Clarke Topp, G. (Eds). 2002. *Methods of soil analysis: Part 4 Physical methods*. Soil Science Society of America, Madison, WI, USA. (At: <http://doi.wiley.com/10.2136/sssabookser5.4>. Accessed: 7/12/2022).
- Daniels, J. & Daniels, C. 1993. Sugarcane in prehistory. *Archaeology in Oceania*, 28, 1–7.
- Dattamudi, S., Wang, J.J., Dodla, S.K., Viator, H.P., DeLaune, R., Hiscox, A., Darapuneni, M., Jeong, C. & Colyer, P. 2019. Greenhouse gas emissions as influenced by nitrogen fertilization and harvest residue management in sugarcane production. *Agrosystems, Geosciences & Environment*, 2, 1–10.

-
- Davidson, E.A., Keller, M., Erickson, H.E., Verchot, L.V. & Veldkamp, E. 2000a. Testing a conceptual model of soil emissions of nitrous and nitric oxides. *BioScience*, 50, 667–680.
- Davidson, E.A. & Verchot, L.V. 2000. Testing the Hole-in-the-Pipe Model of nitric and nitrous oxide emissions from soils using the TRAGNET Database. *Global Biogeochemical Cycles*, 14, 1035–1043.
- Davidson, E.A., Verchot, L.V., Cattânio, J.H., Ackerman, I.L. & Carvalho, J.E.M. 2000b. Effects of soil water content on soil respiration in forests and cattle pastures of eastern Amazonia. *Biogeochemistry*, 48, 53–69.
- De Figueiredo, E.B. & La Scala, N. 2011. Greenhouse gas balance due to the conversion of sugarcane areas from burned to green harvest in Brazil. *Agriculture, Ecosystems & Environment*, 141, 77–85.
- DeForest, J.L., Noormets, A., McNulty, S.G., Sun, G., Tenney, G. & Chen, J. 2006. Phenophases alter the soil respiration–temperature relationship in an oak-dominated forest. *International Journal of Biometeorology*, 51, 135–144.
- Denmead, O.T., Macdonald, B.C.T., Bryant, G., Naylor, T., Wilson, S., Griffith, D.W.T., Wang, W.J., Salter, B., White, I. & Moody, P.W. 2010. Emissions of methane and nitrous oxide from Australian sugarcane soils. *Agricultural and Forest Meteorology*, 150, 748–756.
- Deuss, A. 2012. The economic growth impacts of sugarcane expansion in Brazil: An inter-regional analysis. *Journal of Agricultural Economics*, 63, 528–551.
- Devaraju, N., Bala, G. & Modak, A. 2015. Effects of large-scale deforestation on precipitation in the monsoon regions: Remote versus local effects. *Proceedings of the National Academy of Sciences*, 112, 3257–3262.
- Dexter, A.R. 2004. Soil physical quality. *Geoderma*, 120, 201–214.
- D’Haene, K., Van den Bossche, A., Vandenbruwane, J., De Neve, S., Gabriels, D. & Hofman, G. 2008. The effect of reduced tillage on nitrous oxide emissions of silt loam soils. *Biology and Fertility of Soils*, 45, 213–217.

-
- Ding, W., Cai, Z. & Tsuruta, H. 2004. Cultivation, nitrogen fertilization, and set-aside effects on methane uptake in a drained marsh soil in Northeast China. *Global Change Biology*, 10, 1801–1809.
- Dinh, T.H., Watanabe, K., Takaragawa, H., Nakabaru, M. & Kawamitsu, Y. 2017. Photosynthetic response and nitrogen use efficiency of sugarcane under drought stress conditions with different nitrogen application levels. *Plant Production Science*, 20, 412–422.
- Dobbie, K.E., Smith, K.A., Prieme, A., Christensen, S., Degorska, A. & Orlanski, P. 1996. Effect of land use on the rate of methane uptake by surface soils in Northern Europe. *Atmospheric Environment*, 30, 1005–1011.
- Doetterl, S., Stevens, A., Six, J., Merckx, R., Van Oost, K., Casanova Pinto, M., Casanova-Katny, A., Muñoz, C., Boudin, M., Zagal Venegas, E. & Boeckx, P. 2015. Soil carbon storage controlled by interactions between geochemistry and climate. *Nature Geoscience*, 8, 780–783.
- Dominy, C., Haynes, R. & Antwerpen, R. van. 2002. Loss of soil organic matter and related soil properties under long-term sugarcane production on two contrasting soils. *Biology and Fertility of Soils*, 36, 350–356.
- Don, A., Schumacher, J. & Freibauer, A. 2011. Impact of tropical land-use change on soil organic carbon stocks - a meta-analysis: Soil organic carbon and land-use change. *Global Change Biology*, 17, 1658–1670.
- Drewer, J., Leduning, M.M., Griffiths, R.I., Goodall, T., Levy, P.E., Cowan, N., Comynn-Platt, E., Hayman, G., Sentian, J., Majalap, N. & Skiba, U.M. 2021. Comparison of greenhouse gas fluxes from tropical forests and oil palm plantations on mineral soil. *Biogeosciences*, 18, 1559–1575.
- Du, E., Xia, N. & de Vries, W. 2019. *Effects of nitrogen deposition on growing-season soil methane sink across global forest biomes*. Biogeochemistry: Air - Land Exchange. (At: <https://bg.copernicus.org/preprints/bg-2019-29/>. Accessed: 17/1/2023).
- Dutaur, L. & Verchot, L.V. 2007. A global inventory of the soil CH₄ sink. *Global Biogeochemical Cycles*, 21, 1–9.

-
- Eggeling, W.J. 1947. Observations on the ecology of the Budongo rain forest, Uganda. *The Journal of Ecology*, 34, 20–87.
- Elser, J.J., Bracken, M.E.S., Cleland, E.E., Gruner, D.S., Harpole, W.S., Hillebrand, H., Ngai, J.T., Seabloom, E.W., Shurin, J.B. & Smith, J.E. 2007. Global analysis of nitrogen and phosphorus limitation of primary producers in freshwater, marine and terrestrial ecosystems. *Ecology Letters*, 10, 1135–1142.
- Fanin, N., Hättenschwiler, S., Chavez Soria, P.F. & Fromin, N. 2016. (A)synchronous Availabilities of N and P Regulate the Activity and Structure of the Microbial Decomposer Community. *Frontiers in Microbiology*, 6, 1–13.
- Fanin, N., Hättenschwiler, S., Schimann, H. & Fromin, N. 2015. Interactive effects of C, N and P fertilization on soil microbial community structure and function in an Amazonian rain forest (JK Bailey, Ed.). *Functional Ecology*, 29, 140–150.
- FAO. 1993. *Forest resources assessment 1990: tropical countries*. UN Food and Agriculture Organization, Rome, Italy.
- FAO. 2020. *Global Forest Resources Assessment*. Rome, Italy.
- Fargione, J., Hill, J., Tilman, D., Polasky, S. & Hawthorne, P. 2008. Land clearing and the biofuel carbon debt. *Science*, 319, 1235–1238.
- Faria, L. de A., Nascimento, C.A.C. do, Vitti, G.C., Luz, P.H. de C. & Guedes, E.M.S. 2013. Loss of ammonia from nitrogen fertilizers applied to maize and soybean straw. *Revista Brasileira de Ciência do Solo*, 37, 969–975.
- Faustino, L.I., Moretti, A.P. & Graciano, C. 2015. Fertilization with urea, ammonium and nitrate produce different effects on growth, hydraulic traits and drought tolerance in *Pinus taeda* seedlings (G Goldstein, Ed.). *Tree Physiology*, 35, 1062–1074.
- Feng, J. & Zhu, B. 2019. A global meta-analysis of soil respiration and its components in response to phosphorus addition. *Soil Biology and Biochemistry*, 135, 38–47.
- Finzi, A.C. 2009. Decades of atmospheric deposition have not resulted in widespread phosphorus limitation or saturation of tree demand for nitrogen in southern New England. *Biogeochemistry*, 92, 217–229.

-
- Flores-Jiménez, D.E., Carbajal, N., Algara-Siller, M., Aguilar-Rivera, N., Álvarez-Fuentes, G., Ávila-Galarza, A. & García, A.R. 2019. Atmospheric dispersion of methane emissions from sugarcane burning in Mexico. *Environmental Pollution*, 250, 922–933.
- Forster, P., Ramaswamy, V., Artaxo, P., Berntsen, T., Betts, R., Fahey, D.W., Haywood, J., Lean, J., Lowe, D.C., Myhre, G., Nganga, J., Prinn, R., Raga, G., Schulz, M. & Van Dorland, R. 2007. Forster, P., V. Ramaswamy, P. Artaxo, T. Berntsen, R. Betts, D.W. Fahey, J. Haywood, J. Lean, D.C. Lowe, G. Myhre, J. Nganga, R. Prinn, G. Raga, M. Schulz and R. Van Dorland, 2007: Changes in Atmospheric Constituents and in Radiative Forcing. In: *Climate Change 2007: The Physical Science Basis. Contribution of Working Group I to the Fourth Assessment Report of the Intergovernmental Panel on Climate Change* [Solomon, S., D. Qin, M. Manning, Z. Chen, M. Marquis, K.B. Averyt, M. Tignor and H.L. Miller (eds.)]. Cambridge University Press, Cambridge, United Kingdom and New York, NY, USA. In: *Changes in Atmospheric Constituents and in Radiative Forcing*. [Solomon, S., D. Qin, M. Manning, Z. Chen, M. Marquis, K.B. Averyt, M. Tignor and H.L. Miller. Cambridge University Press, Cambridge, United Kingdom and New York, NY, USA.
- Franco, H.C.J., Otto, R., Faroni, C.E., Vitti, A.C., Almeida de Oliveira, E.C. & Trivelin, P.C.O. 2011. Nitrogen in sugarcane derived from fertilizer under Brazilian field conditions. *Field Crops Research*, 121, 29–41.
- Friedlingstein, P., Jones, M.W., O’Sullivan, M., Andrew, R.M., Hauck, J., Peters, G.P., Peters, W., Pongratz, J., Sitch, S., Le Quéré, C., Bakker, D.C.E., Canadell, J.G., Ciais, P., Jackson, R.B., Anthoni, P., Barbero, L., Bastos, A., Bastrikov, V., Becker, M., Bopp, L., Buitenhuis, E., Chandra, N., Chevallier, F., Chini, L.P., Currie, K.I., Feely, R.A., Gehlen, M., Gilfillan, D., Gkritzalis, T., Goll, D.S., Gruber, N., Gutekunst, S., Harris, I., Haverd, V., Houghton, R.A., Hurtt, G., Ilyina, T., Jain, A.K., Joetzjer, E., Kaplan, J.O., Kato, E., Klein Goldewijk, K., Korsbakken, J.I., Landschützer, P., Lauvset, S.K., Lefèvre, N., Lenton, A., Lienert, S., Lombardozzi, D., Marland, G., McGuire, P.C., Melton, J.R., Metzl, N., Munro, D.R., Nabel, J.E.M.S., Nakaoka, S.-I., Neill, C., Omar, A.M., Ono, T., Peregon, A., Pierrot, D., Poulter, B., Rehder, G., Resplandy, L., Robertson, E., Rödenbeck, C., Séférian, R., Schwinger, J., Smith, N., Tans, P.P., Tian, H., Tilbrook, B., Tubiello, F.N., van der Werf, G.R., Wiltshire, A.J. & Zaehle, S. 2019. Global carbon budget 2019. *Earth System Science Data*, 11, 1783–1838.

- Fujii, K., Hayakawa, C., & Sukartiningsih. 2021. Root exudation and biodegradation of organic acids in a tropical forest soil under dipterocarp and pioneer trees. *Plant and Soil*, 469, 213–226.
- Furtado da Silva, N., Cabral da Silva, E., Muraoka, T., Batista Teixeira, M., Antonio Loureiro Soares, F., Nobre Cunha, F., Adu-Gyamfi, J. & Cavalcante, W.S. da S. 2020. Nitrogen utilization from ammonium nitrate and urea fertilizer by irrigated sugarcane in Brazilian Cerrado Oxisol. *Agriculture*, 10, 1–17.
- Galdos, M.V., Cerri, C.C. & Cerri, C.E.P. 2009. Soil carbon stocks under burned and unburned sugarcane in Brazil. *Geoderma*, 153, 347–352.
- Galloway, J.N., Dentener, F.J., Capone, D.G., Boyer, E.W., Howarth, R.W., Seitzinger, S.P., Asner, G.P., Cleveland, C.C., Green, P.A., Holland, E.A., Karl, D.M., Michaels, A.F., Porter, J.H., Townsend, A.R. & Vöosmarty, C.J. 2004. Nitrogen cycles: past, present, and future. *Biogeochemistry*, 70, 153–226.
- Gao, W., Yang, H., Li, S. & Kou, L. 2017. Responses of soil CO₂, CH₄ and N₂O fluxes to N, P, and acid additions in mixed forest in subtropical China. *Journal of Resources and Ecology*, 8, 154–164.
- Gasparatos, A., von Maltitz, G.P., Johnson, F.X., Lee, L., Mathai, M., Puppim de Oliveira, J.A. & Willis, K.J. 2015. Biofuels in sub-Saharan Africa: Drivers, impacts and priority policy areas. *Renewable and Sustainable Energy Reviews*, 45, 879–901.
- Gee, G.W. & Or, D. 2002. 2.4 Particle-Size Analysis. In: *SSSA Book Series* (eds. Dane, J.H. & Clarke Topp, G.), pp. 255–293. Soil Science Society of America, Madison, WI, USA.
- Geist, H.J. & Lambin, E.F. 2002. Proximate causes and underlying driving forces of tropical deforestation. *BioScience*, 52, 1–8.
- van Genuchten, M.Th. 1980. A Closed-form equation for predicting the hydraulic conductivity of unsaturated soils. *Soil Science Society of America Journal*, 44, 892–898.
- Gerland, P., Raftery, A.E., Ševčíková, H., Li, N., Gu, D., Spoorenberg, T., Alkema, L., Fosdick, B.K., Chunn, J., Lalic, N., Bay, G., Buettner, T., Heilig, G.K. & Wilmoth, J. 2014. World population stabilization unlikely this century. *Science*, 346, 234–237.

-
- Ghiberto, P.J., Libardi, P.L., Brito, A.S. & Trivelin, P.C.O. 2009. Leaching of nutrients from a sugarcane crop growing on an Ultisol in Brazil. *Agricultural Water Management*, 96, 1443–1448.
- Ghiberto, P.J., Libardi, P.L., Brito, A. dos S. & Trivelin, P.C.O. 2011. Nitrogen fertilizer leaching in an Oxisol cultivated with sugarcane. *Scientia Agricola*, 68, 86–93.
- Ghiberto, P.J., Libardi, P.L. & Trivelin, P.C.O. 2015. Nutrient leaching in an Ultisol cultivated with sugarcane. *Agricultural Water Management*, 148, 141–149.
- Gibbs, H.K. & Herold, M. 2007. Tropical deforestation and greenhouse gas emissions. *Environmental Research Letters*, 2, 1–3.
- Gibbs, H.K., Ruesch, A.S., Achard, F., Clayton, M.K., Holmgren, P., Ramankutty, N. & Foley, J.A. 2010. Tropical forests were the primary sources of new agricultural land in the 1980s and 1990s. *Proceedings of the National Academy of Sciences*, 107, 16732–16737.
- Giglio, L., Csiszar, I. & Justice, C.O. 2006. Global distribution and seasonality of active fires as observed with Terra and Aqua Moderate Resolution Imaging Spectro radiometers (MODIS) sensors. *Journal of Geophysical Research: Biogeosciences*, 111, 1–12.
- Gijsman, A.J., Jagtap, S.S. & Jones, J.W. 2002. Wading through a swamp of complete confusion: how to choose a method for estimating soil water retention parameters for crop models. *European Journal of Agronomy*, 18, 77–106.
- Gonzaga, L.C., Zotelli, L. do C., de Castro, S.G.Q., de Oliveira, B.G., Bordonal, R. de O., Cantarella, H. & Carvalho, J.L.N. 2019. Implications of sugarcane straw removal for soil greenhouse gas emissions in São Paulo State, Brazil. *BioEnergy Research*, 12, 843–857.
- Graham, M.H. & Haynes, R.J. 2006. Organic matter status and the size, activity and metabolic diversity of the soil microbial community in the row and inter-row of sugarcane under burning and trash retention. *Soil Biology and Biochemistry*, 38, 21–31.
- Gray, N.D., McCann, C.M., Christgen, B., Ahammad, S.Z., Roberts, J.A. & Graham, D.W. 2014. Soil geochemistry confines microbial abundances across an arctic landscape; implications for net carbon exchange with the atmosphere. *Biogeochemistry*, 120, 307–317.

-
- Griggs, P. 2007. Deforestation and sugar cane growing in Eastern Australia, 1860-1995. *Environment and History*, 13, 255–283.
- Guarracino, L. 2007. Estimation of saturated hydraulic conductivity K_s from the van Genuchten shape parameter α : Estimation of K_s from α . *Water Resources Research*, 43, 1–4.
- Guellouz, L., Askri, B., Jaffré, J. & Bouhlila, R. 2020. Estimation of the soil hydraulic properties from field data by solving an inverse problem. *Scientific Reports*, 10, 1–11.
- Gulledge, J., Hrywna, Y., Cavanaugh, C. & Steudler, P.A. 2004. Effects of long-term nitrogen fertilization on the uptake kinetics of atmospheric methane in temperate forest soils. *FEMS Microbiology Ecology*, 49, 389–400.
- Gundersen, P., Emmett, B.A., Kjønnaas, O.J., Koopmans, C.J. & Tietema, A. 1998. Impact of nitrogen deposition on nitrogen cycling in forests: a synthesis of NITREX data. *Forest Ecology and Management*, 101, 37–55.
- Guo, L.B. & Gifford, R.M. 2002. Soil carbon stocks and land use change: a meta analysis. *Global Change Biology*, 8, 345–360.
- Gupta, S., Papritz, A., Lehmann, P., Hengl, T., Bonetti, S. & Or, D. 2022. Global soil hydraulic properties dataset based on legacy site observations and robust parameterization. *Scientific Data*, 9, 1–15.
- Gütlein, A., Gerschlauser, F., Kikoti, I. & Kiese, R. 2018. Impacts of climate and land use on N₂O and CH₄ fluxes from tropical ecosystems in the Mt. Kilimanjaro region, Tanzania. *Global Change Biology*, 24, 1239–1255.
- Hall, S.J. & Matson, P.A. 1999. Nitrogen oxide emissions after nitrogen additions in tropical forests. *Nature*, 400, 152–155.
- Hall, S.J. & Matson, P.A. 2003. Nutrient status of tropical rain forests influences soil N dynamics after N additions. *Ecological Monographs*, 73, 107–129.
- Hall, S.J., McDowell, W.H. & Silver, W.L. 2013. When Wet gets wetter: Decoupling of moisture, redox biogeochemistry, and greenhouse gas fluxes in a humid Tropical forest soil. *Ecosystems*, 16, 576–589.

-
- Hansen, M.C., Potapov, P.V., Moore, R., Hancher, M., Turubanova, S.A., Tyukavina, A., Thau, D., Stehman, S.V., Goetz, S.J., Loveland, T.R., Kommareddy, A., Egorov, A., Chini, L., Justice, C.O. & Townshend, J.R.G. 2013. High-resolution global maps of 21st-century forest cover change. *Science*, 342, 850–853.
- Hao, M., Zhang, J., Meng, M., Chen, H.Y.H., Guo, X., Liu, S. & Ye, L. 2019. Impacts of changes in vegetation on saturated hydraulic conductivity of soil in subtropical forests. *Scientific Reports*, 9, 1–9.
- Hartemink, A.E. 2008. Chapter 3 Sugarcane for bioethanol. In: *Advances in Agronomy*, pp. 125–182. Elsevier.
- Hashimoto, S., Tanaka, N., Suzuki, M., Inoue, A., Takizawa, H., Kosaka, I., Tanaka, K., Tantasirin, C. & Tangtham, N. 2004. Soil respiration and soil CO₂ concentration in a tropical forest, Thailand. *Journal of Forest Research*, 9, 75–79.
- Hassler, E., Corre, M.D., Tjoa, A., Damris, M., Utami, S.R. & Veldkamp, E. 2015. Soil fertility controls soil–atmosphere carbon dioxide and methane fluxes in a tropical landscape converted from lowland forest to rubber and oil palm plantations. *Biogeosciences*, 12, 5831–5852.
- Hedin, L.O., Vitousek, P.M. & Matson, P.A. 2003. Nutrient losses over four million years of tropical forest development. *Ecology*, 84, 2231–2255.
- Hernandes, T.A.D., de Oliveira Bordonal, R., Duft, D.G. & Leal, M.R.L.V. 2022. Implications of regional agricultural land use dynamics and deforestation associated with sugarcane expansion for soil carbon stocks in Brazil. *Regional Environmental Change*, 22, 1–15.
- Hess, T.M., Sumberg, J., Biggs, T., Georgescu, M., Haro-Monteagudo, D., Jewitt, G., Ozdogan, M., Marshall, M., Thenkabail, P., Daccache, A., Marin, F. & Knox, J.W. 2016. A sweet deal? Sugarcane, water and agricultural transformation in Sub-Saharan Africa. *Global Environmental Change*, 39, 181–194.
- Hicks, L.C., Meir, P., Nottingham, A.T., Reay, D.S., Stott, A.W., Salinas, N. & Whitaker, J. 2019. Carbon and nitrogen inputs differentially affect priming of soil organic matter in tropical lowland and montane soils. *Soil Biology and Biochemistry*, 129, 212–222.

-
- Hira, A. & de Oliveira, L.G. 2009. No substitute for oil? How Brazil developed its ethanol industry. *Energy Policy*, 37, 2450–2456.
- Hobbie, S.E. & Vitousek, P.M. 2000. Nutrient limitation of decomposition in Hawaiian forests. *Ecology*, 81, 1867–1877.
- Högberg, P., Näsholm, T., Franklin, O. & Högberg, M.N. 2017. Tamm Review: On the nature of the nitrogen limitation to plant growth in Fennoscandian boreal forests. *Forest Ecology and Management*, 403, 161–185.
- Holland, E.A., Neff, J.C., Townsend, A.R. & McKeown, B. 2000. Uncertainties in the temperature sensitivity of decomposition in tropical and subtropical ecosystems: Implications for models. *Global Biogeochemical Cycles*, 14, 1137–1151.
- Holzworth, D.P., Huth, N.I., deVoil, P.G., Zurcher, E.J., Herrmann, N.I., McLean, G., Chenu, K., van Oosterom, E.J., Snow, V., Murphy, C., Moore, A.D., Brown, H., Whish, J.P.M., Verrall, S., Fainges, J., Bell, L.W., Peake, A.S., Poulton, P.L., Hochman, Z., Thorburn, P.J., Gaydon, D.S., Dalgliesh, N.P., Rodriguez, D., Cox, H., Chapman, S., Doherty, A., Teixeira, E., Sharp, J., Cichota, R., Vogeler, I., Li, F.Y., Wang, E., Hammer, G.L., Robertson, M.J., Dimes, J.P., Whitbread, A.M., Hunt, J., van Rees, H., McClelland, T., Carberry, P.S., Hargreaves, J.N.G., MacLeod, N., McDonald, C., Harsdorf, J., Wedgwood, S. & Keating, B.A. 2014. APSIM – Evolution towards a new generation of agricultural systems simulation. *Environmental Modelling & Software*, 62, 327–350.
- Hombegowda, H.C., van Straaten, O., Köhler, M. & Hölscher, D. 2016. On the rebound: soil organic carbon stocks can bounce back to near forest levels when agroforests replace agriculture in southern India. *SOIL*, 2, 13–23.
- Houghton, R.A. 2013. The emissions of carbon from deforestation and degradation in the tropics: past trends and future potential. *Carbon Management*, 4, 539–546.
- Hüppi, R., Felber, R., Krauss, M., Six, J., Leifeld, J. & Fuß, R. 2018. Restricting the nonlinearity parameter in soil greenhouse gas flux calculation for more reliable flux estimates (UM Sainju, Ed.). *PLOS ONE*, 13, 1–17.
- Hutson, J.L. 2003. LEACHM - A process-based model of water and solute movement, transformations, plant uptake and chemical reactions in the unsaturated zone, version 4.

-
- Iddris, N.A.-A., Corre, M.D., Yemefack, M., van Straaten, O. & Veldkamp, E. 2020. Stem and soil nitrous oxide fluxes from rainforest and cacao agroforest on highly weathered soils in the Congo Basin. *Biogeosciences*, 17, 5377–5397.
- IPCC. 2021. The Physical Science Basis. Contribution of Working Group I to the Sixth Assessment Report of the Intergovernmental Panel on Climate Change. In: *Climate Change 2021* (eds. Masson-Delmotte, V., Zhai, P., Pirani, A., Connors, S.L., Péan, C., Berger, S., Caud, N., Chen, Y., Goldfarb, L., Gomis, M.I., Huang, M., Leitzell, K., Lonnoy, E., Matthews, J.B.R., Maycock, T.K., Waterfield, T., Yelekçi, O., Yu, R. & Zhou, B.). Cambridge University Press, In press, Cambridge, United Kingdom and New York, NY, USA,.
- Isabirye, M., Raju, D.V.N., Kitutu, M., Yemeline, V., Deckers, J. & Poese, J. 2013. Sugarcane Biomass Production and renewable energy. In: *Biomass Now - Cultivation and Utilization* (ed. Matovic, M.D.), pp. 1–14. InTech.
- Itoh, M., Kosugi, Y., Takanashi, S., Kanemitsu, S., Osaka, K., Hayashi, Y., Tani, M. & Rahim Nik, A. 2012. Effects of soil water status on the spatial variation of carbon dioxide, methane and nitrous oxide fluxes in tropical rain-forest soils in Peninsular Malaysia. *Journal of Tropical Ecology*, 28, 557–570.
- IUSS Working Group WRB. 2014. *World Reference Base for Soil Resources 2014, International soil classification system for naming soils and creating legends for soil maps*. FAO, Rome.
- IUSS Working Group WRB. 2015. *World Reference Base for Soil Resources 2014, update 2015 International soil classification system for naming soils and creating legends for soil maps*. FAO, Rome.
- Jain, R., Shrivastava, A.K., Solomon, S. & Yadav, R.L. 2007. Low temperature stress-induced biochemical changes affect stubble bud sprouting in sugarcane (*Saccharum* spp. hybrid). *Plant Growth Regulation*, 53, 17–23.
- Jarvis, N.J., Bergström, L. & Dik, P.E. 1991. Modelling water and solute transport in macroporous soil. II. Chloride breakthrough under non-steady flow. *Journal of Soil Science*, 42, 71–81.

-
- Jiang, X., Chen, H., Peng, C., Li, Y., He, Y., Chen, D., Lin, M., Hu, J., Ma, T., Liu, L., Liu, X., Xia, M. & Liu, Y. 2016. Soil carbon dioxide fluxes from three forest types of the tropical montane rainforest on Hainan Island, China. *Water, Air, & Soil Pollution*, 227, 1–14.
- Jobbágy, E.G. & Jackson, R.B. 2000. The vertical distribution of soil organic carbon and its relation to climate and vegetation. *Ecological Applications*, 10, 423–436.
- John, R., Dalling, J.W., Harms, K.E., Yavitt, J.B., Stallard, R.F., Mirabello, M., Hubbell, S.P., Valencia, R., Navarrete, H., Vallejo, M. & Foster, R.B. 2007. Soil nutrients influence spatial distributions of tropical tree species. *Proceedings of the National Academy of Sciences*, 104, 864–869.
- Johnston, C. & Meyer, R. 2008. Value chain governance and access to finance: Maize, sugar cane and sunflower oil in Uganda. *Enterprise Development and Microfinance*, 19, 281–300.
- Jolly, L. 2012. Sugar reforms, ethanol demand, and market restructuring. In: *Bioenergy for sustainable development and international competitiveness: the role of sugarcane in Africa*, pp. 1–29. Earthscan, New York.
- Josephat, M. 2018. Deforestation In Uganda: Population Increase, Forests Loss And Climate Change. *Environmental Risk Assessment and Remediation*, 02, 46–50.
- Ju, X. & Zhang, C. 2017. Nitrogen cycling and environmental impacts in upland agricultural soils in North China: A review. *Journal of Integrative Agriculture*, 16, 2848–2862.
- Jusys, T. 2017. A confirmation of the indirect impact of sugarcane on deforestation in the Amazon. *Journal of Land Use Science*, 12, 125–137.
- Kalinda, T. & Chisanga, B. 2014. Sugar value chain in Zambia: An assessment of the growth opportunities and challenges. *Asian Journal of Agricultural Sciences*, 6, 6–15.
- Kaspari, M., Garcia, M.N., Harms, K.E., Santana, M., Wright, S.J. & Yavitt, J.B. 2007. Multiple nutrients limit litterfall and decomposition in a tropical forest. *Ecology Letters*, 0, 1–9.
- Kassa, H., Dondeyne, S., Poesen, J., Frankl, A. & Nyssen, J. 2017. Impact of deforestation on soil fertility, soil carbon and nitrogen stocks: the case of the Gacheb catchment in the White Nile Basin, Ethiopia. *Agriculture, Ecosystems & Environment*, 247, 273–282.

-
- Kim, D.-G. & Kirschbaum, M.U.F. 2014. *The effect of land-use change on the net exchange rates of greenhouse gases: a meta-analytical approach*. Biogeochemistry: Greenhouse Gases. (At: <https://bg.copernicus.org/preprints/11/1053/2014/>. Accessed: 19/1/2023).
- Kingston, G., Anink, M.C. & Allen, D. 2008. Acquisition of nitrogen by ratoon crops of sugar-cane as influenced by waterlogging and split applications. *Proceedings of the 2008 Conference of the Australian Society of Sugar Cane Technologists*, 30, 202–211.
- Koch, P.L. & Barnosky, A.D. 2006. Late quaternary extinctions: State of the debate. *Annual Review of Ecology, Evolution, and Systematics*, 37, 215–250.
- Koehler, B., Corre, M.D., Veldkamp, E. & Sueta, J.P. 2009a. Chronic nitrogen addition causes a reduction in soil carbon dioxide efflux during the high stem-growth period in a tropical montane forest but no response from a tropical lowland forest on a decadal time scale. *Biogeosciences*, 6, 2973–2983.
- Koehler, B., Corre, M.D., Veldkamp, E., Wullaert, H. & Wright, S.J. 2009b. Immediate and long-term nitrogen oxide emissions from tropical forest soils exposed to elevated nitrogen input. *Global Change Biology*, 15, 2049–2066.
- Kostka, G., Polzin, C. & Scharrer, J. 2009. The future of sugar cane in (the) People’s Republic of China and India – Supply constraints and expansion potential. *Applied Energy*, 86, 100–107.
- Kravchenko, A.N., Toosi, E.R., Guber, A.K., Ostrom, N.E., Yu, J., Azeem, K., Rivers, M.L. & Robertson, G.P. 2017. Hotspots of soil N₂O emission enhanced through water absorption by plant residue. *Nature Geoscience*, 10, 496–500.
- La Scala Jr., N., Lopes, A., Spokas, K., Archer, D.W. & Reicosky, D. 2009. First-order decay models to describe soil C-CO₂ Loss after rotary tillage. *Scientia Agricola*, 66, 650–657.
- Lal, R. 2004. Soil carbon sequestration impacts on global climate change and food security. *Science*, 304, 1623–1627.
- Lapola, D.M., Schaldach, R., Alcamo, J., Bondeau, A., Koch, J., Koelking, C. & Priess, J.A. 2010. Indirect land-use changes can overcome carbon savings from biofuels in Brazil. *Proceedings of the National Academy of Sciences*, 107, 3388–3393.

-
- Lawrence, D. & Vandecar, K. 2015. Effects of tropical deforestation on climate and agriculture. *Nature Climate Change*, 5, 27–36.
- Leff, B., Ramankutty, N. & Foley, J.A. 2004. Geographic distribution of major crops across the world. *Global Biogeochemical Cycles*, 18, 1–33.
- Lehto, T., Westerhof, A.B., Lehtonen, M.I., Manninen, T., Mäkitie, H., Virransalo, P., Pokki, J., Härmä, P., Koistinen, T., Saalman, K., Kuosmanen, E., Mänttari, I., Katto, E., Baguma, Z., Kock, G. de & Elepu, D. 2014. Geological Map of Uganda,.
- van Lent, J., Hergoualc'h, K. & Verchot, L.V. 2015. Reviews and syntheses: Soil N₂O and NO emissions from land use and land-use change in the tropics and subtropics: a meta-analysis. *Biogeosciences*, 12, 7299–7313.
- Li, Q., Peng, C., Zhang, J., Li, Y. & Song, X. 2021. Nitrogen addition decreases methane uptake caused by methanotroph and methanogen imbalances in a Moso bamboo forest. *Scientific Reports*, 11, 1–14.
- Li, Y., Sun, J., Tian, D., Wang, J., Ha, D., Qu, Y., Jing, G. & Niu, S. 2018. Soil acid cations induced reduction in soil respiration under nitrogen enrichment and soil acidification. *Science of The Total Environment*, 615, 1535–1546.
- Li, Y., Xu, M. & Zou, X. 2006. Effects of nutrient additions on ecosystem carbon cycle in a Puerto Rican tropical wet forest. *Global Change Biology*, 12, 284–293.
- Li, Q., Yang, A., Wang, Z., Roelcke, M., Chen, X., Zhang, F., Pasda, G., Zerulla, W., Wissemeier, A.H. & Liu, X. 2015. Effect of a new urease inhibitor on ammonia volatilization and nitrogen utilization in wheat in north and northwest China. *Field Crops Research*, 175, 96–105.
- Liu, L. & Greaver, T.L. 2009. A review of nitrogen enrichment effects on three biogenic GHGs: the CO₂ sink may be largely offset by stimulated N₂O and CH₄ emission. *Ecology Letters*, 12, 1103–1117.
- Liu, L., Gundersen, P., Zhang, T. & Mo, J. 2012. Effects of phosphorus addition on soil microbial biomass and community composition in three forest types in tropical China. *Soil Biology and Biochemistry*, 44, 31–38.

-
- Lofton, J. & Tubaña, B. 2015. Effect of nitrogen rates and application time on sugarcane yield and quality. *Journal of Plant Nutrition*, 38, 161–176.
- Lohse, K.A. & Matson, P. 2005. Consequences of nitrogen additions for soil losses from wet tropical forests. *Ecological Applications*, 15, 1629–1648.
- Lu, X., Mao, Q., Wang, Z., Mori, T., Mo, J., Su, F. & Pang, Z. 2021. Long-term nitrogen addition decreases soil carbon mineralization in an N-rich primary tropical forest. *Forests*, 12, 1–9.
- Lukwago, W., Behangana, M., Mwavu, E.N. & Hughes, D.F. 2020. Effects of selective timber harvest on amphibian species diversity in Budongo forest reserve, Uganda. *Forest Ecology and Management*, 458, 1–7.
- Ma, S., Chen, G., Tian, D., Du, E., Xiao, W., Jiang, L., Zhou, Z., Zhu, J., He, H., Zhu, B. & Fang, J. 2020. Effects of seven-year nitrogen and phosphorus additions on soil microbial community structures and residues in a tropical forest in Hainan Island, China. *Geoderma*, 361, 1–10.
- Macedo, I.C., Seabra, J.E.A. & Silva, J.E.A.R. 2008. Greenhouse gases emissions in the production and use of ethanol from sugarcane in Brazil: The 2005/2006 averages and a prediction for 2020. *Biomass and Bioenergy*, 32, 582–595.
- Magill, A.H., Aber, J.D., Hendricks, J.J., Bowden, R.D., Melillo, J.M. & Steudler, P.A. 1997. Biogeochemical response of forest ecosystems to simulated chronic nitrogen deposition. *Ecological Applications*, 7, 402–415.
- Malhi, Y., Baldocchi, D.D. & Jarvis, P.G. 1999. The carbon balance of tropical, temperate and boreal forests. *Plant, Cell and Environment*, 22, 715–740.
- Malhi, Y., Gardner, T.A., Goldsmith, G.R., Silman, M.R. & Zelazowski, P. 2014. Tropical Forests in the Anthropocene. *Annual Review of Environment and Resources*, 39, 125–159.
- Malhi, Y. & Grace, J. 2000. Tropical forests and atmospheric carbon dioxide. *Trends in Ecology & Evolution*, 15, 332–337.

-
- Malhi, Y. & Phillips, O.L. 2004. Tropical forests and global atmospheric change: a synthesis (Y Malhi and OL Phillips, Eds.). *Philosophical Transactions of the Royal Society of London. Series B: Biological Sciences*, 359, 549–555.
- Manu, R., Corre, M.D., Aleeje, A., Mwanjalolo, M.J.G., Babweteera, F., Veldkamp, E. & Straaten, O. 2022. Responses of tree growth and biomass production to nutrient addition in a semi-deciduous tropical forest in Africa. *Ecology*, 103, 1–15.
- Martinelli, L.A., Piccolo, M.C., Townsend, A.R., Vitousek, P.M., Cuevas, E., McDowell, W., Robertson, G.P., Santos, O.C. & Treseder, K. 1999. Nitrogen stable isotopic composition of leaves and soil: Tropical versus temperate forests. *Biogeochemistry*, 46, 45–65.
- Martinson, G.O., Corre, M.D. & Veldkamp, E. 2013. Responses of nitrous oxide fluxes and soil nitrogen cycling to nutrient additions in montane forests along an elevation gradient in southern Ecuador. *Biogeochemistry*, 112, 625–636.
- Martinson, G.O., Müller, A.K., Matson, A.L., Corre, M.D. & Veldkamp, E. 2021. Nitrogen and phosphorus control soil methane uptake in tropical montane forests. *Journal of Geophysical Research: Biogeosciences*, 126, 1–14.
- de Matos, M., Santos, F. & Eichler, P. 2020. Sugarcane world scenario. In: *Sugarcane biorefinery, technology, and perspectives*, pp. 1–19. Elsevier.
- Matson, A.L., Corre, M.D. & Veldkamp, E. 2014. Nitrogen cycling in canopy soils of tropical montane forests responds rapidly to indirect N and P fertilization. *Global Change Biology*, 20, 3802–3813.
- Matson, A.L., Corre, M.D. & Veldkamp, E. 2017. Canopy soil greenhouse gas dynamics in response to indirect fertilization across an elevation gradient of tropical montane forests. *Biotropica*, 49, 153–159.
- Matson, A., Pennock, D. & Bedard-Haughn, A. 2009. Methane and nitrous oxide emissions from mature forest stands in the boreal forest, Saskatchewan, Canada. *Forest Ecology and Management*, 258, 1073–1083.
- McBratney, A.B., Minasny, B. & Tranter, G. 2011. Necessary meta-data for pedotransfer functions. *Geoderma*, 160, 627–629.

-
- McGroddy, M.E., Baisden, W.T. & Hedin, L.O. 2008. Stoichiometry of hydrological C, N, and P losses across climate and geology: An environmental matrix approach across New Zealand primary forests. *Global Biogeochemical Cycles*, 22, 1–14.
- Meier, E.A., Thorburn, P.J., Wegener, M.K. & Basford, K.E. 2006. The availability of nitrogen from sugarcane trash on contrasting soils in the wet tropics of North Queensland. *Nutrient Cycling in Agroecosystems*, 75, 101–114.
- Mello, F.F.C., Cerri, C.E.P., Davies, C.A., Holbrook, N.M., Paustian, K., Maia, S.M.F., Galdos, M.V., Bernoux, M. & Cerri, C.C. 2014. Payback time for soil carbon and sugar-cane ethanol. *Nature Climate Change*, 4, 605–609.
- Menichetti, L., Ågren, G.I., Barré, P., Moyano, F. & Kätterer, T. 2019. Generic parameters of first-order kinetics accurately describe soil organic matter decay in bare fallow soils over a wide edaphic and climatic range. *Scientific Reports*, 9, 1–12.
- Meyer, J.H. & Antwerpen, R. van. 2010. Advances in sugarcane soil fertility research in Southern Africa. *South African Journal of Plant and Soil*, 27, 19–31.
- Meyer, J.H., Schumann, A.W., Wood, R.A., Nixon, D.J. & Van Den Berg, M. 2007. Recent advances to improve nitrogen use efficiency of sugarcane in the South African sugar industry. *Proceedings of the South African Sugar Technologists' Association*, 26, 1–10.
- Minasny, B. & McBratney, Alex.B. 2001. The Australian soil texture boomerang: a comparison of the Australian and USDA/FAO soil particle-size classification systems. *Soil Research*, 39, 1–10.
- Minasny, B., McBratney, A.B. & Bristow, K.L. 1999. Comparison of different approaches to the development of pedotransfer functions for water-retention curves. *Geoderma*, 93, 225–253.
- Mo, J., Zhang, W., Zhu, W., Gundersen, P., Fang, Y., Li, D. & Wang, H. 2008. Nitrogen addition reduces soil respiration in a mature tropical forest in southern China. *Global Change Biology*, 14, 403–412.
- Moitinho, M.R., Ferraudo, A.S., Panosso, A.R., Bicalho, E. da S., Teixeira, D.D.B., Barbosa, M. de A., Tsai, S.M., Borges, B.M.F., Cannavan, F. de S., Souza, J.A.M. de & La Scala, N. 2021. Effects of burned and unburned sugarcane harvesting systems on soil CO₂

- emission and soil physical, chemical, and microbiological attributes. *CATENA*, 196, 104903.
- de Morais, L.K., de Aguiar, M.S., de Albuquerque e Silva, P., Câmara, T.M.M., Cursi, D.E., Júnior, A.R.F., Chapola, R.G., Carneiro, M.S. & Bessalho Filho, J.C. 2015. Breeding of sugarcane. In: *Industrial Crops* (eds. Cruz, V.M.V. & Dierig, D.A.), pp. 29–42. Springer New York, New York, NY.
- Mori, T., Lu, X., Aoyagi, R. & Mo, J. 2018. Reconsidering the phosphorus limitation of soil microbial activity in tropical forests (R Ostertag, Ed.). *Functional Ecology*, 32, 1145–1154.
- Mori, T., Ohta, S., Ishizuka, S., Konda, R., Wicaksono, A., Heriyanto, J. & Hardjono, A. 2010. Effects of phosphorus addition on N₂O and NO emissions from soils of an *Acacia mangium* plantation. *Soil Science and Plant Nutrition*, 56, 782–788.
- Mori, T., Ohta, S., Ishizuka, S., Konda, R., Wicaksono, A., Heriyanto, J. & Hardjono, A. 2013. Effects of phosphorus application on root respiration and heterotrophic microbial respiration in *Acacia mangium* plantation soil. *Tropics*, 22, 113–118.
- Mori, T., Wachrinrat, C., Staporn, D., Meunpong, P., Suebsai, W., Matsubara, K., Boonsri, K., Lumban, W., Kuawong, M., Phukdee, T., Srifai, J. & Boonman, K. 2017. Effects of phosphorus addition on nitrogen cycle and fluxes of N₂O and CH₄ in tropical tree plantation soils in Thailand. *Agriculture and Natural Resources*, 51, 91–95.
- Mosier, A., Wassmann, R., Verchot, L., King, J. & Palm, C. 2004. Methane and nitrogen oxide fluxes in tropical agricultural soils: sources, sinks and mechanisms. *Environment, Development and Sustainability*, 6, 11–49.
- Mualem, Y. 1976. A new model for predicting the hydraulic conductivity of unsaturated porous media. *Water Resources Research*, 12, 513–522.
- Müller, A.K., Matson, A.L., Corre, M.D. & Veldkamp, E. 2015. Soil N₂O fluxes along an elevation gradient of tropical montane forests under experimental nitrogen and phosphorus addition. *Frontiers in Earth Science*, 3, 1–12.

-
- Mwavu, E., Kalema, V., Bateganya, F., Byakagaba, P., Waiswa, D., Enuru, T. & Mbogga, M. 2018. Expansion of Commercial sugarcane cultivation among smallholder farmers in Uganda: Implications for household food security. *Land*, 7, 1–15.
- Mwavu, E.N. & Witkowski, E.T.F. 2008. Land-use and cover changes (1988-2002) around budongo forest reserve, NW Uganda: implications for forest and woodland sustainability. *Land Degradation & Development*, 19, 606–622.
- Nanteza, J., de Linage, C.R., Thomas, B.F. & Famiglietti, J.S. 2016. Monitoring groundwater storage changes in complex basement aquifers: An evaluation of the GRACE satellites over East Africa: GRACE groundwater dynamics in East Africa. *Water Resources Research*, 52, 9542–9564.
- Naseri, H., Parashkoohi, M.G., Ranjbar, I. & Zamani, D.M. 2020. Sustainability of quantitative and qualitative indicators of sugarcane production under different tillage systems (case study: Khuzestan province of Iran). *Environmental and Sustainability Indicators*, 8, 1–24.
- Nasta, P., Szabó, B. & Romano, N. 2021. Evaluation of pedotransfer functions for predicting soil hydraulic properties: A voyage from regional to field scales across Europe. *Journal of Hydrology: Regional Studies*, 37, 1–20.
- Nauer, P.A., Hutley, L.B. & Arndt, S.K. 2018. Termite mounds mitigate half of termite methane emissions. *Proceedings of the National Academy of Sciences*, 115, 13306–13311.
- NEMA. 2017. *State of the environment report for Uganda*. National Environment Management Authority (NEMA). Ministry of Environment and Natural Resources, Kampala, The Republic of Uganda.
- Newbery, D.M., Chuyong, G.B., Green, J.J., Songwe, N.C., Tchuenteu, F. & Zimmermann, L. 2002. Does low phosphorus supply limit seedling establishment and tree growth in groves of ectomycorrhizal trees in a central African rainforest? *New Phytologist*, 156, 297–311.
- Nottingham, A.T., Whitaker, J., Turner, B.L., Salinas, N., Zimmermann, M., Malhi, Y. & Meir, P. 2015. Climate Warming and soil carbon in tropical forests: Insights from an elevation gradient in the Peruvian Andes. *BioScience*, 65, 906–921.

- Obidzinski, K., Kusters, K. & Gnych, S. 2015. Taking the bitter with the sweet: Sugarcane's return as a driver of tropical deforestation. *Conservation Letters*, 8, 449–455.
- Oertel, C., Matschullat, J., Zurba, K., Zimmermann, F. & Erasmi, S. 2016. Greenhouse gas emissions from soils—A review. *Geochemistry*, 76, 327–352.
- Okamoto, K., Goto, S., Anzai, T. & Ando, S. 2021. Nitrogen leaching and nitrogen balance under differing nitrogen fertilization for sugarcane cultivation on a subtropical island. *Water*, 13, 1–13.
- de Oliveira, B.G., Carvalho, J.L.N., Cerri, C.E.P., Cerri, C.C. & Feigl, B.J. 2013. Soil greenhouse gas fluxes from vinasse application in Brazilian sugarcane areas. *Geoderma*, 200–201, 77–84.
- Osher, L.J., Matson, P.A. & Amundson, R. 2003. Effect of land use change on soil carbon in Hawaii. *Biogeochemistry*, 65, 213–232.
- Otieno, H.M., Onduru, G.O. & Okumu, O.O. 2019. Improving Sugarcane (*Saccharum officinarum* L.) yields in Sub-Sahara Africa through the use of existing technologies. *World Journal of Advanced Research and Reviews*, 3, 55–65.
- Otto, R., Castro, S.A.Q., Mariano, E., Castro, S.G.Q., Franco, H.C.J. & Trivelin, P.C.O. 2016. Nitrogen use efficiency for sugarcane-biofuel production: What is next? *BioEnergy Research*, 9, 1272–1289.
- Otto, R., Zavaschi, E., Souza Netto, G.M. de, Machado, B. de A. & Mira, A.B. de. 2017. Ammonia volatilization from nitrogen fertilizers applied to sugarcane straw. *Revista Ciência Agronômica*, 48, 413–418.
- Pachepsky, Y.A. & van Genuchten, M.Th. 2011. Pedotransfer Functions. In: *Encyclopedia of Agrophysics* (eds. Gliński, J., Horabik, J. & Lipiec, J.), pp. 556–561. Springer Netherlands, Dordrecht.
- Pachepsky, Y.A., Rawls, W.J. & Lin, H.S. 2006. Hydropedology and pedotransfer functions. *Geoderma*, 131, 308–316.

-
- Pan, Y., Birdsey, R.A., Phillips, O.L. & Jackson, R.B. 2013. The Structure, distribution, and biomass of the World's forests. *Annual Review of Ecology, Evolution, and Systematics*, 44, 593–622.
- Paradiso, E., Jevon, F. & Matthes, J. 2019. Fine root respiration is more strongly correlated with root traits than tree species identity. *Ecosphere*, 10, 1–15.
- Paredes, D. da S., Alves, B.J.R., dos Santos, M.A., Bolonhezi, D., Sant'Anna, S.A.C., Urquiaga, S., Lima, M.A. & Boddey, R.M. 2015. Nitrous oxide and methane fluxes following ammonium sulfate and vinasse application on sugarcane soil. *Environmental Science & Technology*, 49, 11209–11217.
- Patil, N.G. & Singh, S.K. 2016. Pedotransfer functions for estimating soil hydraulic properties: A review. *Pedosphere*, 26, 417–430.
- Pavelka, M., Acosta, M., Kiese, R., Altimir, N., Brümmer, C., Crill, P., Darenova, E., Fuß, R., Gielen, B., Graf, A., Klemetsson, L., Lohila, A., Longdoz, B., Lindroth, A., Nilsson, M., Jiménez, S.M., Merbold, L., Montagnani, L., Peichl, M., Pihlatie, M., Pumpanen, J., Ortiz, P.S., Silvennoinen, H., Skiba, U., Vestin, P., Weslien, P., Janous, D. & Kutsch, W. 2018. Standardisation of chamber technique for CO₂, N₂O and CH₄ fluxes measurements from terrestrial ecosystems. *International Agrophysics*, 32, 569–587.
- Pearson, T.R.H., Brown, S., Murray, L. & Sidman, G. 2017. Greenhouse gas emissions from tropical forest degradation: an underestimated source. *Carbon Balance and Management*, 12, 1–11.
- Pendall, E., Schwendenmann, L., Rahn, T., Miller, J.B., Tans, P.P. & White, J.W.C. 2010. Land use and season affect fluxes of CO₂, CH₄, CO, N₂O, H₂ and isotopic source signatures in Panama: evidence from nocturnal boundary layer profiles. *Global Change Biology*, 16, 2721–2736.
- Peters, A. & Durner, W. 2008. Simplified evaporation method for determining soil hydraulic properties. *Journal of Hydrology*, 356, 147–162.
- Petitjean, C., Le Gall, C., Pontet, C., Fujisaki, K., Garric, B., Horth, J.-C., Hénault, C. & Perrin, A.-S. 2019. Soil N₂O, CH₄, and CO₂ fluxes in forest, grassland, and tillage/no-tillage croplands in French Guiana (Amazonia). *Soil Systems*, 3, 1–20.

-
- Pinheiro, P.L., Recous, S., Dietrich, G., Weiler, D.A., Giovelli, R.L., Mezzalana, A.P. & Giacomini, S.J. 2018. Straw removal reduces the mulch physical barrier and ammonia volatilization after urea application in sugarcane. *Atmospheric Environment*, 194, 179–187.
- Pinheiro, P.L., Recous, S., Dietrich, G., Weiler, D.A., Schu, A.L., Bazzo, H.L.S. & Giacomini, S.J. 2019. N₂O emission increases with mulch mass in a fertilized sugarcane cropping system. *Biology and Fertility of Soils*, 55, 511–523.
- Popp, J., Lakner, Z., Harangi-Rákos, M. & Fári, M. 2014. The effect of bioenergy expansion: Food, energy, and environment. *Renewable and Sustainable Energy Reviews*, 32, 559–578.
- Powers, J.S., Corre, M.D., Twine, T.E. & Veldkamp, E. 2011. Geographic bias of field observations of soil carbon stocks with tropical land-use changes precludes spatial extrapolation. *Proceedings of the National Academy of Sciences*, 108, 6318–6322.
- Pradhana, A. & Mbohwa, C. 2014. Development of biofuels in South Africa: Challenges and opportunities. *Renewable and Sustainable Energy Reviews*, 39, 1089–1100.
- Prasertsak, P., Freney, J.R., Denmead, O.T., Saffigna, P.G., Prove, B.G. & Reghenzani, J.R. 2002. Effect of fertilizer placement on nitrogen loss from sugarcane in tropical Queensland. *Nutrient Cycling in Agroecosystems*, 62, 229–239.
- Premalatha, R.P., Bhakiyathu Saliha, B., Thiyageshwari, S. & Gurusamy, A. 2016. Influence of various sources and levels of fertilizers on nutrient use efficiencies of sugarcane. *Green Farming*, 7, 1212–1215.
- Pugesgaard, S., Petersen, S.O., Chirinda, N. & Olesen, J.E. 2017. Crop residues as driver for N₂O emissions from a sandy loam soil. *Agricultural and Forest Meteorology*, 233, 45–54.
- R Development Core Team. 2019. A language and environment for statistical computing, R Foundation for Statistical Computing.
- R Development Core Team. 2022.

-
- Rahman, N. & Forrester, P.J. 2021. Ammonium fertilizer reduces nitrous oxide emission compared to nitrate fertilizer while yielding equally in a temperate grassland. *Agriculture*, 11, 1–12.
- Raich, J.W. & Schlesinger, W.H. 1992. The global carbon dioxide flux in soil respiration and its relationship to vegetation and climate. *Tellus B: Chemical and Physical Meteorology*, 44, 1–20.
- Ravishankara, A.R., Daniel, J.S. & Portmann, R.W. 2009. Nitrous Oxide (N₂O): The Dominant ozone-depleting substance emitted in the 21st century. *Science*, 326, 123–125.
- Rawls, W.J., Brakensiek, D.L. & Saxton, K.E. 1982. Estimation of Soil Water Properties. *Transactions of the ASAE*, 25, 1316–1320.
- Reinsch, T., Loges, R., Kluß, C. & Taube, F. 2018. Effect of grassland ploughing and reseeded on CO₂ emissions and soil carbon stocks. *Agriculture, Ecosystems & Environment*, 265, 374–383.
- Riggers, C., Poelau, C., Don, A., Frühauf, C. & Dechow, R. 2021. How much carbon input is required to preserve or increase projected soil organic carbon stocks in German croplands under climate change? *Plant and Soil*, 460, 417–433.
- Roberts, G., Wooster, M.J. & Lagoudakis, E. 2009. Annual and diurnal african biomass burning temporal dynamics. *Biogeosciences*, 6, 849–866.
- Robertson, F.A. & Thorburn, P.J. 2007. Management of sugarcane harvest residues: consequences for soil carbon and nitrogen. *Soil Research*, 45, 1–11.
- Robinson, N., Brackin, R., Vinall, K., Soper, F., Holst, J., Gamage, H., Paungfoo-Lonhienne, C., Rennenberg, H., Lakshmanan, P. & Schmidt, S. 2011. Nitrate paradigm does not hold up for sugarcane (D Bassham, Ed.). *PLoS ONE*, 6, 1–9.
- Runyan, C.W., D’Odorico, P. & Lawrence, D. 2012. Physical and biological feedbacks of deforestation. *Reviews of Geophysics*, 50, 1–32.
- Rütting, T., Björnsne, A.-K., Weslien, P., Kasimir, Å. & Klemedtsson, L. 2021. Low nitrous oxide emissions in a boreal spruce forest soil, despite long-term fertilization. *Frontiers in Forests and Global Change*, 4, 1–7.

-
- Saatchi, S.S., Harris, N.L., Brown, S., Lefsky, M., Mitchard, E.T.A., Salas, W., Zutta, B.R., Buermann, W., Lewis, S.L., Hagen, S., Petrova, S., White, L., Silman, M. & Morel, A. 2011. Benchmark map of forest carbon stocks in tropical regions across three continents. *Proceedings of the National Academy of Sciences*, 108, 9899–9904.
- Sanderman, J., Hengl, T. & Fiske, G.J. 2017. Soil carbon debt of 12,000 years of human land use. *Proceedings of the National Academy of Sciences*, 114, 9575–9580.
- Sarmiento, G., Pinillos, M. & Garay, I. 2005. Biomass variability in tropical American lowland rainforests. *Ecotropicos*, 18, 1–20.
- Satiro, L.S., Cherubin, M.R., Safanelli, J.L., Lisboa, I.P., Rocha Junior, P.R. da, Cerri, C.E.P. & Cerri, C.C. 2017. Sugarcane straw removal effects on Ultisols and Oxisols in south-central Brazil. *Geoderma Regional*, 11, 86–95.
- Satolo, L. & Bacchi, M. 2013. Impacts of the recent expansion of the sugarcane sector on municipal per capita income in São Paulo State. *ISRN Economics*, 2013, 1–14.
- Saunio, M., Jackson, R.B., Bousquet, P., Poulter, B. & Canadell, J.G. 2016. The growing role of methane in anthropogenic climate change. *Environmental Research Letters*, 11, 1–6.
- Schaap, M.G. & Leij, F.J. 1998. Database related accuracy and uncertainty of pedotransfer functions. *Soil Science*, 163, 765–779.
- Schaap, M.G. & Leij, F.J. 2000. Improved prediction of unsaturated hydraulic conductivity with the Mualem-van Genuchten Model. *Soil Science Society of America Journal*, 64, 843–851.
- Schaap, M.G., Leij, F.J. & van Genuchten, M.Th. 2001. Rosetta : A computer program for estimating soil hydraulic parameters with hierarchical pedotransfer functions. *Journal of Hydrology*, 251, 163–176.
- Schlesinger, W.H. & Bernhardt, E.S. 2013. Biogeochemistry: An analysis of global change. (At: <https://oxfordbibliographies.com/view/document/obo-9780199830060/obo-9780199830060-0111.xml>. Accessed: 13/1/2023).

-
- Schwenke, G.D., Manning, W. & Haigh, B.M. 2014. Ammonia volatilisation from nitrogen fertilisers surface-applied to bare fallows, wheat crops and perennial-grass-based pastures on Vertosols. *Soil Research*, 52, 805–821.
- Seghers, D., Top, E.M., Reheul, D., Bulcke, R., Boeckx, P., Verstraete, W. & Siciliano, S.D. 2003. Long-term effects of mineral versus organic fertilizers on activity and structure of the methanotrophic community in agricultural soils. *Environmental Microbiology*, 5, 867–877.
- Shang, Q., Yang, X., Gao, C., Wu, P., Liu, J., Xu, Y., Shen, Q., Zou, J. & Guo, S. 2011. Net annual global warming potential and greenhouse gas intensity in Chinese double rice-cropping systems: a 3-year field measurement in long-term fertilizer experiments. *Global Change Biology*, 17, 2196–2210.
- Shein, E.V. & Arkhangel'skaya, T.A. 2006. Pedotransfer functions: State of the art, problems, and outlooks. *Eurasian Soil Science*, 39, 1089–1099.
- Shishaye, H.A. 2015. Simulations of nitrate leaching from sugarcane farm in Metahara, Ethiopia, using the LEACHN model. *Journal of Water Resource and Protection*, 07, 665–688.
- Shukla, S.K., Yadav, R.L., Singh, P.N. & Singh, I. 2009. Potassium nutrition for improving stubble bud sprouting, dry matter partitioning, nutrient uptake and winter initiated sugarcane (*Saccharum* spp. hybrid complex) ratoon yield. *European Journal of Agronomy*, 30, 27–33.
- da Silva Paredes, D., Lessa, A.C. da R., de Sant'Anna, S.A.C., Boddey, R.M., Urquiaga, S. & Alves, B.J.R. 2014. Nitrous oxide emission and ammonia volatilization induced by vinnasse and N fertilizer application in a sugarcane crop at Rio de Janeiro, Brazil. *Nutrient Cycling in Agroecosystems*, 98, 41–55.
- Silveira, S. & Khatiwada, D. 2019. Sugarcane biofuel production in Indonesia. In: *Sugarcane biofuels* (eds. Khan, M.T. & Khan, I.A.), pp. 285–300. Springer International Publishing, Cham.

-
- Šimůnek, J., Genuchten, M.Th. & Šejna, M. 2008. Development and applications of the HYDRUS and STANMOD software packages and related codes. *Vadose Zone Journal*, 7, 587–600.
- Singh, P., Suman, A., Tiwari, P., Arya, N., Gaur, A. & Shrivastava, A.K. 2008. Biological pretreatment of sugarcane trash for its conversion to fermentable sugars. *World Journal of Microbiology and Biotechnology*, 24, 667–673.
- Six, J., Elliott, E.T., Paustian, K. & Doran, J.W. 1998. Aggregation and soil organic matter accumulation in cultivated and native grassland soils. *Soil Science Society of America Journal*, 62, 1367–1377.
- Sjögersten, S., Aplin, P., Gauci, V., Peacock, M., Siegenthaler, A. & Turner, B.L. 2018. Temperature response of ex-situ greenhouse gas emissions from tropical peatlands: Interactions between forest type and peat moisture conditions. *Geoderma*, 324, 47–55.
- Skocaj, D.M., Everingham, Y.L. & Schroeder, B.L. 2013. Nitrogen management guidelines for sugarcane production in Australia: Can these be modified for wet tropical conditions using seasonal climate forecasting? *Springer Science Reviews*, 1, 51–71.
- Smith, K.A. 1990. Greenhouse gas fluxes between land surfaces and the atmosphere. *Progress in Physical Geography: Earth and Environment*, 14, 349–372.
- Soares, J.R., Cantarella, H., Vargas, V.P., Carmo, J.B., Martins, A.A., Sousa, R.M. & Andrade, C.A. 2015. Enhanced efficiency fertilizers in nitrous oxide emissions from urea applied to sugarcane. *Journal of Environmental Quality*, 44, 423–430.
- Solomon, S. 2014. Sugarcane agriculture and sugar industry in India: At a glance. *Sugar Tech*, 16, 113–124.
- Solomon, S. 2016. Sugarcane production and development of sugar industry in India. *Sugar Tech*, 18, 588–602.
- Soong, J.L., Marañón-Jimenez, S., Cotrufo, M.F., Boeckx, P., Bodé, S., Guenet, B., Peñuelas, J., Richter, A., Stahl, C., Verbruggen, E. & Janssens, I.A. 2018. Soil microbial CNP and respiration responses to organic matter and nutrient additions: Evidence from a tropical soil incubation. *Soil Biology and Biochemistry*, 122, 141–149.

-
- Sousa Neto, E., Carmo, J.B., Keller, M., Martins, S.C., Alves, L.F., Vieira, S.A., Piccolo, M.C., Camargo, P., Couto, H.T.Z., Joly, C.A. & Martinelli, L.A. 2011. Soil-atmosphere exchange of nitrous oxide, methane and carbon dioxide in a gradient of elevation in the coastal Brazilian Atlantic forest. *Biogeosciences*, 8, 733–742.
- Sparovek, G., Barretto, A., Berndes, G., Martins, S. & Maule, R. 2009. Environmental, land-use and economic implications of Brazilian sugarcane expansion 1996–2006. *Mitigation and Adaptation Strategies for Global Change*, 14, 285–298.
- Spracklen, D.V., Arnold, S.R. & Taylor, C.M. 2012. Observations of increased tropical rainfall preceded by air passage over forests. *Nature*, 489, 282–285.
- Stehfest, E. & Bouwman, L. 2006. N₂O and NO emission from agricultural fields and soils under natural vegetation: summarizing available measurement data and modeling of global annual emissions. *Nutrient Cycling in Agroecosystems*, 74, 207–228.
- Stuedler, P.A., Bowden, R.D., Melillo, J.M. & Aber, J.D. 1989. Influence of nitrogen fertilization on methane uptake in temperate forest soils. *Nature*, 341, 314–316.
- Stewart, L.K., Charlesworth, P.B., Bristow, K.L. & Thorburn, P.J. 2006. Estimating deep drainage and nitrate leaching from the root zone under sugarcane using APSIM-SWIM. *Agricultural Water Management*, 81, 315–334.
- van Straaten, H.P. 1976. *Präkambrium und junges western rift im Bunyoro Distrikt, NW Uganda (Ostafrika)*. Schweizerbart Science Publishers, Hannover.
- van Straaten, O., Corre, M.D., Wolf, K., Tchienkoua, M., Cuellar, E., Matthews, R.B. & Veldkamp, E. 2015. Conversion of lowland tropical forests to tree cash crop plantations loses up to one-half of stored soil organic carbon. *Proceedings of the National Academy of Sciences*, 112, 9956–9960.
- van Straaten, O., Doamba, S.W.M.F., Corre, M.D. & Veldkamp, E. 2019. Impacts of burning on soil trace gas fluxes in two wooded savanna sites in Burkina Faso. *Journal of Arid Environments*, 165, 132–140.
- van Straaten, O., Veldkamp, E. & Corre, M.D. 2011. Simulated drought reduces soil CO₂ efflux and production in a tropical forest in Sulawesi, Indonesia. *Ecosphere*, 2, 1–22.

-
- Suman, A., Shrivastava, A.K., Gaur, A., Singh, P., Singh, J. & Yadav, R.L. 2007. Nitrogen use efficiency of sugarcane in relation to its BNF potential and population of endophytic diazotrophs at different N levels. *Plant Growth Regulation*, 54, 1–11.
- Sun, L., Ataka, M., Kominami, Y. & Yoshimura, K. 2017. Relationship between fine-root exudation and respiration of two *Quercus* species in a Japanese temperate forest. *Tree Physiology*, 37, 1011–1020.
- Sundareshwar, P.V., Morris, J.T., Koepfler, E.K. & Fornwalt, B. 2003. Phosphorus limitation of coastal ecosystem processes. *Science*, 299, 563–565.
- Tamale, J., Hüppi, R., Griepentrog, M., Turyagyenda, L.F., Barthel, M., Doetterl, S., Fiener, P. & van Straaten, O. 2021. Nutrient limitations regulate soil greenhouse gas fluxes from tropical forests: evidence from an ecosystem-scale nutrient manipulation experiment in Uganda. *SOIL*, 7, 433–451.
- Tamale, J., van Straaten, O., Hüppi, R., Turyagyenda, L.F., Fiener, P. & Doetterl, S. 2022. Soil greenhouse gas fluxes following conversion of tropical forests to fertilizer-based sugarcane systems in northwestern Uganda. *Agriculture, Ecosystems & Environment*, 333, 1–13.
- Tamatamah, R.A., Hecky, R.E. & Duthie, Hamish C. 2005. The atmospheric deposition of phosphorus in Lake Victoria (East Africa). *Biogeochemistry*, 73, 325–344.
- Tanner, E.V.J., Kapos, V. & Franco, W. 1992. Nitrogen and phosphorus fertilization effects on Venezuelan montane forest trunk growth and litterfall. *Ecology*, 73, 78–86.
- Tanner, E.V.J., Vitousek, P.M. & Cuevas, E. 1998. Experimental investigation of nutrient limitation of forest growth on wet tropical mountains. *Ecology*, 79, 10–22.
- Tate, K.R. 2015. Soil methane oxidation and land-use change – from process to mitigation. *Soil Biology and Biochemistry*, 80, 260–272.
- Täumer, J., Kolb, S., Boeddinghaus, R.S., Wang, H., Schöning, I., Schrumpf, M., Urich, T. & Marhan, S. 2021. Divergent drivers of the microbial methane sink in temperate forest and grassland soils. *Global Change Biology*, 27, 929–940.

- Tavares, R.L.M., Spokas, K., Hall, K., Colosky, E., Souza, Z.M. de & Scala, N.L. 2018. Sugarcane residue management impact soil greenhouse gas. *Ciência e Agrotecnologia*, 42, 195–203.
- Tayade, A.S., Bhaskaran, A. & Anusha, S. 2020. IPNS–STCR-based nutrient management modules for enhancing soil health, fertilizer-use efficiency, productivity and profitability of tropical Indian sugarcane plant–ratoon agro-ecosystem. *Sugar Tech*, 22, 32–41.
- Tchiofo Lontsi, R., Corre, M.D., Iddris, N.A. & Veldkamp, E. 2020. Soil greenhouse gas fluxes following conventional selective and reduced-impact logging in a Congo Basin rainforest. *Biogeochemistry*, 151, 153–170.
- Thorburn, P.J., Biggs, J.S., Attard, S.J. & Kemei, J. 2011. Environmental impacts of irrigated sugarcane production: Nitrogen lost through runoff and leaching. *Agriculture, Ecosystems & Environment*, 144, 1–12.
- Thorburn, P.J., Biggs, J.S., Collins, K. & Probert, M.E. 2010. Using the APSIM model to estimate nitrous oxide emissions from diverse Australian sugarcane production systems. *Agriculture, Ecosystems & Environment*, 136, 343–350.
- Thorburn, P.J., Biggs, J.S., Palmer, J., Meier, E.A., Verburg, K. & Skocaj, D.M. 2017. Prioritizing crop management to increase nitrogen use efficiency in Australian sugarcane crops. *Frontiers in Plant Science*, 8, 1–16.
- Thorburn, P.J., Meier, E.A. & Probert, M.E. 2005. Modelling nitrogen dynamics in sugarcane systems: Recent advances and applications. *Field Crops Research*, 92, 337–351.
- Thorburn, P.J., Wilkinson, S.N. & Silburn, D.M. 2013. Water quality in agricultural lands draining to the Great Barrier Reef: A review of causes, management and priorities. *Agriculture, Ecosystems & Environment*, 180, 4–20.
- Tilman, D., Cassman, K.G., Matson, P.A., Naylor, R. & Polasky, S. 2002. Agricultural sustainability and intensive production practices. *Nature*, 418, 671–677.
- Tomasella, J. & Hodnett, M.G. 1998. Estimating soil water retention characteristics from limited data in Brazilian Amazonia: *Soil Science*, 163, 190–202.

- Townsend, A. R., Vitousek, P. M., and Trumbore, S. E.: Soil organic matter dynamics along gradients in temperature and land use on the island of Hawaii, *Ecology*, 76, 721–733
- Tullberg, J., Antille, D.L., Bluett, C., Eberhard, J. & Scheer, C. 2018. Controlled traffic farming effects on soil emissions of nitrous oxide and methane. *Soil and Tillage Research*, 176, 18–25.
- Tuller, M. & Or, D. 2005. Water retention and characteristic curve. In: *Encyclopedia of Soils in the Environment*, pp. 278–289. Elsevier.
- Tyler, G. 2008. *The African sugar industry—A frustrated success story. Background paper for the competitive commercial agriculture in Africa (CCAA) study*. World Bank, Washington, DC.
- UNFCCC. 2015. *Ad Hoc Working Group on the Durban Platform for Enhanced Action*. Geneva.
- Usman, M. 2016. Contribution of agriculture sector in the GDP growth rate of Pakistan. *Journal of Global Economics*, 4, (At: <http://www.esciencecentral.org/journals/contribution-of-agriculture-sector-in-the-gdp-growth-rate-of-pakistan-2375-4389-1000184.php?aid=71383>. Accessed: 10/12/2022).
- Vadeboncoeur, M.A. 2010. Meta-analysis of fertilization experiments indicates multiple limiting nutrients in northeastern deciduous forests. *Canadian Journal of Forest Research*, 40, 1766–1780.
- Van Looy, K., Bouma, J., Herbst, M., Koestel, J., Minasny, B., Mishra, U., Montzka, C., Nemes, A., Pachepsky, Y.A., Padarian, J., Schaap, M.G., Tóth, B., Verhoef, A., Vanderborght, J., Ploeg, M.J., Weihermüller, L., Zacharias, S., Zhang, Y. & Vereecken, H. 2017. Pedotransfer functions in Earth system science: Challenges and perspectives. *Reviews of Geophysics*, 55, 1199–1256.
- Veber, G., Kull, A., Villa, J.A., Maddison, M., Paal, J., Oja, T., Iturraspe, R., Pärn, J., Teemusk, A. & Mander, Ü. 2018. Greenhouse gas emissions in natural and managed peatlands of America: Case studies along a latitudinal gradient. *Ecological Engineering*, 114, 34–45.
- Veldkamp, E., Koehler, B. & Corre, M.D. 2013. Indications of nitrogen-limited methane uptake in tropical forest soils. *Biogeosciences*, 10, 5367–5379.

- Veldkamp, E., Schmidt, M., Powers, J.S. & Corre, M.D. 2020. Deforestation and reforestation impacts on soils in the tropics. *Nature Reviews Earth & Environment*, 1, 590–605.
- Vennila, A., Palaniswami, C., Durai, A.A., Shanthi, R.M. & Radhika, K. 2021. Partitioning of major nutrients and nutrient use efficiency of sugarcane genotypes. *Sugar Tech*, 23, 741–746.
- Verchot, L.V., Dannenmann, M., Kengdo, S.K., Njine-Bememba, C.B., Rufino, M.C., Sonwa, D.J. & Tejedor, J. 2020. Land-use change and biogeochemical controls of soil CO₂, N₂O and CH₄ fluxes in Cameroonian forest landscapes. *Journal of Integrative Environmental Sciences*, 17, 45–67.
- Verchot, L.V., Davidson, E.A., Cattânio, H., Ackerman, I.L., Erickson, H.E. & Keller, M. 1999. Land use change and biogeochemical controls of nitrogen oxide emissions from soils in eastern Amazonia. *Global Biogeochemical Cycles*, 13, 31–46.
- Vereecken, H., Weynants, M., Javaux, M., Pachepsky, Y., Schaap, M.G. & van Genuchten, M.Th. 2010. Using pedotransfer functions to estimate the van Genuchten-Mualem soil hydraulic properties: A review. *Vadose Zone Journal*, 9, 795–820.
- Vieira-Megda, M.X., Mariano, E., Leite, J.M., Franco, H.C.J., Vitti, A.C., Megda, M.M., Khan, S.A., Mulvaney, R.L. & Trivelin, P.C.O. 2015. Contribution of fertilizer nitrogen to the total nitrogen extracted by sugarcane under Brazilian field conditions. *Nutrient Cycling in Agroecosystems*, 101, 241–257.
- Vitousek, P.M. 1984. Litterfall, nutrient cycling, and nutrient limitation in tropical forests. *Ecology*, 65, 285–298.
- Vrugt, J.A. & Dane, J.H. 2005. Inverse Modeling of Soil Hydraulic Properties. In: *Encyclopedia of Hydrological Sciences* (eds. Anderson, M.G. & McDonnell, J.J.), pp. 1–20. John Wiley & Sons, Ltd, Chichester, UK.
- Wagenet, R.J., Bouma, J. & Grossman, R.B. 1991. Minimum data sets for use of soil survey information in soil interpretive models. In: *SSSA Special Publications* (eds. Mausbach, M.J. & Wilding, L.P.), pp. 161–182. Soil Science Society of America, Madison, WI, USA.

-
- Wang, F., Li, J., Wang, X., Zhang, W., Zou, B., Neher, D.A. & Li, Z. 2014a. Nitrogen and phosphorus addition impact soil N₂O emission in a secondary tropical forest of south China. *Scientific Reports*, 4, 1–8.
- Wang, X., Piao, S., Ciais, P., Friedlingstein, P., Myneni, R.B., Cox, P., Heimann, M., Miller, J., Peng, S., Wang, T., Yang, H. & Chen, A. 2014b. A two-fold increase of carbon cycle sensitivity to tropical temperature variations. *Nature*, 506, 212–215.
- Wang, W.J., Reeves, S.H., Salter, B., Moody, P.W. & Dalal, R.C. 2016. Effects of urea formulations, application rates and crop residue retention on N₂O emissions from sugarcane fields in Australia. *Agriculture, Ecosystems & Environment*, 216, 137–146.
- Wang, C. & Yang, J. 2007. Rhizospheric and heterotrophic components of soil respiration in six Chinese temperate forests. *Global Change Biology*, 13, 123–131.
- Wang, Z., Zhang, X., Liu, L., Cheng, M. & Xu, J. 2020. Spatial and seasonal patterns of atmospheric nitrogen deposition in north China. *Atmospheric and Oceanic Science Letters*, 13, 188–194.
- Wanyama, I., Pelster, D.E., Butterbach-Bahl, K., Verchot, L.V., Martius, C. & Rufino, M.C. 2019. Soil carbon dioxide and methane fluxes from forests and other land use types in an African tropical montane region. *Biogeochemistry*, 143, 171–190.
- Wei, X., Eglinton, J., Piperidis, G., Atkin, F., Morgan, T., Parfitt, R. & Hu, F. 2022. Sugarcane breeding in Australia. *Sugar Tech*, 24, 151–165.
- Wei, Z., Jiangming, M., Yunting, F., Xiankai, L. & Hui, W. 2008. Effects of nitrogen deposition on the greenhouse gas fluxes from forest soils. *Acta Ecologica Sinica*, 28, 2309–2319.
- Weier, K.L. 1998. Sugarcane fields: sources or sinks for greenhouse gas emissions? *Australian Journal of Agricultural Research*, 49, 1–10.
- Welch, B., Gauci, V. & Sayer, E.J. 2019. Tree stem bases are sources of CH₄ and N₂O in a tropical forest on upland soil during the dry to wet season transition. *Global Change Biology*, 25, 361–372.

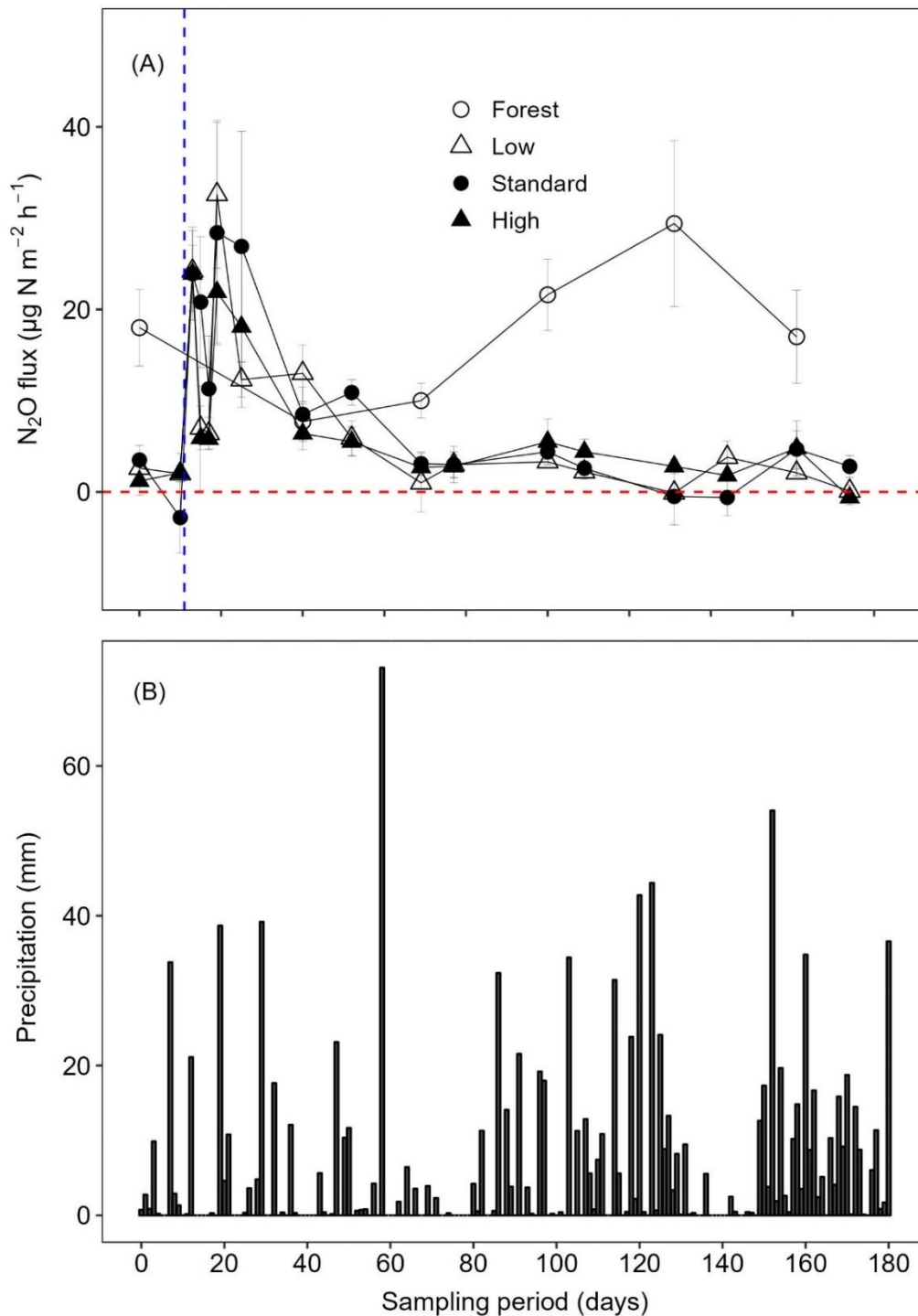
-
- Werner, C., Butterbach-Bahl, K., Haas, E., Hickler, T. & Kiese, R. 2007. A global inventory of N₂O emissions from tropical rainforest soils using a detailed biogeochemical model. *Global Biogeochemical Cycles*, 21, 1–18.
- Weynants, M., Vereecken, H. & Javaux, M. 2009. Revisiting Vereecken pedotransfer functions: Introducing a closed-form hydraulic model. *Vadose Zone Journal*, 8, 86–95.
- Wolf, K., Veldkamp, E., Homeier, J. & Martinson, G.O. 2011. Nitrogen availability links forest productivity, soil nitrous oxide and nitric oxide fluxes of a tropical montane forest in southern Ecuador. *Global Biogeochemical Cycles*, 25, 1–12.
- Wolfgang, D. & Kai, L. 2006. Determining soil hydraulic properties. *Encyclopedia of Hydrological Sciences*, 1–23.
- Wösten, J.H.M., Lilly, A., Nemes, A. & Le Bas, C. 1999. Development and use of a database of hydraulic properties of European soils. *Geoderma*, 90, 169–185.
- Wösten, J.H.M., Pachepsky, Ya.A. & Rawls, W.J. 2001. Pedotransfer functions: bridging the gap between available basic soil data and missing soil hydraulic characteristics. *Journal of Hydrology*, 251, 123–150.
- Wright, S.J. 2019. Plant responses to nutrient addition experiments conducted in tropical forests. *Ecological Monographs*, 89, 1–18.
- Wright, S.J., Turner, B.L., Yavitt, J.B., Harms, K.E., Kaspari, M., Tanner, E.V.J., Bujan, J., Griffin, E.A., Mayor, J.R., Pasquini, S.C., Sheldrake, M. & Garcia, M.N. 2018. Plant responses to fertilization experiments in lowland, species-rich, tropical forests. *Ecology*, 99, 1129–1138.
- Wright, S.J., Yavitt, J.B., Wurzbürger, N., Turner, B.L., Tanner, E.V.J., Sayer, E.J., Santiago, L.S., Kaspari, M., Hedin, L.O., Harms, K.E., Garcia, M.N. & Corre, M.D. 2011. Potassium, phosphorus, or nitrogen limit root allocation, tree growth, or litter production in a lowland tropical forest. *Ecology*, 92, 1616–1625.
- Wu, L., Zhang, Y., Guo, X., Ning, D., Zhou, X., Feng, J., Yuan, M.M., Liu, S., Guo, J., Gao, Z., Ma, J., Kuang, J., Jian, S., Han, S., Yang, Z., Ouyang, Y., Fu, Y., Xiao, N., Liu, X.,

- Wu, L., Zhou, A., Yang, Y., Tiedje, J.M. & Zhou, J. 2022. Reduction of microbial diversity in grassland soil is driven by long-term climate warming. *Nature Microbiology*, 7, 1054–1062.
- Xu, N., Bhadha, J.H., Rabbany, A., Swanson, S., Mccray, J.M., Li, Y., Strauss, S.L. & Mylav-arapu, R. 2022. Sugarcane bagasse amendment mitigates nutrient leaching from a mineral soil under tropical conditions. *Pedosphere*, 32, 876–883.
- Xu, H., Detto, M., Fang, S., Chazdon, R.L., Li, Y., Hau, B.C.H., Fischer, G.A., Weiblen, G.D., Hogan, J.A., Zimmerman, J.K., Uriarte, M., Thompson, J., Lian, J., Cao, K., Kenfack, D., Alonso, A., Bissiengou, P., Memiaghe, H.R., Valencia, R., Yap, S.L., Davies, S.J., Mi, X. & Yao, T.L. 2020. Soil nitrogen concentration mediates the relationship between leguminous trees and neighbor diversity in tropical forests. *Communications Biology*, 3, 1–8.
- Yadav, R.L. 2004. Enhancing efficiency of fertilizer n use in sugarcane by ring-pit method of planting. *Sugar Tech*, 6, 169–171.
- Yan, Y., Sha, L., Cao, M., Zheng, Z., Tang, J., Wang, Y., Zhang, Y., Wang, R., Liu, G., Wang, Y. & Sun, Y. 2008. Fluxes of CH₄ and N₂O from soil under a tropical seasonal rain forest in Xishuangbanna, southwest China. *Journal of Environmental Sciences*, 20, 207–215.
- Yan, G., Xing, Y., Xu, L., Wang, J., Dong, X., Shan, W., Guo, L. & Wang, Q. 2017. Effects of different nitrogen additions on soil microbial communities in different seasons in a boreal forest. *Ecosphere*, 8, 1–19.
- Yang, L., Deng, Y., Wang, X., Zhang, W., Shi, X., Chen, X., Lakshmanan, P. & Zhang, F. 2021. Global direct nitrous oxide emissions from the bioenergy crop sugarcane (*Saccharum* spp. inter-specific hybrids). *Science of The Total Environment*, 752, 1–12.
- Yang, X., Wang, C. & Xu, K. 2017. Response of soil CH₄ fluxes to stimulated nitrogen deposition in a temperate deciduous forest in northern China: A 5-year nitrogen addition experiment. *European Journal of Soil Biology*, 82, 43–49.

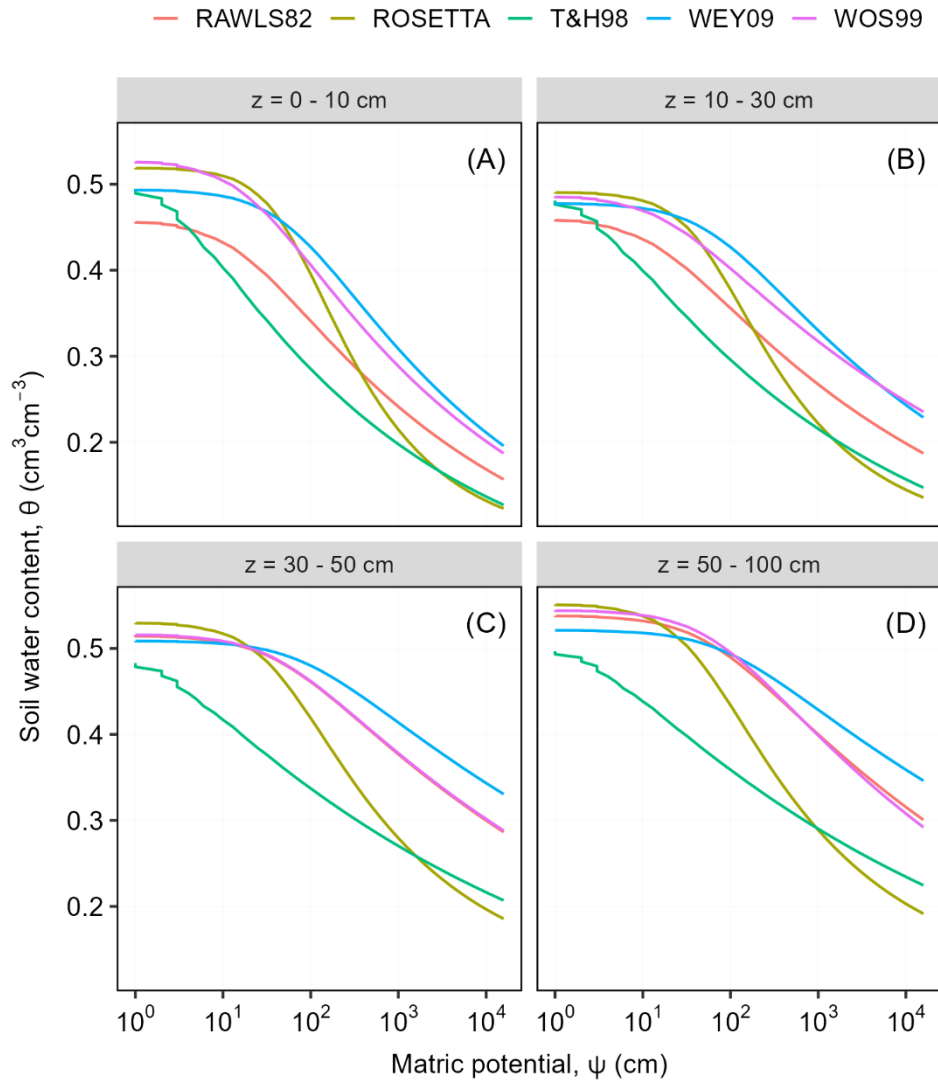
-
- Yu, L., Wang, Y., Zhang, X., Dörsch, P. & Mulder, J. 2017. Phosphorus addition mitigates N₂O and CH₄ emissions in N-saturated subtropical forest, SW China. *Biogeosciences*, 14, 3097–3109.
- Zhang, P., Lü, X.-T., Li, M.-H., Wu, T. & Jin, G. 2022. N limitation increases along a temperate forest succession: evidences from leaf stoichiometry and nutrient resorption (J Xia, Ed.). *Journal of Plant Ecology*, 15, 1021–1035.
- Zhang, Y., Ma, M., Fang, H., Qin, D., Cheng, S. & Yuan, W. 2020. Impacts of nitrogen addition on nitrous oxide emission: Comparison of five nitrous oxide modules or algorithms. *Ecological Modelling*, 421, 1–8.
- Zhang, W., Mo, J., Yu, G., Fang, Y., Li, D., Lu, X. & Wang, H. 2008a. Emissions of nitrous oxide from three tropical forests in Southern China in response to simulated nitrogen deposition. *Plant and Soil*, 306, 221–236.
- Zhang, W., Mo, J., Zhou, G., Gundersen, P., Fang, Y., Lu, X., Zhang, T. & Dong, S. 2008b. Methane uptake responses to nitrogen deposition in three tropical forests in southern China. *Journal of Geophysical Research*, 113, 1–10.
- Zhang, Y. & Schaap, M.G. 2019. Estimation of saturated hydraulic conductivity with pedo-transfer functions: A review. *Journal of Hydrology*, 575, 1011–1030.
- Zhang, W., Zhu, X., Luo, Y., Rafique, R., Chen, H., Huang, J. & Mo, J. 2014. Responses of nitrous oxide emissions to nitrogen and phosphorus additions in two tropical plantations with N-fixing vs. non-N-fixing tree species. *Biogeosciences*, 11, 4941–4951.
- Zhang, T., Zhu, W., Mo, J., Liu, L. & Dong, S. 2011. Increased phosphorus availability mitigates the inhibition of nitrogen deposition on CH₄ uptake in an old-growth tropical forest, southern China. *Biogeosciences*, 8, 2805–2813.
- Zheng, M., Zhang, T., Liu, L., Zhang, W., Lu, X. & Mo, J. 2016a. Effects of nitrogen and phosphorus additions on soil methane uptake in disturbed forests. *Journal of Geophysical Research: Biogeosciences*, 121, 3089–3100.
- Zheng, M., Zhang, T., Liu, L., Zhu, W., Zhang, W. & Mo, J. 2016b. Effects of nitrogen and phosphorus additions on nitrous oxide emission in a nitrogen-rich and two nitrogen-limited tropical forests. *Biogeosciences*, 13, 3503–3517.

- Zhou, J., Gu, B., Schlesinger, W.H. & Ju, X. 2016. Significant accumulation of nitrate in Chinese semi-humid croplands. *Scientific Reports*, 6, 1–8.
- Zommers, Z.A., Johnson, P.J. & Macdonald, D.W. 2012. Biofuels bonanza? Sugarcane production and poverty in villages surrounding Budongo forest, Uganda. *Journal of Eastern African Studies*, 6, 177–195.

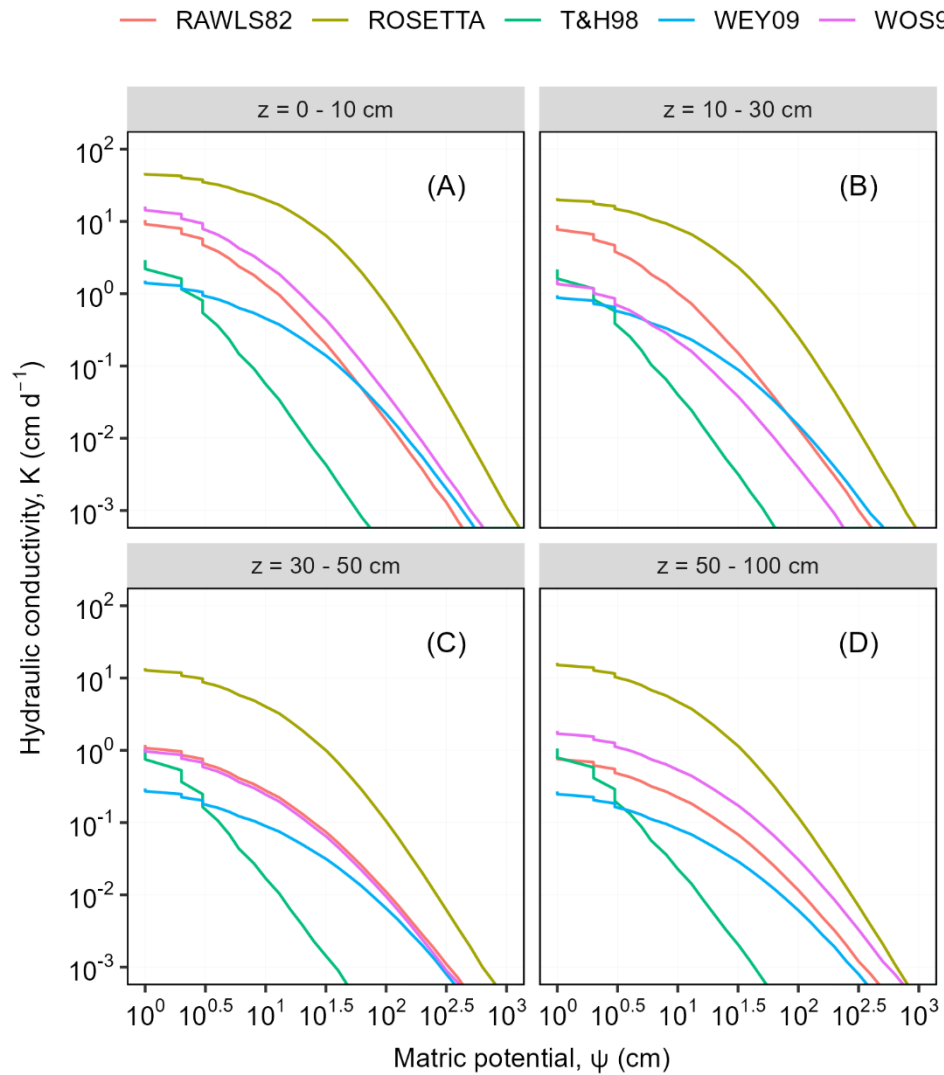
APPENDIX



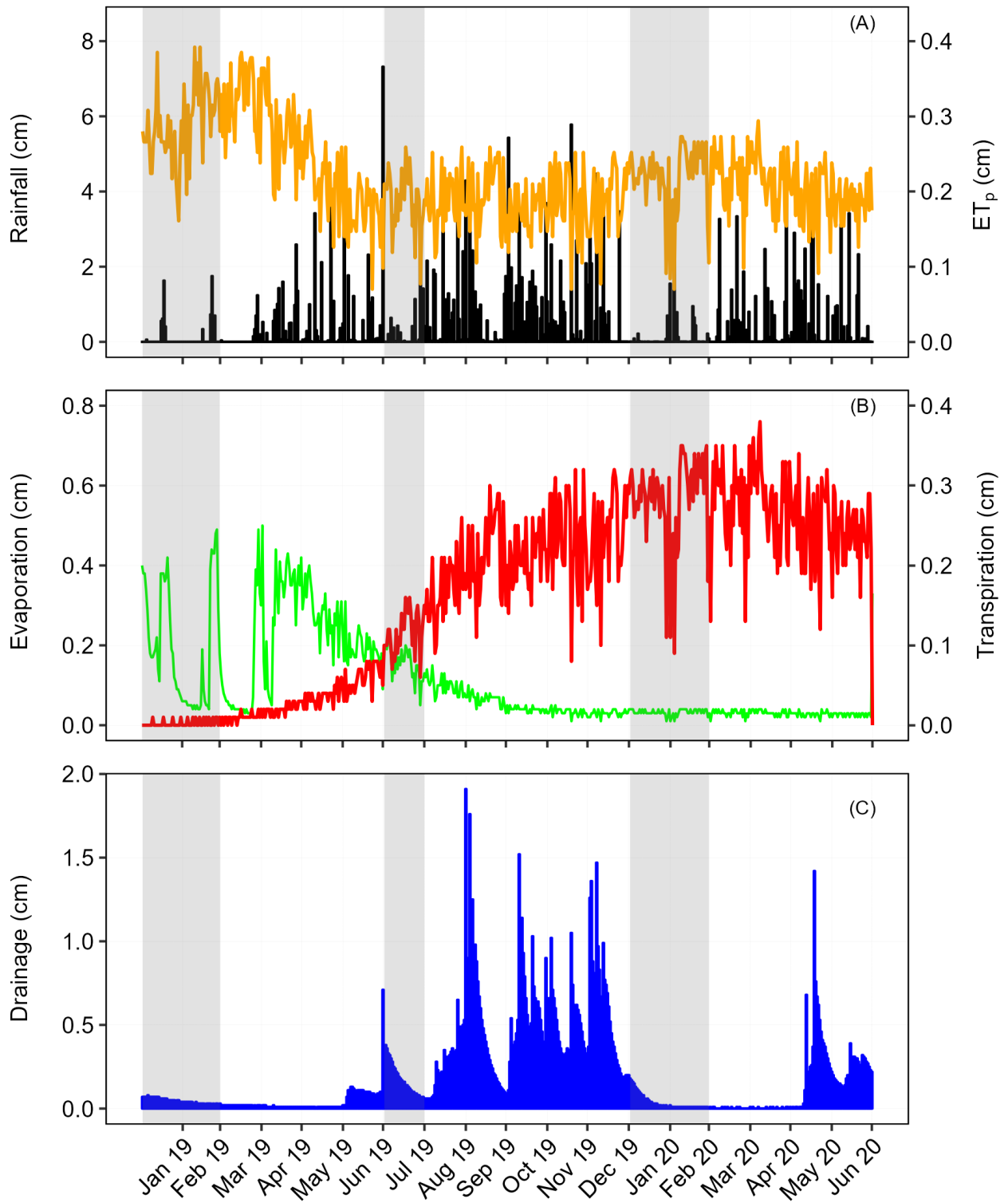
Appendix F.1. (A) Mean (\pm standard error, SE, $n = 4$) soil N_2O fluxes measured between May and October 2019 from the reference forest plots and replicate treatment plots of the completely randomized design (CRD) experiment established in the 20-year-old sugarcane plantation, and (B) the bars represent the daily precipitation measured between May and October 2019 from both the reference forest plots and sugarcane plots. The dashed vertical blue line indicates the timing of the application of the single combined dose of urea and muriate of potash fertilizers in the sugarcane. The dashed horizontal line indicates the background level of the soil N_2O fluxes from both the reference forest and sugarcane plots. Standard equals $70 \text{ kg N} + 23 \text{ kg K ha}^{-1}$ growth cycle⁻¹, low equals 0.5 times standard and high equals 1.5 times standard.



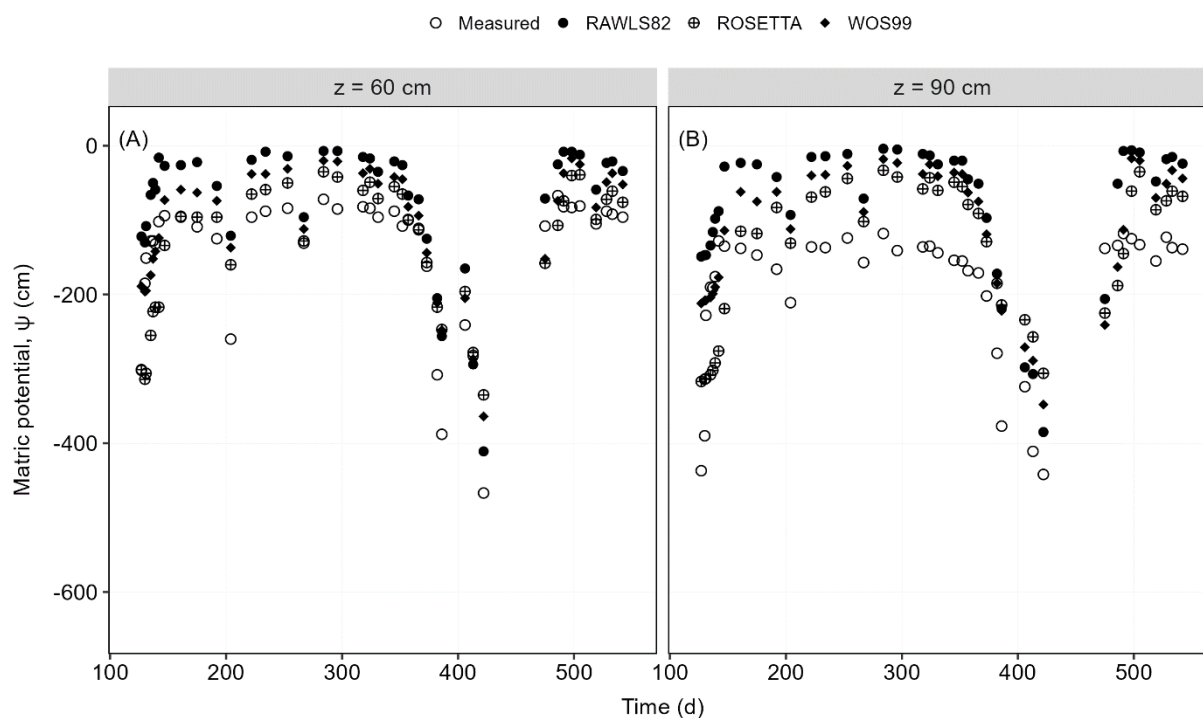
Appendix F.2. Soil water retention curves at four different soil depths (0-10 cm—A; 10-30 cm—B; 30-50 cm—C; and 50-100 cm—D) based on soil hydraulic parameters of the van Genuchten model (θ_r , θ_s , a , and n) estimated using five PTFs (RAWLS82, ROSETTA, T&H98, WEY09, and WOS99).



Appendix F.3. Soil hydraulic conductivity curve at four different soil depths (0-10 cm—A; 10-30 cm—B; 30-50 cm—C; and 50-100 cm—D) based on soil hydraulic parameters of the van Genuchten model (θ_r , θ_s , α , and n) and saturated hydraulic conductivity, K_s , estimated using five PTFs (RAWLS82, ROSETTA, T&H98, WEY09, and WOS99).



Appendix F.4. Panel A shows daily rainfall (cm; measured with ATMOS41 weather station) and potential evapotranspiration (ET_p ; cm), estimated with the Penman-Monteith approach (Allen et al., 1998), panel B shows modeled actual evaporation (cm) and actual transpiration (cm), and panel C shows average modeled drainage (cm) between January 2019 and June 2020 based on ROSETTA; RAWLS82, and WOS99 PTFs. The gray-shaded rectangles in panels A, B, and C represent the lengths of dry periods in 2019 and 2020.



Appendix F.5. Predicted matric potential with ROSETTA, RAWLS82, and WOS99 PTFs and the measured soil matric potential at soil depths of 60 (A) and 90 cm (B) between May 2019 and June 2020.

Appendix T.1. Site-specific topographic, geological, soil and climatic characteristics

Site	Elevation (m a.s.l)	Slope [†] (%)	Geology	Soil type ^{††}	Precipitation [‡] (mm)	Air Temperature [‡] (°C)
Forest	1058	< 5	Precambrian basement complex comprising of granite and gneisses ¹	Haplic Ferralsols to Xanthic Lixisols	2321	23.1 ± 0.0
Sugarcane	1064	< 5	Precambrian basement complex comprising of granite and gneisses ¹	Pisoplinthic Rhodic Ferralsols	2291	22.7 ± 0.1

¹Lehto *et al.* (2014)

[†]Slope extracted from a 30 m digital elevation model obtained from the Department of Geology, Ministry of Lands and Survey, Entebbe, Uganda. ^{††}Soil classification according to IUSS Working Group WRB (2014). [‡]Climatic data for the gas-sampling period (May 2019 to June 2020) obtained from climatic weather stations installed about 2 km and 0.2 km from the forest and sugarcane sites, respectively.

Appendix T.2. Soil physico-chemical characteristics (mean \pm standard error, SE) of the reference forest and sugarcane study sites in north-western Uganda

Depth (cm)	Bulk density (g cm ⁻³)	TOC (Mg ha ⁻¹)	TON (Mg ha ⁻¹)	pH H ₂ O (1:2.5)	C: N	Sand (%)	Silt (%)	Clay (%)
Forest (n = 4)								
0-10	1.6 \pm 0.0 ^a	30.9 \pm 4.9 ^a	1.9 \pm 0.2 ^a	6.8 \pm 0.2 ^a	8.0 \pm 0.4 ^a	-	-	-
10-30	1.2 \pm 0.0	14.0 \pm 2.3 ^a	1.0 \pm 0.1 ^a	6.0 \pm 0.3	7.7 \pm 0.2 ^a	-	-	-
30-50	1.3 \pm 0.0 ^a	26.4 \pm 2.2 ^a	0.6 \pm 0.1 ^a	5.9 \pm 0.4	8.4 \pm 0.3 ^a	46 \pm 2	25 \pm 1	29 \pm 0
50-100	1.3 \pm 0.1 ^a	40.2 \pm 3.9 ^a	4.1 \pm 0.3 ^a	7.2 \pm 0.2 ^a	9.7 \pm 0.1 ^a	59 \pm 0	29 \pm 0	12 \pm 0
Sugarcane (n = 12)								
0-10	1.1 \pm 0.0 ^b	29.0 \pm 0.7 ^b	1.9 \pm 0.0 ^b	5.5 \pm 0.1 ^b	14.8 \pm 0.2 ^b	45 \pm 0	34 \pm 0	21 \pm 0
10-30	1.2 \pm 0.0 ^b	49.0 \pm 1.0 ^b	3.4 \pm 1.1 ^b	5.5 \pm 0.0 ^b	14.4 \pm 0.2 ^b	-	-	-
30-50	1.2 \pm 0.0	26.7 \pm 1.2 ^b	2.3 \pm 0.1 ^b	5.5 \pm 0.0	11.7 \pm 0.2 ^b	-	-	-
50-100	1.1 \pm 0.1 ^b	36.1 \pm 2.0 ^b	3.5 \pm 0.1 ^b	5.4 \pm 0.1	10.4 \pm 0.0 ^b	45 \pm 1	19 \pm 0	36 \pm 1

Notes: Different lowercase letters indicate significant differences between the two land uses (ANOVA with Tukey's HSD test or Kruskal-Wallis with a multiple-comparison extension test at $p \leq 0.05$).

Appendix T.3. List of equations featuring in the five PTFs used to estimate the soil hydraulic parameters of the van Genuchten (1980) soil water retention function and saturated hydraulic conductivity (θ , θ_s , α , and n). Input data are sand (Sa ; %), silt (Si ; %), clay (Cl ; %), soil organic matter (SOM ; %), and bulk density (ρ_b ; g cm⁻³). Soil organic carbon (SOC ; %) is obtained as $SOC = SOM/1.724$ and $topsoil=1$ if soil samples were collected in the uppermost soil layer or $topsoil=0$ if soil samples were collected in the deeper layers of the soil profile. The equations are taken from (Nasta et al., 2021)

RAWLS82: Rawls et al. (1982) developed 12 regression equations to relate soil water content values to prescribed soil matric head values by using the following general equation:

$$\theta(\psi) = a + b Sa + c Si + d Cl + e SOC + f \rho_b \quad (A1)$$

where a , b , c , d , e , and f are the regression coefficients reported in Appendix T.4.

The data pairs, $\theta(\psi)$ were fitted to the van Genuchten water retention curve to optimize its four parameters (θ_r , θ_s , α , and n).

Saturated hydraulic conductivity, K_s (cm d⁻¹), was estimated by using the empirical equation proposed by Guarracino (2007):

$$K_s = 4.65 \cdot 10^4 \theta_s \alpha^2 \quad (A2)$$

ROSETTA was developed by Schaap et al. (2001). It is based on artificial neural network analysis (Zhang & Schaap, 2019) and implemented in HYDRUS-1D, where the five empirical van Genuchten (1980) model parameters (θ_r , θ_s , α , and n) can be derived from measurements of sand, silt, clay, organic matter, and bulk density.

T&H98: Tomasella and Hodnett (1998) developed nine regression equations to relate soil water content (θ) values to prescribed soil matric head (ψ) values by using the following general equation:

$$\theta(\psi) = 0.01 (a SOC + b Si + c Cl + d) \quad (A3)$$

where a , b , c , and d are the regression coefficients reported in Appendix T.5.

The data pairs, $\theta(\psi)$ were fitted to the van Genuchten water retention curve to optimize its four parameters (θ_r , θ_s , α , and n).

Saturated hydraulic conductivity, K_s (cm d⁻¹), was estimated by using the empirical equation proposed by Guarracino (2007) (Eq. A2).

WEY09

$$\theta_s = 0.6355 + 0.0013 * Cl - 0.1631 * \rho_b \quad (A4)$$

$$\theta_r = 0 \quad (A5)$$

$$\alpha = \exp(-4.3003 - 0.0097 * Cl + 0.0138 * Sa - 0.0992 * SOC) \quad (A6)$$

$$n = \exp(-1.0846 - 0.0236 * Cl - 0.0085 * Sa + 1.3699 * 10^{-4} * Sa^2) + 1 \quad (A7)$$

$$m = 1 - \frac{1}{n} \quad (A8)$$

Saturated hydraulic conductivity, K_s (cm d⁻¹), was estimated by using the empirical equation proposed by Guarracino (2007) (Eq. A2).

WOS99

$$\theta_s = 0.7919 + 0.001691 * Cl - 0.29619 * \rho_b - 0.000001491 * Si^2 + 0.0000821 * SOM^2 + \frac{0.02427}{Cl} + \frac{0.01113}{Si} + 0.01472 * \ln(Si) - 0.000073 * SOM * Cl - 0.000619 * \rho_b * Cl - 0.001183 * \rho_b * SOM - 0.0001664 * topsoil * Si \quad (A9)$$

$$\theta_r = 0 \quad (A10)$$

$$\alpha = \exp\left(-14.96 + 0.03135 * Cl + 0.0351 * Si + 0.646 * SOM + 15.29 * \rho_b - 0.192 * \text{topsoil} - 4.671 * \rho_b^2 - 0.000781 * Cl^2 - 0.00687 * SOM^2 + \frac{0.0449}{SOM} + 0.0663 * \ln(Si) + 0.1482 * \ln(SOM) - 0.04546 * \rho_b * Si - 0.4852 * \rho_b * SOM + 0.00673 * \text{topsoil} * Cl\right) \quad (A 1)$$

$$n = 1 + \exp\left(-25.23 - 0.02195 * Cl + 0.0074 * Si - 0.1940 * SOM + 45.5 * \rho_b - 7.24 * \rho_b^2 + 0.0003658 * Cl^2 + 0.002885 * SOM^2 - \frac{12.81}{\rho_b} - \frac{0.1524}{Si} - \frac{0.01958}{SOM} - 0.2876 * \ln(Si) - 0.0709 * \ln(SOM) - 44.6 * \ln(\rho_b) - 0.02264 * \rho_b * Cl + 0.0896 * \rho_b * SOM + 0.00718 * \text{topsoil} * Cl\right) \quad (A12)$$

$$m = 1 - \frac{1}{n} \quad (A13)$$

$$K_s = \exp\left(7.755 + 0.0352 * Si + 0.93 * \text{topsoil} - 0.967 * (\rho_b)^2 - 0.00048 * Cl^2 - 0.000322 * Si^2 + \frac{0.001}{Si} - \frac{0.0748}{SOM} - 0.643 * \ln(Si) - 0.01398 * \rho_b * Cl - 0.1673 * \rho_b * SOM + 0.02986 * \text{topsoil} * Cl - 0.03305 * \text{topsoil} * Si\right) \quad (A14)$$

Appendix T.4. Tabulated regression coefficients (a, b, c, d, e, f) in Eq. (A1) to predict soil water content (θ) values associated with 12 prescribed soil matric head values (ψ)

ψ (cm)	a	b	c	d	e	f
-40	0.790	-0.00370	0	0	0.0100	-0.132
-70	0.714	-0.00300	0	0.00170	0	-0.169
-100	0.412	-0.00300	0	0.00230	0.0317	0
-200	0.312	-0.00240	0	0.00320	0.0314	0
-330	0.258	-0.00200	0	0.00360	0.0299	0
-600	0.207	-0.00160	0	0.00400	0.0275	0
-1,000	0.0349	0	0.00140	0.00550	0.0251	0
-2,000	0.0281	0	0.00110	0.00540	0.0200	0
-4,000	0.0238	0	0.000800	0.00520	0.0190	0
-7,000	0.0216	0	0.000600	0.00500	0.0167	0
-10,000	0.0205	0	0.000500	0.00490	0.0154	0
-15,000	0.0260	0	0	0.00500	0.0158	0

Appendix T.5. Tabulated regression coefficients (a, b, c, d) in Eq. (A3) to predict soil water content (θ) values associated to nine prescribed soil matric head (ψ) values

ψ (cm)	<i>a</i>	<i>b</i>	<i>c</i>	<i>d</i>
-1	2.24	0.298	0.159	37.9
-10	0	0.530	0.255	23.8
-30	0	0.552	0.262	18.5
-60	0	0.576	0.300	12.3
-100	0	0.543	0.321	9.81
-330	0	0.426	0.404	4.05
-1,000	0	0.369	0.351	3.20
-5,000	0	0.258	0.361	1.57
-15,000	0	0.150	0.396	0.91

DECLARATION OF ORIGINALITY AND CERTIFICATE OF OWNERSHIP

I, Joseph Tamale, do hereby declare that I am the sole author of this dissertation entitled “Nutrient availability as a driver of soil greenhouse gas fluxes and nitrogen leaching in a native tropical forest and large-scale sugarcane plantations in north-western Uganda”. All references and data sources that were used in the dissertation have been appropriately acknowledged. I, furthermore, declare that this work has not been submitted elsewhere in any form as part of another dissertation procedure for the award of any academic degree.



Uganda, 2023

(Joseph Tamale)

ABOUT THE AUTHOR

Curriculum Vitae: Joseph Tamale

Personal details

Date of birth: 5.10.1987
Place of birth: Wobulenzi
Nationality: Ugandan

Education

Oct 2018- 2023 PhD in Physical Geography (special inclination towards soil biogeochemistry), University of Augsburg, Germany
Sept 2012-Sept 2014 Master of Science in Physical Land Resources (Soils Option)-Distinction, Ghent University, Belgium
Aug 2007-Jan 2011 Bachelor of Science of Agricultural Land Use and Management- Second Class Upper, Makerere University, Uganda.
2005-2006 Uganda Advanced Certificate of Education
2001-2004 Uganda Certificate of Education

Work experience

Dec 2016-present Research Officer-Soil Fertility, National Agricultural Research Organization, Uganda
Oct 2014-Dec 2018 Pedologist, National Agricultural Research Laboratories-Kawanda, Uganda
Jan 2011-Aug 2012 Professional Agricultural Advisory Service Provider-NAADS Program, Nakasongola District, Uganda
Jan 2008-Jul 2012 Physics and Chemistry Teacher, Advanced Level, Everest College, Luwero, Uganda